# FORMULATION AND *IN VITRO-IN VIVO* EVALUATION OF ROSUVASTATIN CALCIUM INCORPORATED CYCLODEXTRIN, SOLID LIPID AND CHITOSAN BASED DRUG DELIVERY SYSTEMS

**Doctoral Thesis**

**Fawaz Nasser Shekh AL-HEIBSHY**

**Eskişehir, 2017**

# FORMULATION AND *IN VITRO-IN VIVO* EVALUATION OF ROSUVASTATIN CALCIUM INCORPORATED CYCLODEXTRIN, SOLID LIPID AND CHITOSAN BASED DRUG DELIVERY SYSTEMS

**Fawaz Nasser Shekh AL-HEIBSHY**

**DOCTORAL THESIS**

**Department of Pharmaceutical Technology**
**Supervisor: Prof. Dr. Müzeyyen DEMİREL**
**Co-Supervisor: Assoc. Prof. Dr. Ebru BAŞARAN**

**Eskişehir**
**Anadolu University**
**Graduate School of Health Sciences**
**May, 2017**

*This thesis study was supported by Anadolu University Scientific Research Projects Commission (Project No. 1404S289)*

# FINAL APPROVAL FOR THESIS

This thesis titled "Formulation and *in vitro-in vivo* evaluation of rosuvastatin calcium incorporated cyclodextrin, solid lipid and chitosan based drug delivery systems" has been prepared and submitted by Fawaz Nasser Shekh AL-HEIBSHY in partial fulfillment of the requirements in "Anadolu University Directive on Graduate Education and Examination" for the Degree of PhD in Pharmaceutical Technology Department has been examined and approved on 26/05/2017.

| **Committee Members** | | **Signature** |
|---|---|---|
| Member (Supervisor) | : Prof. Dr. Müzeyyen DEMİREL | |
| Member | : Prof. Dr. İsmail Tuncer DEĞİM | |
| Member | : Prof. Dr. Sevgi TAKKA | |
| Member | : Asst. Prof. Dr. Evrim YENİLMEZ | |
| Member | : Asst. Prof. Dr. Arın Gül DAL | |

Prof. Dr. Dilek AK

Director

ANADOLU ÜNİVERSİTESİ FEN BİLİMLERİ ENSTİTÜSÜ MÜDÜRLÜĞÜ

## ABSTRACT

FORMULATION AND *IN VITRO-IN VIVO* EVALUATION OF ROSUVASTATIN CALCIUM INCORPORATED CYCLODEXTRIN, SOLID LIPID AND CHITOSAN BASED DRUG DELIVERY SYSTEMS

Fawaz Nasser Shekh AL-HEIBSHY

Department of Pharmaceutical Technology
Anadolu University, Graduate School of Health Sciences, May 2017

Supervisor: Prof. Dr. Müzeyyen DEMİREL
Co-Supervisor: Assoc. Prof. Dr. Ebru BAŞARAN

Cardiovascular diseases are the main reasons of death worldwide. Considering that many of the active pharmaceutical ingredients (APIs) used for the treatment of the such severe diseases have poor aqueous solubility which leads to insufficient treatment with poor bioavailability data. Therefore, there is a need for formulation of novel drug delivery systems for the enhancement of the efficacy with lowering the side effects of the APIs. In this study Rosuvastatin Calcium (RCa) which is one of the most effective cholesterol-lowering statin group agents was selected as a model drug aiming to prevent the coronary heart diseases with the reduction of the abnormal levels of lipids in the blood. For the enhancement of the efficacy of the API with lowered side effects, cyclodextrin (CDs) complexes, solid lipid nanoparticles (SLNs), polymeric nanoparticles with chitosan (Cs), were formulated. Characteristic properties of CDs complexes as well as the nanoparticles were revealed in detail. And also, stability of the formulations prepared were evaluated during the storage period of 3 months. Cytotoxic evaluations were also conducted with the MTT tests on Caco-2 cell lines. *Ex vivo* permeation performances on Caco-2 cell lines as well as *in vivo* pharmacokinetic studies were also evaluated on selected formulations. The comprehensiveness of the study and uniqueness of selected drug delivery systems are the major original values of our project. And since there is no study has done for the *in vitro-in vivo* efficiency of the CD-polymer based drug delivery systems for the RCa improves the originality of the study.



**Keywords:** Rosuvastatin Calcium, Cyclodextrin, Polyanhydride, Solid Lipid Nanoparticles, Chitosan, Pharmacokinetics.

# ÖZET

ROSUVASTATİN KALSİYUM İÇEREN SİKLODEKSTRİN, KATI LİPİT VE KİTOSAN BAZLI TAŞIYICI SİSTEMLERİN HAZIRLANMASI VE *İN VİTRO-İN VİVO* DEĞERLENDİRİLMESİ

Fawaz Nasser Shekh AL-HEIBSHY

Farmasötik Teknoloji Anabilim Dalı
Anadolu Üniversitesi, Sağlık Bilimleri Enstitüsü, Mayıs, 2017

Danışman: Prof. Dr. Müzeyyen DEMİREL
İkinci Danışman: Doç. Dr. Ebru BAŞARAN

Kardiyovasküler rahatsızlıklar dünya çapında ölüm nedenlerinin ilk sırasında yer almaktadır. Kardiyovasküler rahatsızlıkların tedavisinde kullanılan pek çok etkin madde, sudaki düşük çözünürlükleri nedeni ile düşük biyoyararlanım oluşturarak etkin bir tedavi sağlayamamaktadır. Bu nedenle etkin maddelerin etkinliklerini arttırmanın yanı sıra yan etkilerini de azaltan yeni ilaç taşıyıcı sistemlere ihtiyaç duyulmaktadır. Bu çalışmada, en etkili kolesterol düşürücü statin grubu üyelerinden olan Rosuvastatin Kalsiyum (RCa) kandaki serum lipit oranlarının azaltılması ve bu sayede koroner kalp rahatsızlıklarının önlenmesi amacı ile model etkin madde olarak belirlenmiştir. Etkin maddenin etkisinin arttırılması ve yan etkilerinin azaltılması amacı ile siklodekstrin (CDs) kompleksleri, katı lipit nanopartiküller (SLNs) ve kitosan (Cs) ile hazırlanan polimerik nanopartiküller formüle edilmiştir. CDs komplekslerinin ve nanopartiküllerin karakteristik özellikleri detaylı bir şekilde ortaya konulmuş, ayrıca hazırlanan formülasyonların kararlılıkları 3 ay süresince değerlendirilmiştir. Formülasyonların sitotoksik özellikleri MTT testi ile Caco-2 hücre serileri kullanılarak değerlendirilmiştir. *Ex vivo* permeabilite performansları Caco-2 hücre serileri üzerinde araştırılmış ve ayrıca seçilen formülasyonlar üzerinde *in vivo* farmakokinetik çalışmalar gerçekleştirilmiştir. Çalışmanın kapsamlılığı ve seçilen formülasyonların özgünlüğü araştırmanın asıl değerini oluşturmaktadır. Ayrıca şimdiye kadar hiçbir çalışmada RCa yüklenmiş CDs-polimer yapılı ilaç taşıyıcı sistemlerin *in vitro-in vivo* etkinliklerinin değerlendirilmemiş olması araştırmanın özgünlüğünü artırmaktadır.



**Anahtar Sözcükler:** Rosuvastatin Kalsiyum, Siklodekstrin, Polianhidrit, Katı Lipit Nanopartiküller, Kitosan, Farmakokinetik.

*Dedicated to*
*Almighty Allah*
*then to*
*my loving family*

*This thesis is dedicated to the memory of my life- Adviser, my father NASSER AL-HEBISHY: because I owe it all to you. Thank you for supporting me throughout my life...*

## ACKNOWLEDGEMENTS

My true much gratitude goes to ALLAH all-powerful through whose motivation and celestial course made it possible for me, to finish and accomplished this academic level. I would like to thank my supervisor, **Prof. Dr. MÜZEYYEN DEMİREL** for being very helpful and kind throughout my graduate studies. I appreciate all her support and guidance for my research project. Her knowledge and interest in Pharmaceutical Technology has been a great inspiration to me. She has taught me more than enough and I can't thank her enough for her mentorship. So, I sincerely want to thank you for your hard work and dedication for all the work you do to help me.

I might want to say thanks to my Co-supervisor **Assoc. Prof. Dr. EBRU BAŞARAN** for her kind support amid my graduate reviews. Her recommendation, input and inspiration have been extremely useful at all circumstances. You have dependably been there to guide and support me through this procedure and for that I am very grateful.

I am especially indebted to **Prof. Dr. İMRAN VURAL** and her **Research assistant NAİLE ÖZTÜRK** for their help and support concerning the MTT and permeability tests. My special thanks go to **Assoc. Prof. Dr. RANA ARSLAN and her MSc. Students MERVE KAŞIK** and **KAAN KAYIŞ** for all their helps and discussions during animal's experiments.

It was an extraordinary pleasure working with my lab mate **KADRİ GÜLEÇ**, my graduate experience would not have been the same without his feedback and support. I am extremely thankful for becoming acquainted with him furthermore, have discovered incredible friend like you. My dear friend, without you I would never have had the power to finish my studies.

I am indebted to express my sincere thanks to my sister **WAFA FAROOQ** for her patience, help and insightful comments.

I would also like to thank **Assoc. Prof. Dr. YUSUF ÖZKAY** for allowing me to rotate and work in Doping and Narcotic Laboratory. Further, I would like to thank **Research assistant SERKAN LEVENT** for performing NMR spectra. I would like to thank every member in the Department of **Pharmaceutical Technology** for their understanding and help all through my PhD thesis.

I wanted to take this opportunity to thank Aden University and Turks Abroad and Related Communities (YTB) and all those responsible for the financial support.

I am very grateful to my parents of the considerable number of companions and educators I've had in my life, you both have been the best. My great appreciation goes to my family members for their moral support and advice. Thanks a lot for everything and I cannot forget to express my thanks to my sister **KAMLA HUSSEIN**, who has cheerfully supported me in every circumstance.

Last, but not least, I would like to give special thanks to my wife **WEIAM HUSSEIN** because behind every successful man is a woman. You made me so successful. Thanks for being the best.

26/05/2017

## STATEMENT OF COMPLIANCE WITH ETHICAL PRINCIPLES AND RULES

I hereby truthfully declare that this thesis is an original work prepared by me; that I have behaved in accordance with the scientific ethical principles and rules throughout the stages of preparation, data collection, analysis and presentation of my work; that I have cited the sources of all data and information that could be obtained within the scope of this study, and included these sources in the references section; and that this study has been scanned for plagiarism with scientific plagiarism detection program used by Anadolu University, and that "it does not have any plagiarism" whatsoever. I also declare that, if a case contrary to my declaration is detected in my work at any time, I hereby express my consent to all the ethical and legal consequences that are involved.

Fawaz Nasser Shekh AL-HEIBSHY

## CONTENTS

**Page**

## LIST OF TABLES

## LIST OF FIGURES

## LIST OF ABBREVIATIONS

**AA** : Acetic Acid

**ACN** : Acetonitrile

**AFM** : Atomic Force Microscopy

**AIC** : Akaike Criteria

**API** : Active Pharmaceutical Ingredient

**AsA** : Aspartic Acid

**AUC** : Area Under Curve

**BCS** : Biopharmaceutical Classification System

**Captisol®** : Sulfabutyl Ether Beta-Cyclodextrin

**CAs** : Chitosan Aspartate

**CDs** : Cyclodextrins

**CG** : Chitosan Glutamate

**CHD** : Coronary Heart Disease

**CL** : Chitosan Lactate

**$C_{max}$** : Maximum Plasma Concentration

**$CO_2$** : Carbon Dioxide

**Con.** : Concentration

**Cs** : Chitosan

**CVD** : Cardiovascular Diseases

**CYP3A4** : Cytochromes P3A4

**CYP450** : Cytochromes P450

**DC** : Drug Content

**DL** : Drug Loading

**DLS** : Dynamic Light Scattering

**DMEM** : Dulbecco's Modified Eagle's Medium

**DMSO** : Dimethyl Sulphoxide

**DSC** : Differential Scanning Calorimetry

**DTA** : Differential Thermal Analysis

**DW** : Distilled Water

**EE** : Entrapment Efficacy

**EDTA** : Ethylenediaminetetraacetic Acid

***f1*** : Difference Factor

***f2*** : Similarity Factor

**FBS** : Fetal Bovine Serum

**FTIR** : Fourier Transform Infrared Spectroscopy

**GA** : Glutamic Acid

**GIT** : Gastrointestinal Tract

**GRAS** : Generally Recognized as Safe

**$^{1}$H NMR** : Proton-Nuclear Magnetic Resonance

**HBSS** : Hank's Balanced Salt Solution

**HDL** : High Density Lipoprotein

**HEPES** : 4-(2-Hydroxyethyl)-1-Piperazineethanesulfonic Acid

**HMG-CoA** : 3-hydroxy-3-methyl-glutaryl-coenzyme A

**HPLC** : High-Pressure Liquid Chromatography

**ICH** : International Committee on Harmonisation

**IDL** : Intermediate-Density Lipoprotein

**IS** : Internal Standard

**K** : Kinetic Rate Constant

**KTP** : Ketoprofen

**LD** : Laser Diffraction

**LDL** : Low Density Lipoprotein

**LOD** : The Limit of Detection

**LOQ** : The Limit of Quantitation

**MALDI-TOF** : Matrix-Assisted Laser Desorption/Ionization Time -of- Flight Mass Spectrometer

**MI** : Myocardial Infarction

**MRT** : Mean Residence Time

**MSEAIRC** : Medical and Surgical Experimental Animals Implementation and Research Center

**MTT** : Thiazolyl Blue Tetrazolium Bromide

**MW** : Molecular Weight

**M-β-CDs** : Methyl-Beta-Cyclodextrin

**NMR** : Nuclear Magnetic Resonance

**NPs** : Nanoparticles

**O / W** : Oil in Water Emulsion

**OATP** : Organic Anion Transport Protein

**OATP1B1** : Organic Anion Transporting Polypeptide

**PAD** : Poly (methyl vinyl ether-co-maleic anhydride)

**$P_{Aq}$** : Permeability Coefficient in Aqueous Exterior

**$P_{app}$** : Apparent Permeability Coefficient

**PBS** : Phosphate Buffered Saline

**PCS** : Photon Relationship Spectroscopy

**PDI** : Polydispersity Index

**PMs** : Physical Mixtures

**$P_M$** : Permeability Coefficient

**PS** : Particle Size

**PTC** : Phosphatidylchoine

**$r^2$** : Square Regression

**RCa** : Rosuvastatin Calcium

**RES** : Reticuloendothelial System

**RSD** : Relative Standard Deviation

**Rt** : Retention Time

**SA** : Stearic Acid

**SBE-β-CD** : Sulfobutyl Ether Beta-Cyclodextrin

**SD** : Standard Deviation

**SE** : Standard Error

**SEM** : Scanning Electron Microscopy

**SE(M)** : Standard Error of Mean

**SLNs** : Solid Lipid Nanoparticles

**SNEDDS** : Self-nanoemulsion Drug Delivery System

**$t_{1/2}$** : Half-life

**T80** : Tween 80

**TAS** : Thermodynamic Affinity Structure

**TC** : Total Cholesterol

**TEER** : Transepithelial Electrical Resistance

**TEM** : Transmission Electron Microscopy

**TG** : Triglycerides

**$T_{max}$** : Time of The Maximum Observed Concentration

**TP** : Tripalmitin

**UV** : Ultraviolet Spectroscopy

**UWL** : Unstirred Water Layer

**UPLC** : Ultra-Performance Liquid Chromatography

**USP** : United States Pharmacopeia

**W / O / W** : Water in Oil in Water Emulsion

**W/O** : Water in Oil Emulsion

**WHO** : World Health Organization

**XPS** : X-Ray Photoelectron Spectroscopy

**XRD** : Powder X-Ray Diffraction

**ZP** : Zeta Potential

**α-CDs** : Alpha Cyclodextrin

**β-CDs** : Beta-Cyclodextrins

**γ-CDs** : Gamma Cyclodextrin

# 1. INTRODUCTION

## 1.1. Dyslipidemia

Cardiovascular diseases (CVD) is the primary reason of mortality, furthermore, a standout amongst the most-essential reasons of morbidity around the worldwide. Major contributors are cerebrovascular diseases, such as ischemic stroke, and in addition, myocardial infarction (MI) and coronary heart disease (CHD), all of them place an unbearable load not only on the quality of life of patients, but also on economies and health-care resources (Reiner, 2013, p.453–464).

Dyslipidemia has been decidedly connected to the pathophysiology of coronary disease and it is a key independent modifiable hazard consider for cardiovascular diseases (Nelson, 2014, p.195–211). Dyslipidemia is high and growing in most developed countries, but this growing is not only seen in developed countries, it is now seen in most developing countries because of the irregularities of diet and other lifestyle changes. In 2002, the World Health Organization (WHO) gave an account that Dyslipidemia relates to more than half of the global cause of ischemic heart and cerebrovascular diseases.

The most widely recognized types of Dyslipidemia are:

- High amounts of Low Density Lipoprotein (LDL or terrible) Cholesterol,
- Low levels of High Density Lipoprotein (HDL or great) Cholesterol, and
- High amounts of triglycerides (World Health Organization, 2002, p.1–35).

Fatty deposits in arterial walls are the most serious manifestation of lipid disorders. Cholesterol precipitations and its associated cellular proliferation and fibrous tissue formation produce atheromatous plaques. The lipoproteins, LDL and intermediate-Density Lipoprotein (IDL) are atherogenic in nature. Moreover, plaques narrow the arteries, leading to atherosclerosis, and this is the essential cause of heart attacks, heart disease, peripheral artery disease and may lead to a fatal condition called stroke. Reducing high plasma LDL cholesterol levels lowering the risk of cardiovascular disease. Hypercholesterolemia is one of the leading risks of cardiovascular disease; others include smoking and hypertension (Badimon *et al.*, 2012, p.60–74).

Low levels of HDL and hypertriglyceridemia can also rise fat build-up in the arteries. Raising levels of HDL cholesterol, secures the heart by evacuating the fabricate –up of LDL from the blood vessel walls (Ballantyne, 2000, p.2089–2112).

## 1.2. Statins

Statins were discovered as cholesterol reducing drugs in the 1970s, and are the most widely used around the world as antihyperlipidemic medications (Lyons and Harbinson, 2009, p.362–364). Statins are metabolites of microorganisms (such as mevastatin, lovastatin) or fully synthetic compounds (atorvastatin, fluvastatin, and rosuvastatin). The first described statin, mevastatin, was isolated as a secondary metabolite of a Penicillium citrinum strain (Barrios and Miranda, 2010, p.869–883).

The structures of synthetic statins are dissimilar and are different from the natural statins, except for the 3-hydroxy-3-methylglutaryl-coenzyme A (HMG-CoA)- like moiety, which is responsible for HMG-CoA reductase inhibition which, indirectly results in their cholesterol lowering effects (Manzoni and Rollini, 2002, p.555–564).

Statins cause decrease in (LDL) cholesterol, total cholesterol (TC) and triglycerides (TG) and increase in (HDL) cholesterol. Many clinical trials have demonstrated that statins effectively prevent acute cardiovascular events and decrease mortality in primary and secondary prevention of ischemic heart disease (Pichandi *et al.*, 2011, p.47–56). Independent of their hypolipidemic properties, statins also have potential roles as anti-oxidative, antitumor, anti-inflammatory (Antonopoulos *et al.*, 2012, p.1519–30), antifungal, anti-malarial (Dhiman *et al.*, 2016, p.487–500) and bone forming agents (as both antiresorptive and anabolic) (Jadhav and Jain, 2006, p.3–18).

### 1.2.1. Mechanism of action of statins

Statins perform their major effect – reduction of LDL level – throughout a mevalonic acid – the moiety that competitively inhibits 3-hydroxy-3-methyl-glutaryl-coenzyme A (HMG-CoA) reductase. By blocking the conversion of HMG – CoA to mevalonate, statins inhibit an early and rate – controlling step in cholesterol biosynthesis (Puttananjaiah *et al.*, 2011, p.215–222).

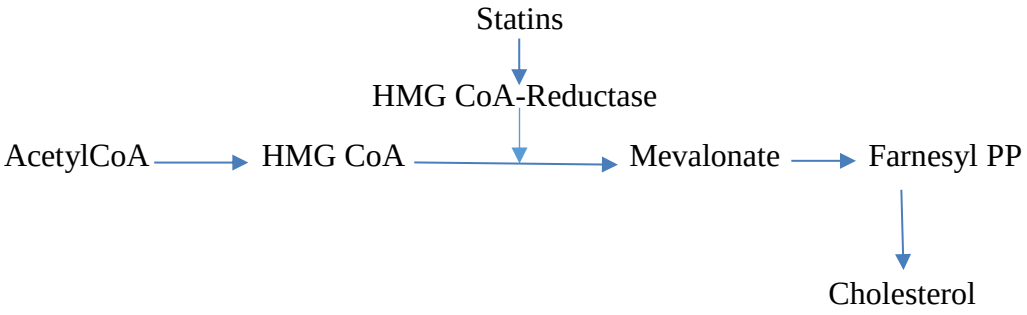

### 1.2.2. Pharmacokinetics of statins

Although all statins share a common mechanism of action, they vary in terms of their chemical structures, pharmacokinetic profiles, and lipid-modifying efficacy. Simvastatin and lovastatin are administered as very lipophilic lactone prodrugs, whereas other statins are given as active acid forms. The chemical structures of statins responsible for their water solubility, which in turn influences their absorption, distribution, metabolism and excretion (Schachter, 2005, p.117–125).

All statins are relatively hepatoselective with respect to inhibition of HMG-CoA reductase. For lipophilic statins, passive diffusion through hepatocyte cell membranes is primarily responsible for effective first pass uptake, while for hydrophilic statins extensive carrier-mediated uptake is the major mechanism. Organic Anion Transporting Polypeptide (OATP1B1) facilitates the hepatic uptake of most statins, but its significance seems to be greatest for hydrophilic statins, such as pravastatin and rosuvastatin (DeGorter *et al.*, 2012, p.1689–97).

While lipophilicity results in effective hepatic shunting, the same property will result in ready passage through nonhepatic cell membranes. This contributes to the fact that hydrophilic statins exhibit greater hepatoselectivity, as well as a reduced potential for uptake by peripheral cells (Unlu *et al.*, 2016, p.340–347).

The currently available statins generally possess a low systemic bioavailability, indicating extensive first-pass extraction (Schachter, 2005, p.117–125). At the pharmacokinetic level, the available statins have important differences, including half-life ($t_{1/2}$), maximum plasma concentration ($C_{max}$), bioavailability, protein binding, lipophilicity, metabolism, existence of active metabolites, and excretion routes (Table 1.1) (Bellosta *et al.*, 2004, p.III-50-III-57).

**Table 1.1.** *Clinical Pharmacokinetics of Statins (HMG - CoA Reductase Inhibitors)*

| Parameter | Atorva-statin | Fluva-statin | Fluva-statin XL | Lova-statin | Prava-statin | Rosuva-statin | Simva-statin |
|---|---|---|---|---|---|---|---|
| **$T_{max}$ (h)** | 2-3 | 0.5-1 | 4 | 2-4 | 0.9-1.6 | 3 | 1.3-2.4 |
| **$C_{max}$ (n. $mL^{-1}$)** | 27-66 | 448 | 55 | 10-20 | 45-55 | 37 | 10-34 |
| **Bioavailability (%)** | 12 | 19-29 | 6 | 5 | 18 | 20 | 5 |
| **Lipophilicity** | Yes | Yes | Yes | Yes | No | No | Yes |
| **Protein binding (%)** | 80-90 | >99 | >99 | >95 | 43-55 | 88 | 94-98 |
| **Metabolism** | CYP3A4 | CYP2C9 | CYP2C9 | CYP3A4 | Sulfation | CYP2C9, 2C19 (minor) | CYP3A4 |
| **Metabolites** | Active | Inactive | Inactive | Active | Inactive | Active (minor) | Active |
| **Transporter protein substrates** | Yes | No | No | Yes | Yes/No | Yes | Yes |
| **$T_{1/2}$ (h)** | 15-30 | 0.5-2.3 | 4.7 | 2.9 | 1.3-2.8 | 20.8 | 2-3 |
| **Urinary excretion (%)** | 2 | 6 | 6 | 10 | 20 | 10 | 13 |
| **Fecal excretion (%)** | 70 | 90 | 90 | 83 | 71 | 90 | 58 |

*Based on a 40-mg oral dose, with the exception of Fluvastatin XL (80mg)*
**Reference***: Bellosta et al., 2004, p.III-50-III-57*

## 1.3. Rosuvastatin Calcium (RCa)

### 1.3.1. Chemistry of RCa

RCa is (3R,5S,6E)–7-[4-(4-fluorophenyl)–6-(1-methylethyl)–2-[methyl (methyl sulfonyl) amino]-5-pyrimidinyl]-3,5-dihydroxy-6-heptenoicacid, calcium salt (2:1). The empirical formula of RCa is $(C_{22}H_{27}FN_3O_6S)_2Ca$, its molecular weight is 1001.14 g. $mol^{-1}$, and its structural formula is presented Figure 1.1.

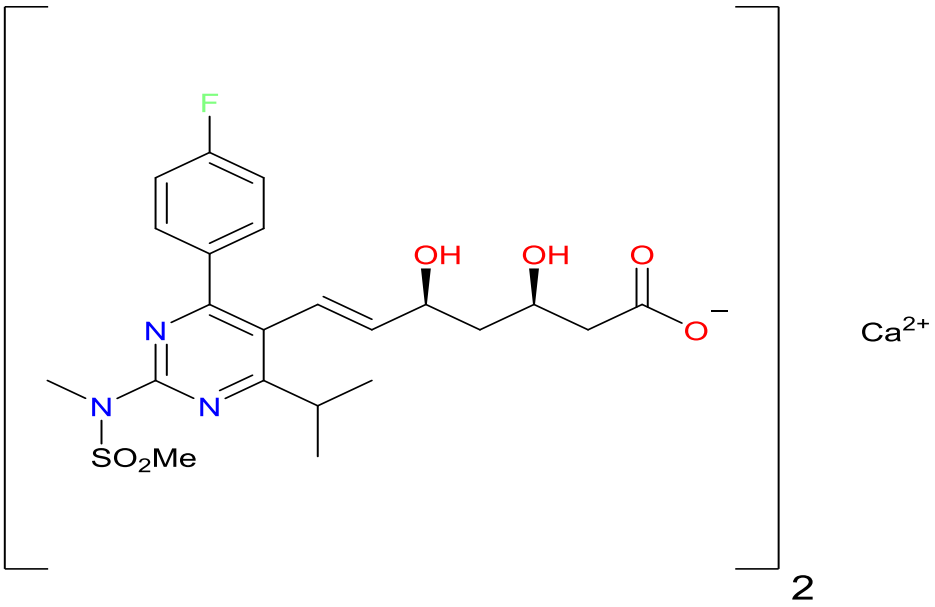


**Figure 1.1.** *Chemical Structure of RCa*
**Reference**: *Remington and Beringer, 2006, p.1368–1369*

### 1.3.2. Description

RCa is a white semi-crystalline powder that is slightly soluble in ethanol and, sparingly soluble in methanol and water. Rosuvastatin compound has hydrophilic property with a partition coefficient (octanol/water) of 0.13 at pH of 7.0. RCa is a salt with pKa of 4.6 (Rivedi and Atel, 2012, p.393–406).

### 1.3.3. Clinical uses

RCa is a synthetic statin. It is a selective and competitive HMG-CoA reductase inhibitor. It is widely used to treat dyslipidemia and to prevent progression of coronary artery diseases. RCa has been reported to reduce serum levels of LDL cholesterol, accompanied by increases in HDL cholesterol and reductions in TG. The dose range for RCa is 5 to 40 mg once daily (McTaggart and Jones, 2008, p.321–338).

Until the approval of rosuvastatin acid in 2003, atorvastatin was the most efficacious drug in the statins class but recent studies reported rosuvastatin acid as a potent inhibitor of HMG-CoA reductase having a more efficient LDL-lowering effects as compared with other statins, which demonstrates that rosuvastatin acid is the leading drug in the statins class (Saku *et al.*, 2011, p.1493–1505).

### 1.3.4. Pharmacokinetics of rosuvastatin

Rosuvastatin is administered orally as a calcium salt of the active hydroxyl acid form. The majority of HMG-CoA reductase inhibitory activity (90%) in plasma is associated with the parent compound. The active moiety, is rapidly absorbed and reaching peak plasma concentration 3 to 5 hours after dosing. Both ($C_{max}$) and area under the curve (AUC) increase in proportion to rosuvastatin acid dose. The absolute bioavailability of RCa is approximately 20% and there is no accumulation on repeated dosing (White, 2002, p.963–970). Mean volume of distribution of RCa is, approximately 134 liters. RCa is 88% bound to plasma proteins reversibly, and independent of plasma concentrations, particularly albumin (Crouse III, 2008, p.287–304).

RCa appears to be actively transported into the liver by an organic anion transport protein (OATP). It undergoes first pass extraction in the liver, and is expected to have less potential for hepatic CYP3A4 drug interactions than other statins. The recovery percentage of radiolabeled dose is approximately 10% as metabolites (Toth and Dayspring, 2011, p.969–986).

Parent rosuvastatin is biotransformed to two metabolites: rosuvastatin-5S lactone (inactive metabolite) and N-desmethyl rosuvastatin (active metabolite) primarily by CYP 2C9, and to a lesser extent, by CYP 2C19, and CYP 3A4 isoenzymes (Figure 1.2). Up to 50% of HMG-CoA reductase inhibitor activity of rosuvastatin has been attributed to N-desmethyl rosuvastatin (Martin *et al.*, 2003, p.2822–2835).

RCa is eliminated primarily unchanged via the fecal route (90%), and approximately 10% of the dose is eliminated renal. Fecal recovery represents unabsorbed drug, metabolites in the bile, and absorbed drug. The elimination ($t_{1/2}$) of RCa is relatively 19 hours (White, 2002, p.963–970).

### 1.3.5. Rosuvastatin interactions

There is also little potential for drug-drug interactions upon co-administration with compounds which are potent inducers or inhibitors of CYP450 since hepatic metabolism is a minor pathway for RCa elimination, which suggests that clinically significant drug interactions via metabolism pathways may be limited. *In vitro* and *in vivo* data indicate that rosuvastatin calcium clearance is not dependent on metabolism by CYP3A4 to a clinically significant extent. This has been confirmed in studies with known CYP3A4 inhibitors (ketoconazole, erythromycin, itraconazole) (Soran and Durrington, 2008, p.2145–2160).

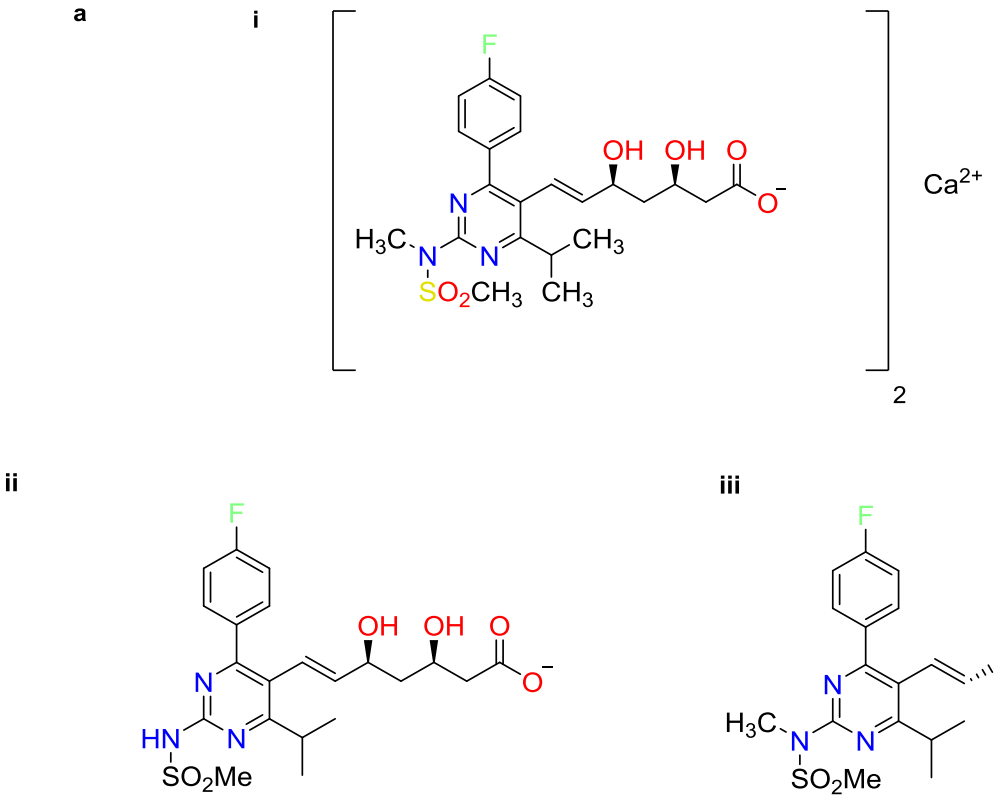


**Figure 1.2**. *Chemical Structure of Radiolabeled Rosuvastatin ([$^{14}$C]-Rosuvastatin), N-Desmethyl Rosuvastatin, and Rosuvastatin-5S-Lactone*
**Reference**: *Martin et al., 2003, p.2822–2835*

Rosuvastatin has minimal drug–drug interactions with many antiretroviral drugs metabolized by CYP3A4. Protease inhibitors such as ritonavir, saquinavir and atazanavir inhibit OATP-1B1, the transporter protein required in the hepatic cell take-up of rosuvastatin. This cause higher serum rosuvastatin concentrations in patients using protease inhibitors. It is recommended that lower doses of rosuvastatin are taken by patients who use protease inhibitors. There are no known drug-drug interactions between rosuvastatin and non-nucleoside reverse transcriptase inhibitors (Kostapanos *et al.*, 2010, p.11–28).

As with other HMG - CoA reductase inhibitors, reports of myopathy with RCa are rare, but higher at the highest marketed dose (40 mg). Cases of rhabdomyolysis have been report in patients on medications which lead to elevation of plasma concentrations of RCa such as gemfibrozil, liponavir and ritonavir (Luvai *et al.*, 2012, p.17–33).

### 1.3.6. Aims of studying new formulations for RCa

Dissolution process is the rate-limiting step for hydrophobic drugs which exhibit irregular and incomplete absorption from the gastrointestinal tract (GIT). Therefore, one

of the main challenges to drug development today is poor solubility, as predestined 40% of all newly developed drugs are poorly or sparingly soluble or insoluble in water.

So, the aims of this study are to improve the bioavailability of RCa by improving the dissolution process, which is the rate-controlling step for the absorption of the drug and consequently, to enhance the efficacy of the drug, to decrease the therapeutic dose and subsequently a reduction in side effects. This will lead to improve patient compliance. Moreover, the reduction of therapeutic dose will lead to reduction in cost which is considered of great importance for both patient and drug manufacturing.

### 1.4. Nanoparticles

Nanoparticles may be defined as particle dispersions or solid particles having sizes in the range of 10-1000 nm. The drug can be solubilized, entrapped, adsorbed, added or encapsulated in the nanoparticle matrix. Depending on the method of preparation, nanoparticles, nanospheres or nanocapsules can be obtained. Nanocapsules are vesicular systems, in which the drug is trapped in a cavity and surrounded by a polymer membrane, while, the nanospheres are matrix systems in which the drug is uniformly dispersed into the nanospheres (Mohanraj *et al.*, 2006, p.561–573). Recently, biodegradable polymeric nanoparticles, particularly long-circulating nanoparticles, which are coated with hydrophilic polymers such as polyethylene glycol, can be targeted to a specific organ through their ability to remain in circulation for a long time, and their ability as potential drug delivery systems to transmit genes (Manmode *et al.*, 2009, p.1020–1027).

The primary goal in designing nanoparticles as drug delivery systems is to control the particle size, surface properties, and release of active pharmaceutical agents so that the drug acts therapeutically at the optimum dose and rate, specifically for the targeted site. Although liposomes are used as potential carriers with their superior advantages such as the ability to protect drugs from degradation, targeting, toxicity or side effects, the applications are limited due to problems such as low encapsulation efficiency, sudden release in the presence of water-soluble drug blood components and low storage stability. In contrast, polymeric nanoparticles have some specific advantages over liposomes (Petros and DeSimone, 2010, p.615–627). For example, they help to increase the stability of the drugs / proteins and have convenient controlled release properties.

Advantages of using nanoparticles as drug delivery systems:

- The particle size and surface properties of nanoparticles can be easily adjusted in both passive and active drug targeting for parenteral administration.
- The extended release of the drug can be controlled during transport and in the circulatory system to improve the drug therapeutic efficacy, pharmacokinetic properties, and to reduce its side effects.
- Controlled release and particle degradation characteristics can be adjusted by selecting the matrix components. Drug loading is relatively high and drugs can be trapped in systems without any chemical reaction, which is an important factor for the protection of drug activity.
- The surfaces of the particles can be targeted to the desired site by adding ligands or using magnetic guidance.
- The system can be used for many routes of administration such as oral, nasal, parenteral, intraocular (Wilczewska *et al.*, 2012, p.1118–1122).

Nanoparticles are of interest in the transport of drugs for various compositions, structures and surface properties. This diversity of nanoparticle compositions and constructions allows the carriers to be tailored for specific applications and targets. Among the targeted drug delivery systems, the most commonly used are liposomes, miscella, dendrimers, nanospheres and nanocapsules. Figure 1.3. (Ageitos *et al.*, 2016, p.1–22) shows the several types of nanoparticles:

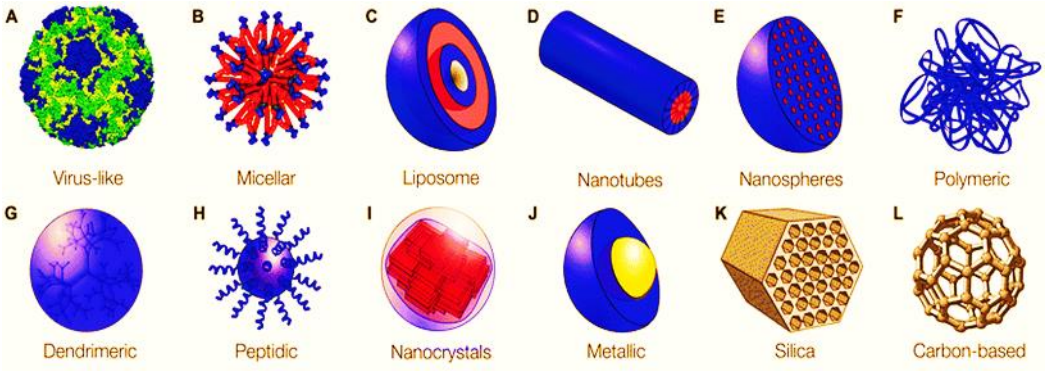


**Figure 1.3.** *Schematic Representation of The Different Types of Nanoparticles*
**Reference:** *Ageitos et al., 2016, p.1–22*

### 1.4.1. Polymeric nanoparticles

Polymeric nanoparticles are matrix systems that are prepared from polymers of natural or synthetic origin, and called nanoparticles or nanocapsules. Their size ranges

from 10 to 1000 nm, and the active substances are solubilized, entrapped and / or adsorbed on their surfaces. The most commonly investigated polymeric nanoparticles as nanoparticulate drug delivery systems are chitosan derivatives, polylactic acid, polyglycolic acid, or copolymers, which are produced from biodegradable and biocompatible polymers such as poly (D, L-lactic-co-glycolic acid) (Bonifácio *et al.*, 2013, p.1–15).

### 1.4.2. Nanoparticle preparation methods

Many methods have been developed to prepare nanoparticles. These methods can be classified into two main categories according to whether the formulation requires polymerization reaction or directly from preformed (macromolecular) polymers (Pinto Reis *et al.*, 2006, p.8–21).

#### 1.4.2.1. *Polymers dispersion*

***Emulsification / solvent evaporation method***

In this method, nanoparticles are prepared by forming a single emulsion oil / water (O / W) or water / oil (W / O) or multiple emulsions water / oil / water (W / O / W) according to drug and polymer solubility. In the case of the single emulsion process, the polymer and the drug dissolve in the same organic solvent. This organic solvent should be a volatile and slightly miscible with water. The emulsifier in the aqueous phase is added to the high volume of organic solvent to form the O / W emulsion. The formation of the nanoparticles is achieved by evaporation or extraction of the organic solvent under mild stirring. In the W / O emulsion, unlike the O / W emulsion, the polymer and the drug are dissolved in the aqueous phase and are added in high volume to the organic phase (Rao and Geckeler, 2011, p.887–913).

In the multiple emulsion method, usually the drug and polymer dissolve in different phases. First, a W / O emulsion is formed in which the water phase and the polymer are in the oil phase. This W / O emulsion is added in high volume to the aqueous phase, thereby forming the W / O / W emulsion. Nanoparticles are obtained by evaporation or extraction of organic solvents (Figure 1.4) (Rao and Geckeler, 2011, p.887–913).

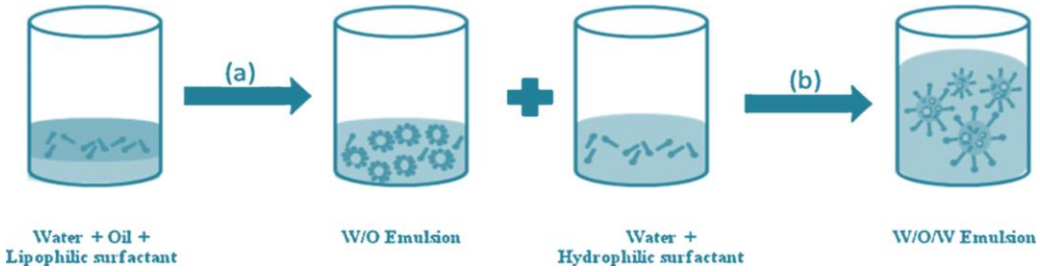


**Figure 1.4.** *Preparation of w/o/w Double Emulsion: (a) High-Shear Emulsification and (b) Low-Shear Emulsification*
**Reference***: Rao and Geckeler, 2011, p.887–913*

***Spontaneous emulsification / solvent diffusion method***

In a modified version of the solvent evaporation method, a water-soluble solvent such as acetone or methanol is used with organic solvent (water-insoluble solvent) such as dichloromethane and chloroform instead of the oil phase. Due to the spontaneous diffusion of the water-soluble solvent (acetone or methanol), inter-surface turbulence between the two phases allows small particles to form. By increasing the concentration of the water-soluble solvent, the particle size can be reduced considerably (Niwa *et al.*, 1993, p.89–98).

***Nano-precipitation method***

The basic principle of this method (also referred to as solvent displacement) is the interfacial accumulation of the polymer after displacement of the water-miscible semi-polar solvent with the lipophilic solvent. Due to the rapid dipping of the non-emulsified solvent, the interface tension decreases and the organic solvent creates small droplets and increases the surface area. In the method, the polymer and the active substance are dissolved in the organic solvent, then the surfactant and the distilled water are mixed at a constant speed, and then the organic solvent is removed by the insufflation method. The aqueous dispersion was lyophilized to prepare nanoparticles (Nagavarma *et al.*, 2012, p.16–23).

***Salting-out method***

In this method, a high amount of the selected salt or sugar is added to the aqueous phase to form a strong satin effect and the emulsion is formulated with the solvent which is completely miscible with the polymer acetone / water. Magnesium chloride, calcium chloride and magnesium acetate are widely used electrolytes. The adverse effect of salt

precipitation by adding water is causing the polymer dissolved in the emulsion droplets to collapse (Rao and Geckeler, 2011, p.887–913).

***Supercritical fluid technology***

The greatest advantage of the supercritical fluid technology, a process used to prepare polymeric nanoparticles is that the precipitated product does not contain solvent. Supercritical fluids are generally defined as liquids that do not change in phase despite the change in pressure over the supercritical temperature. Supercritical carbon dioxide $CO_2$ is the most commonly used supercritical fluid because it is harmless when it is critical (Tc = 31,1 ° C, Pc = 73.8 bar), is not toxic, is not flammable and is cheap. The rapid expansion of the supercritical solution and the supercritical anti-solvent method are the most widely used methods (Girotra *et al.*, 2013, p.22–38).

In the method of rapid expansion of the supercritical solution, the active substance and the polymer are dissolved in the supercritical solvent at high pressure, whereas in the supercritical anti-solvent method, the drug molecules are dissolved in the organic solvent and then released to the supercritical fluid (usually supercritical $CO_2$). The organic phase rapidly dissolves in the supercritical solvent and remains nanoparticles that can be filtered back (Mishra *et al.*, 2010, p.9–24).

***Dialysis method***

Dialysis is a simple and effective method to prepare a nanoparticle with a small and narrow distribution size. The polymer dissolved in the appropriate organic solvent is placed in a dialysis tube having the appropriate molecular size. Due to the solvent displacement throughout the membrane, the solubility decreases, the polymer aggregates and the homogeneous suspension of the nanoparticles is formed (Figure 1.5) (Rao and Geckeler, 2011, p.887–913).

***Spray drying***

Spray drying is usually used for thermodynamically stable substances. In this method, the solution containing the drug and the polymer is sprayed into the hot and dry medium from the liquid state by means of special devices. Thus, solid nanoparticles are obtained (Li and Zhang, 2012, p.295–301).

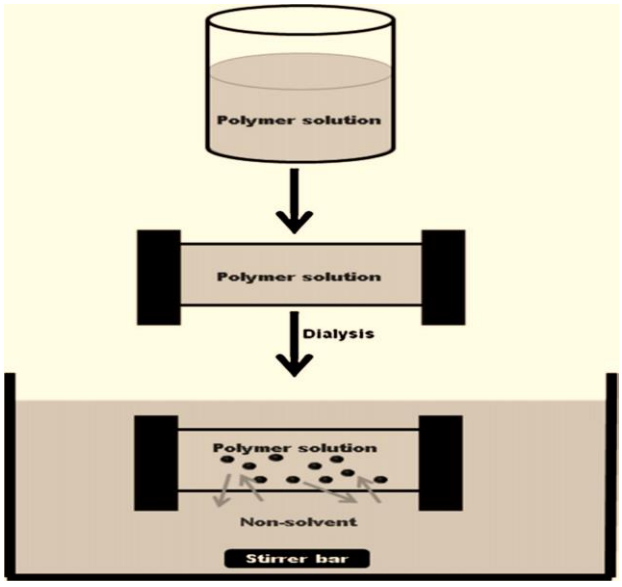


**Figure 1.5.** *Schematic Representation of Dialysis Method for Preparation of Polymer Nanoparticles*
**Reference:** *Rao and Geckeler, 2011, p.887–913*

#### 1.4.2.2. *Polymerization method*

In this method, the monomers are polymerized in an aqueous phase to form nanoparticles. The drug is either adsorbed to the nanoparticles or dissolved in the nanoparticle after dissolution in the polymerization medium or after polymerization. Purification is then carried out using ultracentrifugation to remove the various stabilizers and surfactants used for the polymerization and the particles are resuspended in a surfactant free isotonic environment (Gavandi *et al.*, 2015, p.1–5). This technique has been used to prepare poly(butylcyanoacrylate) or poly(alkylcyanoacrylate) nanoparticles. Nanoparticle formation and particle size depend on the concentration of surfactant and stabilizer used (Mohanraj *et al.*, 2006, p.561–573).

### 1.4.3. Nanoparticle characterization

Nanoparticle characterization parameters involve:

- Surface area and porosity,
- Solubility,
- Resolution,
- Particle size distribution,
- Zeta potential,
- Aggregation,
- Hydrated surface analysis,

- Wettability,
- Adsorption potential,
- Crystallization, and
- Shape and size of interactive surface (Singh, 2016, p.501–531).

Therefore, there are many techniques have been applied to understand the nanoparticle characterization parameters such as:

- Differential Scanning Calorimetry (DSC),
- Dynamic light scattering (DLS),
- Matrix-assisted laser desorption/ionization time-of-flight mass spectrometry (MALDI-TOF),
- Electron microscopy including (TEM) and (SEM),
- Atomic force microscopy (AFM),
- X-ray photoelectron spectroscopy (XPS),
- Powder X-ray diffraction (XRD),
- Fourier transform infrared spectroscopy (FTIR),
- Ultraviolet visible spectroscopy, and
- Nuclear magnetic resonance (NMR) (Singh, 2016, p.501–531).

### 1.4.4. Release of active substance from nanoparticles

Release from nanoparticles is due to particle breakdown, leakage, matrix erosion and diffusion mechanisms depending on the solubility of the drug. The drug is released by polymer degradation from nanoparticles prepared with biodegradable polymers. Degradation rates are based on alkyl chain length. Degradation from the polymer surface can be chemical or enzymatic. If the drug diffusion is faster than the matrix erosion, the release is controlled by the diffusion mechanism. Since the diffusion distance is very short due to particle size, the systems that released by this mechanism are controlled and do not released continuously (Zhang *et al.*, 2003, p.2040–2056).

Poor binding of the drug to the nanoparticles or weak adsorption to the large surface of the nanoparticles causes a burst effect. The immediate release rate can be reduced by charging the drug nanoparticles, thereby extending the release properties. If the nanoparticle is surrounded by a polymer, the release rate is determined by diffusion through the polymeric membrane. In addition, the release rate can be altered by the ionic

interaction between the drug and the adjuvants added. If the drug and excipient form a poorly soluble complex in water, the drug release rate may be reduced and no immediate release effect is observed (Kamaly *et al.*, 2016, p.2602–2663).

### 1.4.5. Stability

Stability is one of the principal factors in evaluating the safety and effectiveness of drug products. Stability problems of drug nanoparticles may occur during production, storage and transportation. For example, high pressure or temperature produced during production can cause crystallinity change to drug particles. Storage and transport of drug products can also cause a variety of stability problems, such as precipitation, agglomeration and crystal growth. For this reason, stability problems associated with drug nanocrystals deserve specific attention in developing pharmaceutical products. There are many techniques used to predict stability of drug nanoparticle and provide suggestions for improving storage and transport conditions. Stability problems with nanoparticle dry powders are often minor (Cui *et al.*, 2015, p.1–15).

Colloidal particles have Brownian motion in dispersion media. This motion is a result of bombardment properties of particles in the dispersion medium. The degree of the motion depends on the viscosity, temperature and molecular size of the dispersion medium. As the particle size decreases, the speed of motion increases, while the viscosity decreases. This motion prevents precipitation and creaming of the nanoparticle dispersion and provide long-term stability (Yu and Xie, 2012, p.228–240).

### 1.4.6. Application areas of nanoparticles

- Anticarcinogenic drugs,
- Anti-inflammatory drugs,
- Anti-parasitic drugs,
- Brain targeting,
- Transdermal application,
- Ocular application,
- Peptide and protein transport,
- Vaccinations,
- Diagnostic items: display of lungs, liver, spleen and bone marrow, and
- Non-medical applications: in disinfection (Mohanraj *et al.*, 2006, p.561–573).

## 1.5. Chitosan Nanoparticles

Chitosan is the N-deacetylated derivative of chitin. Chitin is the second most natural biopolymer in the world after cellulose. Chitosan is a polymer similar to cellulose. Both come from linear β- (1-4) -conjugated monosaccharides. However, the crucial difference of chitosan relative to cellulose is the 2-amino-2-deoxy- [beta] -D-glucan structure linked by the glycoside bonds of chitosan. Chemically they are a polymer consisting of repeating units of β (1- 4) 2-acetamido-2-deoxy-D-glucose ın case of chıtosan or (N-acetylglucosamine) in case of chitin (Figure 1.6.) (Eijsink *et al.*, 2010, p.331–366).

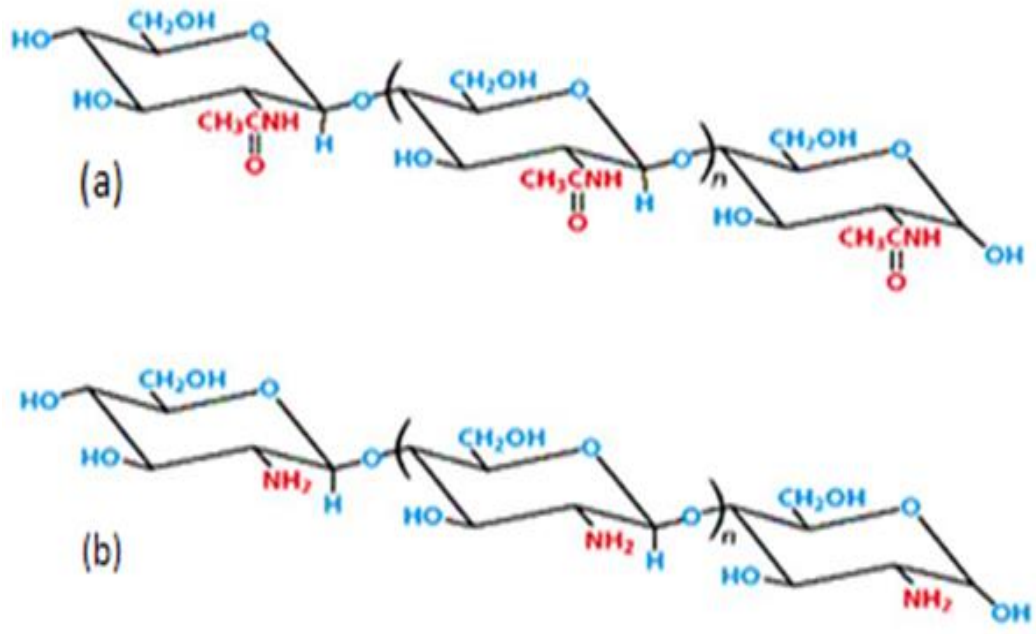


**Figure 1.6.** *Chemical Structure of (a) Chitin and (b) Chitosan*

The commercial chitin and chitosan have high nitrogen percentage (6.89%) in compared with synthetic cellulose (1.25%). This high nitrogen ratio makes them useful chelating agents. Most of the polymers used today are synthetic materials. However, their biocompatibility and biodegradability are rather limited compared to natural polymers such as cellulose, chitin, chitosan. These natural polymers also have limited reactivity and processability. In this regard, chitin and chitosan are recommended as suitable functional materials. Furthermore, these natural polymers have excellent properties such as biocompatibility, biodegradability, non-toxicity, adsorption (Gupta and Kumar, 2000, p.273–308).

Chitosan is widely used in many areas because of its properties such as biocompatibility, antibacterial, antifungal and antitumoral effect, hemostatic, heavy metal, protein and fat absorption, biodegradability (Younes and Rinaudo, 2015, p.1133–1174). The primary uses of chitosan and chitin are, controlled drug release, biosensor applications, cell culture, food and water treatment systems. Many natural polysaccharides such as cellulose, dextran, pectin, alginic acid, agar, agarose and carrageenan are neutral or acidic. Only chitin and chitosan are extremely basic polysaccharides. At neutral or basic pH, the chitosan contains free amino groups and is insoluble in water. At acidic pH, however, the chitosan is water soluble due to the protonation of amino functions, the solubility depends on the distribution of free amino and N-acetyl groups. Chitosan is a linear electrolyte at acidic pH. Thus, chitosan is soluble in dilute acids such as acetic acid, formic acid (Ahmed and Ikram, 2016, p.27–37). The nitrogen content of the chitin varies between 5% and 8% depending on the deacetylation level. Naturally, not all units of the chitin are fully acetylated; About 16% are deacetylated. The nitrogen in the chitin is also mostly present in the form of primary aliphatic amino groups. Therefore, they are exposed to typical reactions of chitosan amines; The most important being the N-acetylation and Schiff reaction (Yuan *et al.*, 2011, p.1399–1416).

Although there are many studies have investigated the use of chitosan in drug delivery systems, but it is also known that chitosan has some disadvantages for its use in this field. These disadvantages are that the dissolution of chitosan in common organic solvents, except dilute acetic acid, has low mechanical properties and also that physical properties are highly dependent on pH. For this reason, when chitosan is used as a drug carrier, it is difficult to control the drug release behavior under different pH values, which are determined by the internal organs of the human body, especially in oral administration. Consequently, it is possible that the excessive release of the drug causes side effects on the human body. On the other hand, modification of chitosan by mixing with other polymers is a convenient and effective method for the development of physical properties in practical use (Elgadir *et al.*, 2015, p.619–629).

### 1.6. Solid Lipid Nanoparticles

Solid lipid nanoparticles (SLNs) introduced in 1991 represent as an alternative system to the existing traditional carriers (emulsions, liposomes and polymeric nanoparticles). They are a new generation of nano-sized lipid emulsions (nano-emulsion)

where the oil phase has been substituted by a solid lipid (Figure 1.7). SLNs exhibit unique characteristics such as small size, large surface area and the interaction of phases at the interfaces, and are appealing for their capability to enhance the execution of pharmaceuticals, neutraceuticals and different materials (Reddy and Shariff, 2013, p.161–171).

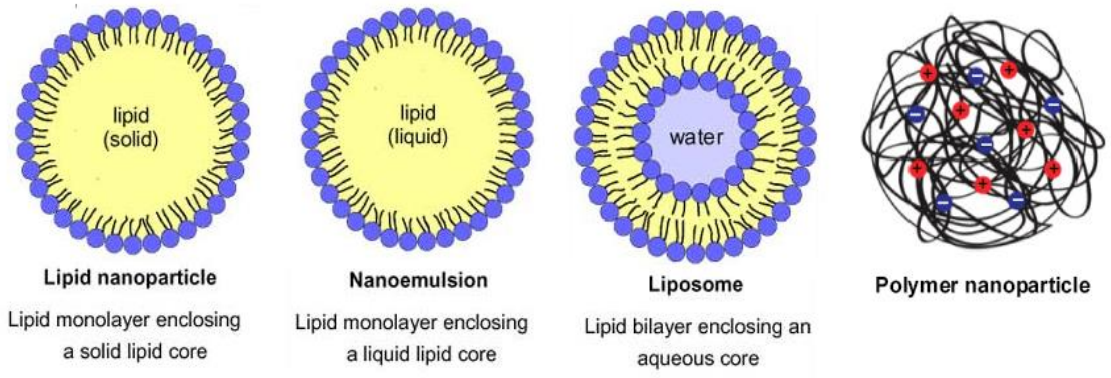


**Figure 1.7.** *Structure of Solid Lipid Nanoparticle (SLNs), Nano-emulsion, Liposome and Polymer Nanoparticle*
**Reference:** *Hoell et al., 2010, p.331–366*

Recently, SLNs are giving major attention as novel colloidal drug carrier for intravenous applications. The SLNs are nanosuspension or colloidal carrier which is composed of physiological lipid, dispersed in water or in an aqueous surfactant solution (Ekambaram *et al.*, 2012, p.80–102). The end goal to beat the disadvantages associated with the liquid state of the oil droplets, the liquid lipid was substituted by a solid lipid, which lately transformed into SLNs. The causes for the increasing concern in lipid based system are numerous factors include.

- Lipids improve oral bioavailability and correct plasma profile variability,
- Better compatibility of lipoid excipients,
- And an enhanced ability to treat the key issues of technology transfer and manufacture scale-up (Hanumanaik *et al.*, 2013, p.928–940).

In conventional o/w emulsion protection of drug against chemical degradation is required. Hence, Incorporation of drug in the solid lipid matrix surely offer a better protection. Moreover, sustained release of drug from emulsion is not practical which can be achieved to a certain degree from SLNs (Table 1.2.). Further, SLNs tend to have lower cost of excipients, lower cytotoxicity than polymeric nanoparticles due to the absence of solvents, and large-scale production is possible by the simple process of high-pressure homogenization. In comparison with liposomes SLNs exhibit better protection to active

ingredient against chemical degradation. However, there are definite limitations associated with SLNs, like low drug loading capacity and drug leakage during storage (Sailaja *et al.*, 2012, p.508–510).

**Table 1.2.** *Comparative Properties of Solid Lipid Nanoparticles, Nano-Emulsions, Liposomes, and Polymeric Nanoparticles*

| Property | SLNs | Nano-emulsion | Liposome | Polymer Nanoparticles |
|---|---|---|---|---|
| **Systemic toxicity** | Low | Low | Low | > or = to SLNs |
| **Cytotoxicity** | Low | Low | Low | > = to SLNs |
| **Residues from organic solvent** | No | No | May or may not | Yes |
| **Large scale production** | Yes | Yes | Yes | No |
| **Conventional sterilization** | Yes | Yes | No | No |
| **Control release** | Yes | No | < or = to SLNs | Yes |
| **RES avoidance** | Depend on size and coating | Yes | Yes | No |

**Reference:** *Ramteke and Dhole, 2012, p.2250–3013*

Advantages of SLNs

- Enhance possibility of drug release and improve drug targeting,
- Solid lipids are biodegradable physiological lipids, which enhance the compatibility, reduce the risk of acute and chronic toxicity and avoidance using of organic solvents in manufacturing method,
- Improve very high long-term stability of pharmaceuticals compared to other Nano-systems,
- Enhanced bioavailability of poor water-soluble compounds,
- Improve the bioavailability of entrapped bioactive molecules and chemical protection of labile incorporated compounds,
- Much easier to manufacture than emulsion and biopolymeric nanoparticles,
- probabilities of loading both lipophilic and hydrophilic compounds,
- Convenient to scale up and sterilize,
- Can be undergo to commercial sterilization methods (Ekambaram *et al.*, 2012, p.80–102).

Disadvantages of SLNs

- Possibility of increasing particle size,
- Unpredictable gelation propensity,
- Drug loading capacity is low,
- Drug leakage due to the possibility of polymeric transition,
- High possibility of infection before drying due to high water content of the dispersions (70-99.9%) (Surender and Deepika, 2016, p.102–114).

Purposes of SLNs preparation

- To improve bioavailability of drug,
- To enhance controlled drug release,
- Increased drug stability,
- Avoidance bio-toxicity of the carrier, and organic solvents,
- Incorporation of poor water-soluble drug.

### 1.6.1. Methods of SLNs preparation

***High shear homogenization***

High shear homogenization is a reliable and suitable method for the preparation of SLNs, and can be performed at elevated temperature (hot high shear homogenization technique) or at below room temperature (cold high shear homogenization technique) (Figure 1.8.). SLNs made from solid lipids or lipid blends produced by high share homogenization of melted lipids disperse in an aqueous as outer phase stabilized by surfactant as Tween 80, sodium dodecyl sulphate, lecithin etc. (Reddy and Shariff, 2013, p.161–171).

- High pressure homogenization pushes a liquid with high pressure (100-2000 bar) through a narrow gap,
- The fluid accelerates on a very short distance to very high velocity (over 100 km/ hr.),
- Very high shear stress and cavitation forces degrade the particles down to the nano-size,
- Generally, 5-10% lipid content is used but up to 40% lipid content has also been investigated (Ekambaram *et al.*, 2012, p.80–102).

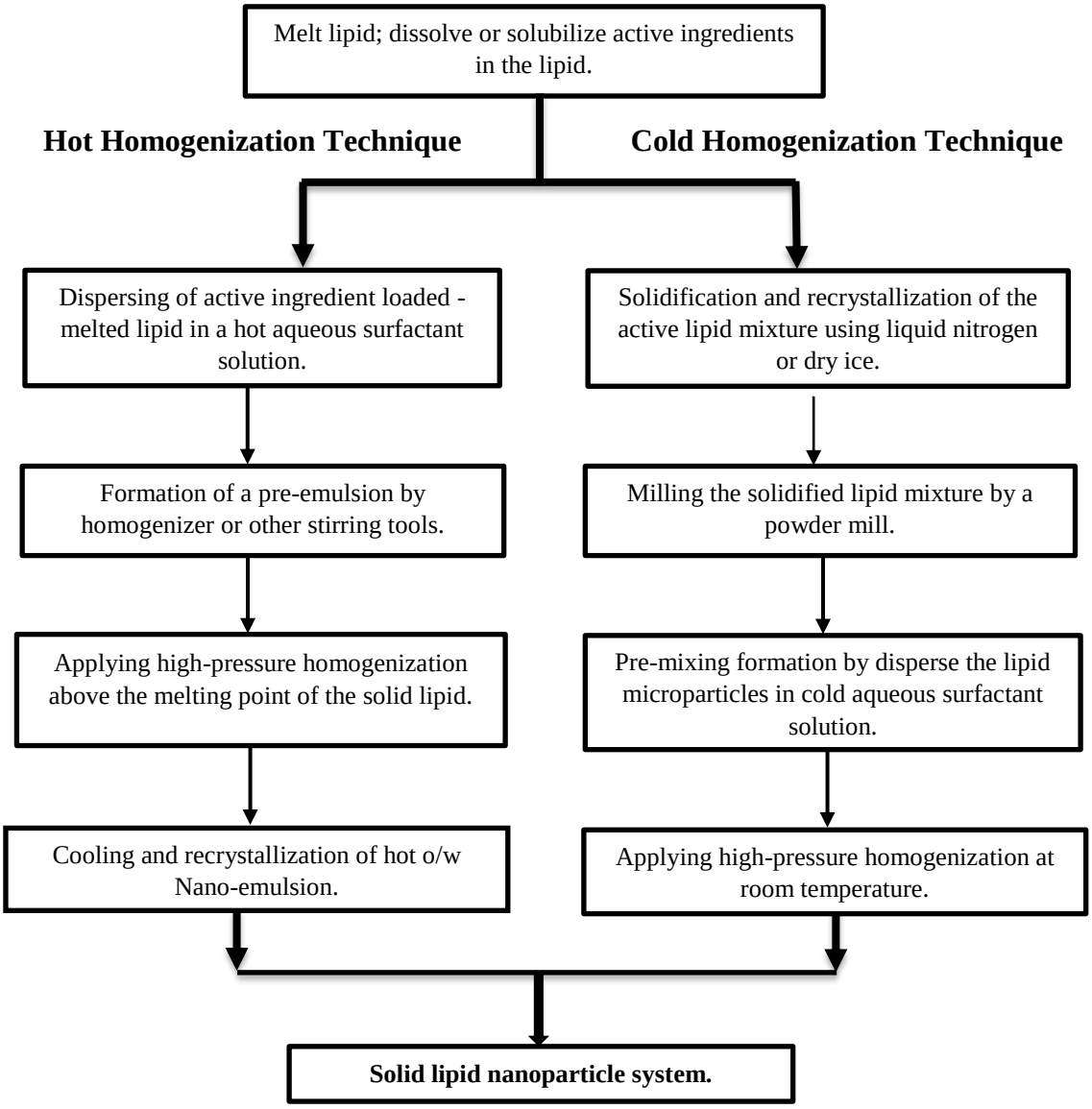


**Figure 1.8.** *Schematic Procedure of Hot and Cold Homogenization Techniques for SLNs Production*

**Reference:** *Surender and Deepika, 2016, p.102–114*

***Ultrasonication or high-speed homogenization***

SLNs were also made by quick blending or sonication. A most usefulness point is that, equipment whatever usage here are to a great degree common in every lab. The problem of this method is the particle dispensing index ranging into micrometer range. This leads to physical instabilities likes particle growth during storage. Furthermore, the possibility of mental contamination represents a big disadvantage of ultrasonication method. So, for preparing a stable formulation, studies have been carried out by many research groups that very high speed stirring and ultrasonication are used combined and carried out at high temperature (Sailaja *et al.*, 2012, p.508–510).

***SLNs prepared by solvent emulsification/evaporation***

In preparation of solid nanoparticle dispersions by precipitation in o/w emulsions, the dissolved solid lipid substance in water-immiscible organic solvent (e.g. cyclohexane), is emulsified in an aqueous phase. Then, the organic solvent is evaporated to make the nanoparticle dispersion by precipitation of the lipid in the aqueous medium. The average diameter of the formed particles is ranging in submicron size (Ramteke *et al.*, 2012, p.2250–3013).

***Microemulsion based SLNs preparations***

This technique depends on the dilution of microemulsions. Like microemulsions are two phase systems composed of an inner and outer phase (e.g. o/w microemulsions). They are prepared by stirring an optically transparent solution at 65-70 °C, which contains low melting fatty acid (e.g. palmitic acid), an emulsifier (e.g. Tween 80), co-emulsifiers (e.g. Polysorbate 60) and water. The hot microemulsifying droplets is solidifying in cold water (2-3 °C) under stirring. SLNs dispersion can be dried by spray dryer or lyophilization to form solid granules which are transformed in to solid product (tablets, pellets) by granulation process. Wide-temperature gradients enhance prompt lipid crystallization and inhibit aggregation. Because of the dilution step; accomplishable lipid contents are extremely lower contrasted with the high shear homogenization based formulations (Mahajan *et al.*, 2015, p.3698–3712).

***SLNs preparation by using supercritical fluid***

This is a generally new method for SLNs formulation and has the feature of solvent-less consuming. There are some variances in this stage technology for powder and nanoparticle production. The fast expansibility of supercritical carbon dioxide at (99.99%) percentage is one SLNs preparation methods (Kumar and Karimulla, 2012, p.35–55).

***Double emulsion method***

Solvent emulsification-evaporation technique has been represented a new method for preparation of hydrophilic loaded SLNs. However, in double emulsion method the active ingredient is encapsulated with a stabilizer to block drug leakage to outer aqueous phase during solvent evaporation from the outer water phase of w/o/w double emulsion (Yadav *et al.*, 2014, p.1152–1162).

***Precipitation technique***

Precipitation technique is one of SLNs preparation methods which characterized by consuming a lot of solvents. The solid lipid (e.g. triglycerides) is dissolved in an organic solvent (e.g. chloroform) and the dispersion is formed by emulsifying lipid solution in an aqueous phase. After that, the lipid is precipitated forming Nanoparticles by evaporation of the organic solvent (Mukherjee *et al.*, 2009, p.349–358).

***Film ultrasound dispersion***

The solid lipid and the drug are put into convenient organic solvent, after that, the solution is subjected to decompression, rotation and evaporation of the organic solvent, a lipid film is created, then the hydrophilic solution which contains the emulsions is added. Utilizing the ultrasound with the test to diffuser finally, the SLNs with the little and uniform molecule size is created (Gupta *et al.*, 2016, p.351–367).

***Solvent injection technique***

This technique is known as solvent displacement or solvent injection method in which the solid lipid and active ingredient are mixed together in a hydrophilic organic solvent (e.g. acetone, ethanol) and this dispersion are injected by a syringe needle to water under stirring: solid lipid precipitates will be formed when they will be in contact with water. Lipid type, surface active agent and solvent can affect the SLNs particle size and degree of dispersion viscosity (Schubert and Müller-Goymann, 2003, p.125–131) (Figure 1.9.).

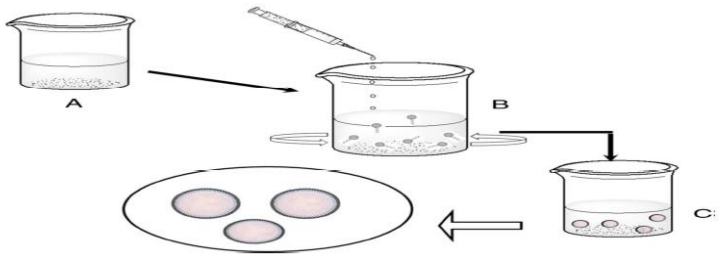


**Figure 1.9.** *Preparation of SLNs by Solvent Injection Technique*
**Reference:** *Surender and Deepika, 2016, p.102–114*

***Membrane contractor method***

Recently, a new technique has been used for preparation of SLNs by squeezing the lipid phase at temperatures above the fusing point and through a membrane of nano size pores to allow the formation of tiny droplets. While, at the same time the aqueous phase

diffuses inside the membrane compartment and sweeps away the formed droplets at the pores outlet. Subsequently, the SLNs are created by cooling the solution at room temperature. There are few parameters affecting this process; Membrane pore size, pressure applied to lipid phase, the viscosity of the aqueous phase, and lipid phase and aqueous phase temperature (Charcosset *et al.*, 2005, p.112–120) (Figure 1.10).

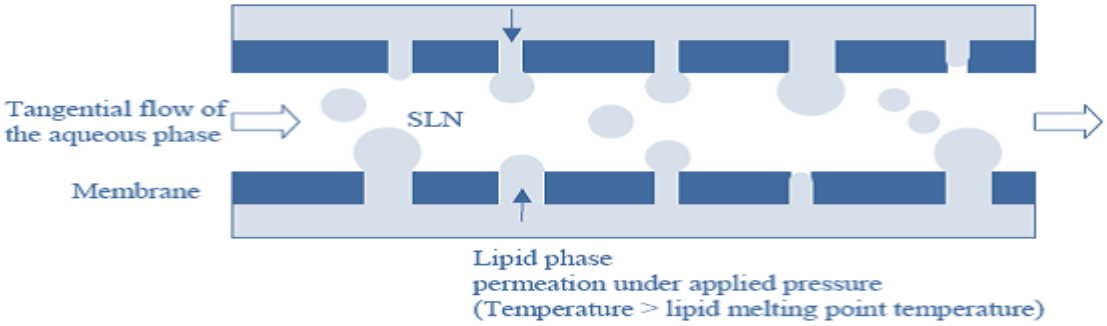


**Figure 1.10.** *A Schematic Diagram of Membrane Contractor for Technique of SLNs*
**Reference:** *Charcosset et al., 2005, p.112–120*

### 1.6.2. Characterization tests of SLNs

Qualification of SLNs product is required by applying adequate characterization methods which should be susceptible to the of SLN performance key parameters. However, SLNs characterization is a serious challenge due to their sub-micron size and the complication of the system, which has also dynamic property. The significant parameters that characterize the SLNs involve particle size, polydispersity index, zeta potential, *in-vitro* drug release, SLNs surface morphology, entrapment efficacy, drug content, degree of polymorphism, and co-existence of another dispersion system (e.g. liposome) (Urbán-Morlán *et al.*, 2010, p.611–620).

***Particle size and zeta potential***

The physical soundness of SLNs relies on upon their particle size. Photon relationship spectroscopy (PCS) and laser diffraction (LD) are the most intense technique for measuring of particle size. PCS (otherwise called dynamic light dispersing) measure the change of the power of the scattered light, which is brought on by nanoparticles motion. The SLNs size measurement by PCS determines the size limit of 3 nm to 3µm and by LD in size scope of 100 nm to 180 µm. Even though PCS is a decent apparatus to study nanoparticles, however, is fit for the location of bigger microparticles. The LD technique depends on the reliance of the diffraction angle on the SLNs size (Fraunhofer

spectra). Smaller particles cause more extraordinary diffusing at high edges contrasted with the bigger ones (Soni *et al.*, 2015, p.1–18).

Another characterization technique, acoustic spectroscopy, estimates the alleviation of sound waves as a tool of measuring size through the fitting of physically related equations. Furthermore, the oscillating electric field developed due to the motion of the charged particles under the impact of acoustic energy, provides information on the charged surfaces (Pardeshi *et al.*, 2012, p.433–72).

Zeta potential estimation can be completed utilizing zeta potential analyzer or zeta meter. Before estimation, SLNs preparations are diluted 50 time with the first colloidal medium for size measuring and zeta potential estimation. The elevated value of zeta potential may prompt to degradation of particles without the other holding agent, for example, steric stabilizers or hydrophilic surface members. Zeta potential evaluations allow expectation about the storage stability of colloidal dispersion systems (Luo *et al.*, 2006, p.53–59).

***Surface morphology***

Physical properties like general shape and morphology of SLNs are estimated by using either transmission electron microscopy (TEM) or scanning electron microscopy (SEM). They allow the emphasis of particle size and distributions. SEM applies electrons transmitted from the surface of the particle while TEM applies electrons transmitted through the example. TEM has a minimal particle size limit of detection (Gaba *et al.*, 2015, p.147–159).

AFM is a sophisticated microscopic technique which is used as a new device to designate the main unchanged form and surface characteristics of the particles. AFM measures the strength acting between the surface of the sample and the head of the probe, when the probe remains stable in closeness to the sample which results in a locative resolution of up to 0.01 mm for imaging (Peixoto *et al.*, 2005, p.52–55).

***Differential scanning calorimetry (DSC)***

The determination of the crystallinity degree of the colloidal particles is carried out by using DSC. DSC measures the rate of crystalline indirectly by comparing the melting enthalpy energy of the standard material with the melting enthalpy energy of the dispersion medium (Bunjes and Unruh, 2007, p.379–402).

***Nuclear magnetic resonance spectroscopy (NMR)***

NMR is used to qualitatively measures the nature of Nanoparticles. The selectivity managed by chemical rotation enhances the sensitivity to molecular versatility to give information on the physicochemical properties of components included in the Nanoparticles (Pardeshi *et al.*, 2012, p.433–72).

***X-ray diffraction (powder X-ray diffraction)***

X-ray powder diffraction technique can be used to measure the degree of crystallinity of solid nanoparticles by analyzing the geometric scattering of radiation that reflected from the crystal surfaces of that nanoparticles (Ingham, 2015, p.1–75).

***Determination of drug content***

Determination the incorporated amount of drug in SLNs is very important due to its impact on the release characteristics. The free drug and SLN separate from the dispersion medium by using centrifugation, filtration, ultracentrifugation, or gel permeation chromatography to determine the quantity of drug encapsulated in each unit of weight. The active ingredient can be analyzed by a basic analytical approach such as HPLC, UPLC, a spectrophotometry, a spectro-fluorophotometer, or liquid scintillation counting (Basu *et al.*, 2010, p.84–92).

### 1.6.3. *In vitro* drug release

*In vitro* drug release can be carried out by:

- Dialysis tubing,
- Reverse dialysis, or
- Franz diffusion cell.

***Dialysis tubing***

*In vitro* drug release could be carried out using dialysis tubing. The SLNs preparation is put in a rinsed dialysis tubing which should be well sealed. The dialysis bag is then dialyzed versus a suitable dissolution medium, either simulated gastric fluid or simulated intestinal fluid at body temperature; the samples are collected from the medium at definite time and analyzed for drug content using a proper analytical method (HPLC, UPLC, or UV spectroscopy, etc.). The applying of sink condition is mandatory (Pragati *et al.*, 2014, p.187–237).

***Reverse dialysis***

The direction of active ingredient released in reverse dialysis is opposite to dialysis tubing in which many small dialysis bags, including (1 mL) of dissolution medium are put in SLNs preparation, then the SLNs are diffused into the dialysis bags. A fast release couldn't be quantified by applying this technique (Basu *et al.*, 2010, p.84–92).

***Franz diffusion cell***

Under maintenance of sink condition, the SLNs medium pass across a cellophane membrane which is fitted in a Franz diffusion cell (the donor) into the suitable dissolution medium at body temperature. After that, the analysis of the withdrawn samples from dissolution medium at definite interval times is carried out to measure the drug content utilizing common analytical methods (Pragati *et al.*, 2009, p.509–516).

### 1.6.4. Permeability test with *ex vivo* model

Animal's tissue is clean, rinsed and cut into small pieces. Each piece is fitted to a cell of two chambers of an exposed tissue area of 1 $cm^2$ and the SLNs dispersion is placed in mucosal side, the samples are withdrawn at definite intervals for analyzing the drug content (Reddy and Shariff, 2013, p.161–171).

### 1.6.5. Storage stability of SLN

The physicochemical characteristics of SLN's during long term storage can be studied by observing the changes in particle size (PS), zeta potential (ZP), polydispersity index (PDI), drug content, and organoleptic properties (Surender and Deepika, 2016, p.102–114).

The different conditions of storage are

- At 4°C which is most appropriate storage temperature.
- At 20°C, long period storage should not be lead to decrease in drug content or aggregation in SLNs dispersion.
- At 50°C a quick development of particle size may be detected (Surender and Deepika, 2016, p.102–114).

### 1.6.6. Applications of SLNs

SLNs have a superior stability and facility for developing to large production scale in compared with other colloidal drug delivery systems (e.g. liposomes). Furthermore, SLNs have good biological behavior and biodegradable properties reinforce targeted drug

delivery and drug protection against biological environment (e.g. reticuloendothelial system (RES)) (Mudshinge *et al.*, 2011, p.129–141). There are many efficient applications of SLNs like:

- Encapsulating of cancer chemotherapeutics,
- Delivery system for peptides and proteins,
- Targeted brain drug delivery system, and
- Drug delivery of some antiparasites and antivirals etc.

SLNs can be administered by oral, parenteral, ocular, rectal, respiratory, and topical with clear efficacy (Üner and Yener, 2007, p.289–300).

### 1.6.7. Toxicity of SLNs

SLNs are prepared from lipids (e.g. phospholipids, triglyceride, fatty acids and waxes), surfactants (Poloxamer 188, Tween 80 etc.) and water. However, many of lipids classified as harmless due to their biological activity or being part of cytomembrane and degraded by lipases, the cytotoxicity of SLNs can be occur due to a nonionic property of emulsifying agents and preservative compounds (Schubert and Müller-Goymann, 2003, p.125-131).

Schubert and Müller-Goymann, improved that lipid concentration up to 2.5% do not exhibit cytotoxicity. Moreover, the lipids concentration up to 10% have been produced in 80% of viable human cell in culture. The MTT assay was carried out by Caco-2 model which simulates the intestinal wall cells and is usually applied to estimate the permeability of oral administered drugs (Schubert and Müller-Goymann, 2003, p.125-131). Other studies have established that SLNs exhibit good biocompatibility which make them attractive drug delivery system (Severino *et al.*, 2012, p.1–10).

## 1.7. Cyclodextrins (CDs)

### 1.7.1. Natural CDs and their physicochemical properties

Cyclodextrins (CDs) are cyclic oligosaccharides as a class of carbohydrates, accidentally discovered by the French scientist A. Villiers in 1891 and they were named "cellulosine". Later, the Austrian microbiologist Franz Schardinger identified α-dextrin and β-dextrin crystal compounds which were isolated from potato starch. Pringsheim in Germany during the 25 years (1911-1935) was the main researcher in this field, proved the ability of CDs to form stable and freely soluble complexes with a variety of chemical compounds (Das *et al.*, 2013, p.1694–1720) CDs are molecules that are chemically

formed by the enzymatic transformation of starch. CDs are cyclic glucose oligomers linked by 1,4-α-glucosidic bonds with the lipophilic internal cavity and hydrophilic outer surface and with six, seven or eight glucose units called alpha (α), beta (β) and gamma (γ), respectively. Due to their special configurations, CDs can form inclusion complexes with many lipophilic molecules. Nine glucose units of CD are called δ-CDs but have poor ability to form complex with other chemicals (Alves-Prado *et al.*, 2008, p.3–13). The α-CD, β-CD and γ-CD structures are shown in Figure 1.11. (Jin, 2010, p. 5).

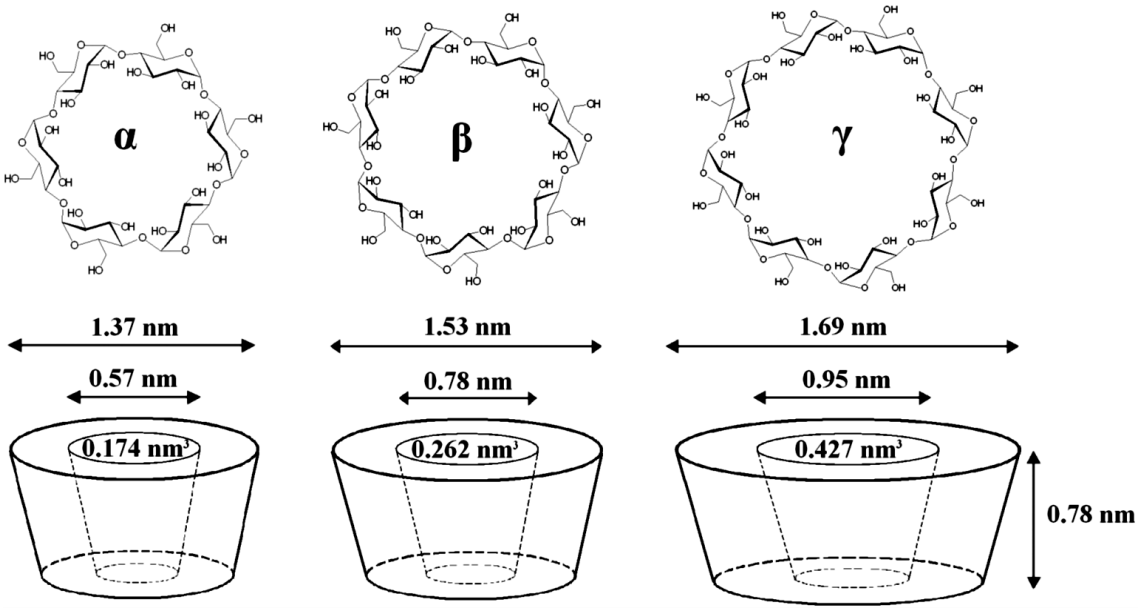


**Figure 1.11.** *Structures, Approximate Geometric Dimensions and Approximate Cavity Volumes of α-, β- and γ-CD*
**Reference:** *Jin, 2010, p. 8*

The hydrophobic cavities of CDs (host) are suitable for both polar and non-polar (guest) molecules or polymers to form stable complexes. When the host molecule forms an inclusion complex with the guest molecules, the stability of the guest molecule is increased by the strong bonds between them (van der waals, hydrogen, hydrophobic etc.) (Khan and Durakshan, 2013, p. 858–865).

CDs inclusion complexes of poorly soluble drug molecules are positively affecting the physicochemical properties of the drugs such as solubility, dissolution rate, bioavailability, stability and biocompatibility. CDs inclusion complexes have been used to improve the stability of liquid substances when they are prepared in powder form by protect them against microorganism's infection and bad storage conditions. Recently,

CDs have also been used as nanostructuring functional components that respond to biological stimuli to achieve the desired drug release behavior and to increase the therapeutic efficacy of drugs (Salústio *et al.*, 2011, p.1276–1292).

In the mid-1970s, the structural and chemical properties of natural CDs were characterized and intensively studied. Some physicochemical properties of the CDs are shown in Table 1.3. Currently, CDs are being studied extensively for industrial and pharmacological applications. CDs are often used to prevent or reduce eye, stomach, intestinal irritation, to remove unpleasant odors and tastes, to prevent drug-drug or drug additive interactions etc (Divya and Sathasivasubramanian, 2013, p.279–283).

**Table 1.3.** *Physicochemical Properties of Cyclodextrins*

| **Properties** | **Cyclodextrin type** | | |
|---|---|---|---|
| | **α-Cyclodextrin** | **β- Cyclodextrin** | **γ- Cyclodextrin** |
| **Semisystematic name** | cyclomaltohexaose | cyclomaltoheptaose | cyclomaltooctaose |
| **Glucopyranose unit number** | 6 | 7 | 8 |
| **Molecular weight (g. mol$^{-1}$)** | 972 | 1135 | 1297 |
| **Central cavity diameter (Å)** | 4.7-5.3 | 6.0-6.5 | 7.5-8.3 |
| **Solubility in water at 25 ºC** | 14.5 | 18.5 | 23.2 |
| **Cavity volume (Å$^3$)** | 174 | 262 | 427 |
| **Outer diameter (Å)** | 14.6 | 15.4 | 17.5 |
| **Height of torus (Å)** | 7.9 | 7.9 | 7.9 |

**Reference**: *Jambhekar and Breen, 2016, p.356–362; Jin, 2010, p. 8.*

CDs can be classified according to polarization, size and biological activities. β-CDs and their hydroxypropylated derivatives, acetylated γ-CDs and in some cases α-CDs is often used as drug carriers. Hydroxypropylated β-CDs, sulphobutylated β-CDs and basic γ-CDs are only considered for parenteral use because of their toxicological values at acceptable levels. Generally, CDs derivatives include methyl CDs, hydroxypropyl CDs, sulfoalkylated CDs, and sulfated CDs. There are over 100 commercially available CDs Table 1.4. It has been found that the diameters of β-CDs cavities are suitable for guest molecules. For this reason, β-CDs are the most frequently used CDs for

biocompatibility in drug applications. However, β-CDs have a limited effect on water solubility and the inclusion complex formation due to strong hydrogen bonds between molecules between secondary hydroxyl groups (Jambhekar and Breen, 2016, p.356–362).

**Table 1.4.** *Cyclodextrins That Can be Found in Marketed Pharmaceutical Products*

| Cyclodextrin | Substitution* | MW (Da) | Solubility in water (mg. $mL^{-1}$) ** | Applications |
|---|---|---|---|---|
| **α-Cyclodextrin** | - | 972 | 145 | Oral, parenteral, topical |
| **β-Cyclodextrin** | - | 1135 | 18.5 | Oral, topical |
| **2 Hydroxypropyl-β-cyclodextrin** | 0.65 | 1400 | > 600 | Oral, parenteral, topical, rectal |
| **Randomly methylated-β-cyclodextrin** | 1.8 | 1312 | > 500 | Oral, topical |
| **β-Cyclodextrin sulfobutyl ether sodium salt** | 0.9 | 2163 | > 500 | Oral, parenteral, topical |
| **γ-Cyclodextrin** | - | 1297 | 232 | Oral, parenteral, topical |
| **2-Hydroxypropyl-γ-cyclodextrin** | 0.6 | 1576 | > 500 | Oral, parenteral, topical, eye drops |

**Average number of substituents per glucopyranose repeat unit. ** Solubility in pure water at ∼25°C. §In very limited amounts. MW: Molecular weight.*
**Reference***: Jambhekar and Breen, 2016, p.356–362; European Medicines Agency, 2014, p.1–17*

### 1.7.2. Approaches for preparation of inclusion complexes

#### *Milling or co-grinding technique*

In this method, guest molecules and CDs are milled together without using water and organic solvent to form inclusion complexes resulting in dynamic and thermodynamic interactions. It is a simple and fast technique. Although, in physical mixing method, water or organic solvent are not required, this method is not applied to

all active ingredients and not suitable for large scale due the possibility of inclusion complexes breakdown by the effect of moisture (Patil *et al.*, 2010, p.29–34).

***Kneading method (paste complexation)***

In order to form a paste, water is added in small quantities mixed with CDs using mortar (or kneading machine in large scale production). The time required depends on the guest. The resulting complex can be directly dried or washed with a little water and then subjected to filtration or centrifugation. Pastes sometimes dry up to form a hard mass instead of fine powder. This depends on the guest molecule and the amount of water used in the pastry. Usually these hard masses are dried and milled to obtain the powder form of the complex (Patil *et al.*, 2010, p.29–34).

***Co-precipitation technique***

It is the most widely used technique in laboratories. The hot solution of the guest material (active pharmaceutical ingredient) (API) that dissolved in the organic solvent is slowly added to the water-soluble cyclodextrin solution, during which the cyclodextrin solution is continuously stirred. The complex between the cyclodextrin and the guest molecule occurs and the resulting complex is precipitated. The precipitate can be separated from the cake by coarse transfer, centrifugation and filtration. The precipitate may be washed with a small amount of water or with other water miscible solvents such as ethyl alcohol, methanol, acetate (Del Valle, 2004, p.1033–1046).

***Solution-solvent evaporation method***

This involves dissolving the drug and CDs in two different suitable solvents, mixing both solutions to obtain the molecular dispersion of the drug and complexing agents, and finally evaporating the solvent under vacuum, thereby obtaining the inclusion compound in solid powder form. Generally, aqueous solutions of CDs are added to the alcoholic drug solution. The resulting dispersion is mixed for 24 hours and the solvents are evaporated under vacuum at 45 °C. The obtained pulverized mass is passed through a 60-mesh sieve. This method is considered to be completely simple and economical in both laboratory and large scale production and as an alternative to spray drying technique (Güleç and Demirel, 2016, p.1–8),(Patil *et al.*, 2010, p.29–34).

***Neutralization precipitation method***

Basic guest molecules are dissolved in an acidic solution and acidic guest molecules are dissolved in a basic solution. Once all is dissolved, the cyclodextrin is added to the solution with constant stirring. It is stirred until a clear solution is formed. By changing the pH of the obtained clear solution, the water solubility of the guest molecule is reduced. Thus, cyclodextrin inclusion complex is formed. The resulting solid complex is separated from the solvent by centrifugation and filtration (Özkan *et al.*, 2000, p.365–370).

***Spray drying or atomization method***

The CDs and the guest molecule dissolve in the organic solvent / water mixture and are sprayed through a nozzle into a heated cabinet. The inclusion complex is formed by rapidly removing the solvents from the medium. The inside and outside temperatures of the device, pump speed and nozzle size are important parameters (Mura *et al.*, 1999, p.279–287).

***Lyophilization (freeze drying) technique***

Lyophilization is a convenient method for the heat-labile substances (e.g. volatile compounds) of low stability to stand drying methods where temperature, flow velocity, and pressure are high. It is a particularly useful method for soluble complexes such as heat sensitive guest molecules and hydroxy propyl CDs complexes. These methods have advantages such as the obtaining of more amount of product, being suitable for soluble active substances, and being able to produce on a large scale. However, it is an expensive and time-consuming method, as well as beside the obtained inclusion complex, there is a possibility of containing free active substance and free CDs in the product (Güleç and Demirel, 2016, p.444–452).

***Microwave irradiation method***

This technique utilizes the microwave irradiation interaction between the drug and the CDs using a microwave oven. The CDs and the active ingredient in the given molar are dissolved in a solution of water and organic solvent in a flask at a certain ratio. The solution is left for two minutes in the microwave at 60°C until completing of the reaction between the drug and CDs. The residual of free complex-free drug and CDs is removed by adding a sufficient amount of the co-solvent, and the precipitate is obtained using a filter paper and dried in a vacuum oven at 40°C for two days. Microwave irradiation is a

new method for industrial scale preparation because of the shorter reaction time and higher yield of the product (Badr-Eldin *et al.*, 2013, p.1223–1231).

### 1.7.3 Analysis methods of CD inclusion complexes

Inclusion complexes can be analyzed quickly and directly by physicochemical and thermodynamic methods. The energy and stability constant required for the formation of the CDs inclusion complexes are determined by various methods.

***X-ray diffraction method***

This method is often used in the determination of inclusion complex formation. If the X-ray is shed at a certain angle from the source onto the powdered materials, it is refracted according to the crystal structure of the material, giving peaks at the height of the material and perceivable by a detector. Rolled curves that can be perceived with diffraction end detectors of the crystal structure are characteristic for each substance examined. If the inclusion complex is formed, there are significant differences in the X-ray analysis results of the complex (Mura, 2015, p.226–238).

***Thermal methods***

These methods involved the following techniques: thermodynamic affinity structure (TAS), thermodynamic gradient structure, differential scanning calorimetry (DSC) and differential thermal analysis (DTA) methods. From these methods, the DTA method determines the endothermic and exothermic enthalpy changes caused by phase transformation as a function of temperature. DSC quantitatively detects the conversion temperatures of the phases. The purity control of the chemical substance can also be performed with DSC (Mura, 2015, p.226–238).

***Nuclear magnetic resonance method (NMR)***

NMR is one of the most important methods used in the qualitative evaluation of the CDs inclusion complexes. The interaction between CDs and the active substance can be determined from changes in magnetic field signals of CDs and certain drug sites. If the CDs inclusion complex has a variation in the NMR spectra from the guest molecule and the host CDs molecule, it means that there is an interaction between the CDs and the guest molecule (Mura, 2014, p.238–250).

***Scanning electron microscopy (SEM)***

SEM has been used for the characterization of CDs inclusion complexes solid form to investigate the impact of kneading and evaporation methods on the morphological properties of the product. Furthermore, SEM is the best technique to obtain micrographs that utilized for evaluation the different crystal forms and homogeneity through the particles (Mura, 2015, p.226–238).

***Chromatographic method***

This method is usually used for volatile substances. If it is stable in a complex solution, thin layer chromatography can be applied. Liquid chromatography is performed using the minimum amount of guest molecule and used to determine the stability constants of CDs inclusion complexes (Mura, 2014, p.238–250).

***Spectrophotometric method***

Ultraviolet (UV), infrared spectroscopy (IR) and fluorescence spectroscopy are suitable methods to determine if the CDs inclusion complex is formed. The interaction and bonding states of the active substance with CDs can be concluded by looking at the peaks when the UV and visible spectrum are examined (Mura, 2014, p.238–250; Mura, 2015, p.226–238).

### 1.7.4. Stability of CDs inclusion complex

CDs inclusion complexes have enhanced the stability of many unstable drugs against high temperature, hydrolysis, oxidation-reduction reactions and photodegradation. It was reported that improving drug stability may be a consequence of the protection of the CDs-drug complex against the interaction of drug-vehicles, microbiological degradation and / or the inhibition of drug bio-conversion at the site of absorption (Rasheed *et al.*, 2008, p.567–598).

### 1.7.5. Toxicity of CDs

α-CDs are well tolerated when given orally and have not significant side effects. Furthermore, small amount of α-CDs are absorbed undamaged from the GIT and the intravenous administrated dose of α-CDs is excreted as unchanged form in the urine. β-CDs cannot be given intravenously because they have low water solubility and nephrotoxicity. However, it is safe when administered orally.

The nephrotoxicity of α- and β-CDs, following intravenous administration, as well as problems with many modified CDs, have been well documented. The metabolism of γ-CDs like that of starch and other linear dextrins, and only a small fraction of γ-CDs is absorbed undamaged from the GIT. Following intravenous injection, γ-CDs are mainly excreted in intact form in the urine (Duchene and Bochot, 2016, p.58–72).

Aqueous soluble CDs specifically, HP-β-cyclodextrin and SBE-β-cyclodextrin, are rated nontoxic when given in minimum to moderate doses, orally or intravenously. HP-β-cyclodextrin is more hydrophilic, so that its more toxic than β-cyclodextrin and can cause recurrent diarrhea and cecal growth in animals and therefore humans. Water poorly soluble CDs derivatives, such as methylated CDs, are absorbed considerably from the GIT into the systemic circulation and have been shown to be toxic after intravenous administration. Currently, oral administration of methylated β-cyclodextrin is restricted because of its probable toxicity (Jambhekar and Breen, 2016, p.356–362).

### 1.7.6. CDs application fields

CDs have formed inclusion complexes with many polar and even apolar aliphatic and aromatic compounds. For this reason, they can significantly change the physical and chemical properties of guest molecules. CDs are widely used in the pharmaceutical (e.g.), food, cosmetic, agricultural and chemical industries due to their complexity. Inclusion complexes formed by host CDs molecules with guest molecules have many advantages. Some of these are given below:

- CDs increase the solubility of water-insoluble or slightly soluble compounds.
- The volatility of aromatic compounds can be reduced by formation of CDs inclusion complexes.
- CDs inclusion complexes improve stability of light or oxygen sensitive molecules.
- Bad odors and tastes of drug compounds can be masked by CDs inclusion complexes.
- CDs inclusion complexes prevent some compounds from being destroyed by microorganisms due to changing the physical properties of liquid compounds (Chaudhary and Patel, 2013, p.68–76).

CDs applications in drug delivery as:

- Oral Drug Delivery,

- Parenteral Drug Delivery,
- Ocular Delivery,
- Nasal Drug Delivery,
- Rectal Drug Delivery,
- Controlled Drug Delivery,
- Colon-Specific Drug Delivery,
- Peptide and Protein Delivery,
- Gene and Oligonucleotide Delivery,
- Dermal and Transdermal Delivery, and
- Brain Drug Delivery or Brain targeting (Challa *et al.*, 2005, p.E329–E357).

CDs applications in the design of some novel delivery systems for example:

- Liposomes,
- Microspheres,
- Microcapsules, and
- Nanoparticles (Challa *et al.*, 2005, p.E329–E357).

### 1.7.7. Cyclodextrin-poly(anhydride) nanoparticles

The biopharmaceutical classification system (BCS) classify drugs into four categories according to their water solubility and membrane permeability characteristics and in general allows the prognostication of the rate-limiting step in the intestinal absorption process following oral administration. Many drugs remain poorly available when administered by this route, owing to the physicochemical properties of the drug, physiological factors and factors related to the dosage form. It has been demonstrated that two of these factors, namely the aqueous solubility of a drug and its permeability across the cellular membranes, strongly determine the oral bioavailability of the drug. Whenever a dosage form is administered orally, first the drug should be released and dissolve in the surrounding gastrointestinal fluid to form a solution. The adsorption of orally administered drugs is restricted to transport through the enterocytes or between the enterocytes and transport through M cells. Once the drug is dissolved in intestinal fluid, it passes across the membranes of the cells lining the gastrointestinal tract. A low solubility and very low solubility of the compound result in low dissolution rate in the mucosal fluids and elimination of a fraction of the drug before absorption (Dahan *et al.*, 2009, p.740–746).

In some specific models, drugs may be absorbed by fluid-phase endocytosis, an energy-dependent saturable process in which the molecule trans inside membrane vesicles. Drug molecules absorbed by the transcellular pathway are in general, low-molecular-mass hydrophobic structures that can diffuse through the membrane, either on their own or connected with a particular membrane transporter (Xu *et al.*, 2013, p.1–15).

In the absence of a convenient membrane transporter, the paracellular route of drug molecules transportation through M cells are the only ones available for their absorption. In the paracellular space, the presence of tight junctions between adjacent cells limits the passage of large molecules through the intercellular space. Furthermore, M cells are phagocytic enterocytes found in the follicle-associated epithelium of the Peyer's patches. They are specialized in the catching and transport of bacteria, viruses, macromolecules and particles from the gut lumen to immune cells across the epithelial barrier, and consequently, they are important in activating mucosal immunity (Agüeros *et al.*, 2011, p.721–734). Unlike their neighboring cells, they have the unique ability to take up compounds from the lumen of the small intestine by means of endocytosis or phagocytosis and then deliver them via transcytosis to dendritic cells and lymphocytes located in a unique pocket-like structure on their basolateral side. In any case, the total contribution of the paracellular pathway or transit through M cells to general drug transport is in general, very discrete. The surface of intercellular pores and M cells represents only 0.01 - 0.1% and < 1% of the intestinal epithelial cells, respectively (Mabbott *et al.*, 2013, p.666–77).

Apart from the solubility and absorption pathways, an extensive presystemic metabolism is also a handicap that limits the oral bioavailability of many drugs. During and after the adsorption many drugs can be degraded by the cytochrome P450 system. Enzymes of the CYP family are expressed at high levels in the villus tip enterocytes of the small intestine at concentrations equal to or higher than in the liver. Finally, in addition to the first-pass metabolism, active secretion of absorbed drug is now recognized as a significant factor in oral drug bioavailability. One of particular interest, is the MDR1 gene product P-glycoprotein, a multidrug efflux pump. As CYP3A, P-gp is located in the intestinal villus enterocytes. This colocalization and the sharing of a remarkable number of substrates and inhibitors suggest that CYP3A and P-gp may form a concerted barrier to drug absorption and that intestinal drug metabolism and counter transport processes

are a major determinant of oral drug bioavailability and variability (Gavhane and Yadav, 2012, p.331–344).

Several strategies have been suggested to avoid these limitations, including pro-drug synthesis, reduction of drug particle size, administration with P-gp or CYP inhibitors, or salt formation. Another interesting method depends on encapsulation of the drug inside nanosized carrier systems such as polymeric nanoparticles, micelles, liposomes and other lipid carriers. This transitory immobilization results in a delay in the transit time of the particles in the GIT and, in this way, an increase in the drug concentration gradient from the lumen to the epithelia or direct contact with intestinal cells, which is the first step before drug adsorption (Xu *et al.*, 2013, p.1–15). Sometimes, nanoparticles themselves can cross the epithelial membrane and transfer the drug particles from the lumen to the blood or lymph. Nanoparticles should be taken up by M cells or translocate between epithelial cells, both pathways with an inconsequential contribution to the whole drug adsorption (Agüeros *et al.*, 2011, p.721–734).

Recently, the bio-adhesive properties of cyclodextrin-poly(anhydride) nanoparticles and their performance for improving the oral bioavailability of poorly water-soluble drugs such as Paclitaxel, or Atovaquone were investigated. These copolymers allow the production of nanoparticles under 'soft' conditions and the resulting delivery systems have established, a high ability to enhance bio-adhesive interactions within the GIT (Agüeros et al., 2010, p.2–8; Lakkakula and Macedo, 2014, p.877–94). This phenomenon may be due to the formation of carboxylic groups during the hydrolysis of the anhydride residues of the copolymer. These carboxylic groups would develop hydrogen bonds with components of the mucosa. Basically, the surface of these poly(anhydride) nanoparticles can be easily modulated by simple incubation with several additives or ligands in order to change their physicochemical and biological properties as well as their fate within the GIT (Agüeros *et al.*, 2011, p.721–734).

## 2. MATERIALS

### 2.1. Chemicals

| Substance | Company |
|---|---|
| **Acetic Acid** | : Sigma-Aldrich, Germany |
| **Acetone** | : Sigma-Aldrich, Germany |
| **Acetonitrile** | : Sigma-Aldrich, Germany |
| **Caco-2 Cell line** | : American Type Culture Collection (ATCC), USA |
| **Chitosan medium molecular weight** | : Sigma-Aldrich, Germany |
| **Chitosan oligosaccharide lactate** | : Sigma-Aldrich, Germany |
| **Deuterated chloroform** | : Merck, USA |
| **Deuterated dimethyl sulphoxide** | : Merck, USA |
| **Dimethyl sulphoxide *(cell culture grade) DMSO*** | : AppliChem GmBH, Germany |
| **Dulbecco's Modified Eagle's Medium (DMEM),** | : Biochrom AG, Germany |
| **Ethanol** | : Sigma-Aldrich, Germany |
| **Fetal bovine serum (FBS)** | : Biochrom AG, Germany |
| **Formic acid** | : Sigma-Aldrich, Germany |
| **Hank's Balanced Salt Solution (HBSS)** | : Biochrom AG, Germany |
| **Heparin vial** | : Mustafa Nevzat İlaç Sanayii A.Ş., Turkey |
| **Ketamine vial** | : EGE-VET, Turkey |
| **Ketoprofen** | : Gift |
| **L-Aspartic acid** | : Sigma-Aldrich, Germany |
| **L-Glutamic acid** | : Sigma-Aldrich, Germany |
| **Methyl-beta-cyclodextrin** | : Sigma-Aldrich, Germany |
| **Penicillin / Streptomycin** | : Biochrom AG, Germany |
| **Phosphate buffered saline (PBS) tablets** | : Sigma, USA |
| **Phosphatidylcholine** | : Sigma-Aldrich, Germany |
| **Polyanhydride** | : Sigma-Aldrich, Germany |

| | |
|---|---|
| **Rosuvastatin Calcium (RCa) as (API)** | : Abdi İbrahim İlaç, Türkiye (Gift) |
| **Stearic Acid** | : Sigma-Aldrich, Germany |
| **Sulfobutyl ether beta-cyclodextrin (Captisol®)** | : Sigma-Aldrich, Germany |
| **Thiazolyl blue tetrazolium bromide (MTT)** | : AppliChem GmBH, Germany |
| **Trehalose** | : Sigma-Aldrich, Germany |
| **Tripalmitin** | : Fluka, France |
| **Trypan blue** | : Sigma, UAS |
| **Trypsin-EDTA solution** | : Biochrom AG, Germany |
| **Tween® 80** | : Sigma-Aldrich, Germany |
| **Xylazine vial** | : EGE-VET, Turkey |

## 2.2. Devices

| **Device** | **Company** |
|---|---|
| **96 well sterile plate** | : Grenier Bio-one, Germany |
| **Biosafety cabinet** | : Faster, BHG 2004, Class 2, Italy |
| **Carbon dioxide incubator** | : Sanyo, Japan |
| **Cell culture dishes** | : Grenier Bio-one, Germany |
| **Cell culture inserts** | : Grenier Bio-one, Germany |
| **Cell culture wells** | : Grenier Bio-one, Germany |
| **Centrifuge** | : Eppendorf, Centrifuge 5417r, Germany |
| **Centrifuge** | : Nüve NF400, Turkey |
| **Centrifuge** | : Nüve, NF 615, Turkey |
| **Column** | : GL sciences, C18, Japan |
| **Deep freeze** | : Libherr LGEX 3410 Medline, Germany |
| **Differential Scanning Calorimetry** | : Shimadzu DSC-60, Japan |
| **Electric resistance system** | : Millipore, Millicell-ERS, USA |
| **Fourier Transform Infrared Spectrophotometer (FTIR)** | : Perkin Elmer Spectrum 2000, UK |
| **Gavage Needle** | : Fine Science Tools Inc., USA |

| | |
|---|---|
| **High Performance Liquid Chromatography (HPLC)** | : Shimadzu, 20-A, Japan |
| **Horizontal Shaker** | : WiseShake SHR-1D, Korea |
| **Horizontal shaker, digital** | : Memmert GmBH Co. KG / Germany |
| **Incubator** | : Nüve EN120, Turkey |
| **Injector filter 0.2 µm, sterile** | : Sartorius, Stedim Biotech GmbH, Germany |
| **Inverted microscope, Camera system** | : Leica, DMIL, Germany |
| **Lyophilizer** | : Leybold-Heraeus Lyovac GT-2, Germany |
| **Magnetic stirrer** | : Wisd Laboratory Instruments, Daihan SMH5-3, Korea |
| **Micropipette** | : Eppendorf, Germany |
| **Micropipette tip** | : Eppendorf, Germany |
| **Microplate reader** | : VersaMax, USA |
| **Nylon filter** | : Agilent technologies, USA |
| **Oven** | : Nüve FN 500, Turkey |
| **pH meter** | : WTW Profi Lab pH 597, Germany |
| **Polypropylene tube, capped, 15 mL** | : Grenier Bio-one, Germany |
| **Proton-Nuclear Magnetic Resonance Spectrophotometer ($^1$H-NMR)** | : Bruker, Ultra Shield CP MAS NMR 500 MHz, Germany |
| **Pure Water Device** | : Millipore, Milli-Q Synthesis A10 Ultra-Pure, France |
| **Refrigerator** | : Arçelik 5274 NMS No Frost, Turkey |
| **Rotary evaporator** | : Buchi R-205, Japan |
| **Scanning Electron Microscope (SEM)** | : Zeiss, Supratm 50 VP, Germany |
| **Sensitive balances** | : Mettler AM 100, USA |
| **Spray Drying Device** | : Büchi, Nano Spray-Dryer B-90, Switzerland |

| | |
|---|---|
| **Sterile pipettes** | : Grenier Bio-one, Germany |
| **Ultrasonic bath** | : Elma T470 / H Singen, Germany |
| **Ultrasonic processor** | : VCX 130 PB, USA |
| **Ultra-Turrax Homogenizer** | : IKA T25, USA |
| **Vacuum 0ven** | : Jeio tech, OV-12, Korea |
| **Vortex** | : Jeiotech VM-96B, Korea |
| **Vortex** | : IKA, Brazil |
| **Water bath** | : Nüve BM 302, Turkey |
| **X-ray Diffraction (XRD)** | : Rikagu, D / Max-3C, Japan |
| **Zeta potential analyzer** | : Zetasizer Nano ZS Malvern, UK |

# 3. METHODS

## 3.1. Analytical Validation Studies

### 3.1.1. Chromatographic conditions optimization

The analytical validation processes were carried out in this research; for *in vitro* study, permeability study and for *in vivo* study. In each time a few of chromatographic conditions (Kumar *et al.*, 2006, p.881–887) had been developed which will be mentioned later in validation steps. In high pressure liquid chromatography (HPLC), the validation studies are of immense importance for subsequent analyzes. By carrying out validation; accurate, reliable and reproducible data are obtained from analytical studies. Analytical parameters such as linearity, precision, accuracy, specificity, and sensitivity were analyzed and statistically evaluated using the International Harmonization Committee (ICH), analytical process validation guidelines (ICH, 1996, p.4–5).

**Table 3.1.** *HPLC Operating Conditions*

| | |
|---|---|
| **Device** | **Shimadzu, LC 20-AT, Japan** |
| **Column** | GL sciences column $C_{18}$ (250 × 4.6 mm, 5 µm) |
| **Oven Temperature** | 25 °C |
| **Mobile Phase** | Formic acid (0.05 M) and Acetonitrile (ACN) 55:45 (v/v) |
| **Detector** | Diode Array |
| **Wavelength** | 240 nm |
| **Flow rate** | 1.0 $mL.min^{-1}$ |
| **Injection Volume** | 20 µL (*in vitro* test and permeability test) and 100 µL (*in vivo* test) |

### 3.1.2. Linearity

Linearity is a test of whether, the analytic work done is a linear relationship throughout the entire study. In the linearity study, it is expected that the material to be analyzed at different concentration will be directly proportional to the peak area measured in the chromatogram. The peak areas obtained at different concentrations allow the determination of the straight-line equation which had been used throughout the entire study.

The linearity of the selected methods was established from the calibration curves constructed at seven RCa concentrations within the level of 1-100 μg. $mL^{-1}$ in mobile phase in case of *in vitro* study, at six RCa concentrations within the level of 1-25 RCa μg. $mL^{-1}$ in Hank's Balanced salt solution (HBSS) in case of permeability study, and 0.1 -10 μg. $mL^{-1}$ in mobile phase with internal standard (IS) ketoprofen (KTP) (1 μg. $mL^{-1}$) after extraction from the plasma in case of *in vivo* study. Calibration curves were constructed for RCa in the mobile phase and spiked plasma samples by plotting their relative peak area against their respective concentrations using a linear least squares regression analysis. The solution in each concentration was analyzed by HPLC and the work was repeated three times.

### 3.1.3. Range

It is the range of the upper and lower concentrations of the analyte in the sample to show that the analytical method used has linearity, accuracy and precision conditions. The working range is usually determined by the linearity studies and the intended application of the process. The following minimum specified ranges should be considered (ICH, 1996, p.4–5):

- For drug and finished product analysis, it should be between 80% and 120% of the test concentration,
- The active substance must be at least 70% to 130% of the test concentration for testing the quantity determination or within a wider range, and
- It is necessary to work within ± 20% of the range determined for the dissolution test.

### 3.1.4. Accuracy

The accuracy of the analytical method refers to the closeness of the found value to the actual value or accepted reference value. In order to determine the accuracy, the analysis of known concentration samples is carried out and the quantities calculated with the straight-line equation are compared to the actual quantities. When this parameter is examined, it should be calculated by repeating at least three (3) different concentrations, three (3) times. The results are given as (% recovery), standard error (SE), standard deviation (SD) and relative standard deviation (RSD %).

### 3.1.5. Precision

The precision of an analytical method defined as the closeness of agreement (degree of scatter) between a set of measurements obtained from multiple sampling of the same homogeneous or artificial sample under the definite conditions. Precision should be investigated using standard samples. However, if it is not possible to obtain a standard sample it may be investigated using artificial sample solutions. In this work, a standard solution of RCa was used for the precision study.

Precision may be investigated at three levels: repeatability (intra-day precision), intermediate precision (inter-day precision) and reproducibility (between laboratories precision). Confidence intervals and relative standard deviation are given to demonstrate the precision of the method. The repeatability parameter is obtained by measuring the same stock solution several times in short time intervals. In this work repeatability (intra-day precision) and intermediate precision (inter-day precision) were done by six (6) times repeatedly at three (3) different concentrations for three days.

### 3.1.6. Selectivity

Selectivity is one of the most important analytical parameters that show that the concentration of a single substance in a mixture, in its formulation, or the presence of other substances in the environment can be accurately determined. The measurement that has been made for a single component should not be affected by interference from other components (adjuvants, biological compounds, biological metabolites, known metabolites, impurities, known or unknown degradation products) that may be present in the environment (ICH, 1996, p.4–5). The selectivity was carried out in this work in case of validation method for permeability test and validation method of *in vivo* test.

### 3.1.7. Sensitivity

The ability of the analytical method to detect low concentrations. The detection limit (LOD) is the lowest level of the exact concentration of the analyte in the sample. This value may not be a definitive quantitative value.

The limit of quantitation (LOQ) is the minimum amount of the analyte in the sample that can be detected with appropriate accuracy and strictly quantitatively. There are different approaches depending on whether the method is instrumental or not in order to determine both the detection limit and the quantity detection limit:

- Visual evaluation,
- Signal-noise, and
- Standard deviation of obtained response and slope
    - Standard deviation of empty samples, and
    - Use of the calibration curve

In sensitivity studies, the limit of detection (LOD) value, which does not fall within the quantitative limits of the system, is calculated using Equation 3.1 below. (ICH, 1996, p.4–5)

$$LOD = \frac{3.3\ x\ SD}{Slope} \tag{3.1}$$

The limit of quantitation (LOQ) is the minimum amount of material required to accurately measure a standard material in a reliable manner. The methods used to determine the LOD are also valid for LOQ and are calculated by Equation 3.2 below (ICH, 1996, p.4–5).

$$LOQ = \frac{10\ x\ SD}{Slope} \tag{3.2}$$

In both equations (3.1, 3.2) SD is the standard deviation of y-intercepts of regression lines.

### 3.1.8. Robustness

It is the measurement of the analytical method's ability to remain unaffected by slight changes. However, this parameter has not been tested in this study since a new method was not developed and the method already specified by literature review that has been modified and used.

### 3.1.9. System suitability test

The system suitability test is an integral part of many analytical procedures. The test includes hardware, analytical processing and electronic status. System suitability test parameters have been validated depending on the type of the planned operation.

The system suitability test parameters defined by the USP (United States Pharmacopeia) are given below.

- Peak morphology,
- Theoretical number of layers,
- Queuing and asymmetry factors,
- Capacity factor,
- Selectivity factor,
- Separation power, and
- % Relative standard deviation of the peak height or area.

At least two of these criteria indicate the system suitability of the required conditional method (U.S.P, 2016, p.463–468).

### 3.2. RCa Solubility in Water

In order to determine the solubility of standard RCa in water, 35 mg of RCa was added to 2 ml of distilled water to form saturated solution. The solution was shaken in a horizontal shaker for one hour at room temperature after that the solution was filtered by 0.2 μm nylon filter and then analyzed by HPLC. The experiment was repeated three times.

### 3.3. The Characterization Tests of Pure Substances

#### 3.3.1. Thermal analysis

Approximately 4-6 mg as sample of material was placed in aluminum cell and covered with the assist of pressure. Then, by using Differential scanning calorimetry (DSC) the thermal analysis was done and the thermograms of the RCa and the other excipients were obtained. The analysis was carried out with nitrogen gas at a flow rate of 50 $mL.min^{-1}$ and a temperature increase of 10 °C. $min^{-1}$ regarding an empty aluminum sample cell as a reference.

#### 3.3.2. Proton nuclear magnetic resonance ($^1$H-NMR) analysis

NMR spectras of the active ingredient and the excipient were obtained using deuterated chloroform and deuterated dimethylsulphoxide (DMSO).

#### 3.3.3. Infrared (FT-IR) analysis

Spectra were taken between 500-4000 $cm^{-1}$ for FT-IR analysis of RCa and excipient used in this study.

#### 3.3.4. X-ray diffraction analysis

X-ray diffraction analysis of the active substance and the excipient used were carried out at $4^{o}$ - $40^{o}$ using a generator of 40 kV voltage and 20 mA current.

### 3.3.5. Morphological examination

The surface properties and dispersion patterns of RCa and the used excipient were examined using scanning electron microscope (SEM) after coating with gold on carbon tape.

## 3.4. Preparation of Chitosan Nanoparticles (Cs NPs)

Chitosan (Cs) acid salts were prepared in a laboratory-scale using organic acetic acid (AA), aspartic acid (AsA), and glutamic acid (GA) as solvent. Formulations of Cs NPs were carried out for the four derivatives of Cs: AA, AsA, GA and chitosan lactate (CL) using spray drying method (Başaran *et al*., 2015, p.1180-1188).

### 3.4.1. Preformulation studies

The suitable solvents or co-solvents were selected for preparation of Cs NPs according to the following steps, thus at the beginning:

- Cs acid salts solution were added to the dimethyl sulfoxide solvent to form miscible solution and the RCa was added to this solution, but the precipitation occurred.
- After that, 500 mg of Cs were added to a solution of (150 mL of % 2 AA and 50 mL of Acetone) to prepare miscible solution which was mixed for 16 hours and sprayed but the Cs NPs were not formed because the end solution was thick and didn't properly injected throughout the nozzle of spray dryer.
- The same solvents in step two were used in addition to ethanol but the same problem was occurred.
- Then, the solutions of Cs salts were added to ethanol to form miscible solution which sprayed to get the Cs NPs.

To improve the Cs NPs properties and get high quantity of product further steps were carried out in preparation of Cs aspartate and Cs glutamate NPs as following:

- Cs and AsA were added in a ratio of (1:2 mmol) to 250 mL distilled water (DW) with a continuous stirring to get miscible solution but the AsA didn't dissolve and precipitated.
- The same ratio of Cs and AsA (1:2 mmol) was added to the co-solvent of (125 mL distilled water and 125 mL ethanol) and, also AsA didn't dissolved.

- Then, 500 mg of Cs was added to a 250 mL % 0.6 solution of AsA with a continuous stirring for 16 hours to form a little bit viscous solution which would not be convenient to sprayed.
- After that, a suitable amount of Cs was added to (250 mL of % 0.3 AsA) solution and a solution of (125 mL of % 0.3 AsA and 125 mL of ethanol) separately and mixed by magnetic stirrer for 16 hours to form clear and miscible Cs aspartate salt solutions which sprayed to get Cs NPs.
- By same ways, Cs NPs prepared from % 0.3 GA solution and ethanol.

### 3.4.2. Formulation of chitosan nanoparticles Cs NPs

The formulations of Cs NPs were carried out by a laboratory-scale spray dryer. The organic acids AA, AsA, and GA were used as solvent in the formulation process for the medium molecular weighted Cs (Luangtan-anan *et al*., 2005, p.189-196). The already prepared chitosan lactate (CL) powder was directly hydrated in distilled water and the medium molecular weighted Cs powder was hydrated in 0.3 % GA, 0.3% AsA and 2 % AA solutions with a continuous stirring on a magnetic stirrer at 300 rpm at room temperature for 16 hours. RCa and ethanol (99.8%) were added to the homogenous mixture of CL and Cs salt solutions with a continuous stirring about one hour. Spray drying process was accomplished for homogenous mixtures at flow rate 1 mL. $min^{-1}$ using a 0.5 mm nozzle. The inlet temperature was set to 160 °C and the outlet temperature was 95 °C. The produced dried NPs were put in well closed containers and stored in a desiccator at 25 ± 0.5 °C until being analyzed. Compositions of the RCa loaded NPs are shown in Table 3.2.

**Table 3.2.** *Compositions of RCa Incorporated Cs NPs*

| Code | RCa (mg) | Cs (mg) | CL (mg) | AA 2% v/v (mL) | AsA 3% v/v (mL) | GA 3% v/v (mL) | Ethanol 99.8% (mL) | DW (mL) |
|---|---|---|---|---|---|---|---|---|
| **F1** | 150 | 1000 | - | 150 | - | - | 150 | - |
| **F2** | 75 | - | 500 | - | - | - | 250 | 250 |
| **F3** | 50 | 500 | - | - | 500 | - | - | - |
| **F4** | 75 | 500 | - | - | 500 | - | 500 | - |
| **F5** | 50 | 500 | - | - | - | 500 | - | - |
| **F6** | 75 | 500 | - | - | - | 250 | 250 | - |

### 3.4.3. Cs NPs preparations yield value

The yield value was calculated by using Equation 3.3.

$$Nanoparticle\ yield = \frac{Mass\ of\ Nanoparticle\ \ Recovered}{Mass\ of\ Drug\ and\ Polymer} \times 100 \qquad (3.3)$$

### 3.4.4. Determination of drug content (DC %)

For determining the drug content percentage (DC %) of the prepared Cs NPs formulations, 1 mg of the formula was dissolved in 1 mL of mobile phase, and the resulting solution was diluted with mobile phase at a ratio of (1:10) and analyzed under HPLC operating conditions. Equality 3.4 was used for calculating the percentage of drug loaded (Gupta *et al.*, 2010, p.324–333). All analyses were repeated in triplicate.

$$DC\ (\%) = \frac{Amount\ of\ Drug\ Actually\ Present\ in\ the\ Nanoparticles}{Amount\ of\ Drug\ Used} \times 100 \quad (3.4).$$

### 3.4.5. Physicochemical characterization tests of Cs NPs

#### 3.4.5.1. *Particle size (PS), polydispersity index (PDI) and zeta potential (ZP) measurements*

The particle size and zeta potential measurements of Cs NPs were carried out using Malvern Zetasizer Nano-ZS. The preparation of samples for analysis was achieved by diluting proper amounts of dry NPs in bidistilled water adjusted to a constant conductivity of 50 $\mu S.cm^{-1}$ with 0.9% NaCl and suspended completely for several minutes using vortex. All analyses were repeated in triplicate at 25 °C.

#### 3.4.5.2. *Morphology of Cs NPs*

Photomicrographs were taken at a voltage of 3 kV and 5.00 K X, 9.59 K X, 10.00 K X or 250 X magnification using a Scanning Electron Microscope (SEM).

#### 3.4.5.3. *Thermal analysis of Cs NPs*

Melting transitions and changes in heat capacity of the drug and polymers were analyzed using DSC. The samples of constant amount of were put in hermetically sealed aluminum crucibles and purged with inert nitrogen gas at the rate of 50 $mL.min^{-1}$. Thermograms were obtained at 30-250 °C with an increase rate of $10°C.min^{-1}$.

#### 3.4.5.4. *Infrared (FT-IR) analysis*

In order to verify the interaction possibilities between the drug and NPs (FT-IR) spectra were recorded by FT-IR spectrophotometer at the wavelength range of 4000-500 $cm^{-1}$.

#### 3.4.5.5. *XRD (X-ray diffraction)*

The crystallinity of the spray dried powders was evaluated using powder X-ray diffractometer. XRD studies were performed on the samples by exposing them to CuKα radiation (40kV, 20mA) and scanned from $2^o$ to $40^o$, 2θ at a scanning rate $2^o$. $min^{-1}$.

#### 3.4.5.6. *$^1$H-NMR analysis*

Nuclear magnetic resonance ($^1$H-NMR) spectra were obtained in order to demonstrate the modifications in the pure materials and polymeric matrixes during the formulation stages using a Bruker NMR equipment (500 MHz) (Germany). Deuterated chloroform was used as a solvent.

### 3.4.6. *In vitro* release studies

26 mg RCa are soluble in 10 mL at pH 6.8 (Salih *et al.*, 2013, p.525–535). So, to provide perfect sink conditions, 3 mg pure RCa or the NPs containing an equivalent amount of RCa were placed in dialysis bag and then in 50 mL phosphate buffer (pH) 6.8 (Akbari *et al.*, 2011, p.1–8; Klose *et al.*, 2011, p.75–82). Therefore, sink conditions were achieved with the drug concentration in the release medium does not exceed 10% of the solubility of the drug in this medium at any time point. The study was performed at 37 ± 0.5 $^o$C with a stirring rate of 100 rpm using a magnetic stirrer. At predetermined time intervals (5, 10 ,15 min, 0.5, 1, 2, 3, 4, 6, 8, 12 and 24 h) 1 mL samples were collected and fresh medium was added immediately to the release media with same amount to maintain sink conditions. The withdrawn samples were filtered through 0.2 μm nylon filter and analyzed by HPLC. The experiments were repeated in triplicate.

### 3.4.7. Kinetics and mechanism of release

To investigate the release kinetics, the data obtained from *in vitro* drug release studies in phosphate buffer (pH 6.8) were analyzed by DDSolver software program (Zhang *et al.*, 2010, p.263–271).

### 3.5. Preparation of Solid Lipid Nanoparticles (SLNs)

#### 3.5.1. Preformulation study

Stearic acid (SA) and tripalmitin (TP) were used as solid lipids for preparation of SLNs. The SLNs were prepared by the high shear homogenization (ultra-turrax) method for the two types of solid lipids SA and TP (Ekambaram and Abdul Hasan Sathali, 2011, p.216-220). In preformulation study different: RCa concentrations, lipid concentrations and surfactant types and concentrations were experimented to get the optimal concentration for all ingredients. Furthermore, different methods were examined for cooling the obtained coarse emulsion from the preparation method which carried out as follow:

The lipid was melted at 10 °C above its melting point and RCa was added to it. Separately, the surfactant/ or surfactants were dissolved in bidistilled water and heated to the temperature of lipid mixture. Then, the hot aqueous surfactant solution was added to the clear homogenous hot lipid phase, and homogenization was carried out (at 9500 rpm) by using ultra-turrax homogenizer for three minutes. Table 3.3 and 3.4 show the different conditions and ingredients concentrations that were used in preformulation study.

**Table 3.3.** *Preformulation Ingredients of SA SLNs*

| Code | RCa (mg) | SA (g) | Tween® 80 (g) | Bidistilled Water (mL) | Advice Used for Further Mixing after Homogenization | Cooling Temperature |
|---|---|---|---|---|---|---|
| **F 1** | - | 5 | 1 | 50 | - | 25 ºC |
| **F 2** | - | 5 | 1 | 50 | A magnetic stirrer (300 rpm) for 24 hours | 25 ºC |
| **F 3** | - | 5 | 1 | 50 | A magnetic stirrer (300 rpm) for 24 hours | Ice bath |
| **F 4** | - | 5 | 1 | 50 | Homogenizer (3500 rpm) for 10 minutes | 25 ºC |
| **F 5** | - | 5 | 1 | 50 | Ultrasonication for 10 min at %20 Amp | Ice bath |
| **F 6** | - | 5 | 1 | 50 | Ultrasonication for 10 min at % 20 Amp | 25 ºC |
| **F 7** | - | 5 | 1 | 50 | Ultrasonication for 10 min at % 40 Amp | 40 ºC |
| **F 8** | - | 2 | 1 | 50 | A magnetic stirrer 300 (rpm) for 24 hours | 25 ºC |
| **F 9** | - | 2 | 1 | 50 | Ultrasonication for 10 min at % 20 Amp | 25 ºC |
| **F 10** | - | 2 | 1 | 50 | Ultrasonication for 10 min at % 20 Amp | 4 ºC |
| **F 11** | 40 | 1.960 | 1 | 50 | Ultrasonication for 10 min at % 20 Amp | 4 ºC |
| **F 12** | 80 | 1.920 | 1 | 50 | Ultrasonication for 10 min at % 20 Amp | 4 ºC |
| **F 13** | 10 | 1.990 | 1 | 50 | Ultrasonication for 10 min at % 20 Amp | 25 ºC |
| **F 14** | 20 | 1.980 | 1 | 50 | Ultrasonication for 10 min at % 20 Amp | 4 ºC |

**Table 3.4** *Preformulation Ingredients of TP SLNs*

| Code | RCa (mg) | TP (g) | Surfactants (g) | Bidistilled Water (mL) | Advice Used for Further Mixing after Homogenization | Cooling Temperature |
|---|---|---|---|---|---|---|
| **F 15** | - | 2 | 1 T80 | 50 | - | 25 ºC |
| **F 16** | - | 2 | 1 T80 | 50 | A magnetic stirrer (300 rpm) for 24 hours | 25 ºC |
| **F 17** | - | 2 | 1 T80 | 50 | A magnetic stirrer (300 rpm) for 24 hours | Ice bath |
| **F 18** | - | 2 | 1 T80 | 50 | Homogenizer (3500 rpm) for 10 minutes | 25 ºC |
| **F 19** | - | 2 | 1 g T80 | 50 | Ultrasonication for 10 min at %20 Amp | 25 ºC |
| **F 20** | - | 2 | 1 T80 | 50 | Ultrasonication for 10 min at % 20 Amp | 4 ºC |
| **F 21** | 40 | 2 | 1 T80 | 50 | Ultrasonication for 10 min at % 20 Amp | 4 ºC |
| **F 22** | 20 | 1.980 | 1 T80 | 50 | Ultrasonication for 10 min at % 20 Amp | 4 ºC |
| **F 23** | - | 2 | 1 PTC | 50 | Ultrasonication for 10 min at % 20 Amp | 4 ºC |
| **F 24** | - | 2 | 1 PTC | 50 | Ultrasonication for 10 min at % 40 Amp | 4 ºC |
| **F 25** | 20 | 2 | 0.5 T80 – 0.5 PTC | 50 | Ultrasonication for 10 min at % 20 Amp | 4 ºC |
| **F 26** | 80 | 1.980 | 0.5 T80 – 0.5 PTC | 50 | Ultrasonication for 10 min at % 20 Amp | 4 ºC |
| **F 27** | 10 | 1.990 | 0.5 T80 – 0.5 PTC | 50 | Ultrasonication for 10 min at % 20 Amp | 4 ºC |
| **F 28** | 5 | 1.995 | 0.5 T80 – 0.5 PTC | 50 | Ultrasonication for 10 min at % 20 Amp | 4 ºC |

* PTC: Phosphatidylcholine

### 3.5.2. Formulation of SLNs

Fundamentally, after evaluation of all prepared formulations, the best formulations of SA-SLNs and TP-SLNs were chosen from preformulation step (Table 3.3 and Table 3.4) according to their particle size, polydispersity index, and zeta potential in addition to their physical appearance. The selected formulations from SA-SLNs were (F11, F14) which were recoded as F1 and F2 and the selected formulations from TP-SLNs were (F22, F28) which were recoded as F3 and F4.

### 3.5.3. Determination of entrapment efficacy (EE%) and drug loading (DL%) of SLNs

Entrapment efficacy (EE%) and and drug loading (DL%) were estimated using the total added drug, drug in precipitate (total drug added – free drug) and added excipients, Equations (3.5 and 3.6) (Kheradmandnia *et al.*, 2010, p.753–759).

$$EE\% = \frac{Drug\ in\ precipitate}{Total\ added\ drug} \times 100 \quad (3.5)$$

$$DL\% = \frac{Drug\ in\ precipitate}{Drug\ in\ precipitate + Added\ excipients} \times 100 \quad (3.6)$$

### 3.5.4. Physicochemical characterization tests of SLNs

#### *3.5.4.1. Particle size, polydispersity index, and zeta potential measurements*

Malvern Zetasizer Nano-ZS was used to measure the particle size, polydispersity index and zeta potential of SLNs. The samples were prepared by diluting proper volume of SLNs dispersion in distilled water of 50 μS. $cm^{-1}$ with 0.9 % NaCl constant conductivity and mixed by vortex. For each formulation three sample were prepared and analyzed at 25 °C.

#### *3.5.4.2. Morphology of SLNs*

A field emission scanning electron microscope (SEM) was used to evaluate the photomicrographs of SLNs which were taken at a voltage of 3 kV and 5.00 K X, 9.59 K X, 10.00 K X or 250 X magnification.

#### *3.5.4.3. Thermal analysis of SLNs*

Melting transitions and changes in heat capacity of the drug and solid lipids were analyzed using differential scanning calorimetry. The samples of constant amount of lyophilized SLNs dispersion were put in hermetically sealed aluminum crucibles and

purged with inert nitrogen gas at the rate of 50 mL. $min^{-1}$. Thermograms were obtained at 30-300 °C with an increase rate of 10 °C. $min^{-1}$.

#### *3.5.4.4. Infrared (FT-IR) analysis*

To check the interaction possibilities between the drug and SLNs in the four selected formulations (FT-IR) spectra were recorded at the wavelength range of 4000-500 $cm^{-1}$.

#### *3.5.4.5. XRD (X-ray diffraction)*

The X-ray diffraction analysis of the formulations prepared was carried out by exposing the samples to CuKα radiation (40kV, 20mA) and scanned from $2^o$ to $40^o$, 2θ at a scanning rate $2^o$. $min^{-1}$.

#### *3.5.4.6. $^1$H-NMR analysis*

$^1$H-NMR spectra of SLNs were obtained using deuterated chloroform as a solvent to verify the modifications in the pure RCa and SLNs during the formulation stages using a Bruker NMR equipment (500 MHz).

### 3.5.5. *In vitro* SLNs release studies

A modified dialysis bag diffusion method was used to carry out the *in vitr*o release of RCa from selected SLNs formulations. A definite dispersion volumes of the four selected RCa-SLNs formulations (F 1, F 2, F3, and F 4) that equivalent to (2 mg, 1 mg, 0.5 mg, 0.4 mg of RCa) respectively were transferred to a dialysis bag included magnet. The dialysis bag was transferred to a beaker contained 50 mL phosphate buffer of pH (6.8). The study was carried out at 37 ± 0.5 °C with a magnetic stirrer at a stirring speed of 100 rpm. 1 mL samples were taken at predetermined time intervals (0.5, 1, 2, 3, 4, 6, 8, 12, 24, and 48 hours) and the same fresh media fluid was added the main medium to maintain sink conditions. The samples were analyzed by the validated HPLC method. The study was repeated in triplicate.

### 3.5.6. Kinetics and mechanism of release

The DDSolver software program was used to investigate the release kinetics data that were obtained from *in vitro* release study of RCa-SLNs in phosphate buffer (pH6.8) (Zhang *et al.*, 2010, p.263–271).

### 3.6. Preparation of CDs Inclusion complexes

#### 3.6.1. Phase solubility studies

The phase solubility studies were carried out to investigate the proportions of both materials either (RCa or Methyl-β-CDs (M-β-CDs)) or (RCa and Captisol® (sulfabutyl ether beta-cyclodextrin)) in order to form their inclusion compounds.

##### 3.6.1.1. *Determine the phase solubility diagram of RCa / M-β-CDs*

1.331 g of M-β-CDs which equivalent to 10 x $10^{-3}$ M were added to a little amount of distilled water until completely dissolved at 25 ºC and then the volume of the solution was up to 100 mL with distilled water. This solution was used as a stock solution to prepare different concentrations of (M-β-CDs) solutions (2 x $10^{-3}$ M, 4 x $10^{-3}$ M, 6 x $10^{-3}$ M, and 8 x $10^{-3}$ M). An amount of RCa was added to each of the prepared solutions of (M-β-CDs) and mixed to form supersaturated solutions which agitated by horizontal shaker at 300 rpm and 25 ºC for 24 hours. After that, the solutions were filtered using nylon (0.45 µm) filter and analyzed by HPLC. The resulted data were used to determine the phase solubility diagram.

##### 3.6.1.2. *Determine the phase solubility diagram of RCa / Captisol®*

The study of the phase solubility diagram of RCa / Captisol® was carried out by the same method that were done to determine the phase solubility diagram of RCa / M-β-CDs. The Captisol® concentrations were (1 x $10^{-3}$ M, 2 x $10^{-3}$ M, 3 x $10^{-3}$ M, 4 x $10^{-3}$ M, and 5 x $10^{-3}$ M).

#### 3.6.2. Preparation of RCa / M-β-CDs and RCa / Captisol® inclusion complexes

Two different methods: kneading method and modified lyophilization method were carried out to prepare the inclusion complexes of RCa/M-β-CDs which were coded as (F1, F2, and F3) and RCa/Captisol® inclusion complexes which in turn were coded as (F4, F5, and F6). The RCa/CDs (1: 1) molar ratio that obtained from the RCa / M-β-CD and RCa / Captisol® phase solubility studies, was used in the preparation of RCa/CDs inclusion complex formulations.

##### 3.6.2.1. *Kneading method*

The desired amounts of RCa and CDs (M-β-CDs or Captisol®) were weighted in a ratio of (1:1) molar. Mortar and pestle were used to prepare a homogenous paste of CDs by adding small quantities of (water: ethanol) mixture (1: 1) or pure distilled water. RCa

powder was added to the CDs homogenous paste in portions and with continuous kneading for about three hours. During kneading a suitable amount of (water: ethanol) (1: 1) mixture or distilled water was added to maintain the paste consistency. The homogenous paste was dried in air shadow at 25 $^{o}$C for 48 hours. The dried CDs complexes were triturated and passed through sieve (No. 100) and stored in a hermetic glass bottle Table 3.5 (Ai *et al*., 2014, p.1115-1123).

### 3.6.2.2. *Lyophilization method*

A definite amount of CDs (M-β-CDs or Captisol®) which equivalent to one molar, were added to 50 mL of distilled water and mixed to form homogeneous solutions. An accurate quantity of RCa which also equivalent to one molar was added to the CDs solutions to form (RCa / M-β-CD or RCa / Captisol®) solutions of (1: 1) molar concentration. The (RCa / CDs) solutions were mixed thoroughly at 25 $^{o}$C using a horizontal shaker at 300 rpm for 24 hours. After that, the (RCa / CDs) solutions were centrifuged at 1500 rpm for 15 minutes and filtered using 0.45 µm nylon filter. Trehalose (5 %) was added to the obtained cleared solutions and mixed well. The final (RCa / CDs) solutions were freezed and dried by lyophylization dryer at – 120 ± 0.5 $^{o}$C for 24 hours. The dried powders were collected, filled in tightly closed containers and stored in a suitable place Table 3.5 (Ai *et al*., 2014, p.1115-1123).

**Table 3.5.** *Compositions and Methods of Preparation of RCa/CDs Inclusion Complexes.*

| Code | RCa (mole) | M-β-CDs (mole) | Captisol® (mole) | Ethanol 99.8% | Bidistilled water | Method of Preparation |
|---|---|---|---|---|---|---|
| **F1** | 1 | 1 | - | + | + | Kneading Method |
| **F2** | 1 | 1 | - | - | - | Kneading Method |
| **F3** | 1 | 1 | - | - | 50 (mL) | Lyophilization Method |
| **F4** | 0.5 | - | 0.5 | + | + | Kneading Method |
| **F5** | 0.5 | - | 0.5 | - | - | Kneading Method |
| **F6** | 0.5 | - | 0.5 | - | 50 (mL) | Lyophilization Method |

### 3.6.3. Determination of Drug content (DC) %

In order to determine the amount of drug RCa loaded (DC %) in the prepared CDs inclusion complexes, 1 mg of the formula was dissolved in 1 mL of mobile phase and the

resulting solution was diluted with mobile phase to proper concentration and analyzed under HPLC operating conditions. Equation 3.4 was used for the calculation of (DC %):

$$\text{DC\%} = \frac{The\ amount\ of\ drug\ (RCa)\ in\ CDs\ complexes}{actual\ (RCa)\ amount\ used\ in\ formulation} \times 100 \qquad (3.4)$$

### 3.6.4. Physicochemical Characterization of CDs inclusion complexes

#### 3.6.4.1. *Particle size, polydispersity index, and zeta potential of CDs inclusion complexes*

The particle size and zeta potential measurements of CDs inclusion complexes were carried out using Malvern Zetasizer Nano-ZS. The preparation of samples for analysis was accomplished by diluting proper amounts of dry CDs complexes in distilled water adjusted to a constant conductivity of 50 μS. $cm^{-1}$ with 0.9 % NaCl and completely mixed using vortex. All analyses were repeated in triplicate at 25 °C.

#### 3.6.4.2. *Morphology of CDs inclusion complexes*

Photomicrographs of the samples were taken using a scanning electron microscope (SEM) at a voltage of 3 kV and 5.00 K X, 9.59 K X, 10.00 K X or 250 X magnification.

#### 3.6.4.*3. Thermal analysis of CDs inclusion complexes*

Thermal analyzes of CD inclusion complexes prepared by different methods were carried out by using DSC device. The samples were put in the aluminum cells which were tightly closed by pressure. A nitrogen flow rate of 50 mL. $min.^{-1}$, was applied to the aluminum reference at a temperature range of 30-300 ºC with a temperature increase of 10ºC. $min^{-1}$.

#### 3.6.4.4. *FT-IR analysis of CDs inclusion complexes*

The CDs complexes (FT-IR) spectra were recorded by FT-IR spectrophotometer at the wavelength range of 4000-500 $cm^{-1}$.

#### 3.6.4.5. *XRD analysis CDs inclusion complexes*

The X-ray diffraction analysis of the CDs inclusion complex formulations prepared was carried out by exposing the samples to CuKα radiation (40kV, 20mA) and scanned from $2^o$ to $40^o$, 2θ at a scanning rate $2^o$. $min^{-1}$.

#### 3.6.4.6. *$^1$H-NMR analysis of CDs inclusion complexes*

$^1$H-NMR spectra were obtained using a Bruker NMR instrument (500 MHz) (USA). In this work, CDs inclusion complexes samples were prepared using deuterated DMSO.

### 3.6.5. *In vitro* drug release studies for the CDs inclusion complexes

The dissolution test for the CDs inclusion complexes was carried out using a modified dialysis bag diffusion method. Accurate amount of the CDs inclusion complex formulations which equivalent to 2 mg of RCa were transferred to a dialysis bag included capsule magnet. The dialysis bag was transferred to a beaker contained 50 mL phosphate buffer of pH (6.8). The study was carried out at 37 ± 0.5 °C with a magnetic stirrer at a stirring speed of 100 rpm. One mL was taken as a sample at predetermined time intervals (0.5, 1, 2, 3, 4, and 6 hours) and replaced by the same fresh media fluid to maintain sink conditions. The samples were analyzed by the validated HPLC method. The study was repeated in triplicate.

### 3.6.6. Investigation of similarity of dissolution profiles for CDs inclusion complexes

Statistically, two methods named as $f_1$ (difference factor) and $f_2$ (similarity factor), which are accepted as official authorities, have been developed to evaluate whether the dissolution profiles are "close enough" (Shah *et al.*, 1998, p.889–896). DDSolver software program was used to calculate the similarity factor values of the CDs inclusion complexes dissolution rate profiles according to Equation 3.7 (Zhang *et al.*, 2010, p.263–271).

$$f_2 = 50 \log \left\{ \left( \sqrt{1 + \frac{1}{n} \sum_{t=1}^{n} (R_t + T_t)^2} \right)^{-1} \times 100 \right\} \quad (3.7)$$

### 3.6.7. Solubility study of RCa in CDs inclusion complexes

Excess amounts of each CDs inclusion complex formulations and physical mixture (RCa / M-β-CD and RCa / Captisol®) were added separately to 2 mL of distilled water to form supersaturated solutions which thoroughly mixed using vortex for 5 minutes at 25 °C. The formed supersaturated solutions were filtered using polyamide 0.45 μm filter and the supernatants were diluted and analyzed using the validated HPLC method. The study was repeated in triplicate for each formulation. The solubility of RCa was calculated in molar concentration.

## 3.7. Preparation of Cyclodextrin-Poly(anhydride) Nanoparticles (CDs-PAD NPs)

### 3.7.1. Preformulation studies

After characterization test of CDs inclusion complex formulations, the best formulation of each CDs derivatives (M-β-CD and Captisol®) (F2 and F6) were selected

and used to coat them by Poly (methyl vinyl ether-co-maleic anhydride) (PAD) i.e. formulations of (CDs-PAD NPs). F1 (CDs-PAD) was prepared by using (F2-M-β-CD) and F2 was prepared by using (F6-Captisol®). Different amounts of formulations which included an accurate concentration of RCa were used in preformulation step to get the optimal RCa concentration for preparation the (CDs-PAD NPs). The poly(anhydride) amount also was varied between (100 to 200 mg) which was dissolved in 5 mL of acetone. The technique of preparation was the same in each experiment.

### 3.7.2. Formulation of (CDs-PAD NPs)

The CD-PAD NPs were prepared using solvent displacement modified method (Agüeros *et al*., 2011, p.721-734). An accurate quantity of CDs inclusion complex formulations which equivalent to 10 mg RCa was added to the PAD acetone solution which was prepared by adding 200 mg of PAD to 5 mL acetone then, thoroughly mixed using a magnetic stirrer at 300 rpm for an hour at room temperature. 20 mL of the water: ethanol (1 :1) solution were dropped gently to the (CDs-PAD) suspension with continuous stirring for 30 minutes. The organic solvents (acetone and ethanol) were evaporated using a rotary evaporator at 160 bar vacuum pressure and 45 ± 0.5 °C. The obtained suspension centrifuged at 11000 rpm at room temperature for 20 minutes. After that, the supernatant was disposed and 10 mL of distilled water were added to the dispersion and centrifuged another time to clean the dispersion from free RCa and organic solvents. The cleaning process was repeated two times and the 5 % trehalose was added to the dispersion and mixed well. The dispersion was placed in refrigerator at – 84 °C for 24 hours and dried by using lyophilization technique at – 120 ± 0.5 °C for 48 hours to get the final powder product of CDs-PAD NPs.

### 3.7.3. Determination of drug content (DC) % of CDs-PAD NPs

The actual amount of RCa in CDs-PAD NPs was investigated by taking 4 mg of each CDs-PAD NPs formulation and added them to 2 mL of mobile phase and mixed well using a magnetic stirrer at 300 rpm for 15 minutes. The obtained dispersion was filtered using 0.2 μm nylon filter, and the RCa in the filtrate was analyzed using the validated HPLC method. The equation 3.4 was used for calculating the amount of RCa in (CDs-PAD NPs) and the analysis was repeated in triplicate.

### 3.7.4. Physicochemical properties of CDs-PAD NPs

#### 3.7.4.1. *Particle size, polydispersity index, and zeta potential of CDs-PAD NPs*

The particle size and zeta potential measurements of CDs-PAD NPs were carried out using Malvern Zetasizer Nano-ZS. The analysis samples were prepared by weighting one mg of each dry CDs-PAD NPs formulations which were added to bidistilled water adjusted to a constant conductivity of 50 μS. $cm^{-1}$ with 0.9 % NaCl and suspended completely for several minutes using vortex. All analyses were repeated in triplicate at 25 °C.

#### 3.7.4.2. *Morphology*

A scanning electron microscope (SEM) was used to evaluate the photomicrographs of CDs-PAD NPs which were taken at a voltage of 3 kV and 5.00 K X, 9.59 K X, 10.00 K X or 250 X magnification.

#### 3.7.4.3. *Thermal analysis of CDs-PAD NPs*

Thermal analyzes of CDs-PAD NPs were carried out by using DSC device. The samples were put in the aluminum sample containers which were tightly closed by pressure. A nitrogen flow rate of 50 mL. $min^{-1}$, was applied to the aluminum reference at a temperature range of 30-300 ºC with a temperature increase of 10ºC. $min^{-1}$.

#### 3.7.4.4. *FT-IR analysis of CDs-PAD NPs*

To check the interaction possibilities between the drug and CDs and PAD in the end product, (FT-IR) spectra were recorded at the wavelength range of 4000-500 $cm^{-1}$.

#### 3.7.4.5. *XRD of CDs-PAD NPs*

The X-ray diffraction analysis of the formulations prepared was carried out by exposing the samples to CuKα radiation (40kV, 20mA) and scanned from $2^o$ to $40^o$, 2θ at a scanning rate $2^o$. $min.^{-1}$.

#### 3.7.4.6. *$^1$H-NMR analysis of CDs-PAD NPs*

$^1$H-NMR spectra of CDs-PAD NPs were obtained using deuterated chloroform as a solvent to verify the modifications in the pure RCa and CDs-PAD NPs during the formulation stages using a Bruker NMR equipment (500 MHz).

### 3.7.5. *In vitro* release studies of RCa of CDs-PAD NPs

A definite quantity of the CDs-PAD NPs formulations which equivalent to 2 mg of RCa were transferred to a dialysis bag included magnet. The dialysis bag was put in a

beaker contained 50 mL phosphate buffer of pH (6.8). The experiment was carried out at 37 ± 0.5 °C with a magnetic stirrer at a stirring speed of 100 rpm. 1 mL samples were taken at predetermined time intervals (0.5, 1, 2, 3, 4, 6, 8, and 24 hours). The same and fresh media fluid was added to the main medium to maintain sink conditions. The samples were analyzed by the validated HPLC method. The study was repeated in three times.

### 3.7.6. Kinetics and mechanism of release of CDs-PAD NPs

To analyze the kinetics of drug (RCa) release from CDs-PAD NPs, the data obtained from *in vitro* drug release studies in phosphate buffer (pH 6.8) were analyzed by DDSolver software program (Zhang *et al.*, 2010, p.263–271).

## 3.8. Cell Culture and Cytotoxicity Studies

Caco-2 cell line was used for cell viability and migration experiments in cell culture studies. The Caco-2 cells used in the experiments had a passage number range of 25-30 and were incubated at 37 ° C in an atmosphere containing 5% carbon dioxide. The effects of the formulations on Caco-2 cell viability were investigated by MTT method. The formulations to be applied in permeability studies were determined according to the results of cell viability tests in which these formulations were examined in the Caco-2 cell monolayer model in permeability studies.

Dulbecco's Modified Eagle's Medium (DMEM) was prepared for the growth of Caco-2 cells. The whole culture medium was contained 10% (v / v) fetal bovine serum (FBS), 2 mM L-glutamine, 50 units/mL penicillin and 50 μg/mL streptomycin. HBSS pH 7,4 containing 10 mM HEPES was used for transient studies.

### 3.8.1. Growth of Caco-2 cells

The vial containing Caco-2 cells was taken from a nitrogen tank at -180 °C and submerged in a water bath at 37 °C. A 15 mL vial containing the complete culture medium was emptied in a slightly vial laminar flow chamber. After the tube was centrifuged for 3 minutes at 2000 rpm, the supernatant from the tube was carefully drained and the precipitated cells were dispersed in fresh culture medium and transferred to cell culture flasks. These flasks were incubated at 37 °C in a humidified atmosphere containing 5% carbon dioxide and growth of the cells was monitored under a microscope. The environment of the cells was changed day after day and after about 5 days, passivation was performed when the cell density in the flask reached about 80-90%. For this purpose, the medium on the cells was discarded and the cells were washed twice with phosphate

buffer solution (PBS). The cells were then separated from the vaccine using trypsin-EDTA solution (0.05% trypsin, 0.02% w / v EDTA). Cells separated from the flask surface were pipetted, 15 mL of the complete culture medium in the tube was added and centrifuged at 2000 rpm for 3 minutes. At the end of the centrifugation, the medium above the cells that had been settled was discarded. The cells were suspended in fresh culture medium and the suspension was transferred to new flasks and incubated in an incubator. The cell count method was used with trypan blue to determine the number of cells to be used for cell viability and migration studies. For this purpose, the cell suspension was diluted 2 folds with trypan blue and the suspension was counted on a hemocytometer under microscope and the number of cells in mL was calculated.

### 3.8.2. *In vitro* cell viability studies

The Caco-2 cells were removed from the flask with trypsin-EDTA and centrifuged with the complete culture medium, after which the cells were suspended in fresh culture medium. This cell suspension is counted by trypan blue method and the number of cells in mL is determined and added to 100 µL per hole of 96-hole plate which were 5000 cells in total culture medium. Cells were left to hold onto the plate surface for a night. The following day, placebo and the active ingredient solution which prepared using DMSO were added to holes of the whole culture medium in serial dilutions. Furthermore, serial dilutions containing 0.5% DMSO were added to whole culture medium as controls. After the plates were allowed to incubate in 5% $CO_2$ at 37 °C for 24 hours, 25 µL MTT (1 mg. $mL^{-1}$) was added to the holes and incubated for 4 hours at 37 °C. At the end of the period, the plate was discarded and 200 µL of DMSO was added to the holes and the absorbance at 570 nm was read with a microplate reader. The cell viability (%) was calculated according to Equation 3.8 (Yong *et al.*, 2016, p.651–657).

$$\text{Cell viability (\%)} = \frac{number\ of\ viable\ cells/mL\ (sample)}{average\ number\ of\ viable\ cells/\ mL\ (control)} \times 100 \qquad (3.8)$$

### 3.8.3. *In-vitro* permeation studies

#### 3.8.3.1 *Preparing cells for permeability studies*

The replicated Caco-2 cells were counted with trypan blue and the inserts (ThinCert ™, 12 holes, 1.0 µm por diameter) were added as cell suspensions were 60,000 cells / insert. 0.5 mL was placed in the apical part of the inserts used and 1 mL in the basolateral part of the used inserts. Cells were incubated with 5% $CO_2$ at 37 °C. For the first three

days, the cells were allowed to grow without any treatment. Then the environment of the cells was changed day after day. At the end of 21 days, TEER (transepithelial electrical resistance) measurements of Caco-2 cells in the inserts were performed using Millicell - ERS epithelial voltmeter and monolayer integrity was verified. TEER values were calculated using the following Equation (3.9):

$$TEER_{\text{cell single layer}} = (R_{\text{sample}} - R_{\text{empty}}) \times A \quad (3.9)$$

$R_{\text{sample}}$ = measured resistance

$R_{\text{empty}}$ = resistance of control inserts without cells

A = surface area of cell culture insert ($cm^2$)

**3.8.3.2.** ***RCa permeability studies***

Permeability studies were performed after confirmation of monolayer integrity TEER measurements of Caco-2 cells grown for 21 days. Before applying the formulations, apical and basolateral compartments were added to pH 7.4 HBSS solution containing 10 mM HEPES and incubated for 30 minutes in this medium. Then these environments were thrown away. The formulations were prepared in HBSS containing 0.5 µM DMSO which contain 50 µM of RCa and were applied at a rate of 0.5 mL to the apical portion of the inserts. The formulations employed are: formulations (CDs inclusion complex F3 and F6, CDs-PAD NPs F1 and F2, and SLNs F2) and the solution of RCa active substance. The basolateral portion was supplemented with 1 mL of pH 7.4 HBSS containing 10 mM HEPES. Plates were placed in a horizontal shaker and incubated at 37 °C for 2 hours at 60 rpm. Two hours later, 1 mL samples were taken from the basolateral side and the samples were stored at -20 °C. The samples stored at -20 °C were then dissolved and analyzed by HPLC.

The calculation of the apparent permeability coefficient ($P_{app}$) for the pure RCa and studied formulation was carried out using the following Equation (3.10)

$$P_{app}\ (cm.sec^{-1}) = V\ \text{basolateral}\ (cm^3) \times C\ \text{basolateral} / (A \times C_0 \times T(sec)) \quad (3.10)$$

Where $P_{app}$ is an apparent permeability coefficient, V basolateral is a volume of basolateral, C basolateral is a receiver concentration, A is the surface area of the filter ($cm^2$), $C_0$ is donor concentration and T is the time in seconds (Blaser, 2007, p.25–34).

### 3.9. Formulation Stability Studies

The stability studies were applied on three formulations which had the best permeability test results F1 (CDs-PAD) and F2 (CDs-PAD), and SLNs-F2). Drug content DC %, particle size, polydispersity index PDI, and zeta potential were studied during three months. The prepared formulations were stored at temperature conditions of 25 ± 1 ° C, 4 ± 1 ° C and 40 ± 1 ° C for stability studies at certain periods (first day, $30^{th}$ day, $60^{th}$, and $90^{th}$ day). The stability studies for drug content, particle size, polydispersity index, and zeta potential were repeated in triplicate at every time for every condition.

### 3.10. *In Vivo* Studies (Pharmacokinetic Studies)

Pharmacokinetic studies were performed on male (Spraque Dawley) rats to evaluate the effectiveness of the SLN-F2 and F2 (CD-PAD) formulations in ameliorating oral bioavailability of RCa. The rats were divided into three groups of five animals, where the first group was given 2.2 $mg.kg^{-1}$ as standard RCa aqueous suspension and the second and third groups were given SLN-F2 and F2 (CD-PAD) formulations of the same dose, respectively using 75 mm round tip gavage. The pure drug and formulations were given orally to animals, using 18-gauge oral-feeding needle. The animals were anesthetized using ketamine (90 mg/kg) as anesthetic agent and xylazine (10 mg/kg) as muscle relaxant. The blood samples (0.5 mL) were withdrawn from the rat's tail at 0.5, 1, 2, 4, 6, 9, 24, 48, and 72 hours into eppendorf tubes containing anticoagulant agent (heparin) (Kumar *et al.*, 2006, p.881–887).

Rats (250-300 g) were obtained from the Eskişehir Osmangazi University, Medical and Surgical Experimental Animals Implementation and Research Center (MSEAIRC). The animals were maintained in a room with controlled temperature (22 ± 2 °C) for a light/ dark photoperiod of 12:12, with free access to food and water. Before each experiment, in order to avoid a possible interaction with food, the animals received only water for 12 h. Animal care and research protocols were based on the principles and guidelines adopted in the Guide for the Care and Use of Laboratory Animals (NIH Publication No: 85- 23, revised in 1985) and were approved by the local ethics committee of Eskişehir Osmangazi University (Appendix 1).

### 3.10.1. Samples preparation (liquid-liquid extraction) for bioanalysis

A modified liquid-liquid extraction method was used for sample preparation (Kumar *et al.*, 2006, p.881–887). The tubes containing blood sample were centrifuged at 5000 rpm for 10 min at 25 ± 1 ℃. Two mL acetonitrile (ACN) were added to the separated plasma. The samples were vortexed for 2.5 min followed by sonication for 5 minutes in sonication bath and then centrifuged at 4500 rpm for 10 min. The supernatant was separated and samples were reconstituted using 200 µL mobile phase for analysis by HPLC. Figure 3.1 is shown the pharmacokinetic study steps.


**Figure 3.1.** *Pharmacokinetic Studies of Pure RCa, SLN-F2 and F2 (CD-PAD) Formulations on Rat*

# 4. RESULTS

## 4.1 Validation Studies

### 4.1.1. Validation process for analysis of *in vitro* studies

The results obtained from the validation study were evaluated under the titles of linearity, accuracy, precision, working range, selectivity, sensitivity, robustness/ consistency and system suitability test.

#### 4.1.1.1. *Linearity*

Solutions of RCa were prepared in the mobile phase and analyzed by HPLC. Concentrations of (1, 5, 10, 30, 50, 80, and 100) µg. $mL^{-1}$ of RCa were used in the study. The linearity graph was plotted using area under the curve (AUC) versus concentrations. The linearity was examined by using the least square regression equation. The standard RCa chromatogram is shown in Figure 4.1 and the AUC values obtained by HPLC analysis for the standard RCa concentrations are shown in Table 4.1.

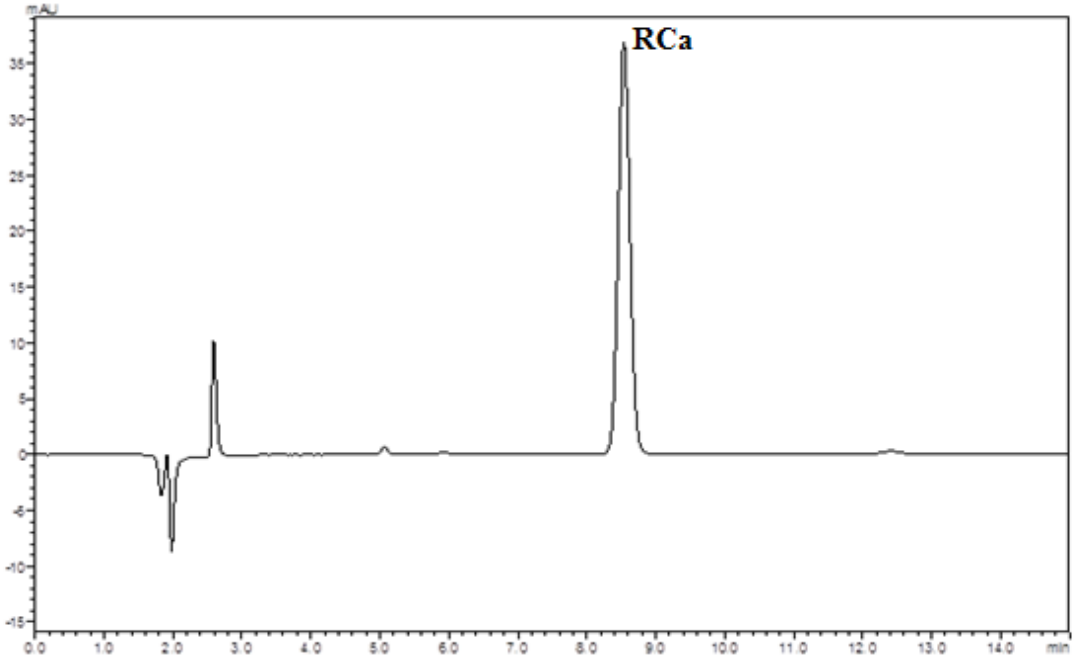


**Figure 4.1**. *Chromatogram of Standard RCa*

**Table 4.1.** *AUC Values Obtained by Standard RCa HPLC Analysis*

| RCa Concentrations µg. mL$^{-1}$ | Area Under the Curve (AUC) | | | |
|---|---|---|---|---|
| | 1.Set | 2. Set | 3. Set | Mean ± SE |
| **1** | 55296 | 54198 | 52274 | 53922.67 ± 883.17 |
| **5** | 234101 | 253639 | 264858 | 250866.00 ± 8986.38 |
| **10** | 508557 | 521160 | 508594 | 512770.33 ± 4194.84 |
| **30** | 1482834 | 1494637 | 1540997 | 1506156.00 ± 17750.57 |
| **50** | 2515060 | 2514528 | 2597368 | 2542318.67 ± 27525.09 |
| **80** | 4004548 | 4176433 | 4096775 | 4092585.33 ± 49663.12 |
| **100** | 4928813 | 5031438 | 5103277 | 5021176.00 ± 50624.11 |

The right equation in the result of the work done is y = 50538.71 *x* + 4444.51 and regression square is $r^2$ = 0.9998. The linearity graph is shown in Figure 4.2.

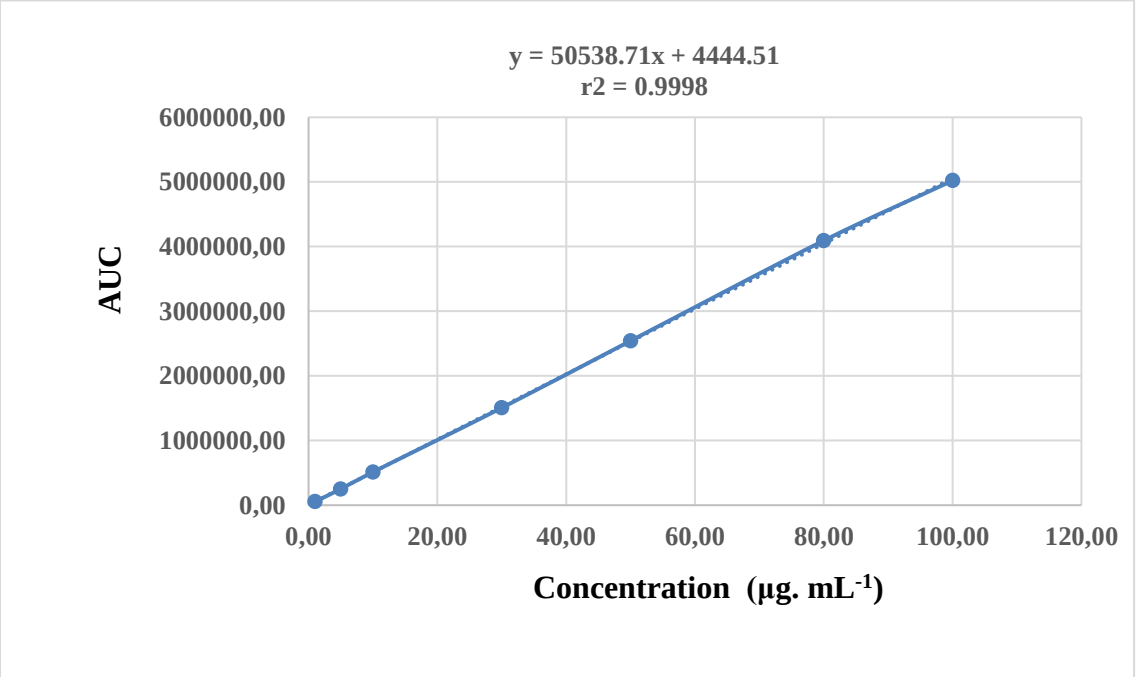


**Figure 4.2.** *Calibration Curve and Linearity Equation of Standard RCa*

#### 4.1.1.2. *Range*

The range of analytical method was studied in this limit of concentration (1- 200 µg. $mL^{-1}$). The calibration curve was selected at the concentration limit (1-100 µg. $mL^{-1}$).

#### 4.1.1.3. *Accuracy*

Three different concentrations known to be (1, 50, and 100) µg. $mL^{-1}$ of active substance RCa were prepared for 3 repetitions for each concentration. The results obtained were calculated using the linearity equation and the correctness of the method was calculated as % recovery by comparison with known concentrations. Acceptance interval of % recovery for accuracy, is ± 2 %. According to the obtained results, it has been proved that the method is suitable for recovery and accuracy. The results are presented in Table 4.2.

**Table 4.2.** *Recovery % of Standard RCa Analysis by HPLC*

| **Day 1 ($n$ = 3)** | **Added (µg. $mL^{-1}$)** | **1** | **50** | **100** |
|---|---|---|---|---|
| | **Found (mean ± SD)** | 0.9925 ± 0.01630 | 50.7289 ± 0.1977 | 101.7392 ± 0.8027 |
| | **Recovery%** | 99.2517 | 101.4578 | 101.7392 |
| | **SD** | 1.6304 | 0.3954 | 0.8027 |
| | **SE(M)** | 0.9413 | 0.2283 | 0.4634 |
| | **RSD%** | 1.6427 | 0.3897 | 0.7890 |
| **Day 2 ($n$ = 3)** | **Added (µg. $mL^{-1}$)** | **1** | **50** | **100** |
| | **Found (mean ± SD)** | 1.0065 ± 0.0025 | 49.1965 ± 0.1182 | 98.2399 ± 0.9742 |
| | **Recovery%** | 100.6467 | 98.3931 | 98.2399 |
| | **SD** | 0.2547 | 0.2365 | 0.9742 |
| | **SE(M)** | 0.1470 | 0.1365 | 0.5624 |
| | **RSD%** | 0.2530 | 0.2403 | 0.9916 |
| **Day 3 ($n$ = 3)** | **Added (µg. $mL^{-1}$)** | **1** | **50** | **100** |
| | **Found (mean ± SD)** | 0.9900 ± 0.0061 | 50.6535 ± 0.2362 | 99.0957 ± 0,4916 |
| | **Recovery%** | 99.0005 | 101.3070 | 99.0957 |
| | **SD** | 0.6062 | 0.4723 | 0.4916 |
| | **SE(M)** | 0.3500 | 0.2727 | 0.2838 |
| | **RSD%** | 0.6123 | 0.4662 | 0.4961 |

#### 4.1.1.4. *Precision*

The measurement of repeatability (intra-day) and intermediate precision (inter-days) was done to verify the precision of the analysis method. Standard solution of RCa at concentrations of (1, 50 and 100 $\mu$g. mL$^{-1}$) were analyzed on three successive days, six times in a day. The calculated RSD value is lower than 2% deviation from the nominal value of precision for RCa standard solution. This indicates that the current method is highly precise and analytically acceptable. The statistical evaluation is shown in Tables 4.3, 4.4, and 4.5.

**Table 4.3.** *Results of Standard Precision Study for Standard RCa 1 µg. mL$^{-1}$*

| 1 µg. mL$^{-1}$ | Intra-day (n = 6) | | | Inter-day (n = 18) |
|---|---|---|---|---|
| | 1.Day | 2. Day | 3. Day | |
| **Average** | 52689.00 | 54886.00 | 55463.00 | 54346.00 |
| **Standard Deviation** | 504.11 | 599.47 | 140.63 | 414.74 |
| **Standard Error** | 205.80 | 244.73 | 57.41 | 169.32 |
| **RSD** | 0.96 | 1.09 | 0.25 | 0.77 |

**Table 4.4.** *Results of Standard Precision Study for Standard RCa 50 µg. mL$^{-1}$*

| 50 µg. mL$^{-1}$ | Intra-day (n = 6) | | | Inter-day (n = 18) |
|---|---|---|---|---|
| | 1.Day | 2. Day | 3. Day | |
| **Average** | 2454883.67 | 2467441.00 | 2564406.00 | 2495576.89 |
| **Standard Deviation** | 5514.60 | 17008.34 | 11935.23 | 11486.05 |
| **Standard Error** | 2251.32 | 6943.62 | 4872.54 | 4689.16 |
| **RSD** | 0.22 | 0.60 | 0.47 | 0.46 |

**Table 4.5.** *Results of Standard Precision Study for Standard RCa 100 µg. mL$^{-1}$*

| 100 µg. mL$^{-1}$ | Intra-day (n = 6) | | | Inter-day (n = 18) |
|---|---|---|---|---|
| | 1.Day | 2. Day | 3. Day | |
| **Average** | 5162880.76 | 4969363.67 | 5012611.00 | 5048285.11 |
| **Standard Deviation** | 18962.90 | 49232.19 | 24844.98 | 31013.36 |
| **Standard Error** | 7741.57 | 20098.96 | 10142.92 | 12661.15 |
| **RSD** | 0.37 | 0.99 | 0.50 | 0.62 |

#### 4.1.1.5. *Specificity*

Analyzes of RCa and the placebo solutions of the formulations in mobile phase for specificity studies which were performed by HPLC operating method. The chromatograms of the placebo solutions showed that there were no interfering peaks at the retention time of RCa (Retention Time = Rt = 8.71 minutes), so the HPLC operating method was confirmed to be specific for RCa. The chromatograms related to specificity are shown in Figure 4.3.

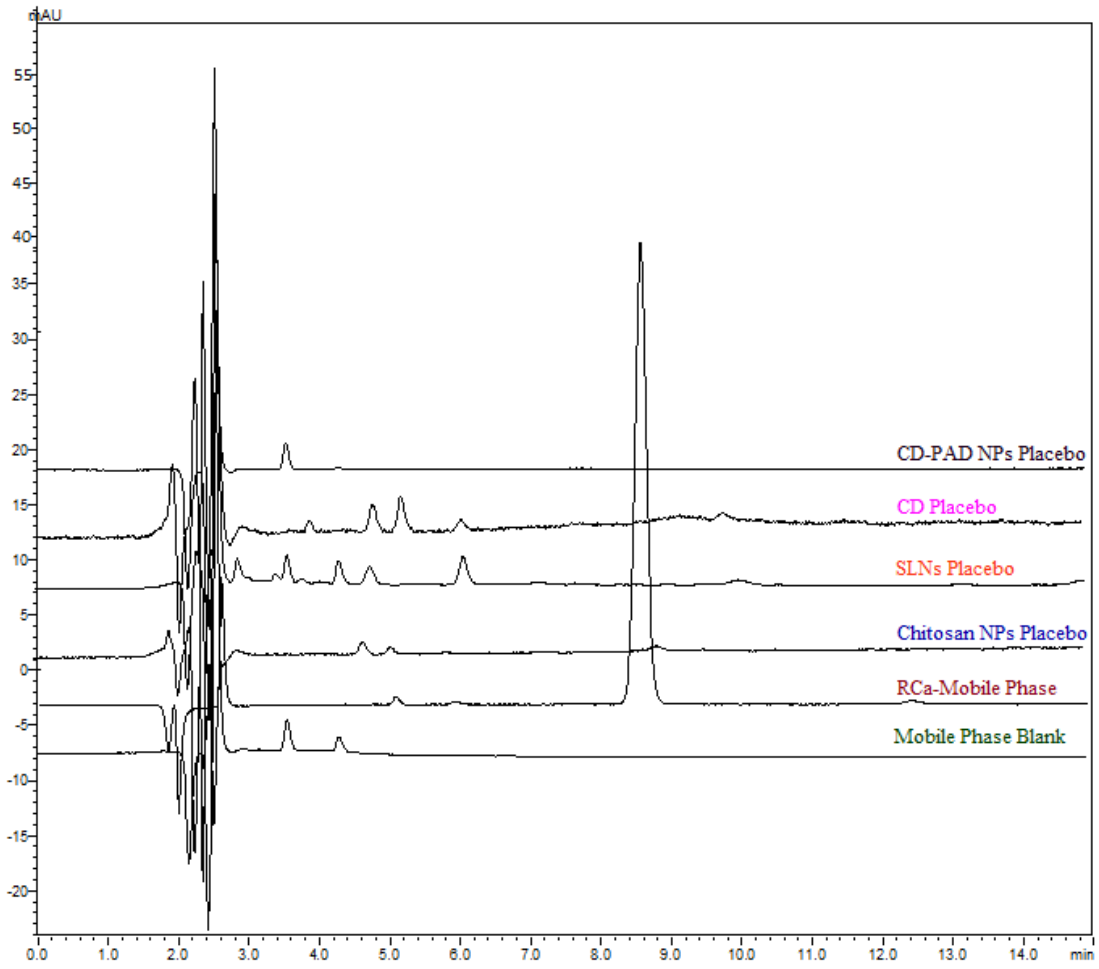


**Figure 4.3.** *Chromatograms of Analyzes of the Selectivity Studies*

#### 4.1.1.6. *Sensitivity*

The sensitivity of the HPLC operating method was determined by evaluation of LOD and LOQ. The LOD and LOQ were calculated by using equations (3.1 and 3.2) which were mentioned in section (3.1.7). LOD is 0.3340 µg. $mL^{-1}$ and LOQ is 1.0120 µg. $mL^{-1}$. The smallest concentration that can be measured with acceptable accuracy and precision for the sensitivity of the method is 1 µg. $mL^{-1}$ and the calculated LOD value is below this value. These results show that the method is sensitive.

#### 4.1.1.7. *System suitability test*

The system suitability test of the HPLC operating method was evaluated by lab. solution software. The results of the studied parameters are shown in Table 4.6. (U.S.P, 2016, p.463–468).

**Table 4.6.** *HPLC System Suitability Test Parameters*

| Parameters | RCa | Recommended value |
|---|---|---|
| **Theoretical Plate (N)** | 11.510.521 | >2000 |
| **Retention time** | 8.71 | |
| **Tailing factor** | 1.084 | < 2 |
| **Asymmetry factor** | 1.082 | $0.95<A_S< 1.2$ |
| **Capacity factor** | 2,297 | 2<K< 10 |

**Reference**: *U.S.P, 2016, p.463–468*

### 4.1.2. Validation process for permeability studies

For permeability studies, another HPLC analysis method validation was carried out by the same condition of the validation method in section (4.1.1). The only different was in the sample preparation co-solvent where HBSS and 2 % DMSO solution were used as co-solvent at pH 7.4 for standard RCa during validation study.

The results obtained from the validation study were evaluated under the titles of linearity, accuracy, precision, working range, selectivity, sensitivity, and system suitability test.

#### 4.1.2.1. *Linearity*

Solutions of RCa were prepared in the (HBSS + 2 % DMSO) solution and analyzed by HPLC. Concentrations of (1, 5, 10, 15, 20, and 25) µg. $mL^{-1}$ of RCa were used in the study. The linearity graph was plotted using AUC versus concentrations. The linearity was studied by using the least square regression equation. The standard RCa chromatogram is illustrated in Figure 4.4 and the AUC values obtained by HPLC analysis for the standard RCa concentrations are shown in Table 4.7.

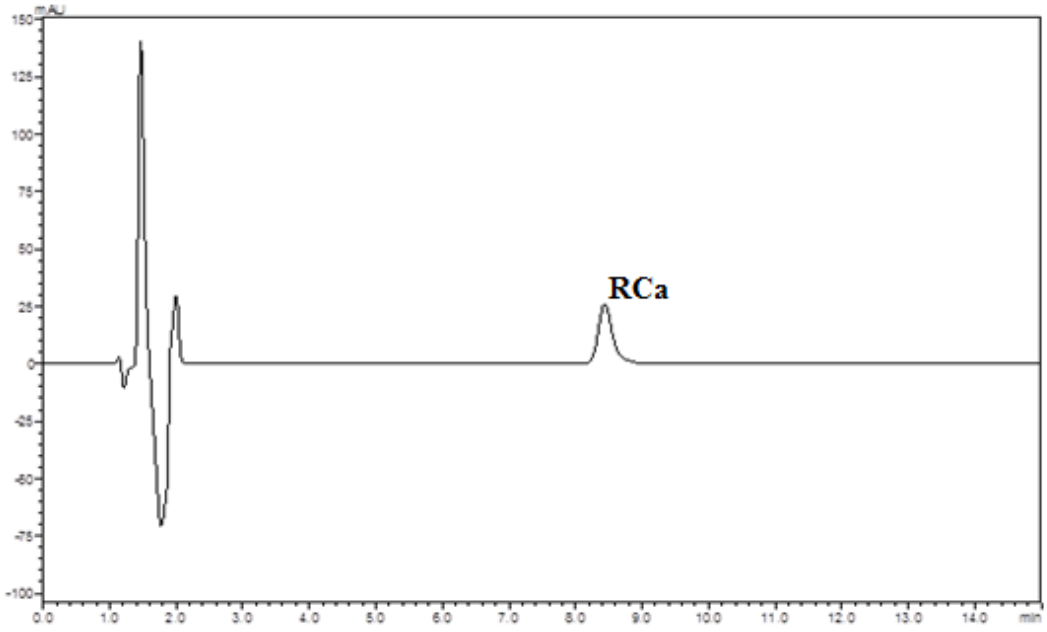


**Figure 4.4.** *Chromatogram of Standard RCa in HBSS + 2 % DMSO Solution*

**Table 4.7.** *AUC Values Obtained by Standard RCa HPLC Analysis in HBSS + 2 % DMSO Solution*

| RCa Concentrations µg. mL$^{-1}$ | AUC | | | |
|---|---|---|---|---|
| | 1.Set | 2. Set | 3. Set | Mean ± SE |
| 1 | 45034 | 46605 | 44374 | 45337.67 ± 661.69 |
| 5 | 220172 | 227534 | 221868 | 223191.33 ± 2225.85 |
| 10 | 447773 | 452054 | 457202 | 452343.00 ± 2725.75 |
| 15 | 665976 | 686362 | 682252 | 678196.67 ± 6224.46 |
| 20 | 886054 | 901441 | 906227 | 897907.33 ± 6085.57 |
| 25 | 1123202 | 1137211 | 1133685 | 1131366.00 ± 4206.99 |

The right equation in the result of the study done is y = 45180 *x* – 886.78 and regression square is $r^2$ = 1. The linearity graph is demonstrated in Figure 4.5.

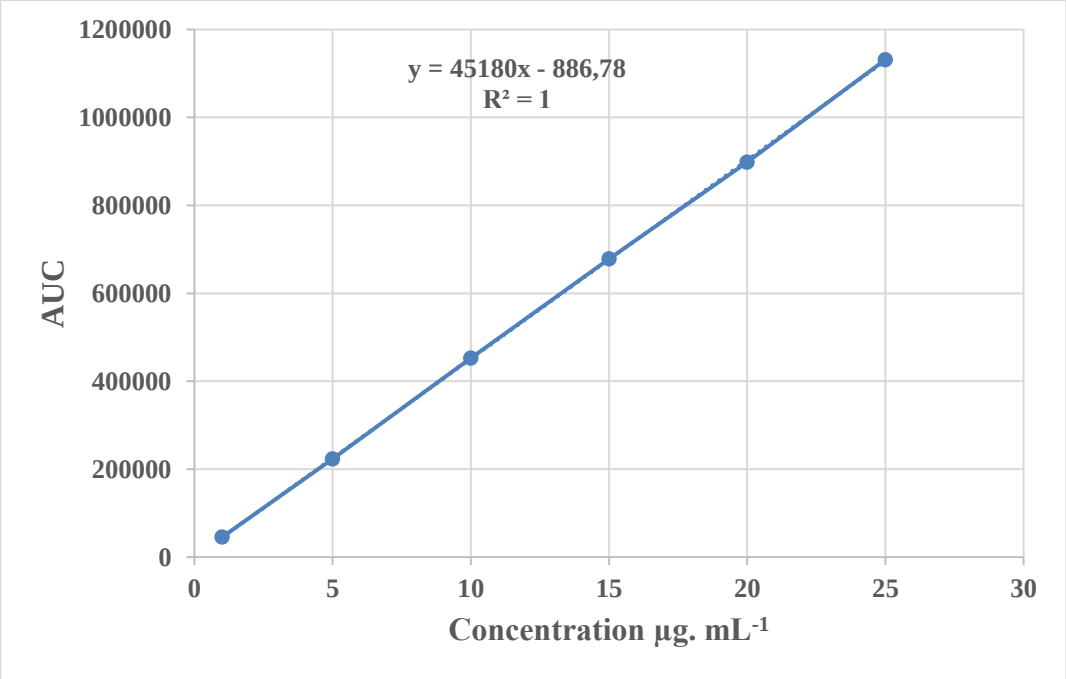


**Figure 4.5.** *Calibration Curve and Linearity Equation of Standard RCa in HBSS + 2 % DMSO Solution*

#### 4.1.2.2. *Range*

The range of analytical method was studied in this limit of concentration (0.1- 25 µg. $mL^{-1}$). The calibration curve was selected at the concentration limit (1-25 µg. $mL^{-1}$).

#### 4.1.2.3. *Accuracy*

The accuracy study was carried out by selecting three concentrations (1, 10, and 25 µg. $mL^{-1}$) of active substance RCa in HBSS + 2 % DMSO solution which prepared in 3 repetitions for each concentration and analyzed by HPLC. The results obtained were calculated using the linearity equation and the accuracy of the method was calculated as % recovery by comparison with known concentrations. Acceptance interval of % recovery for accuracy, is ± 2%. According to the obtained data, it has been proved that the method is suitable for recovery and accuracy. The results are presented in Table 4.8.

**Table 4.8.** *Recovery % of Standard RCa Analysis in HBSS + 2 % DMSO Solution by HPLC*

| **Day 1 ($n$ = 3)** | **Added (µg. $mL^{-1}$)** | **1** | **10** | **25** |
|---|---|---|---|---|
| | **Found (mean ± SD)** | 1.0157 ± 0.01364 | 10.0317 ± 0.10450 | 25.0655 ± 0.16139 |
| | **Recovery%** | 101.5745 | 100.3170 | 100.2620 |
| | **SD** | 1.3635 | 1.0450 | 0.6520 |
| | **SE(M)** | 0.7872 | 0.6033 | 0.3764 |
| | **RSD%** | 1.3424 | 1.0417 | 0.6503 |
| **Day 2 ($n$ = 3)** | **Added (µg. $mL^{-1}$)** | **1** | **10** | **25** |
| | **Found (mean ± SD)** | 1.0180 ± 1.6934 | 10.1788 ± 0.05469 | 24.5251 ± 0.38121 |
| | **Recovery%** | 101.8047 | 101.7882 | 98.1004 |
| | **SD** | 1.6934 | 0.5469 | 1.5248 |
| | **SE(M)** | 0.9777 | 0.3157 | 0.8804 |
| | **RSD%** | 1.6634 | 0.5373 | 1.5544 |
| **Day 3 ($n$ = 3)** | **Added (µg. $mL^{-1}$)** | **1** | **10** | **25** |
| | **Found (mean ± SD)** | 1.0111 ± 0.01307 | 9.8459 ± 0.06200 | 25.2905 ± 0.16290 |
| | **Recovery%** | 101.1060 | 98.4589 | 101.1622 |
| | **SD** | 1.3071 | 0.6200 | 0.6516 |
| | **SE(M)** | 0.7547 | 0.3580 | 0.3762 |
| | **RSD%** | 1.2928 | 0.6297 | 0.6441 |

#### 4.1.2.4. *Precision*

The measurement of repeatability (intra-day) and intermediate precision (inter-days) was achieved to evaluate the precision of the analysis method. Standard solution of RCa at concentrations of (1, 10 and 25 $\mu$g. $mL^{-1}$) in in HBSS + 2 % DMSO solution were analyzed on three consecutive days, six times in a day. The calculated RSD value is lower than 2% deviation from the nominal value of precision for RCa standard solution. This elucidates that the current method is highly precise and analytically acceptable. The statistical estimation is demonstrated in Tables 4.9-4.11.

**Table 4.9.** *AUC Values of Standard RCa 1 $\mu g.mL^{-1}$ in HBSS + 2 % DMSO Solution Obtained for Precision Study*

| **1 µg.mL$^{-1}$** | **Intra-day (n = 6)** | | | **Inter-day (n = 18)** |
|---|---|---|---|---|
| | **1.Day** | **2. Day** | **3. Day** | |
| **Average** | 44007.67 | 44128.00 | 44032.67 | 44056.11 |
| **Standard Deviation** | 104.41 | 169.92 | 136.65 | 136.99 |
| **Standard Error** | 42.6252 | 69.3695 | 55.7871 | 55.9273 |
| **RSD** | 0.24 | 0.39 | 0.31 | 0.31 |

**Table 4.10.** *AUC Values of Standard RCa 10 $\mu g.mL^{-1}$ in HBSS + 2 % DMSO Solution Obtained for Precision Study*

| **10 µg.mL$^{-1}$** | **Intra-day (n = 6)** | | | **Inter-day (n = 18)** |
|---|---|---|---|---|
| | **1.Day** | **2. Day** | **3. Day** | |
| **Average** | 460710.00 | 460517.00 | 460659.67 | 460628.89 |
| **Standard Deviation** | 194.49 | 667.46 | 186.62 | 349.53 |
| **Standard Error** | 79.4002 | 272.4894 | 76.1873 | 142.6923 |
| **RSD** | 0.04 | 0.14 | 0.04 | 0.076 |

**Table 4.11.** *AUC Values of Standard RCa 25 $\mu g.mL^{-1}$ in HBSS + 2 % DMSO Solution Obtained for Precision Study*

| **25 µg.mL$^{-1}$** | **Intra-day (n = 6)** | | | **Inter-day (n = 18)** |
|---|---|---|---|---|
| | **1.Day** | **2. Day** | **3. Day** | |
| **Average** | 1124671.00 | 1124785.67 | 1124748.33 | 1124735.00 |
| **Standard Deviation** | 439.14 | 247.08 | 194.88 | 293.70 |
| **Standard Error** | 179.2782 | 100.8670 | 79.5594 | 119.9025 |
| **RSD** | 0.04 | 0.02 | 0.02 | 0.03 |

#### 4.1.2.5. *Specificity*

Analyzes of RCa prepared in (HBSS + 2 % DMSO) solution with in (HBSS and 2 % DMSO) solution for specificity studies which were carried out by HPLC analysis method. The chromatograms of the (HBSS + 2 % DMSO) solution showed that there were no interfering peaks at the retention time of RCa (Rt = 8.65 minutes), so the HPLC analysis method was approved to be specific for RCa in (HBSS and 2 % DMSO) solution. The chromatograms related to specificity are shown in Figure 4.6.

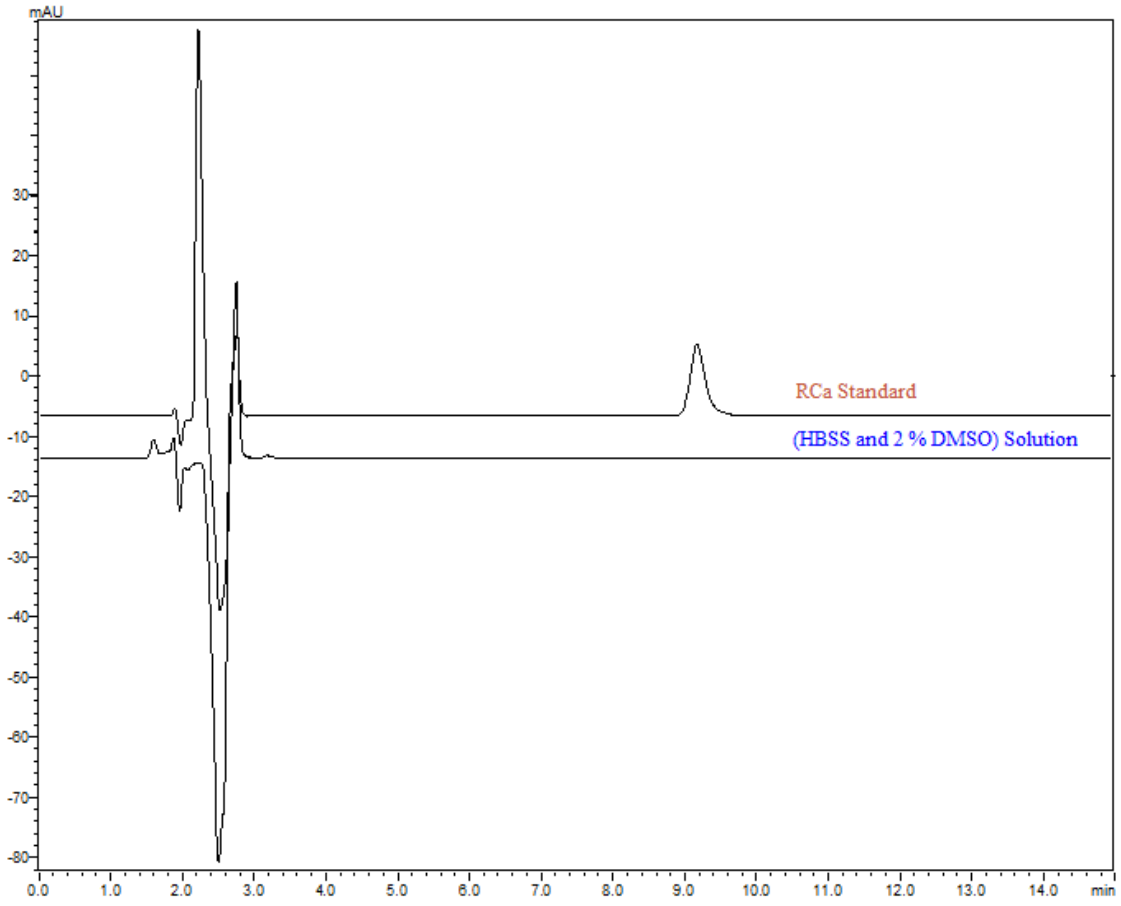


**Figure 4.6.** *Chromatograms of the Selectivity Studies for HBSS + 2 % DMSO*

#### 4.1.2.6. *Sensitivity*

The sensitivity of the HPLC analysis method was examined by evaluation of LOD and LOQ. The LOD and LOQ were calculated by using equations (3.1 and 3.2) which were mentioned in section (3.1.7). LOD is 0.23 $\mu g.mL^{-1}$ and LOQ is 0.69 $\mu g.mL^{-1}$. The smallest concentration that can be measured with acceptable accuracy and precision for the sensitivity of the method is 1 $\mu g.mL^{-1}$ and the calculated LOD, LOQ values are below this value. These results show that the method is sensitive.

#### 4.1.2.7. *System suitability test*

The system suitability test of the HPLC analysis method was estimated by lab. solution software. The results of the evaluated parameters are illustrated in Table 4.12 (U.S.P, 2016, p.463–468).

**Table 4.12.** *HPLC System Suitability Test Results of HBSS + 2 % DMSO*

| Parameters | RCa | Recommended value |
|---|---|---|
| **Theoretical Plate(N)** | 9,606.955 | >2000 |
| **Retention time** | 8.65 | |
| **Tailing factor** | 1.236 | < 2 |
| **Asymmetry factor** | 1.192 | $0.95<A_S< 1.2$ |
| **Capacity factor** | 2.354 | 2<K< 10 |

**Reference**: *U.S.P, 2016, p.463–468*

### 4.1.3. Validation process for *in vivo* studies

For *in vivo* (pharmacokinetics) studies, a modified HPLC analysis method (Kumar *et al.*, 2006, p.881–887), validation was carried out by the same condition of the validation method in section (4.1.1). The sample preparation was carried out as mentioned in section (3.10.1)

The results obtained from the validation study were evaluated under the titles of linearity, accuracy, precision, working range, selectivity, sensitivity, and system suitability test.

#### 4.1.3.1. *Linearity*

The linearity study was carried out in extracted rat plasma. The three sets of calibration curves were obtained by plotting the peak area ratio of RCa/IS (KTP) against the nominal concentrations of standard RCa. The concentrations used were 0.1, 0.2, 0.5, 1.0, 2.0, 5.0, and 10.0 µg. $mL^{-1}$. The concentration of (IS) KTP was 1 µg. $mL^{-1}$. The linearity was studied by using the least square regression equation. The chromatogram is illustrated in Figure 4.7 and the RCa AUC/ KTP AUC values obtained by HPLC analysis are shown in Table 4.13

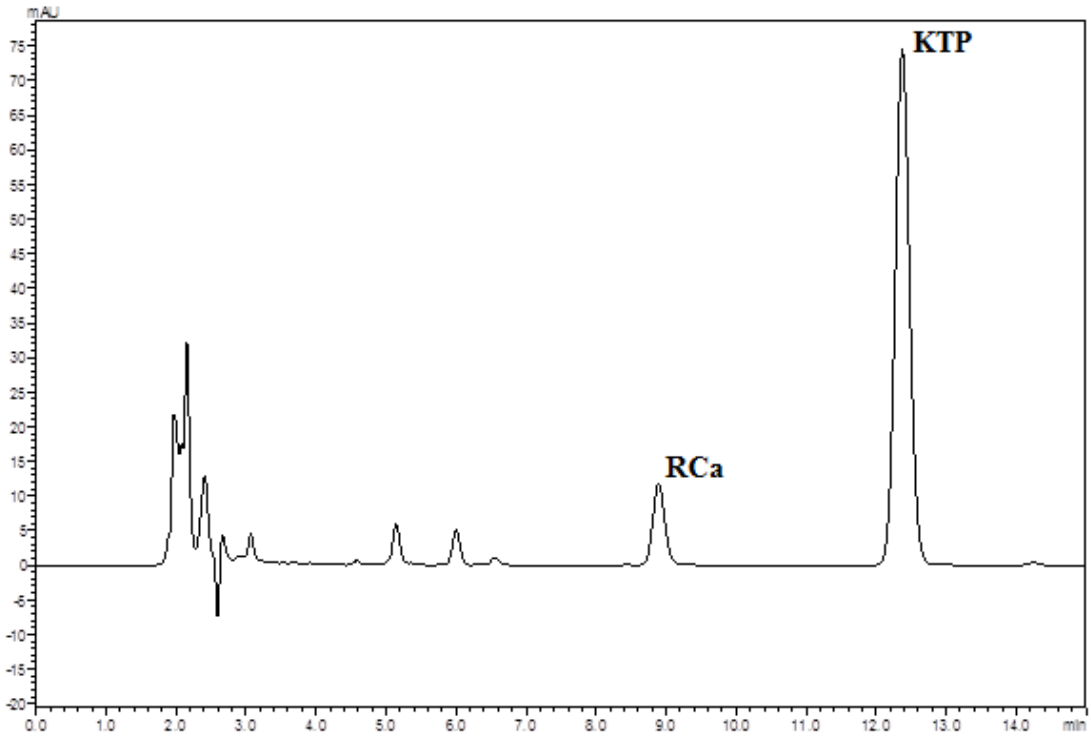


**Figure 4.7.** *Chromatogram of Standard RCa + KTP in Rat Plasma*

**Table 4.13.** *RCa AUC/ KTP AUC Values Obtained by HPLC Analysis in Rat Plasma*

| RCa Concentrations µg. mL$^{-1}$ | RCa AUC/ KTP AUC | | | |
|---|---|---|---|---|
| | 1.Set | 2. Set | 3. Set | Mean ± SE |
| **0.1** | 0.1017 | 0.1049 | 0.1089 | 0.1052 ± 0.0017 |
| **0.2** | 0.1815 | 0.1891 | 0.2020 | 0.1909 ± 0.0049 |
| **0.5** | 0.4803 | 0.4702 | 0.4850 | 0.4785 ± 0.0036 |
| **1** | 0.9609 | 0.8972 | 0.9540 | 0.9374 ± 0.0165 |
| **2** | 1.8882 | 1.8565 | 1.9828 | 1.9092 ± 0.0309 |
| **5** | 4.9169 | 4.6320 | 4.7252 | 4.7580 ± 0.0685 |
| **10** | 9.5238 | 9.2914 | 9.6328 | 9.4827 ± 0.0822 |

The right equation in the result of the study done is y = 0.9484x + 0.0046 and regression square is $r^2$ = 0.9999. The linearity graph is demonstrated in Figure 4.8.

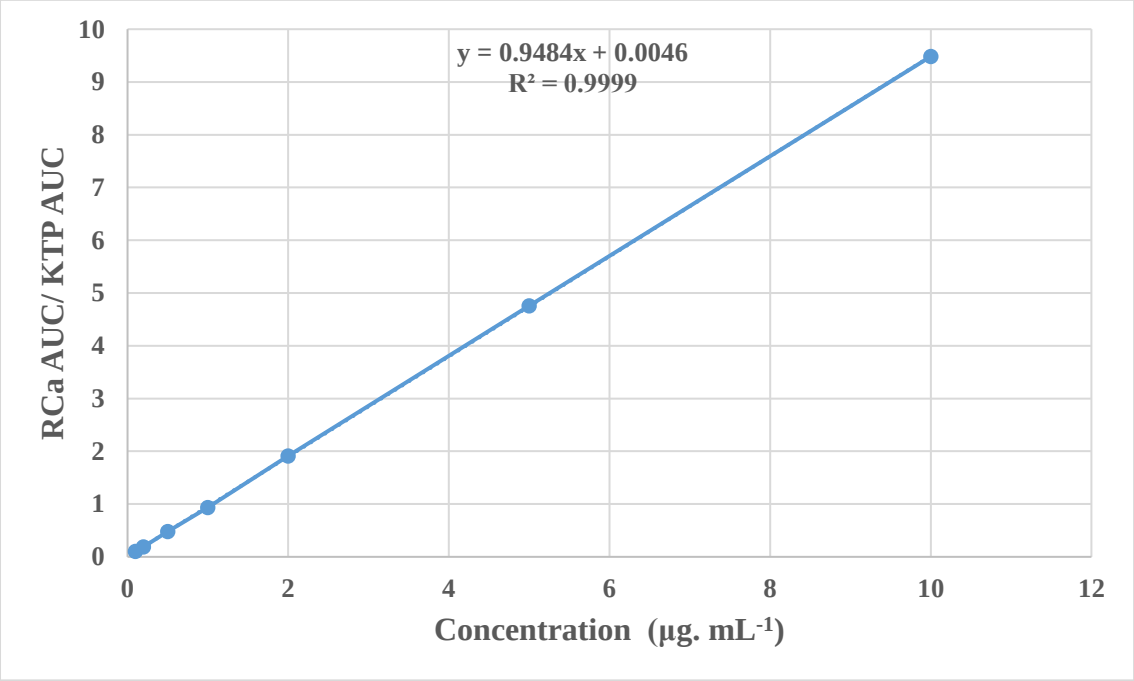


**Figure 4.8.** *Calibration Curve and Linearity Equation of Standard RCa + KTP in Rat Plasma*

#### 4.1.3.2. *Range*

The range of analytical method was studied in this limit of concentration (0.05- 10 µg. $mL^{-1}$). The calibration curve was selected at the concentration limit (0.1-10 µg. $mL^{-1}$).

#### 4.1.3.3. *Recovery*

The recovery study was carried out by selecting three concentrations (0.2, 2, and 10 µg. $mL^{-1}$) of active substance RCa and 1 µg. $mL^{-1}$ of KTP in extracted plasma solution which prepared in 3 repetitions for each concentration and analyzed by HBLC. The results obtained were calculated using the linearity equation and the recovery of the method was calculated as % recovery by comparison with known concentrations. Acceptance interval of % recovery for accuracy, is ± 15 % (EMA, 2012, p.1–23). According to the obtained data, it has been proved that the method is suitable for recovery and accuracy. The results are presented in Table 4.14.

**Table 4.14.** *Recovery % of Standard RCa+KTP Analysis in Rat Plasma by HPLC*

| **Day 1 ($n$ = 3)** | **Added (µg. $mL^{-1}$)** | **0.2** | **2** | **10** |
|---|---|---|---|---|
| | **Found (mean ± SD)** | 0.2106 ± 0.01282 | 2.0733 ± 0.07301 | 10.463 ± 0.7025 |
| | **Recovery%** | 105.32 | 103.66 | 104.63 |
| | **SD** | 6.4093 | 3.6508 | 7.0248 |
| | **SE(M)** | 3.7004 | 2.1078 | 4.0557 |
| | **RSD%** | 6.0856 | 3.5218 | 6.7139 |
| **Day 2 ($n$ = 3)** | **Added (µg. $mL^{-1}$)** | **0.2** | **2** | **10** |
| | **Found (mean ± SD)** | 0.2056 ± 0.00856 | 2.0239 ± 0.04345 | 10.193 ± 0.3050 |
| | **Recovery%** | 102.80 | 101.20 | 101.93 |
| | **SD** | 4.2817 | 2.1726 | 3.0504 |
| | **SEM** | 2.4720 | 1.2543 | 1.7612 |
| | **RSD%** | 4.1649 | 2.1468 | 2.9927 |
| **Day 3 ($n$ = 3)** | **Added (µg. $mL^{-1}$)** | **0.2** | **2** | **10** |
| | **Found (mean ± SD)** | 0.2064 ± 00798 | 2.0416 ± 0.03289 | 10.198 ± 0.24938 |
| | **Recovery%** | 103.18 | 102.08 | 101.98 |
| | **SD** | 3.9918 | 1.6444 | 2.4939 |
| | **SE(M)** | 2.3047 | 0.9494 | 1.4398 |
| | **RSD%** | 3.8690 | 1.6109 | 2.4454 |

#### 4.1.3.4. *Precision*

The measurement of repeatability (intra-day) and intermediate precision (inter-days) was achieved to evaluate the precision of the analysis method. Standard solution of RCa at concentrations of (0.2, 2 and 10 $\mu$g. mL$^{-1}$) + KTP (1 $\mu$g. mL$^{-1}$) concentration in extracted rat plasma solution were analyzed on three consecutive days, six times in a day. The calculated RSD value is lower than 15 % deviation from the nominal value of precision for RCa standard solution (EMA, 2012, p.1–23). This elucidates that the current method is highly precise and analytically acceptable. The statistical estimation is demonstrated in Tables 4.15, 4.16, and 4.17.

**Table. 4.15**. *AUC RCa/AUC KTP Values of Standard RCa 0.2 µg.mL$^{-1}$+KTP 1 µg.mL$^{-1}$ Obtained for Precision Study*

| **0.2 µg. mL$^{-1}$** | **Intra-day (n = 6)** | | | **Inter-day (n = 18)** |
|---|---|---|---|---|
| | **1.Day** | **2. Day** | **3. Day** | |
| **Average** | 0.2097 | 0.2105 | 0.2093 | 0.2098 |
| **Standard Deviation** | 0.0029 | 0.0032 | 0.0022 | 0.00278 |
| **Standard Error** | 0.0012 | 0.0013 | 0.0001 | 0.0011 |
| **RSD** | 1.3790 | 1.5380 | 1.0555 | 1.3242 |

**Table. 4.16**. *AUC RCa/AUC KTP Values of Standard RCa 2 µg.mL$^{-1}$+KTP 1 µg.mL $^{-1}$ Obtained for Precision Study*

| **2 µg. mL$^{-1}$** | **Intra-day (n = 6)** | | | **Inter-day (n = 18)** |
|---|---|---|---|---|
| | **1.Day** | **2. Day** | **3. Day** | |
| **Average** | 1.9929 | 1.9416 | 1.8917 | 1.9421 |
| **Standard Deviation** | 0.0317 | 0.0162 | 0.0143 | 0.0207 |
| **Standard Error** | 0.0129 | 0.0066 | 0.0058 | 0.0085 |
| **RSD** | 1.5912 | 0.8333 | 0.7561 | 1.0602 |

**Table. 4.17**. *AUC RCa/AUC KTP Values of Standard RCa 10 µg.mL$^{-1}$+KTP 1 µg.mL$^{-1}$ Obtained for Precision Study*

| **10 µg. mL$^{-1}$** | **Intra-day (n = 6)** | | | **Inter-day (n = 18)** |
|---|---|---|---|---|
| | **1.Day** | **2. Day** | **3. Day** | |
| **Average** | 10.2996 | 9.7766 | 9.3397 | 9.8053 |
| **Standard Deviation** | 0.1691 | 0.1017 | 0.1250 | 0.1319 |
| **Standard Error** | 0.0690 | 0.0415 | 0.0510 | 0.0539 |
| **RSD** | 1.6419 | 1.0405 | 1.3386 | 1.3403 |

#### 4.1.3.5. *Specificity*

Analyzes of RCa in extracted rat plasma with KTP solution for specificity studies which were carried out by HPLC analysis method. The chromatograms of the pure plasma and IS (KTP) in plasma showed that there were no interfering peaks at the retention time of RCa (Rt of RCa = 8.85 minutes and Rt of KTP = 12.26 minutes), so the HPLC analysis method was approved to be specific for RCa in plasma and KTP solution. The chromatograms related to specificity are shown in Figure 4.9

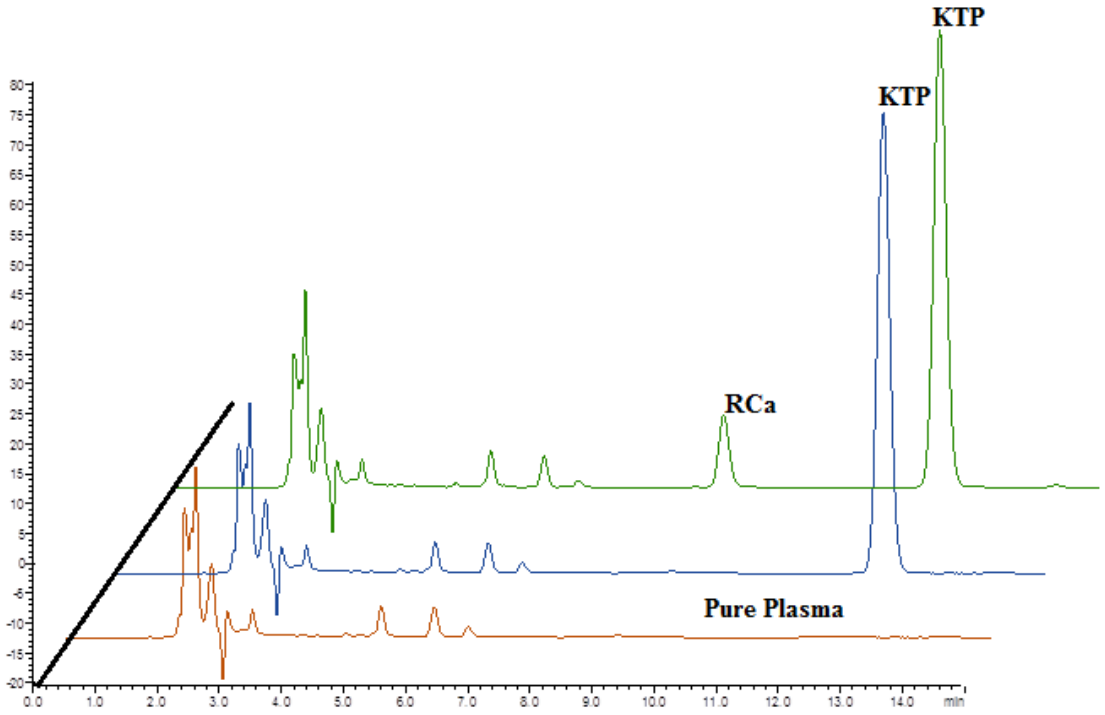


**Figure 4.9.** *Chromatograms of the Selectivity Studies for RCa in Plasma, Pure Plasma and KTP in Plasma*

#### 4.1.3.6. *Sensitivity*

The sensitivity of the HPLC analysis method was examined by evaluation of LOD and LOQ. The LOD and LOQ were calculated by using equations (3.1 and 3.2) which were mentioned in section (3.1.7). LOD is 0.035 µg. $mL^{-1}$ and LOQ is 0.107 µg. $mL^{-1}$. The smallest concentration that can be measured with acceptable accuracy and precision for the sensitivity of the method is 0.1 µg. $mL^{-1}$ and the calculated LOD, LOQ values are at this value. These results show that the method is sensitive.

#### 4.1.3.7. *System suitability test*

The system suitability test of the HPLC analysis method was estimated by lab. solution software. The results of the evaluated parameters are illustrated in Table 4.18 (U.S.P, 2016, p.463–468).

**Table 4.18.** *HPLC System Suitability Test Results of In Vivo Studies*

| Parameters | RCa | KTP | Recommended value |
|---|---|---|---|
| **Theoretical Plate(N)** | 9,984.558 | 14,655.611 | >2000 |
| **Retention time** | 8.85 | 12.26 | |
| **Tailing factor** | 1.169 | 1.111 | < 2 |
| **Asymmetry factor** | 1.151 | 1.102 | $0.95<A_S< 1.2$ |
| **Capacity factor** | 2.364 | 3.679 | 2<K< 10 |
| **Resolution** | - | 9.096 | >2 |

**Reference**: *U.S.P, 2016, p.463–468*

## 4.2. RCa Solubility in Water

According to the study performed, the solubility of RCa in bidistilled water was found to be 7.32 ± 0.082 mg. $mL^{-1}$ (mean ± SE). The study was repeated three times.

### 4.3. Cs NPs Formulation Studies

#### 4.3.1. Cs NPs preparation yield

The production performance was calculated using equation (3.3) as the ratio of the dried product and the sum of the RCa and Cs masses. The yields were found, 10.43, 27.48, 41.82, 80.00, 41.82 and 27.83% for F1-F6 formulations respectively.

#### 4.3.2. Determination of drug content of Cs NPs

The drug content was calculated using equation (3.4) which varied from 16.5 ± 0.7% to 99.1 ± 1.9% for the formulations prepared. Table 4.19.

#### 4.3.3. Physicochemical characterization tests of Cs NPs

##### 4.3.3.1. *Particle size, polydispersity index, and zeta potential measurements*

PS analyses results have demonstrated nanometer range with the particle sizes of 446.9 ± 13.1, 240.0 ± 10.7, 388.1 ± 8.9, 355.4 ± 14.7, 356.4 ± 6.5 and 247.2 ± 46.0 nm for F1-F6 formulations, respectively, with relatively homogenous size distribution (with PDI data range of 0.490 ± 0.032 - 0.790 ± 0.090). An important parameter; ZP values were recorded as 37.3 ± 0.2, 21.9 ± 0.9, 63.7 ± 0.5, 24.9 ± 0.1, 49.4±0.8 and -6.9±0.1 mV for F1-F6 formulations, respectively. ZP values of NP formulations were found indicating a good physical stability being in the range of 20-65 mV for most of the formulations Table 4.19.

**Table 4.19.** *PS, PDI, ZP, and DC % (Mean ± SE) of Cs NPs*

| Code | PS (nm) | PDI | ZP (mV) | DC (%) |
|---|---|---|---|---|
| **F1** | 446.9 ± 13.1 | 0.595 ± 0.009 | 37.3 ± 0.2 | 80.8 ± 3.1 |
| **F2** | 240.0 ± 10.7 | 0.693 ± 0.064 | 21.9 ± 0.9 | 99.1 ± 1.9 |
| **F3** | 388.1 ± 8.9 | 0.620 ± 0.024 | 63.7 ± 0.5 | 4.9 ± 0.2 |
| **F4** | 355.4 ± 14.7 | 0.671 ± 0.073 | 24.9 ± 0.1 | 16.5 ± 0.7 |
| **F5** | 356.4 ± 6.5 | 0.490 ± 0.032 | 49.4 ± 0.8 | 4.3 ± 0.7 |
| **F6** | 247.2 ± 46.0 | 0.790 ± 0.090 | -6.9 ± 0.1 | 21.2 ± 1.3 |

#### 4.3.3.2. *Morphology of Cs NPs*

For the evaluation of morphological structures of the Cs NPs and RCa, SEM microphotographs were illustrated in the Figure 4.10.

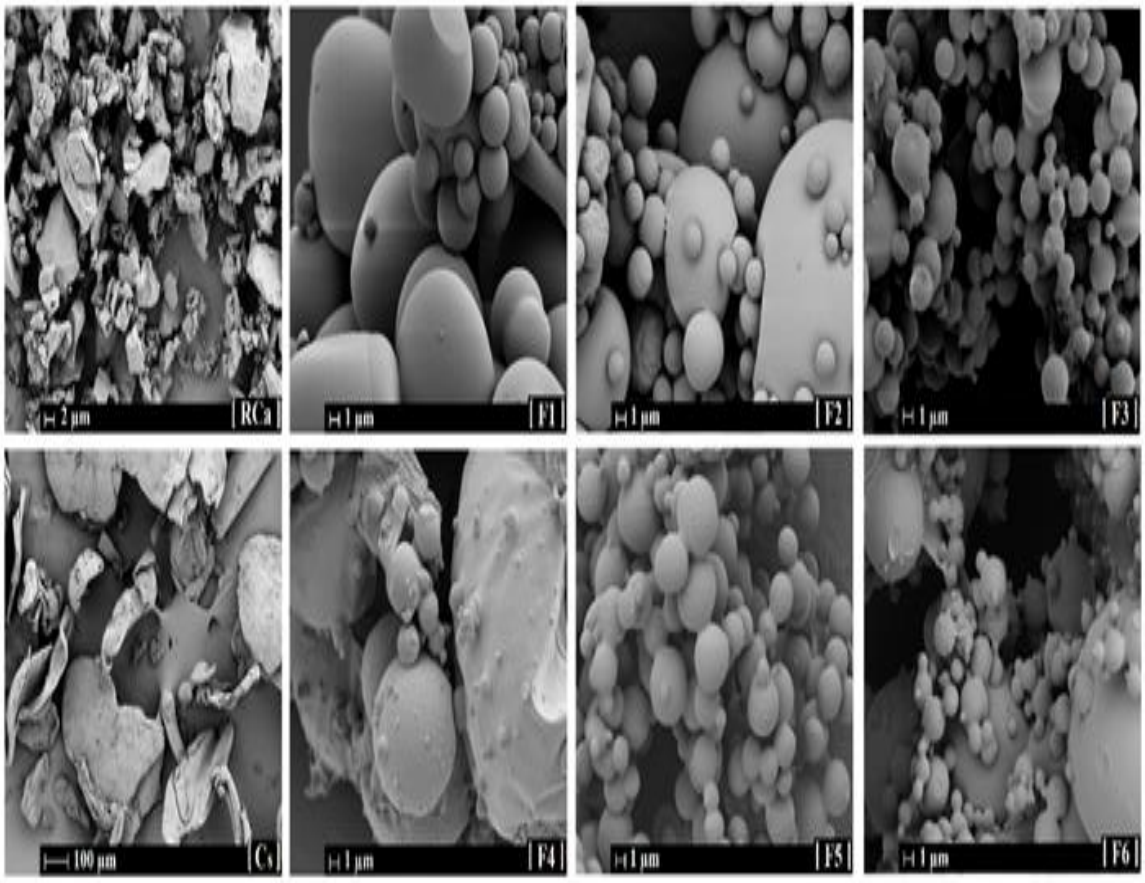


**Figure 4.10.** *SEM Images of RCa, and Formulations of Cs NPs*

#### 4.3.3.3. *Thermal analysis of Cs NPs*

Thermodynamic variations related to morphological changes before and after formulation steps can be detected by DSC. Figure 4.11 shows the DSC curves of the pure components, physical mixtures (PMs) as well as of the final Cs NPs prepared. No sharp peaks were appeared in the thermograms showing the formation of amorphous structures. The thermograms showed no evidence of the any chemical interaction between drug and polymer, however no structural changes were revealed related to the formulation steps.

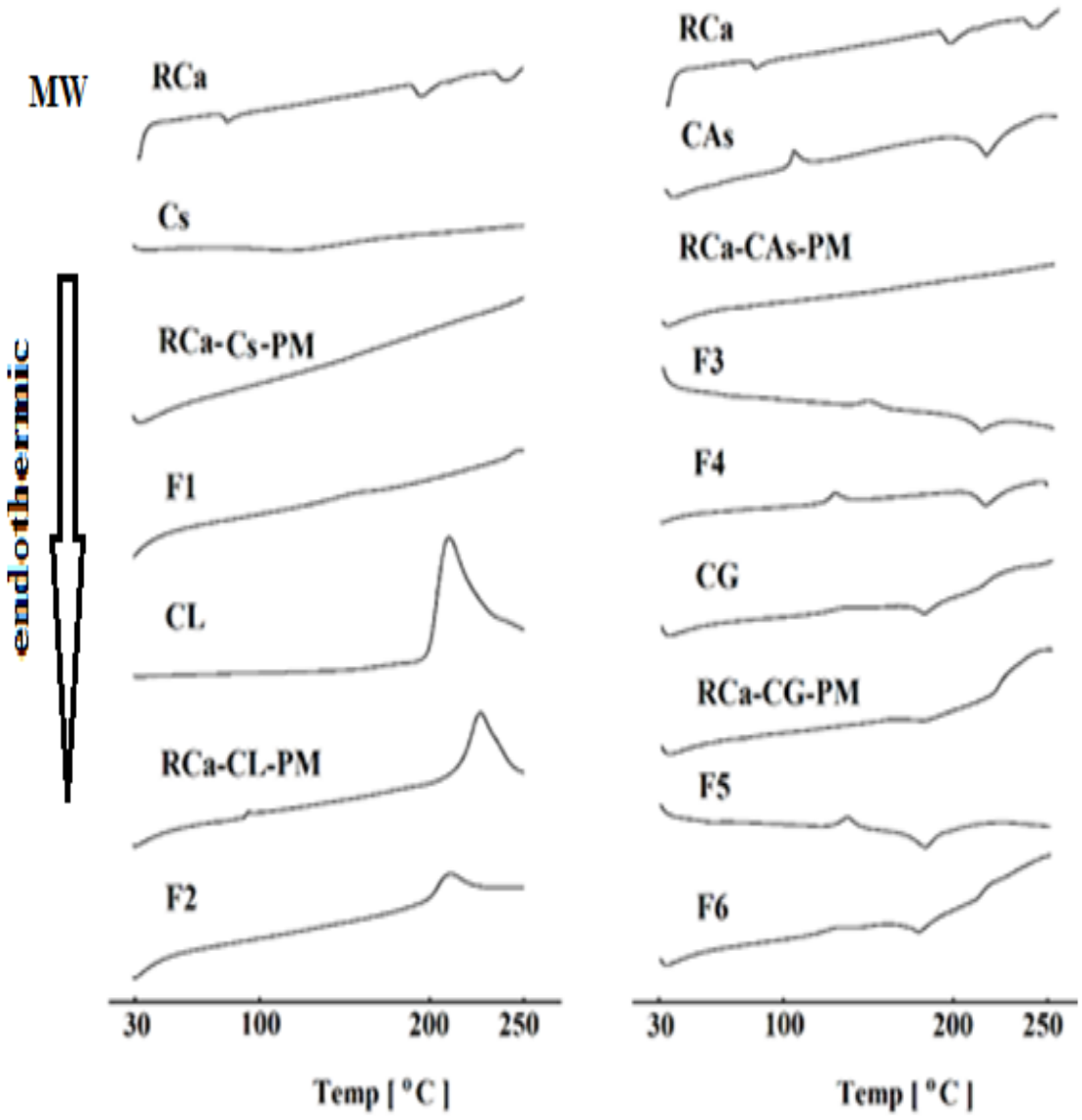


**Figure 4.11.** *DSC Thermograms of RCa, Cs, Cs Salts, PMs and Cs NPs Formulations*

#### 4.3.3.4. *Infrared (FT-IR) analysis*

FT-IR analyses were proposed as the possible way to investigate the interactions between substances. In our study interaction possibilities between the Cs salts and active agent were evaluated by FT-IR. The FT-IR spectra of pure materials, PMs, Cs salts and prepared formulations of Cs NPs are given in Figure 4.12 which were suggested the absence of chemical interaction between RCa and any of the Cs salts used in the preparation of spray dried products.

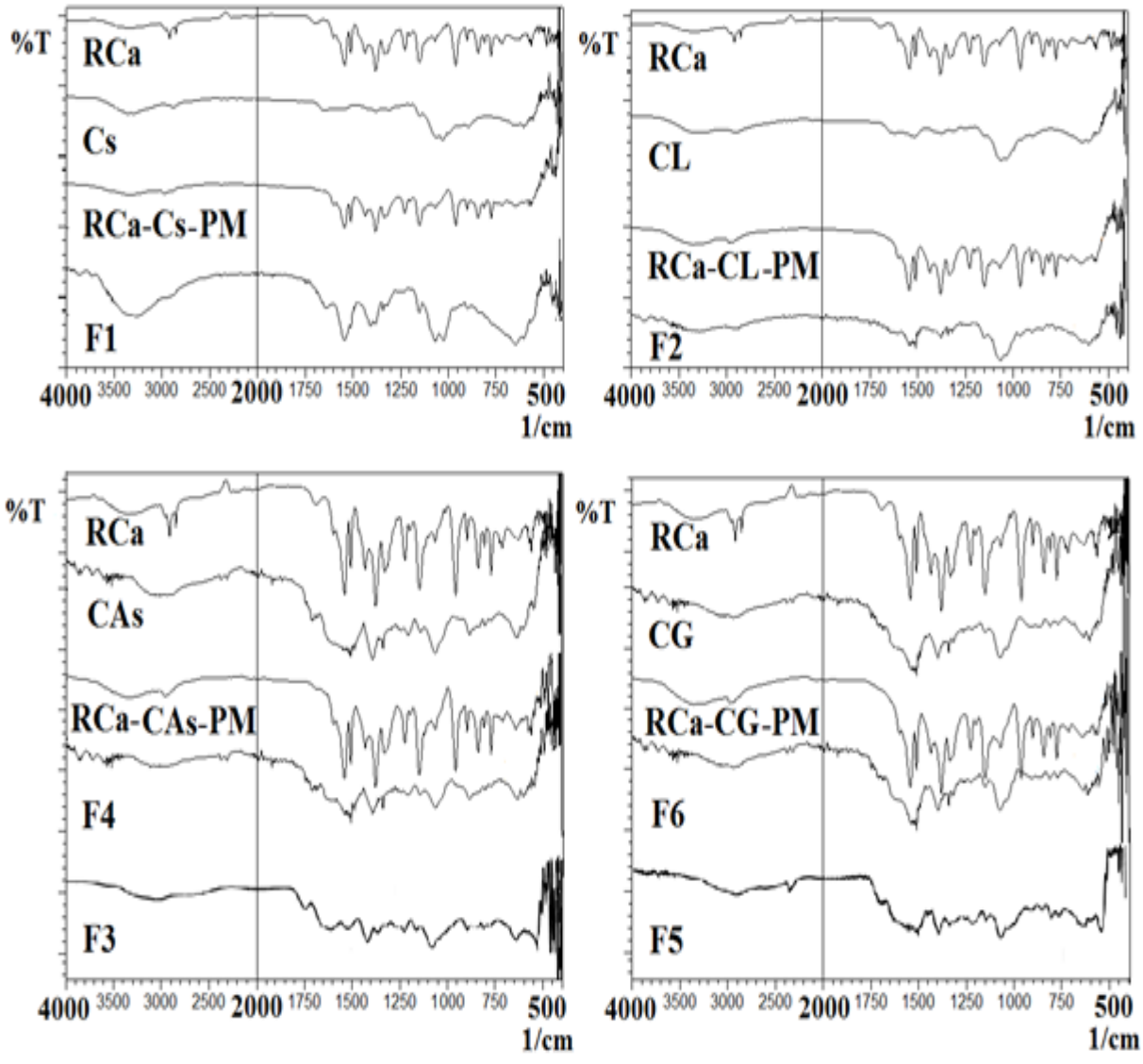


**Figure 4.12.** *FT-IR Spectra of RCa, Cs, Cs Salts, PMs and Cs NPs Formulations*

#### 4.3.3.5. *XRD (X-ray diffraction)*

The Figure 4.13 shows the XRD patterns of RCa, Cs, Cs salts, PMs and Cs NPs prepared formulations. The XRD patterns of pure RCa, Cs, Cs salts and Cs NPs prepared showed broad diffraction peaks at 2θ values indicating the amorphous status as expected.

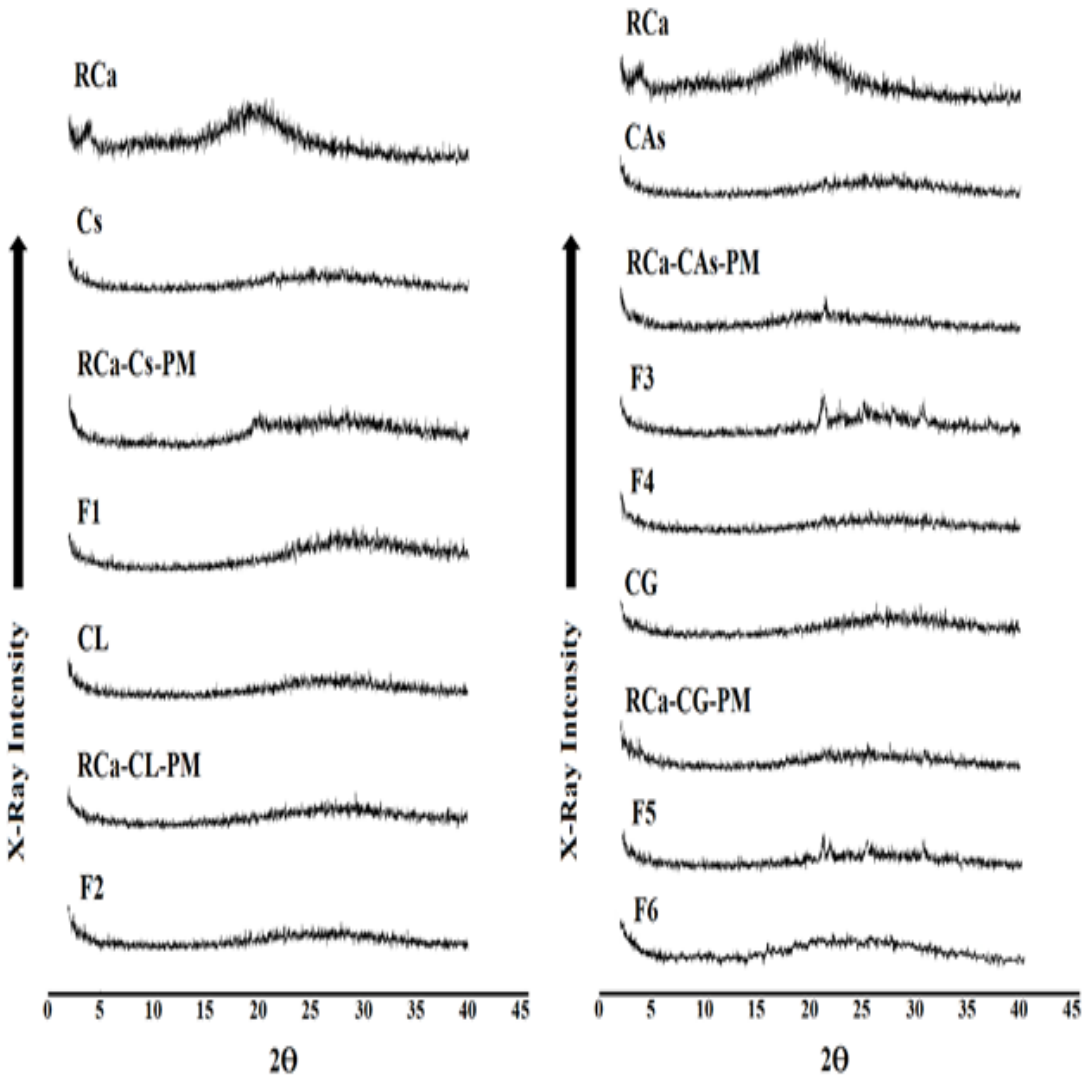


**Figure 4.13.** *XRD Spectra of RCa, Cs, Cs Salts, PMs and Cs NPs Formulations*

### 4.3.3.6. *[1]H-NMR analysis*

[1]H-NMR analyses of the NPs were performed in order to reveal the ionic interactions between RCa and Cs salts. Figure 4.14 shows the characteristic peaks for Cs at 3 ppm (due to the acetyl group), and 7.5 ppm (considering H-3/6) for the ring structure of the sugar (marked with arrows).

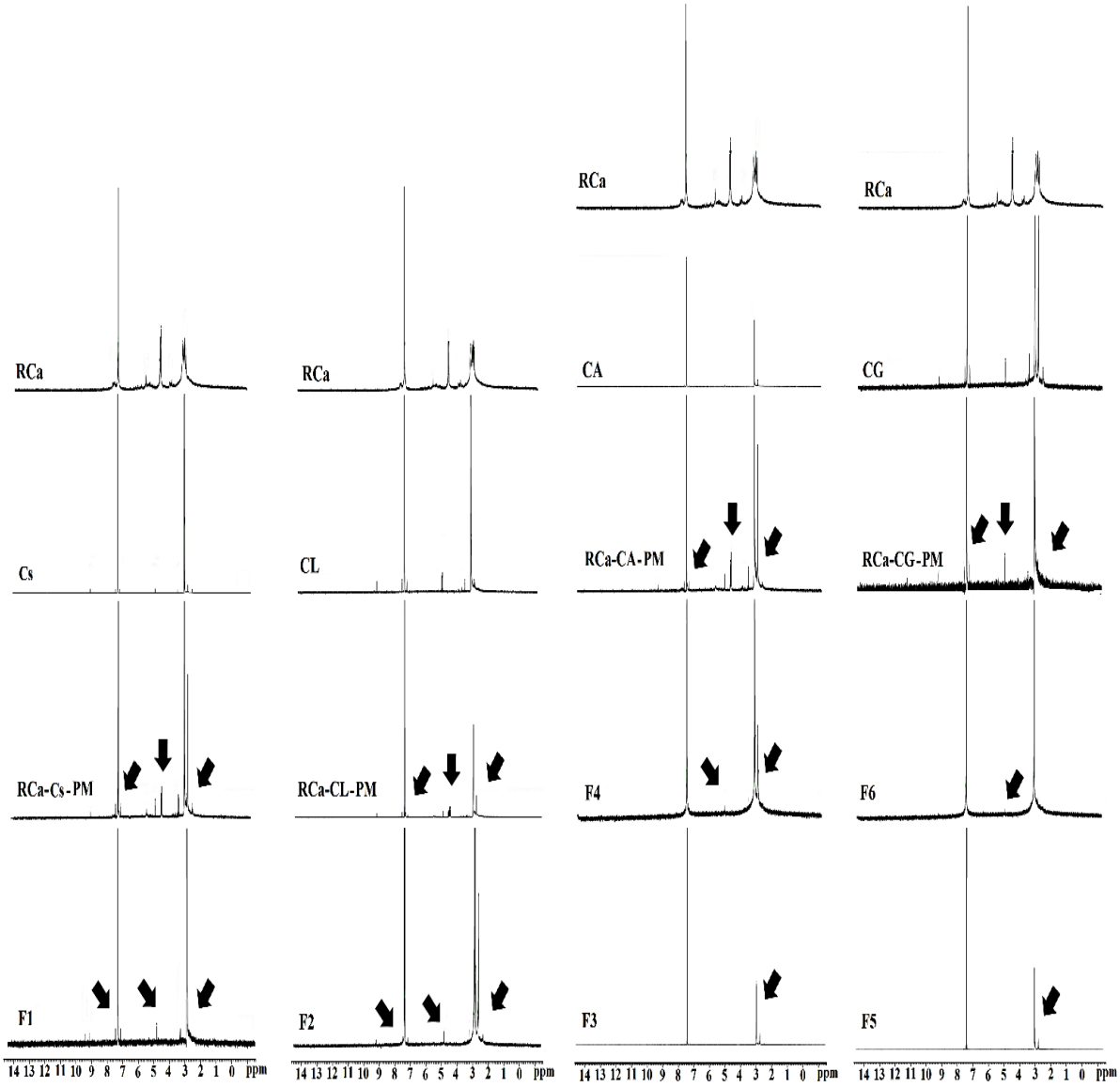


**Figure 4.14.** *[1]H-NMR Spectra of RCa, Cs, Cs Salts, PMs and Cs NPs Formulations*

### 4.3.4. *In vitro* release studies

Four Cs NPs were selected according to the results of physicochemical characterization tests. *In vitro* release studies performed for selected formulations (F1, F2, F4, and F6). The results of dissolution studies in phosphate buffer (pH 6.8) performed on Cs NPs formulations were shown in Table.4.20, Figure.4.15. and Figure.4.16. The release data clearly indicated that RCa is released from the NPs under physiological conditions. An initial burst release achieved for the F1 and F2 formulations, which was approximately 58% just within 5 minutes. On the contrary, the release rate of pure RCa was relatively slower and sustained compared to F1 and F2 with 53% of drug release within 1 hour. The release rate of pure RCa was 32%, whereas 85%, 81%, 58% and 63% releases were observed from F1, F2, F4 and F6 in phosphate buffer (pH 6.8) within 0.5 hour respectively. Extended RCa releases (~91%) from pure substance and three formulations (F1, F2 and F6) were observed after 4 hours Table.4.20.

**Table 4.20.** *% Cumulative Release of RCa from Pure Form RCa, Cs NPs at pH 6.8*

| (Time Hour) | % Cumulative Release (mean ± SE) | | | | |
|---|---|---|---|---|---|
| | **Pure RCa** | **F1** | **F2** | **F4** | **F6** |
| **0.08** | 8.01 ± 0.36 | 57.54 ± 15.60 | 58.77 ± 8,26 | 25.64 ± 1.58 | 40.06 ± 5.65 |
| **0.17** | 13.99 ± 0.89 | 73.39 ± 1.97 | 68.01 ± 7.48 | 32.59 ± 1.4 | 44,68 ± 4,36 |
| **0.25** | 19.37 ± 1.37 | 80.84 ± 3.33 | 71.16 ± 7.47 | 35.30 ± 1.69 | 47.61 ± 4.36 |
| **0.5** | 31.96 ± 2.31 | 85.06 ± 1.59 | 81.03 ± 2.27 | 57.66 ± 9.11 | 62.85 ± 5.84 |
| **1** | 53.07 ± 3.75 | 88.77 ± 2.29 | 88.70 ± 0.32 | 69.60 ± 9.78 | 73.20 ± 4.14 |
| **2** | 75.81 ± 4.69 | 89.76 ± 2.49 | 90.67 ± 0.86 | 70.90 ± 7 36 | 83,61 ± 3.33 |
| **3** | 86.22 ± 5.0 | 90.14 ± 0.39 | 91.16 ± 0.94 | 74.57 ± 6.7 | 89.38 ± 2.86 |
| **4** | 91.60 ± 4.97 | 90.26 ± 2.58 | 91.27 ± 0.94 | 75.21 ± 6.28 | 92.48 ± 2.46 |
| **6** | 95.46 ± 4.73 | 91.46 ± 2.32 | 91.65 ± 0.94 | 78.20 ± 7.3 | 94.03 ± 3.65 |
| **8** | - | 91.46 ± 2.43 | 91.66 ± 0.81 | 87.83 ± 7.34 | 104.93 ± 0.12 |
| **12** | - | 91.78 ± 3.08 | 93.13 ± 0.81 | 93.16 ± 7.5 | 109.87 ±1.65 |
| **24** | - | 92.04 ± 2.34 | 92.12 ± 0.76 | 104.1 ± 6.35 | 115.28 ± 65 |

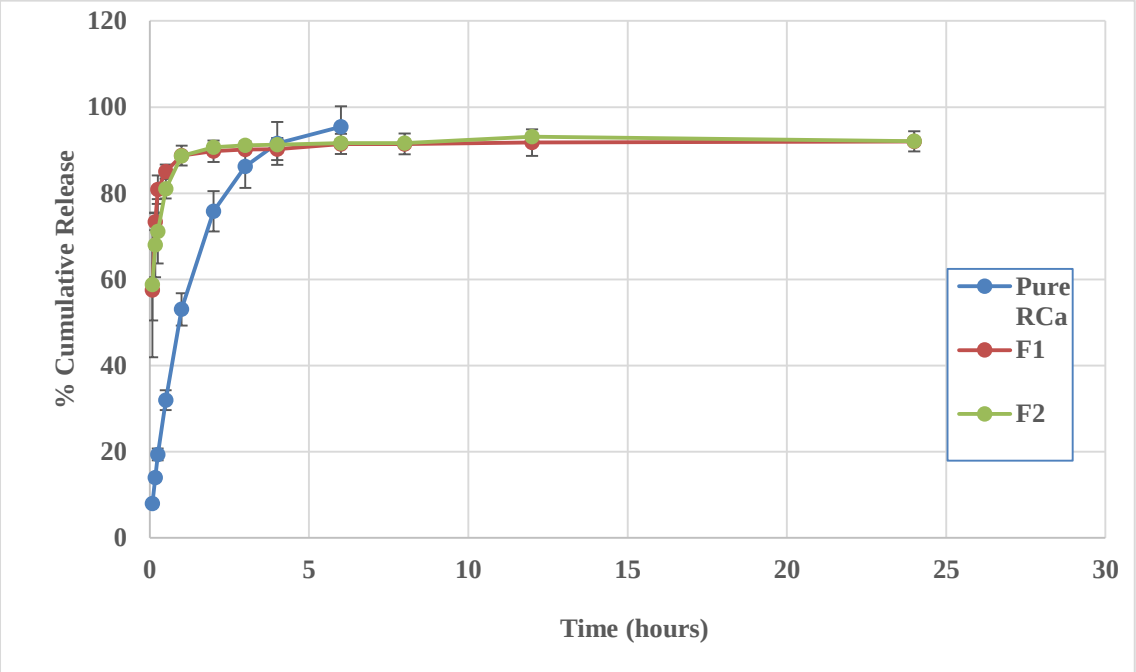


**Figure 4.15.** *In Vitro Release of RCa from F1and F2 Cs NPs versus Pure RCa Release in Phosphate Buffer (pH 6.8) (mean ± SE) (n =3)*

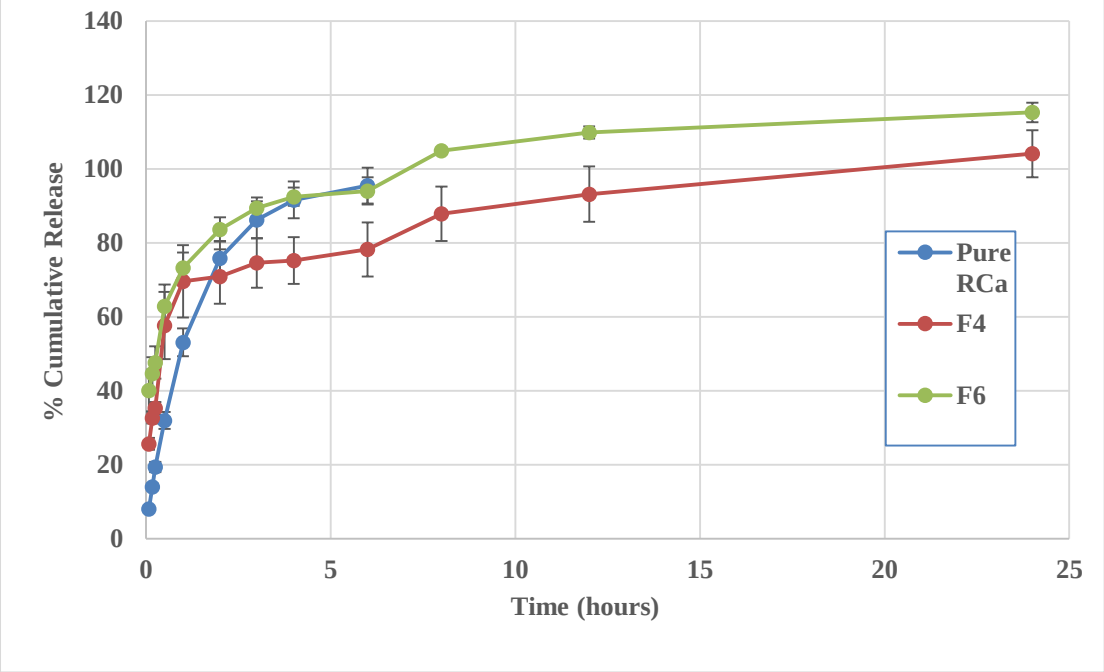


**Figure 4.16.** *In Vitro Release of RCa from F4 and F6 Cs NPs versus Pure RCa Release in Phosphate Buffer (pH 6.8) (mean ± SE) (n =3)*

### 4.3.5. Kinetics and mechanism of release

*In vitro* release profiles in phosphate buffer (pH 6.8) for the selected NPs were applied to various kinetic models (zero order kinetics, first order kinetics, Higuchi model, Korsmeyer-Peppas model and Hixson-Crowell model). The release data were evaluated by rate constant (k), r-values ($r^2$) and Akaike criteria (AIC) for the selection of best suited kinetic model. The pure RCa release was fitted to the first order kinetic model, while all of the NPs (F1, F2, F4 and F6) were fitted to Korsmeyer-Peppas model according to the highest k and r values with lowest AIC data Table 4.21, Figure 4.17.

**Table 4.21.** *Kinetic Modeling of RCa Release from, Pure RCa and Cs NPs by DDsolver Software Program*

| Code | | Kinetic Model | | | | |
|---|---|---|---|---|---|---|
| | | **Zero order** | **First order** | **Higuchi** | **Korsmeyer-Peppas*** | **Hixson-Crowell** |
| **Pure RCa** | **k** | 0.021 | 0.001 | 0.045 | 0.048 | 0.000 |
| | **$r^2$** | 0.001 | 0.001 | 0.001 | 0.001 | 0.001 |
| | **AIC** | 0.078 | 0.048 | 0.059 | 0.065 | 0.051 |
| **F1** | **k** | 0.007 | 0.000 | 0.032 | 0.082 | 0.000 |
| | **$r^2$** | - 0.043 | - 0.022 | -0.021 | 0.001 | -0.026 |
| | **AIC** | 0.132 | 0.125 | 0.124 | 0.075 | 0.127 |
| **F2** | **k** | 0.007 | 0.000 | 0.032 | 0.080 | 0.000 |
| | **$r^2$** | - 0.032 | - 0.016 | - 0.015 | 0.001 | - 0.019 |
| | **AIC** | 0.132 | 0.123 | 0.123 | 0.074 | 0.126 |
| **F4** | **k** | 0.007 | 0.000 | 0.030 | 0.062 | 0.000 |
| | **$r^2$** | - 0.003 | 0.000 | 0.000 | 0.001 | 0.000 |
| | **AIC** | 0.123 | 0.105 | 0.109 | 0.084 | 0.113 |
| **F6** | **k** | 0.008 | 0.001 | 0.034 | 0.073 | 0.000 |
| | **$r^2$** | - 0.004 | 0.000 | - 0.001 | 0.001 | - 0.001 |
| | **AIC** | 0.128 | 0.102 | 0.114 | 0.079 | 0.118 |

**Reference:** *DDsolver Program, Zhang et al., 2010, p.263–271.*

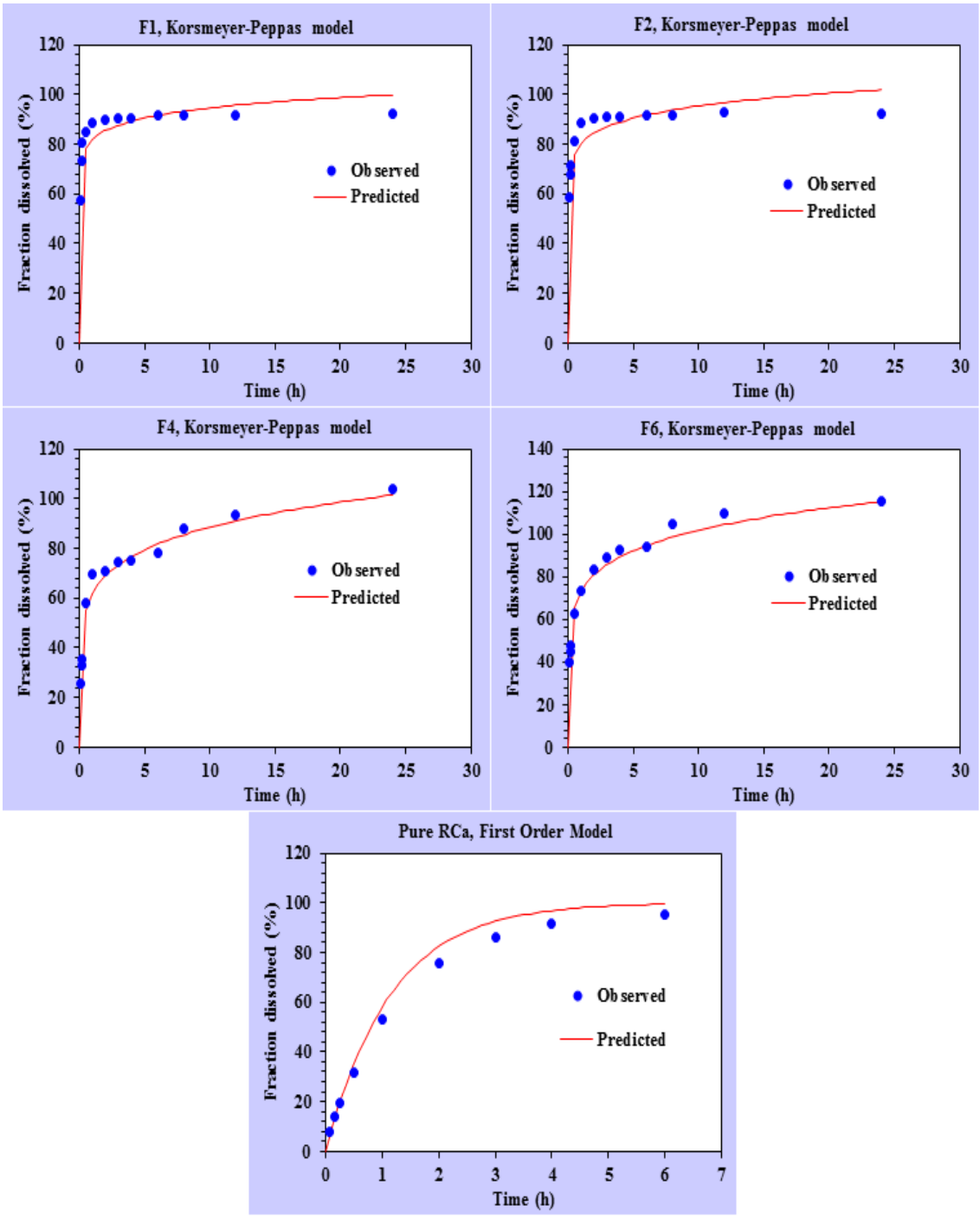


**Figure 4.17.** *Kinetic Modeling of RCa Release from, Pure RCa and Cs NPs by DDsolver Software Program*

**Reference:** *DDsolver Program, Zhang et al., 2010, p.263–271.*

### 4.4. Formulation of SLNs

The selected formulations from SA-SLNs were (F11, F14) which put into a different code (F1 and F2) and the selected formulations from TP-SLNs were (F22, F28) put into a different code (F3 and F4).

#### 4.4.1. Determination of EE % of SLNs

The drug-entrapment efficiency of SLNs was estimated using equation (3.5) which ranged from 71.5 ± 0.07 % to 103.10 ± 0.01 % (mean ± SE) for the formulations prepared which have different drug concentrations (F1, F2, F3 and F4) Table 4.22.

#### 4.4.2. Determination of DL % of SLNs

The drug loading percentage of SLNs were calculated using Equation (3.6) and the results are shown in Table 4.22.

**Table 4.22.** *EE % and DL % (Mean ± SE) of SLNs*

| Code | EE (%) | DL (%) |
|---|---|---|
| **F1** | 71.5 ± 0.07 | 0.71 ± 0.01 |
| **F2** | 80.2 ± 0.06 | 1.57 ± 0.01 |
| **F3** | 103.10 ± 0.01 | 1.03 ± 2.00 |
| **F4** | 100.14 ± 0.65 | 0.25 ± 0.01 |

#### 4.4.3. Physicochemical characterization tests of SLNs

##### 4.4.3.1. *Particle size, polydispersity index, and zeta potential measurements*

The measured PS, PDI and ZP of the prepared SLNs formulations are presented in Table 4.23.

**Table 4.23.** *PS, PDI, and ZP* (*Mean ± SE) of SLNs*

| Code | PS (nm) | PDI | ZP (mV) |
|---|---|---|---|
| **F1** | 351.13 ± 1.39 | 0.33 ± 0.025 | -17.03 ± 0.53 |
| **F2** | 134.37 ± 0.91 | 0.13 ± 0.01 | -18.77 ± 0.20 |
| **F3** | 240.2 ± 22.9 | 0.2 ± 0.00 | -23 ± 1.5 |
| **F4** | 267.7 ± 18.7 | 0.3 ± 0.00 | -40.8 ± 1.2 |

### 4.4.3.2. *Morphology of SLNs*

For the evaluation of morphological structures of the SLNs and standard RCa, SEM microphotographs were shown in the Figure 4.18. and 4.19

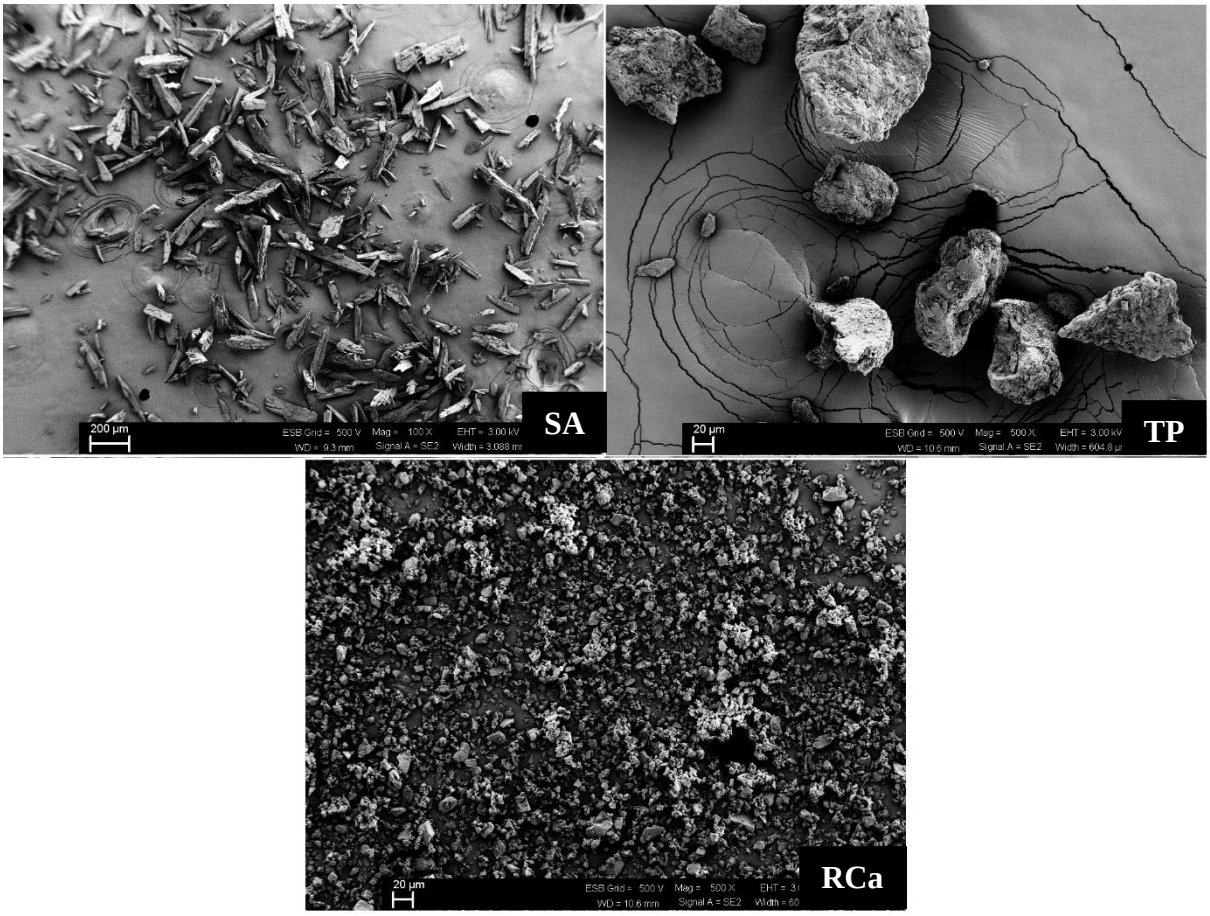


**Figure 4.18.** *SEM images of RCa, SA, and TP*

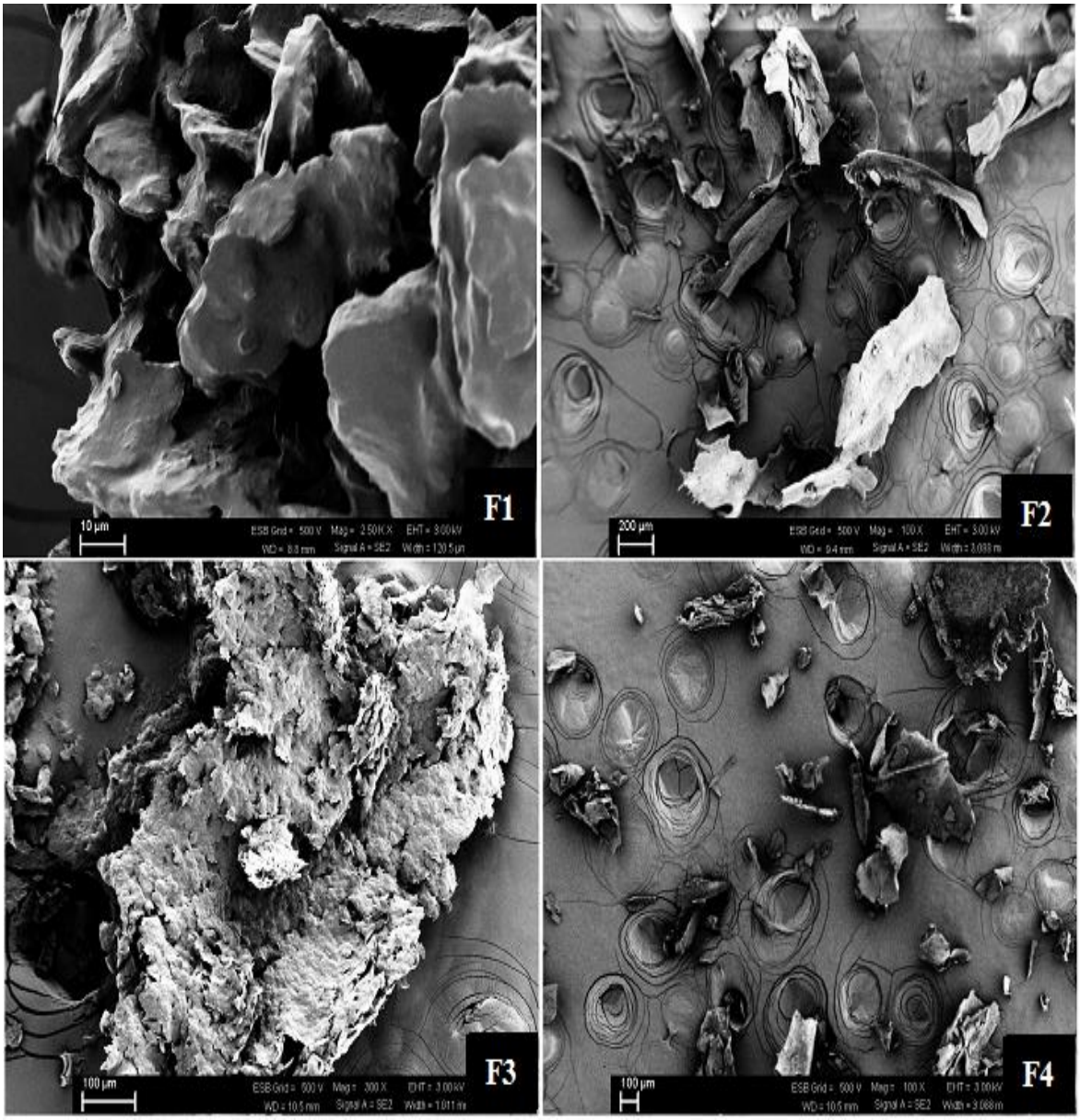


**Figure 4.19.** *SEM images of F1, F2, F3, and F4 SLNs Formulations*

#### 4.4.3.3. *Thermal analysis of SLNs*

The thermogram of the pure substances, freshly prepared SLNs formulations containing the active agent and the placebo are presented in Figure 4.20 and 4.21.

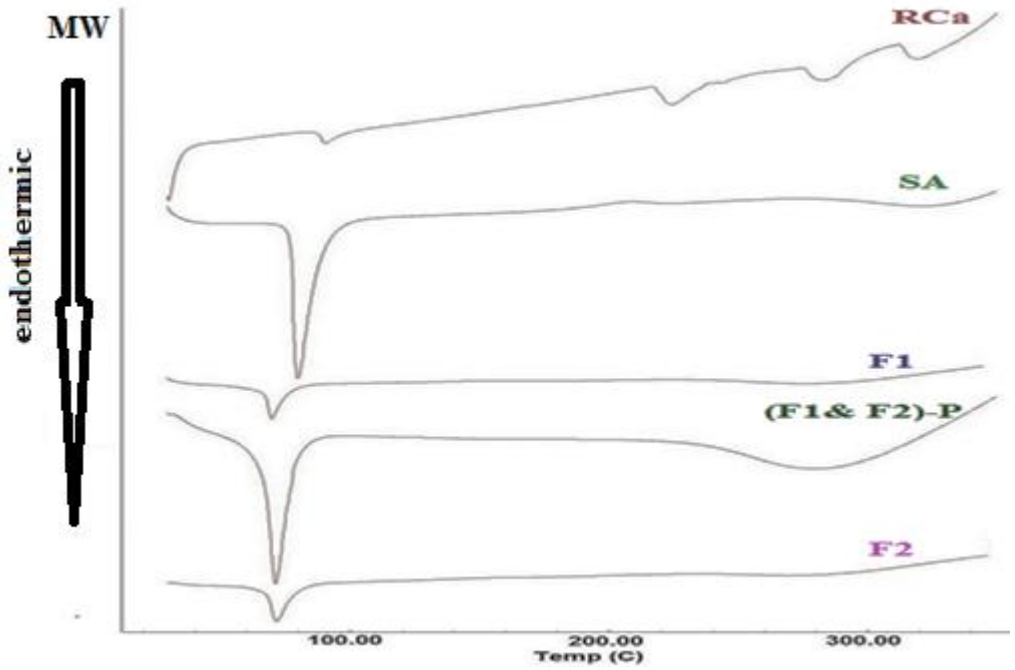


**Figure 4.20.** *DSC Thermograms of RCa, SA, SA- SLNs Formulations and Placebo*

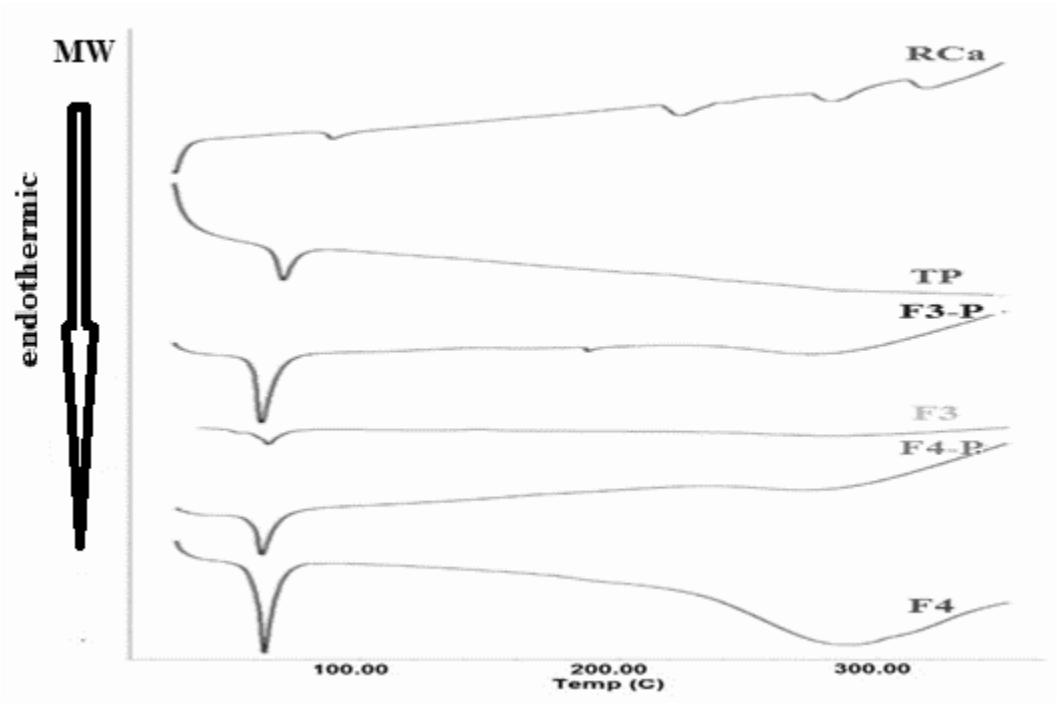


**Figure 4.21.** *DSC Thermograms of RCa, TP, TP- SLNs Formulations and Placebo*

#### 4.4.3.4. *Infrared (FT-IR) analysis of SLNs*

In SLNs formulation, the interaction possibilities between the SLNs formulation's ingredients and active agent were investigated by FT-IR. The FT-IR spectra of standard RCa and prepared formulations of SLNs are given in Figure 4.22 and 4.23, which were proposed the absence of chemical interaction between RCa and any of the formulation's ingredients used in the preparation of SLNs.

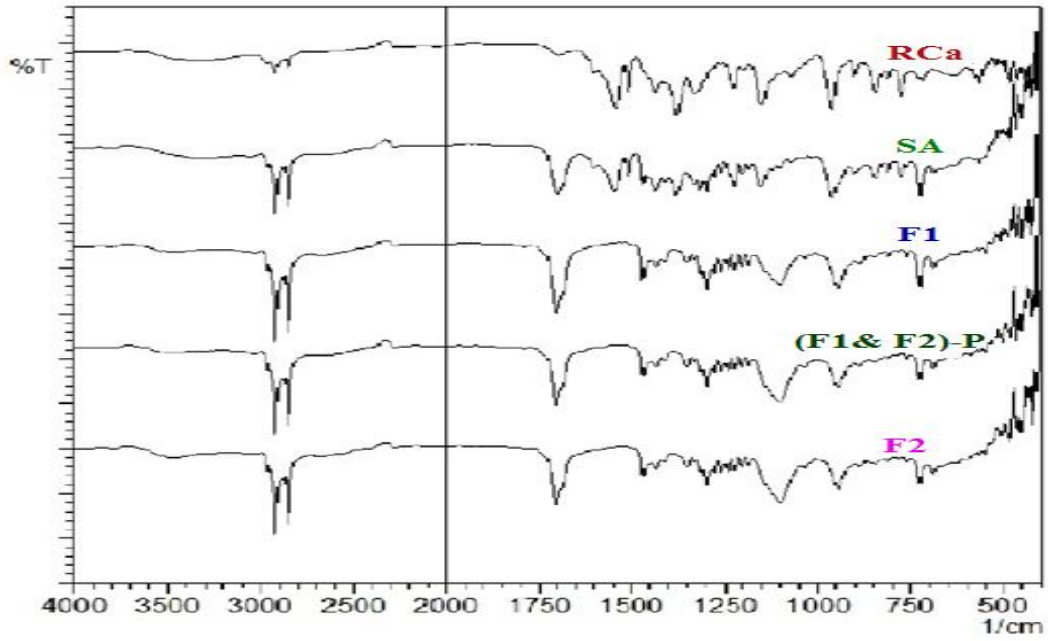


**Figure 4.22.** *FT-IR Spectra of RCa, SA, SA- SLNs Formulations and Placebo*

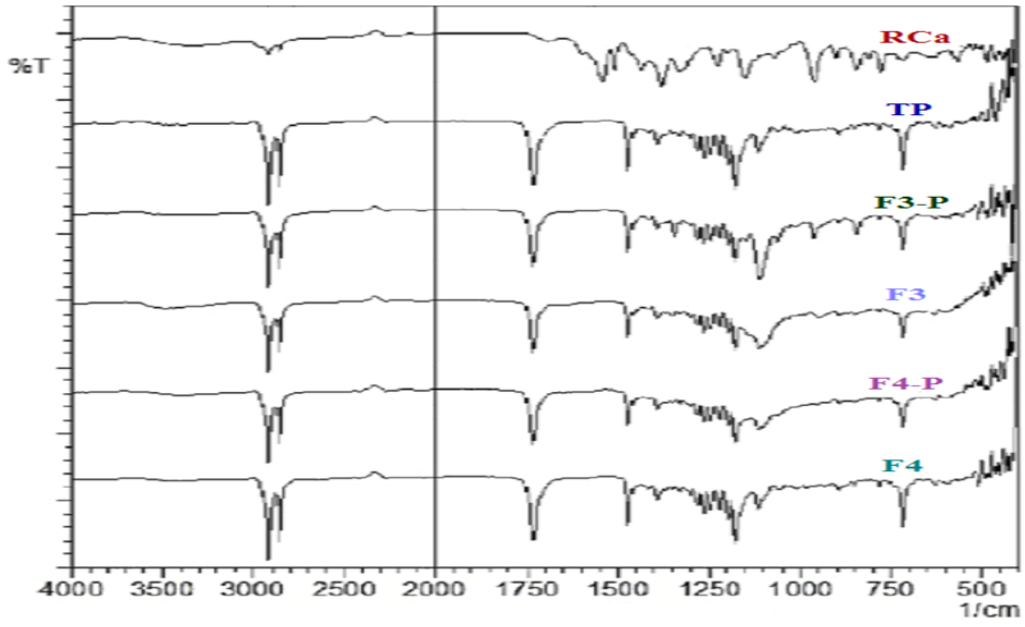


**Figure 4.23.** *FT-IR Spectra of RCa, TP, TP- SLNs Formulations and Placebo*

#### 4.4.3.5. *XRD analysis of SLNs*

The XRD patterns of RCa, prepared SLNs, placebo formulation, SA and TP are shown in Figure 4.24 and 4.25.

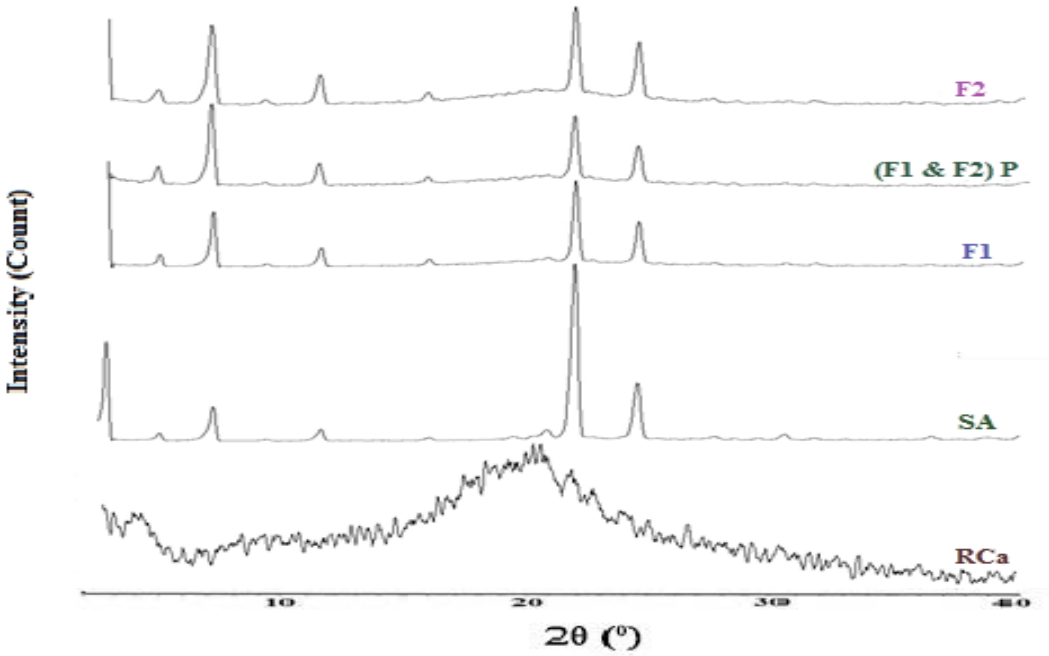


**Figure 4.24.** *XRD Spectra of RCa, SA, SA- SLNs Formulations and Placebo*

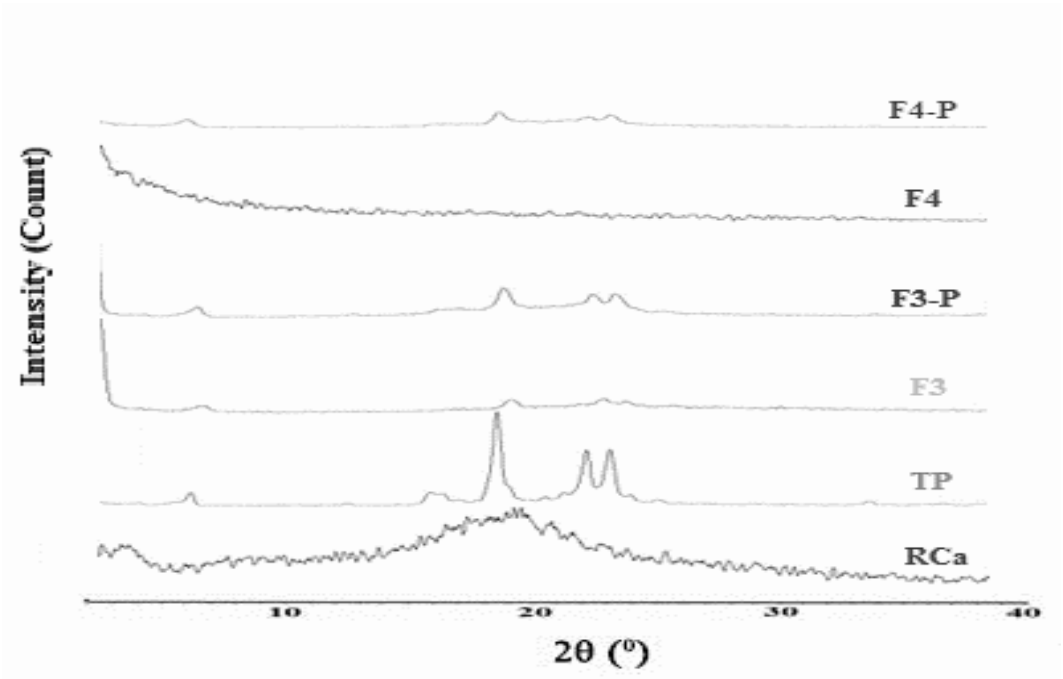


**Figure 4.25.** *XRD Spectra of RCa, TP, TP- SLNs Formulations and Placebo*

### 4.4.3.6. *$^{1}$H-NMR analysis of SLNs*

The $^{1}$H-NMR spectra of the SLNs formulations, RCa, SA, TP, and placebo are shown in Figure 4.26 and 4.27.

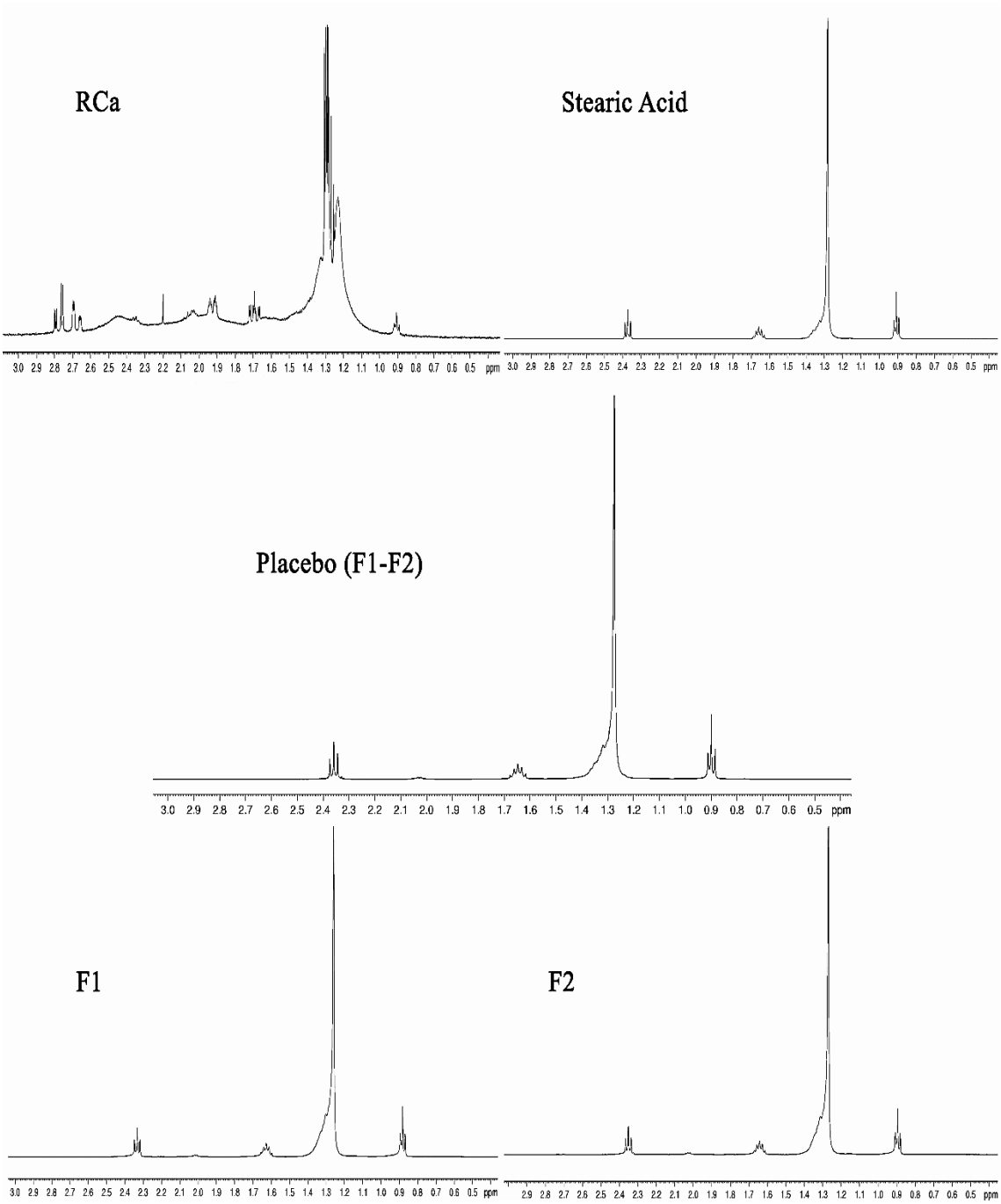


**Figure 4.26.** *$^{1}$H-NMR Spectra of RCa, SA, SA- SLNs Formulations and Placebo*

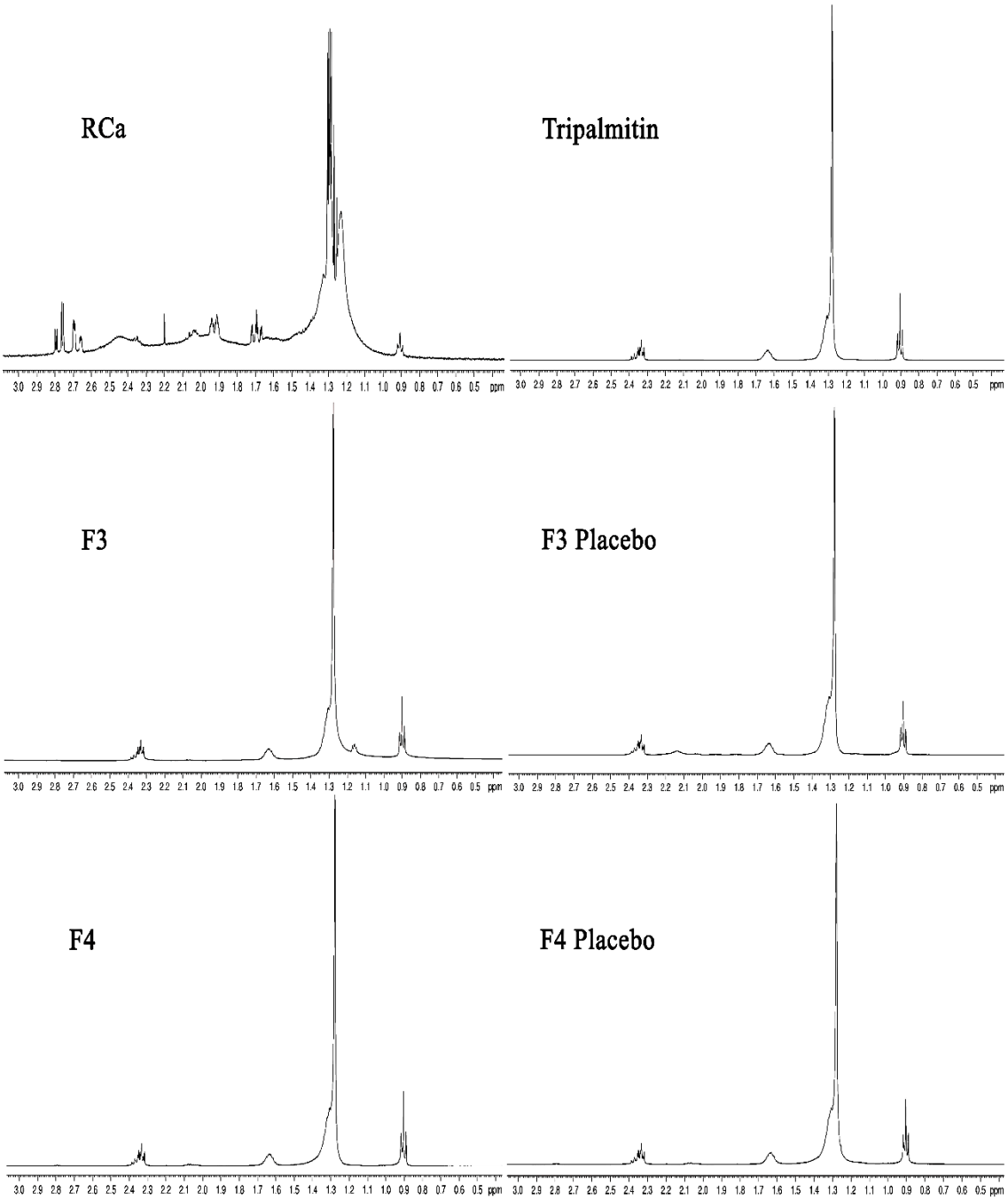


**Figure 4.27.** *$^{1}$H-NMR Spectra of RCa, TP, TP- SLNs Formulations and Placebo*

### 4.4.4. *In vitro* release studies

The profiles and data of *in vitro* release of RCa from the pure RCa and the selected SLNs formulations are illustrated in Table 4.24 and Figure 4.28.

**Table 4.24.** *% Cumulative Release of RCa From SLNs Formulations at pH 6.8 (n =3)*

| Time (Hour) | % Cumulative Release (mean ± SE) | | | | |
|---|---|---|---|---|---|
| | Pure RCa | F1 | F2 | F3 | F4 |
| **0.5** | 31.96 ± 2.31 | 14.73 ± 0.369 | 17.16 ± 0.66 | 33.53 ± 2.43 | 21.50 ± 0.50 |
| **1** | 53.07 ± 3.75 | 28.10 ± 1.58 | 29.45 ± 1.12 | 54.89 ± 2.82 | 37.83 ± 1.02 |
| **2** | 75.81 ± 4.69 | 45.16 ± 2.28 | 46.39 ± 1.51 | 73.17 ± 3.72 | 59.18 ± 1.42 |
| **3** | 86.22 ± 5.0 | 57.00 ± 1.48 | 57.40 ± 1.65 | 83.26 ± 2.76 | 73.33 ± 0.66 |
| **4** | 91.60 ± 4.97 | 65.76 ± 1.57 | 64.54 ± 1.69 | 87.17 ± 1.88 | 82.50 ± 0.55 |
| **6** | 95.46 ± 4.73 | 78.88 ± 1.44 | 74.36 ± 1.61 | 92.16 ± 1.04 | 92.40 ± 0.47 |
| **8** | - | 85.16 ± 1.06 | 78.27 ± 1.50 | 93.10 ± 0.94 | 96.13 ± 0.09 |
| **12** | - | 91.97 ± 0.46 | 83.41 ± 1.05 | 93.80 ± 0.73 | 99.64 ± 0.05 |
| **24** | - | 97.62 ± 0.25 | 89.34 ± 0.68 | 88.30 ± 0.49 | 97.78 ± 0.44 |
| **48** | - | 105.63 ± 0.72 | 98.34 ± 0.57 | 86.25 ± 0.15 | 97.09 ± 0.66 |

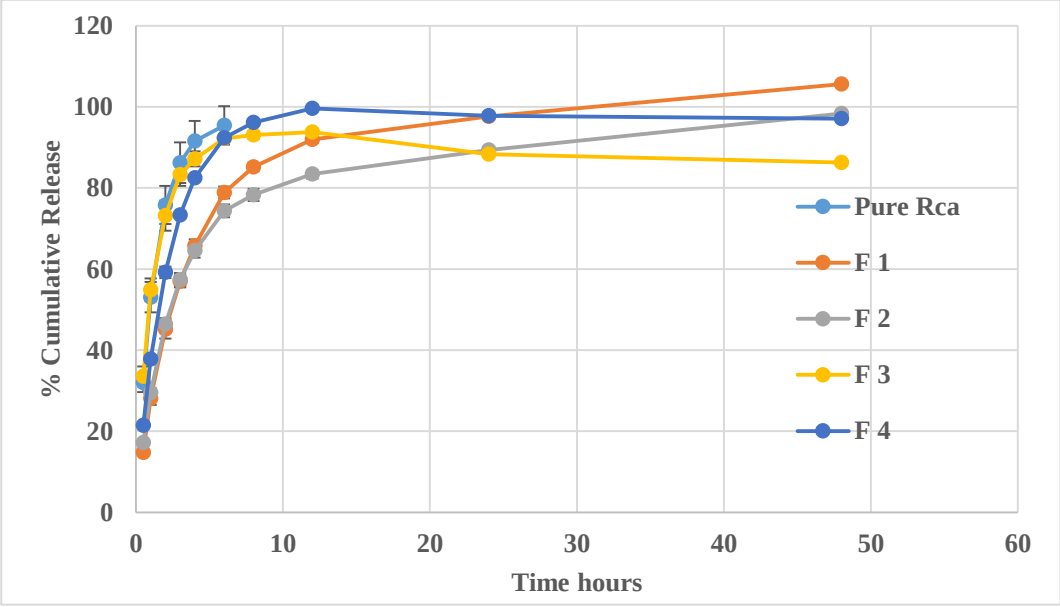


**Figure 4.28.** *% Cumulative Release of RCa From SLNs Formulations at pH 6.8 (mean ± SE), (n =3)*

### 4.4.5. Kinetics and mechanism of release

*In vitro* release profiles in phosphate buffer (pH 6.8) for the selected SLNs were used to different kinetic models (zero order kinetics, first order kinetics, Higuchi model, Korsmeyer-Peppas model and Hixson-Crowell model). The release data were estimated by rate constant (k), r-values ($r^2$) and Akaike criteria (AIC) for the selection of best appropriate kinetic model Table 4.25., Figure 4.29.

**Table 4.25.** *Kinetic Modeling of RCa Release from SLNs Formulations by DDsolver Software Program*

| Code | | Kinetic Model | | | | |
|---|---|---|---|---|---|---|
| | | **Zero order** | **First order** | **Higuchi** | **Korsmeyer-Peppas*** | **Hixson-Crowell** |
| **Pure RCa** | **k** | 0.021 | 0.001 | 0.045 | 0.048 | 0.000 |
| | **$r^2$** | 0.001 | 0.001 | 0.001 | 0.001 | 0.001 |
| | **AIC** | 0.078 | 0.048 | 0.059 | 0.065 | 0.051 |
| **F1** | **k** | 0.003 | 0.000 | 0.021 | 0.042 | 0.000 |
| | **$r^2$** | -00.001 | 00.001 | 00.000 | 00.001 | 00.000 |
| | **AIC** | 00.101 | 00.049 | 00.087 | 00.076 | 00.089 |
| **F2** | **k** | 0.003 | 0.000 | 0.020 | 0.048 | 0.000 |
| | **$r^2$** | -00.002 | 00.001 | 00.000 | 00.001 | 00.000 |
| | **AIC** | 00.100 | 00.079 | 00.086 | 00.075 | 00.088 |
| **F3** | **k** | 0.003 | 0.000 | 0.022 | 0.057 | 0.000 |
| | **$r^2$** | -00.009 | -00.003 | -00.003 | 00.000 | -00.004 |
| | **AIC** | 00.107 | 00.098 | 00.098 | 00.080 | 00.101 |
| **F4** | **k** | 0.003 | 0.000 | 0.022 | 0.063 | 0.000 |
| | **$r^2$** | -00.003 | 00.000 | 00.000 | 00.001 | -00.001 |
| | **AIC** | 00.105 | 00.086 | 00.094 | 00.082 | 00.095 |

**Reference:** *DDsolver Program, Zhang et al., 2010, p.263–271.*

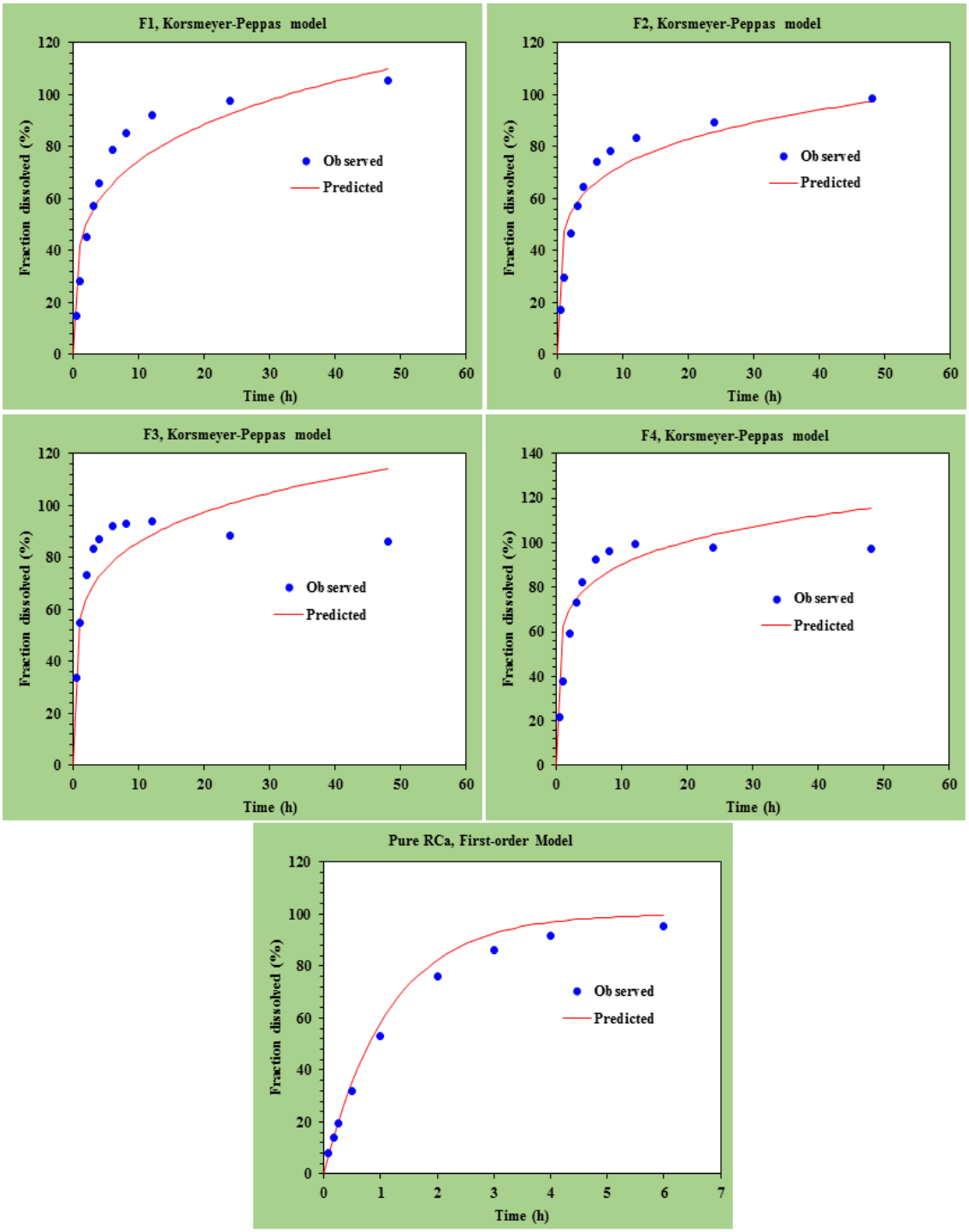


**Figure 4.29.** *Kinetic Modeling of RCa Release from SLNs Formulations by DDsolver Software Program*

**Reference:** *DDsolver Program, Zhang et al., 2010, p.263–271.*

## 4.5. Formulation of CDs Inclusion Complexes

### 4.5.1. Phase solubility studies

Experiments carried out in the manner described in the methods section (3.6.1). In the results; the RCa solubility increased in CDs solution with relative to the shaking time.

#### 4.5.1.1. *Determine the phase solubility diagram of RCa / M-β-CDs*

The resolution phase diagram shows that when different RCa concentrations are plotted against different M-β-CDs concentrations on the graph, the solubility diagram shows the solubility phase of Higuchi. It has been determined that the $A_L$ type diagram conforms to the diagrams Figure 4.30. Relevant to the $A_L$ type diagram, the preparation of RCa / M-β-CDs complexes were carried out at ratio of 1: 1 molar (Higuchi and Connors, 1965, p.117–210).

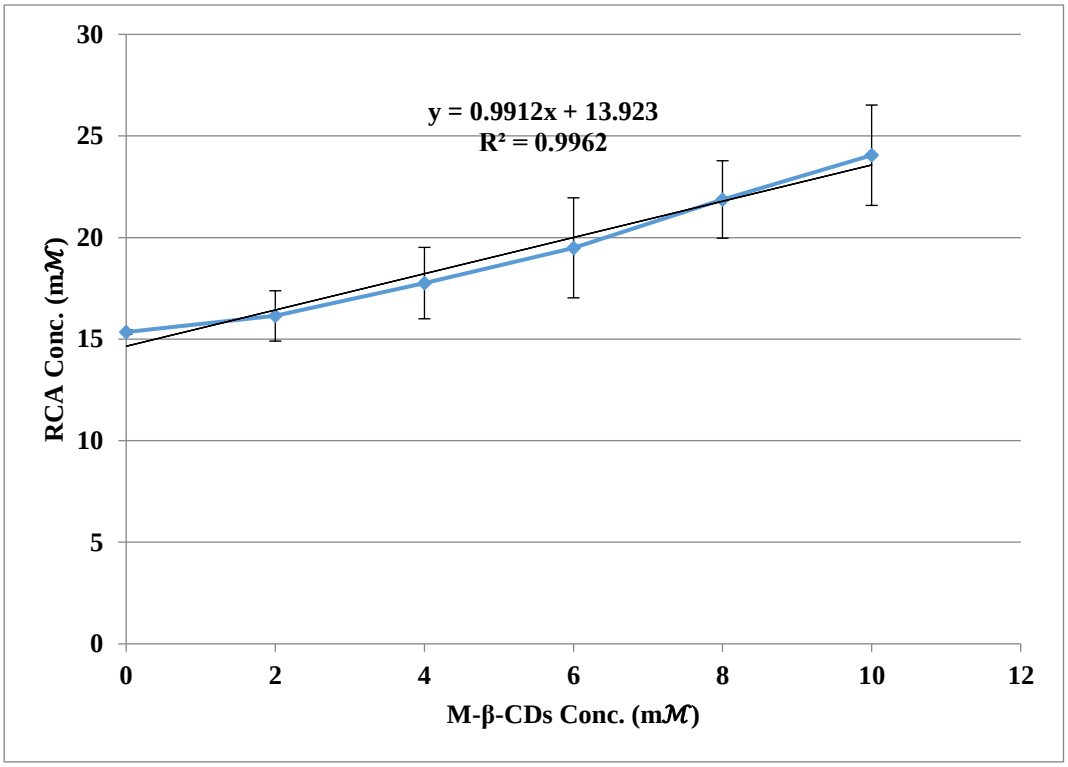


**Figure 4.30.** *Phase Solubility Diagram of RCa / M-β-CDs (mean ± SE), (n = 3)*

#### 4.5.1.2. *Determine the phase solubility diagram of RCa / Captisol®*

The resolution phase diagram shows that when different RCa concentrations are plotted against different Captisol® concentrations on the graph, the solubility diagram shows the solubility phase of Higuchi. It has been determined that the $A_L$ type diagram conforms to the diagrams Figure 4.31. Relevant to the $A_L$ type diagram, the preparation of RCa / Captisol® complexes were carried out at ratio of 1: 1 molar (Higuchi and Connors, 1965, p. 117–210).

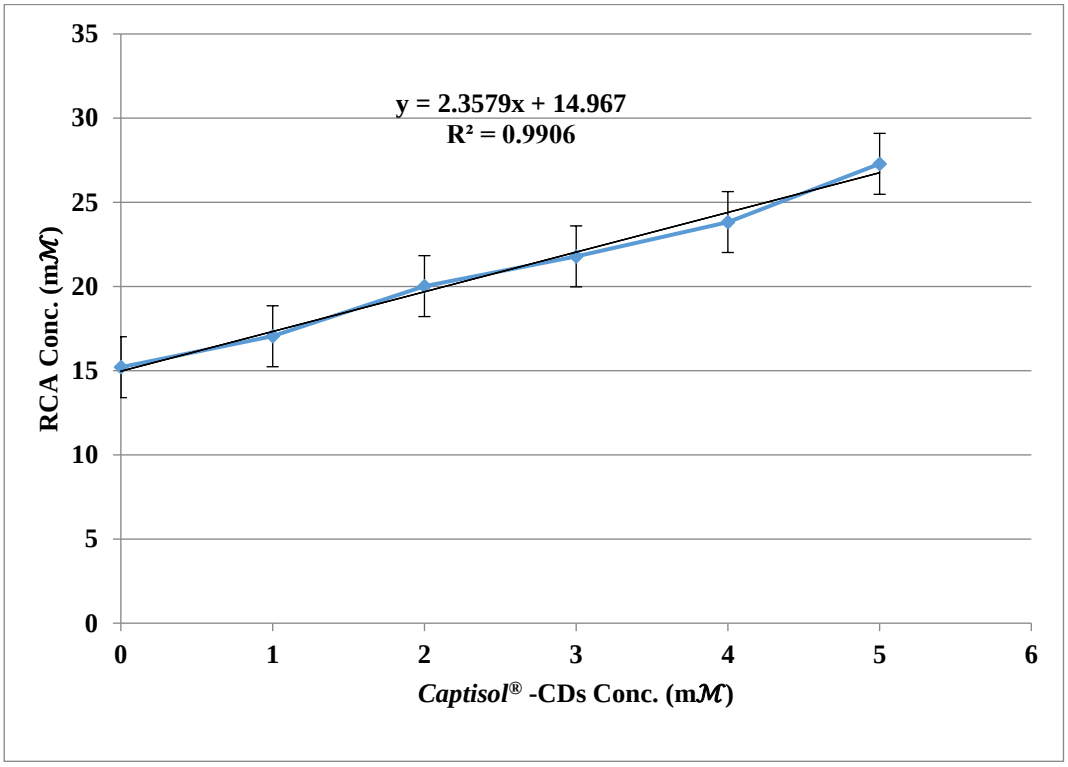


**Figure 4.31.** *Phase Solubility Diagram of RCa / Captisol® (mean ± SE) (n = 3)*

### 4.5.2. Preparation of CDs inclusion complex formulations

The RCa/M-β-CDs inclusion complexes were prepared by kneading method using (water: ethanol) (1:1) for formulation F1 and only distilled water used for F2 while the formulation F3 was prepared by the lyophilization method. The RCa/ Captisol® formulations F4 and F5 were prepared by kneading method using (water: ethanol) (1:1, v/v) and distilled water, respectively whereas the formulation F6 was prepared by lyophilization method.

### 4.5.3. Physicochemical Characterization of CDs inclusion complexes

#### 4.5.3.1. *PS, PID, ZP, and DC % of CDs inclusion complexes*

The measured PS, PDI and ZP of the prepared CDs inclusion complex formulations are shown in Table 4.26. The drug contents percentage was calculated using equation (3.4) Table 4.26.

**Table 4.26.** *PS, PDI, ZP and DC %* (*Mean ± SE) of CDs Inclusion Complexes*

| Code | PS (nm) | PDI | ZP (mV) | DC (%) |
|---|---|---|---|---|
| **F1** | 455.97 ± 14.73 | 0.327 ± 0.06 | - 8.33 ± 0.48 | 105.40 ± 0.93 |
| **F2** | 192.60 ± 4.78 | 0.364 ± 0.02 | - 21.80 ± 0.36 | 100.26 ± 2.04 |
| **F3** | 532.80 ± 15.35 | 0.310 ± 0.03 | - 14.73 ± 0.54 | 106.22 ± 1.01 |
| **F4** | 321.77 ± 5.23 | 0.426 ± 0.01 | - 13.90 ± 0.17 | 97.06 ± 1.36 |
| **F5** | 210.30 ± 5.70 | 0.448 ± 0.02 | - 18.70 ± 0.13 | 93.50 ± 1.70 |
| **F6** | 220.33 ± 4.80 | 0.382 ± 0.01 | - 11.13 ± 0.03 | 104.31 ± 1.58 |

#### 4.5.3.2. *Morphology of CDs inclusion complexes*

The morphological structures as SEM microphotographs of RCa, M-β-CDs, Captisol®, and the CDs inclusion complex formulations and their placebo are illustrated in the Figures 4.32. and 4.33.

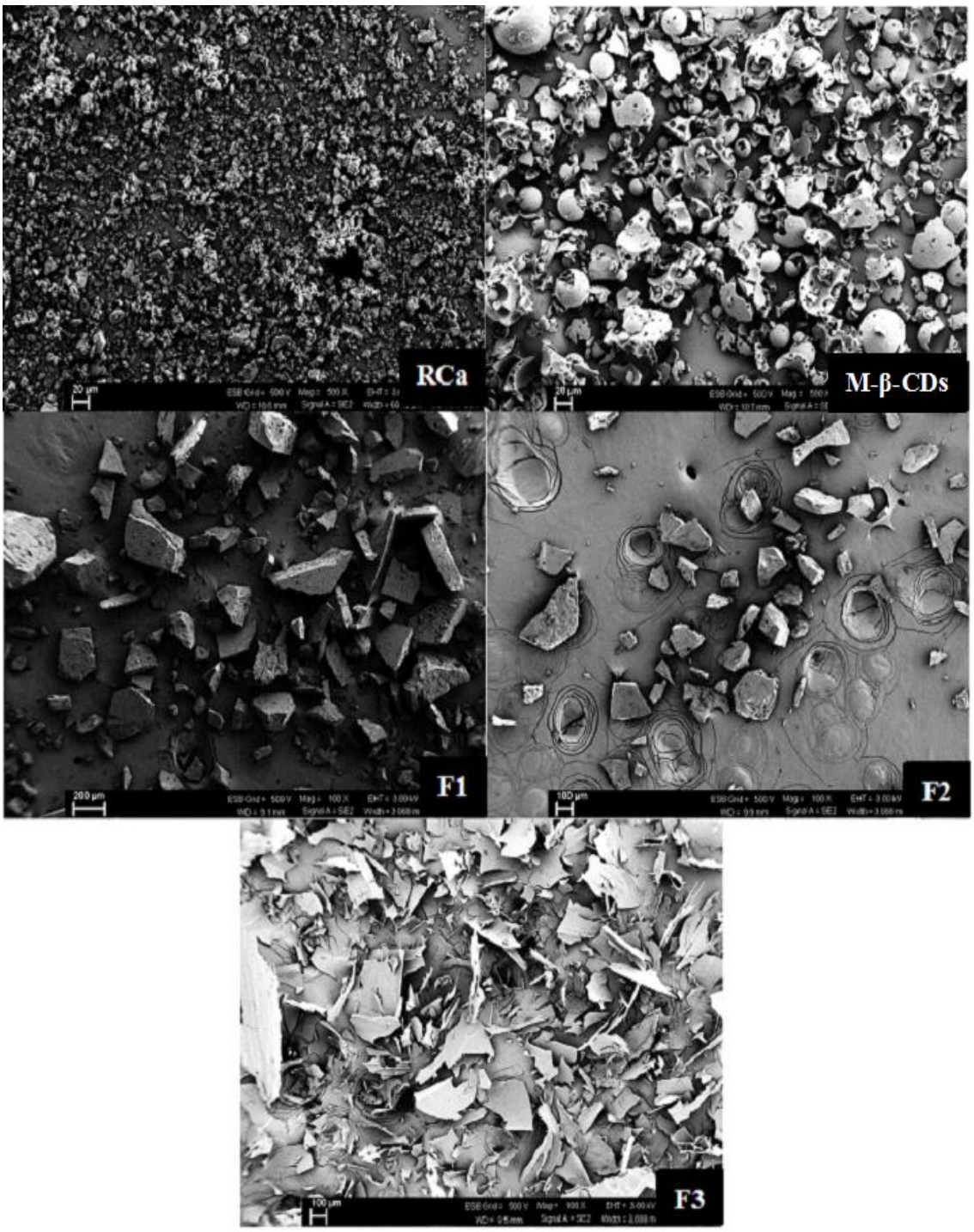


**Figure 4.32.** *SEM Images of RCa, M-β-CD, and Inclusion Complexes of M-β-CD*

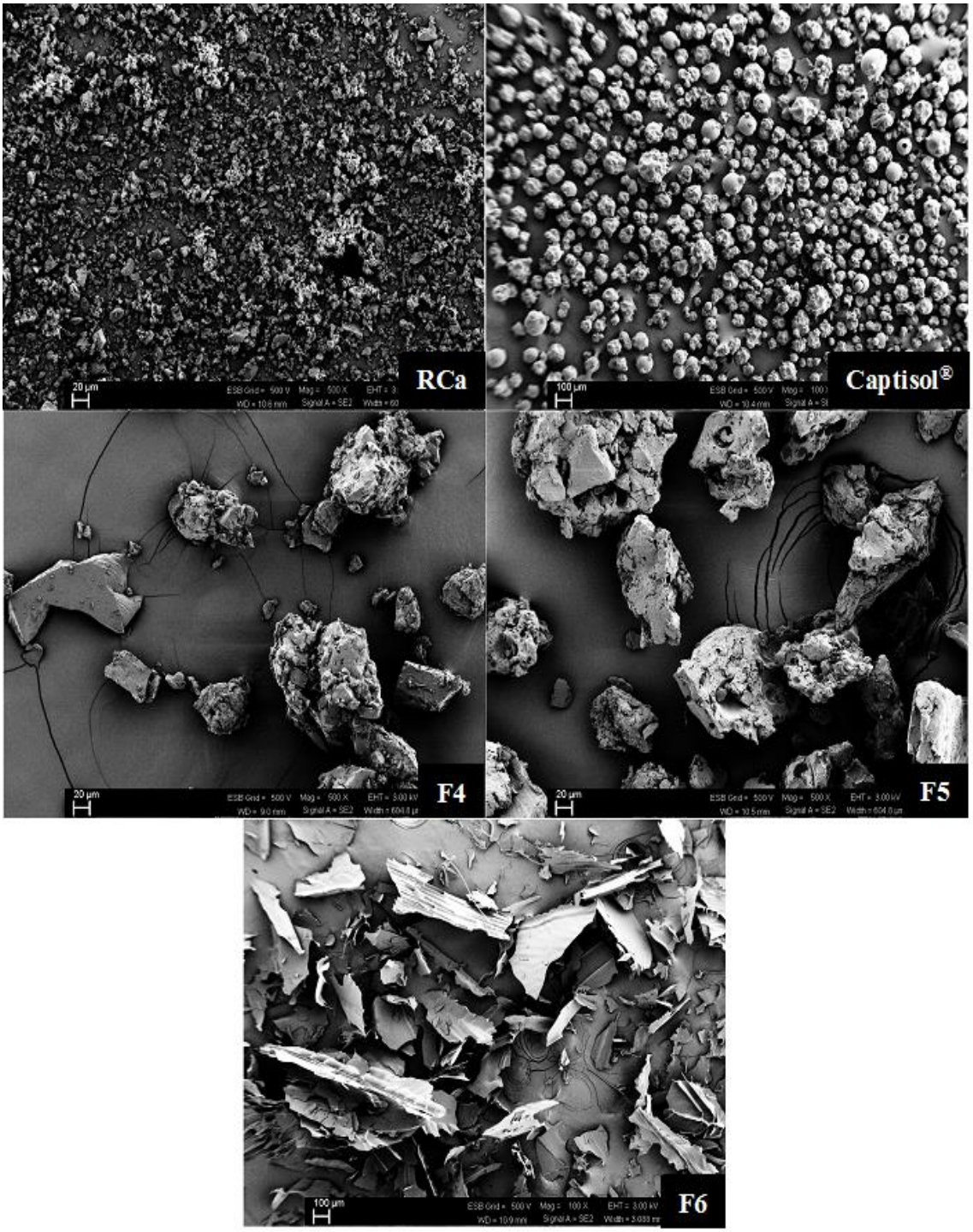


**Figure 4.33.** *SEM Images of RCa, Captisol®, and Inclusion Complexes of Captisol®*

#### 4.5.3.3. *Thermal analysis of CDs inclusion complexes*

The thermogram of RCa, M-β-CDs, Captisol®, and the CDs inclusion complex formulations and their placebo are shown in the Figures 4.34. 4.35.

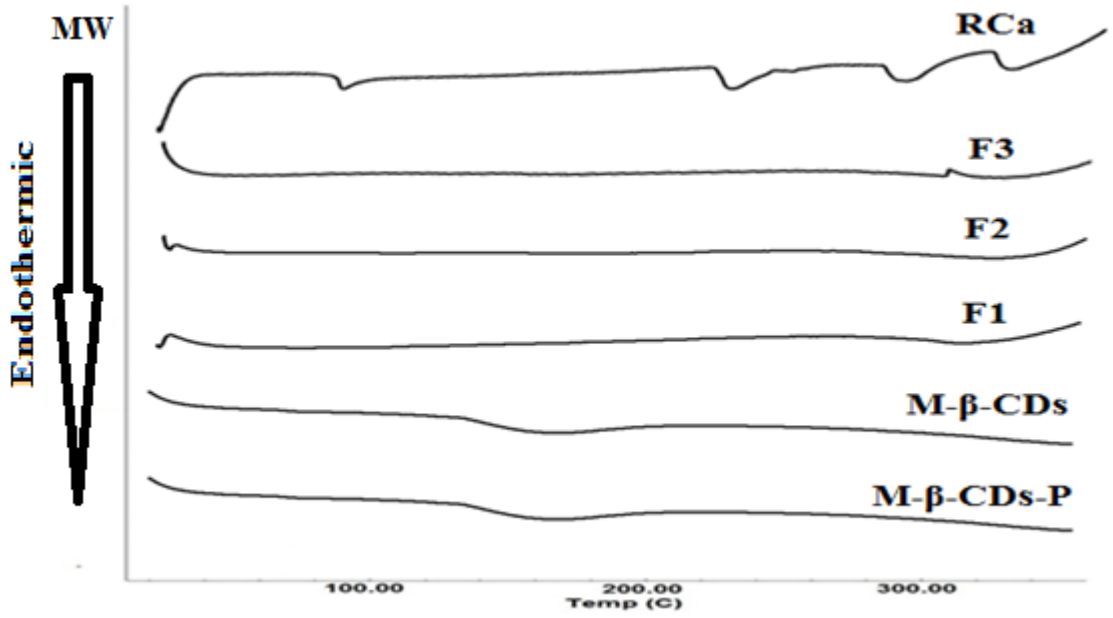


**Figure 4.34.** *DSC Thermograms of RCa, M-β-CD, M-β-CD-P and CDs Inclusion Complexes of M-β-CD*

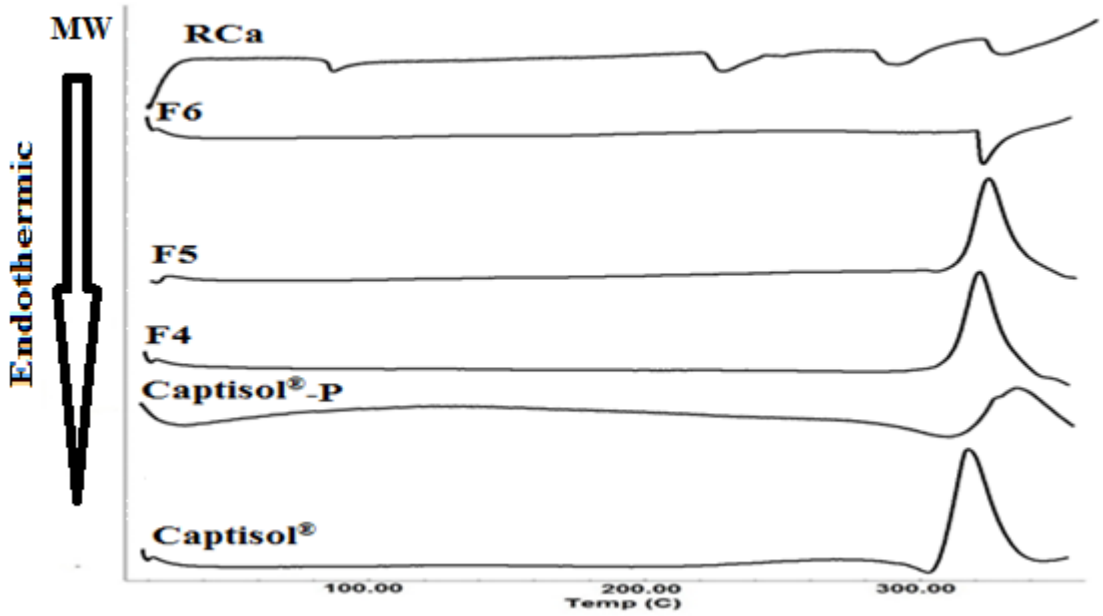


**Figure 4.35.** *DSC Thermograms of RCa, Captisol®, Captisol®-P and CDs Inclusion Complexes of Captisol®*

#### 4.5.3.4. *FT-IR analysis of CDs inclusion complexes*

The CDs complex formation was also confirmed in the FT-IR spectra analysis by investigating the characteristic peaks of the active molecule RCa, M-β-CD, Captisol®, placebo, RCa/ M-β-CD complex and RCa/ Captisol® complex. Figures 4.36.

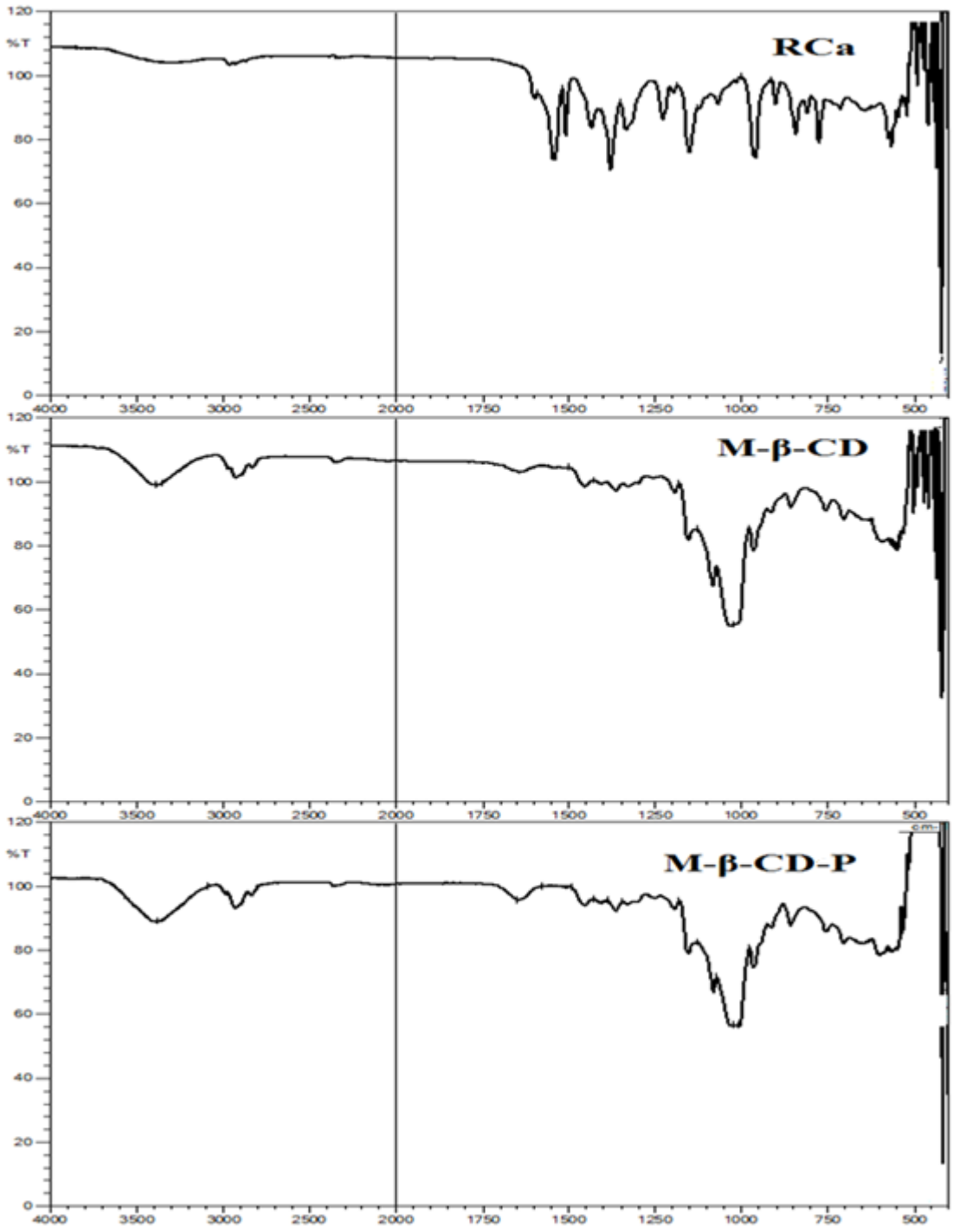


**Figure 4.36.** *FT-IR Spectra of RCa, M-β-CD, Captisol®, Placebo and Inclusion Complexes*

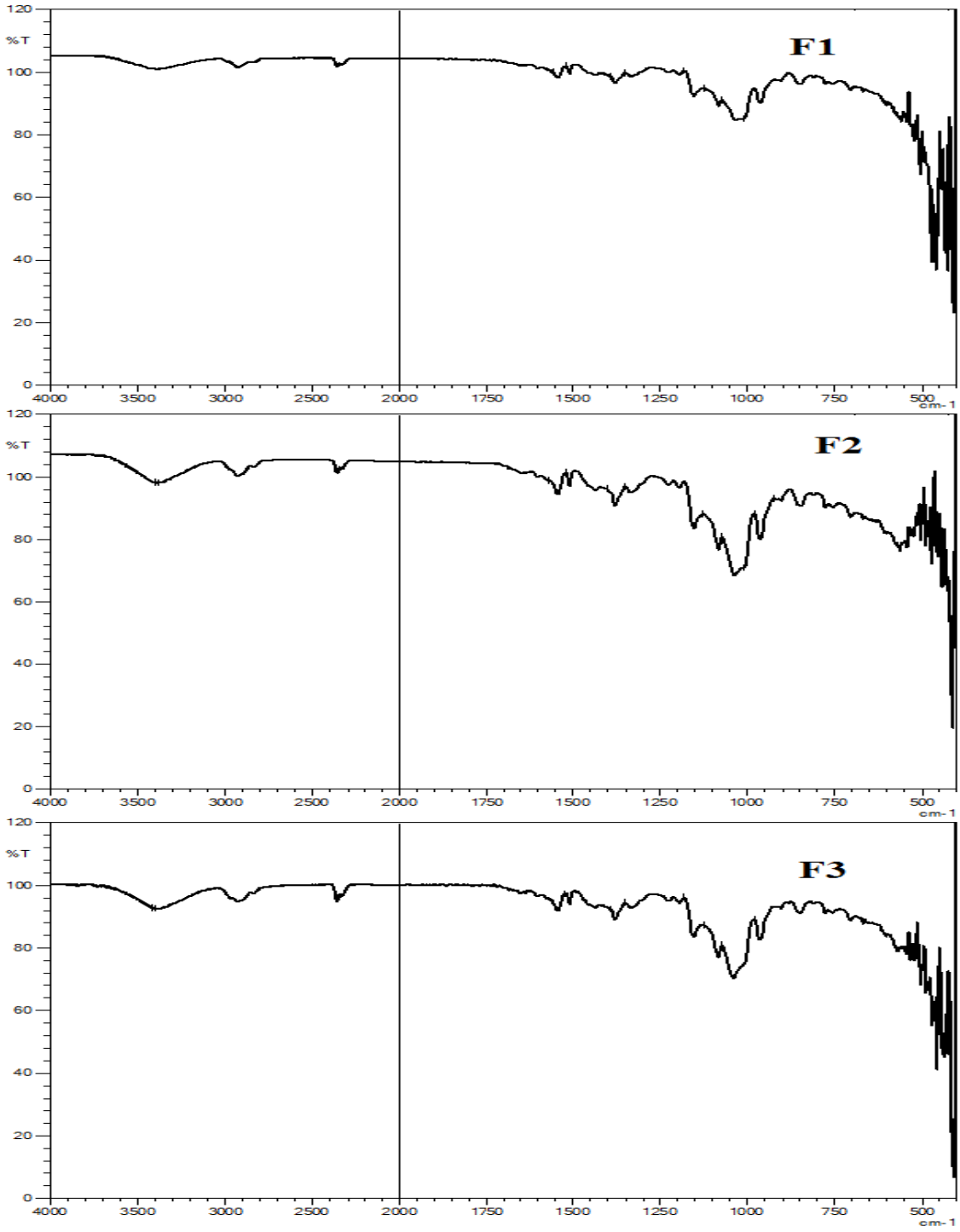


**Figure 4.36. (continued)** *FT-IR Spectra of RCa, M-β-CD, Captisol®, Placebo and Inclusion Complexes*

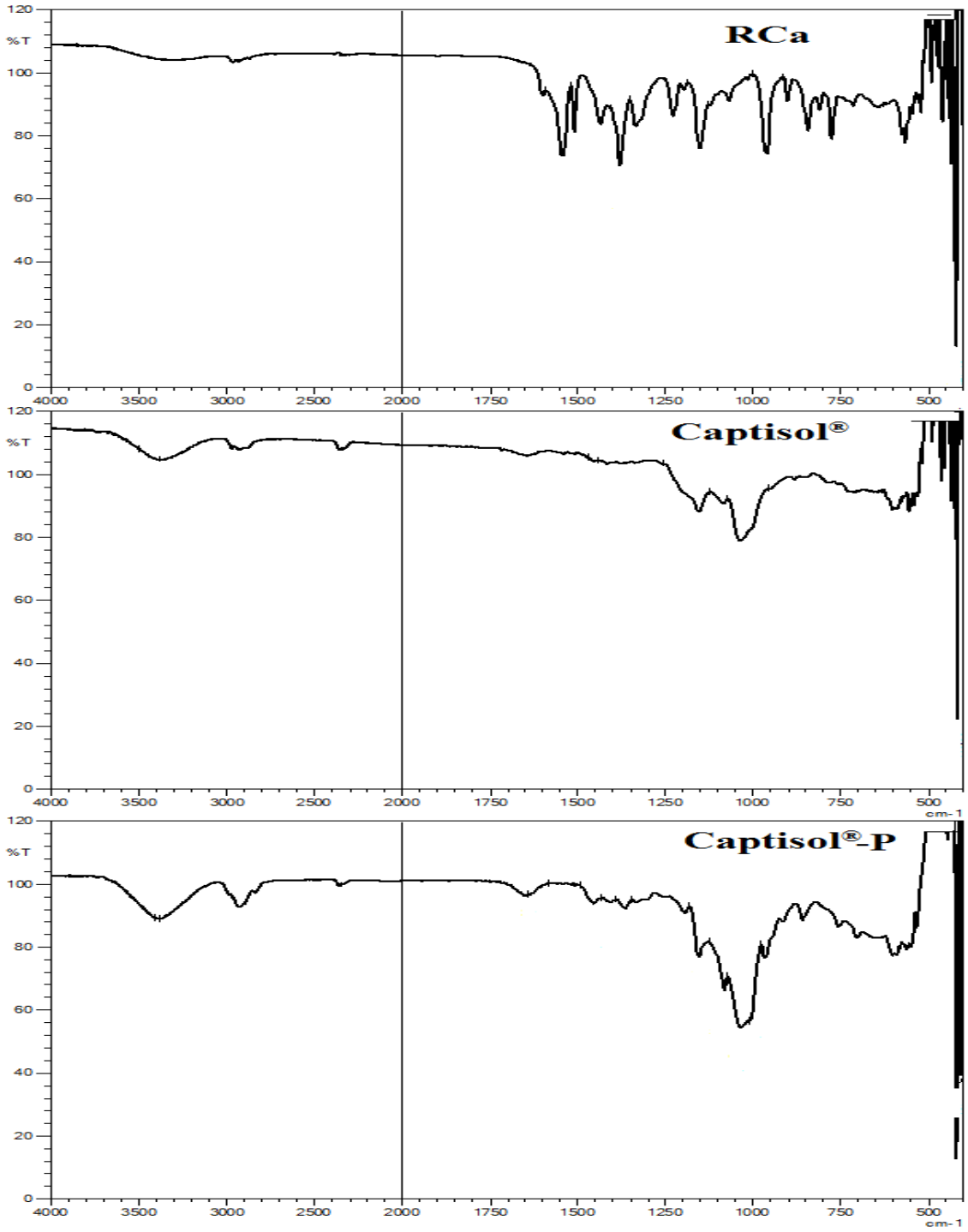


**Figure 4.36. (continued)** *FT-IR Spectra of RCa, M-β-CD, Captisol®, Placebo and Inclusion Complexes*

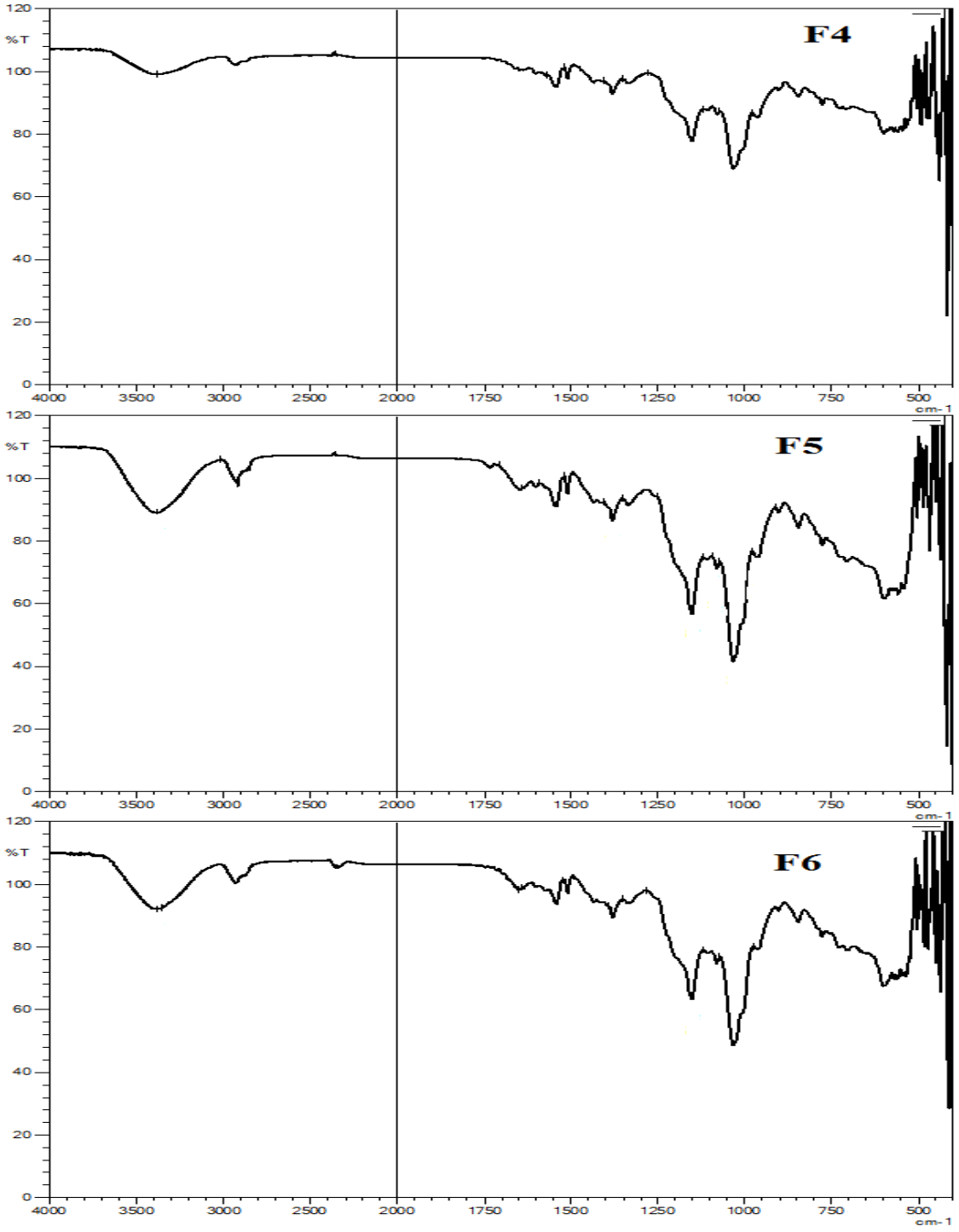


**Figure 4.36. (continued)** *FT-IR Spectra of RCa, M-β-CD, Captisol®, Placebo and Inclusion Complexes*

#### 4.5.3.5. *XRD analysis of CDs inclusion complexes*

The XRD patterns of RCa, M-β-CD, Captisol®, and the CDs inclusion complex formulations and their placebo are demonstrated in the Figures 4.37.

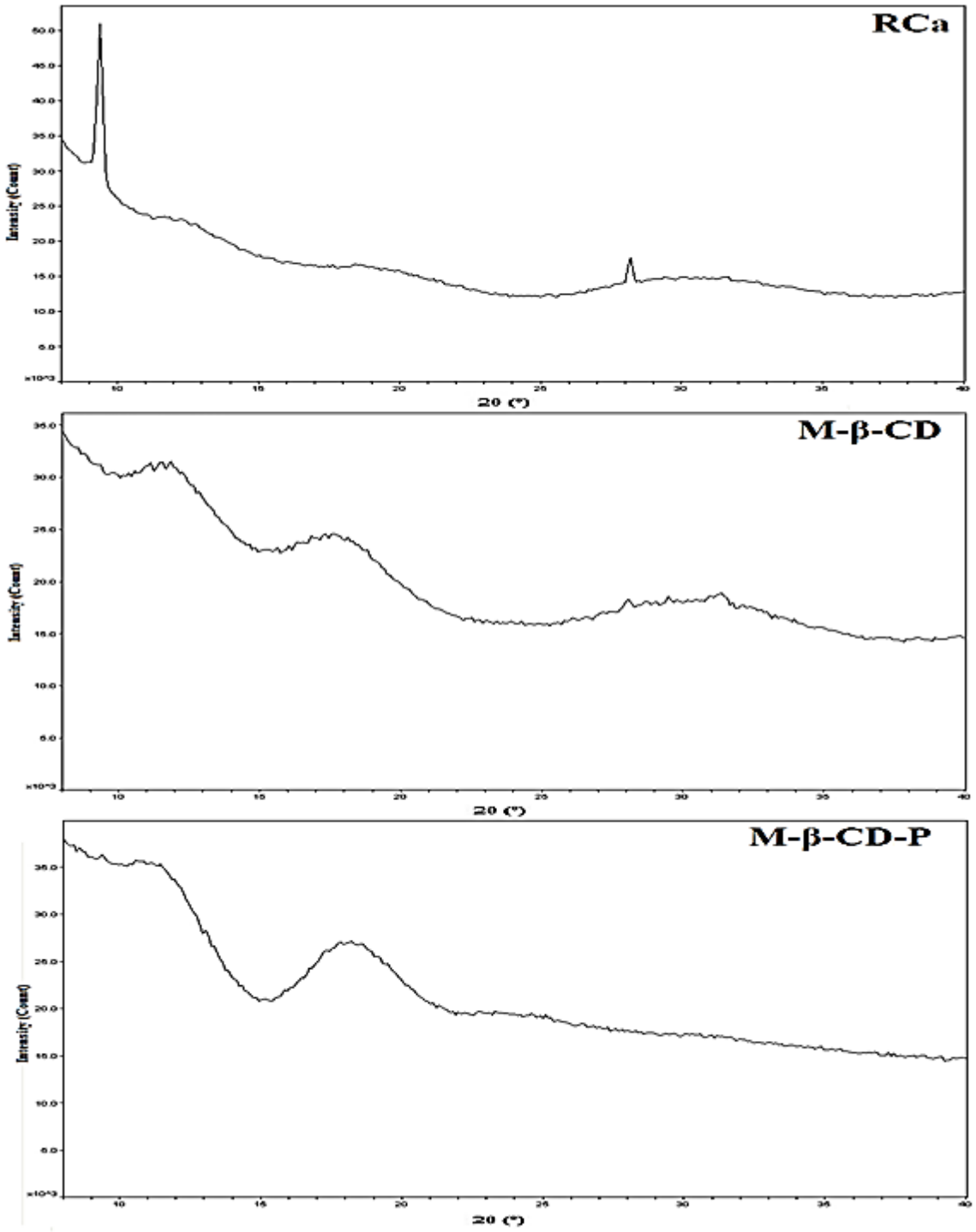


**Figure 4.37.** *XRD Spectra of RCa, M-β-CD, Captisol®, Placebo and Inclusion Complexes*

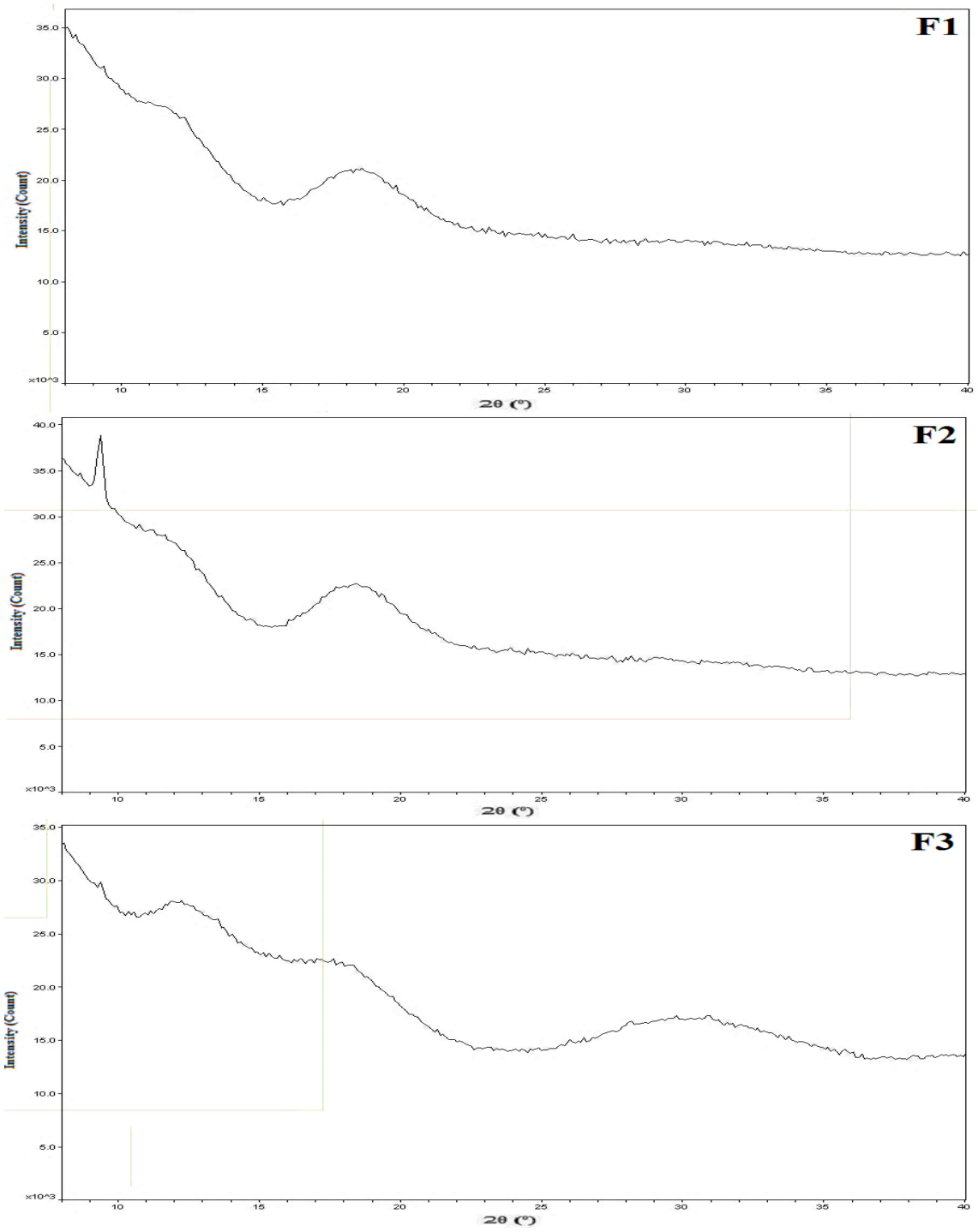


**Figure 4.37. (continued)** *XRD Spectra of RCa, M-β-CD, Captisol®, Placebo and Inclusion Complexes*

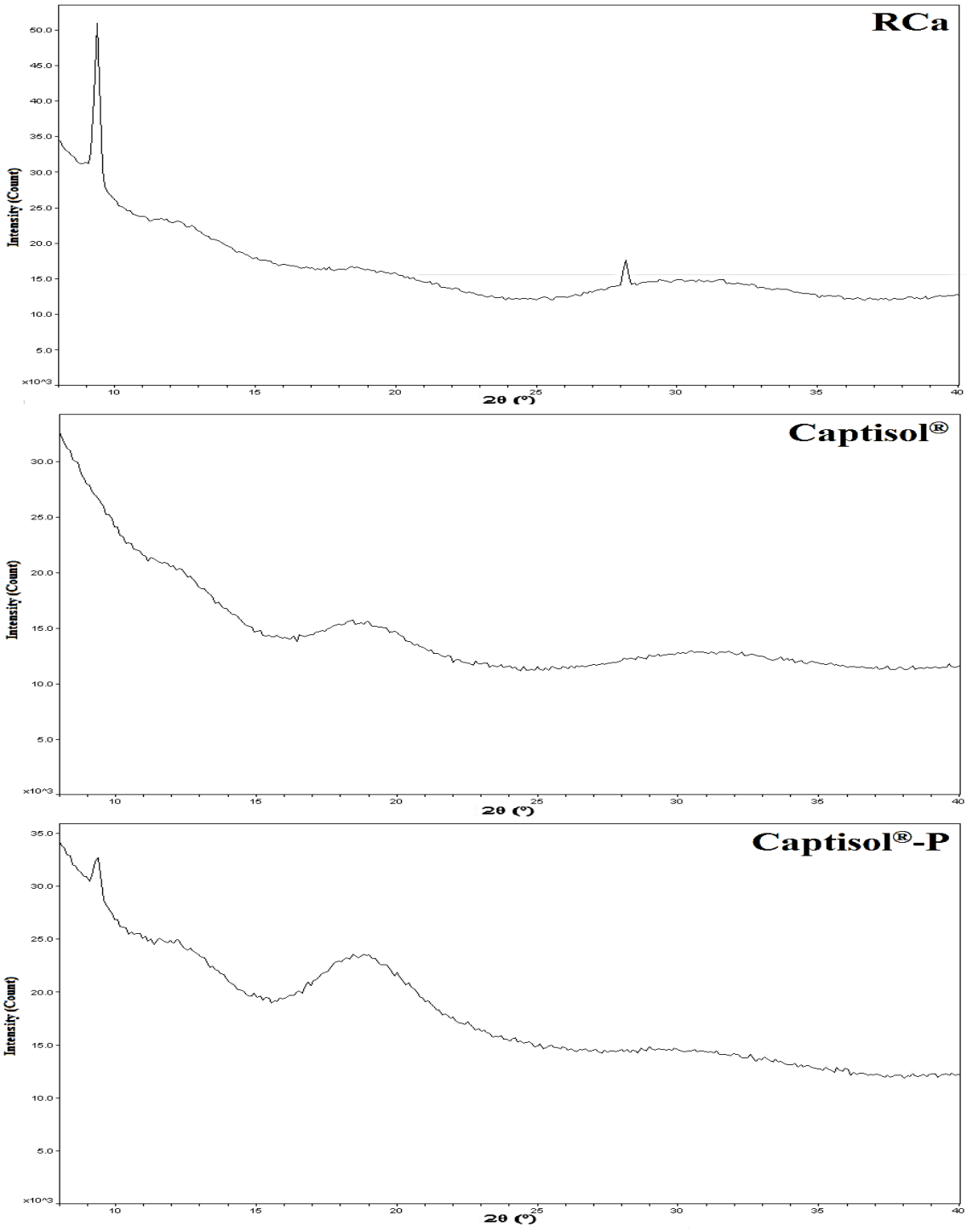


**Figure 4.37. (continued)** *XRD Spectra of RCa, M-β-CD, Captisol®, Placebo and Inclusion Complexes*

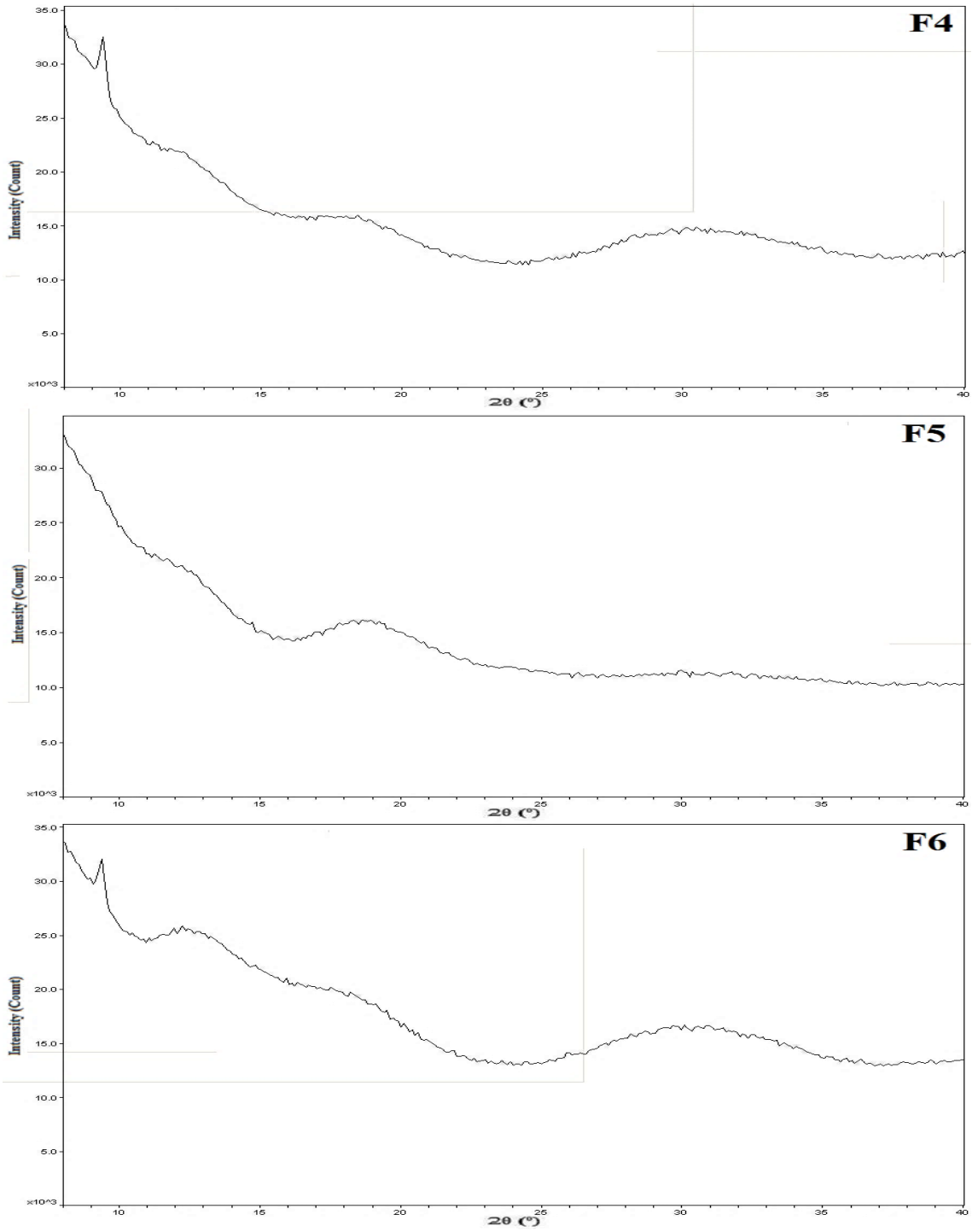


**Figure 4.37. (continued)** *XRD Spectra of RCa, M-β-CD, Captisol®, Placebo and Inclusion Complexes*

### 4.5.3.6. *$^{1}$H-NMR analysis of CDs inclusion complexes*

The $^{1}$H-NMR spectra of RCa, M-β-CDs, Captisol®, the CDs inclusion complex formulations and their placebo are illustrated in the Figures 4.38.

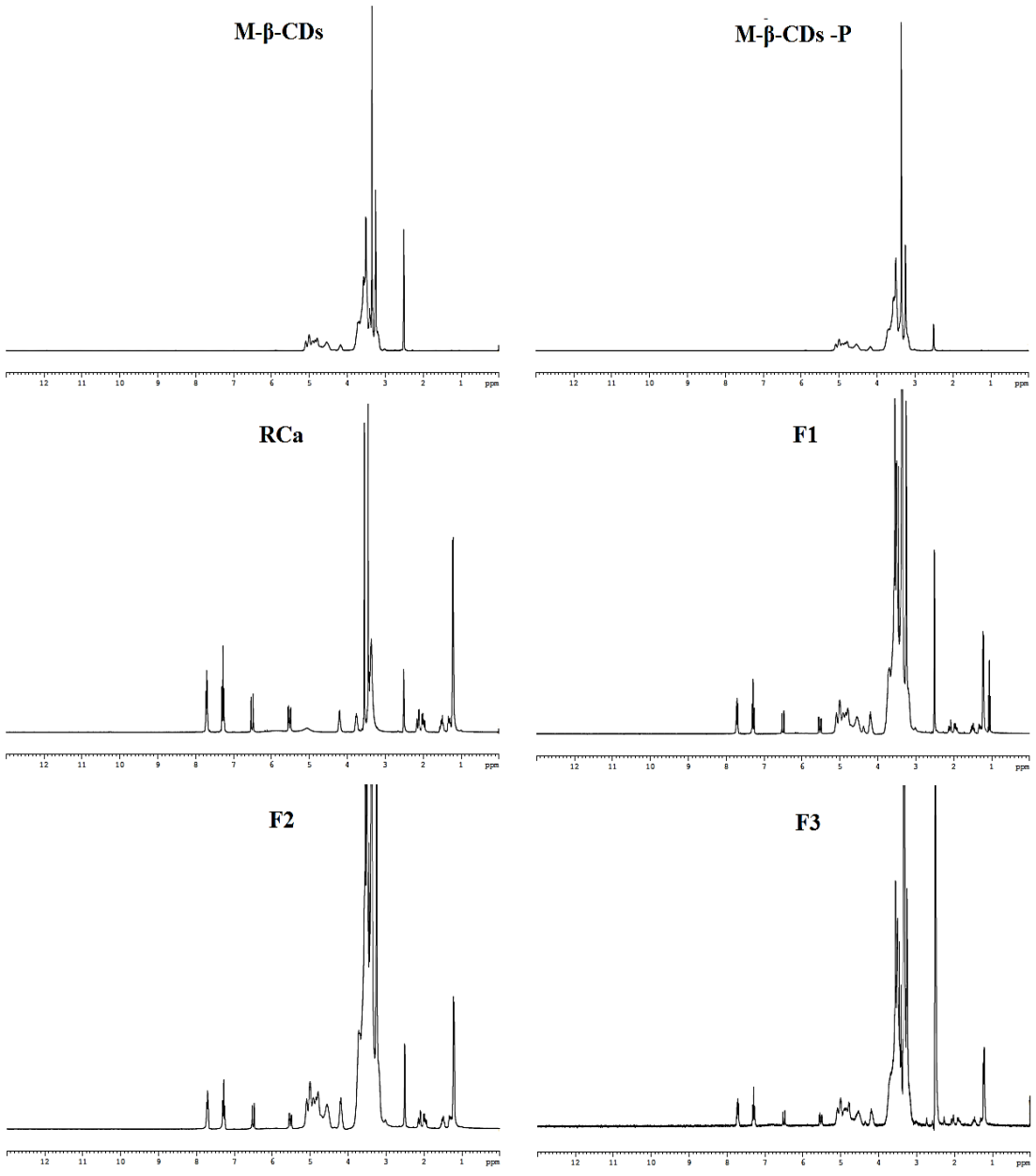


**Figure 4.38.** *$^{1}$H-NMR spectra of RCa, M-β-CD, Captisol®, Placebo and Inclusion Complexes*

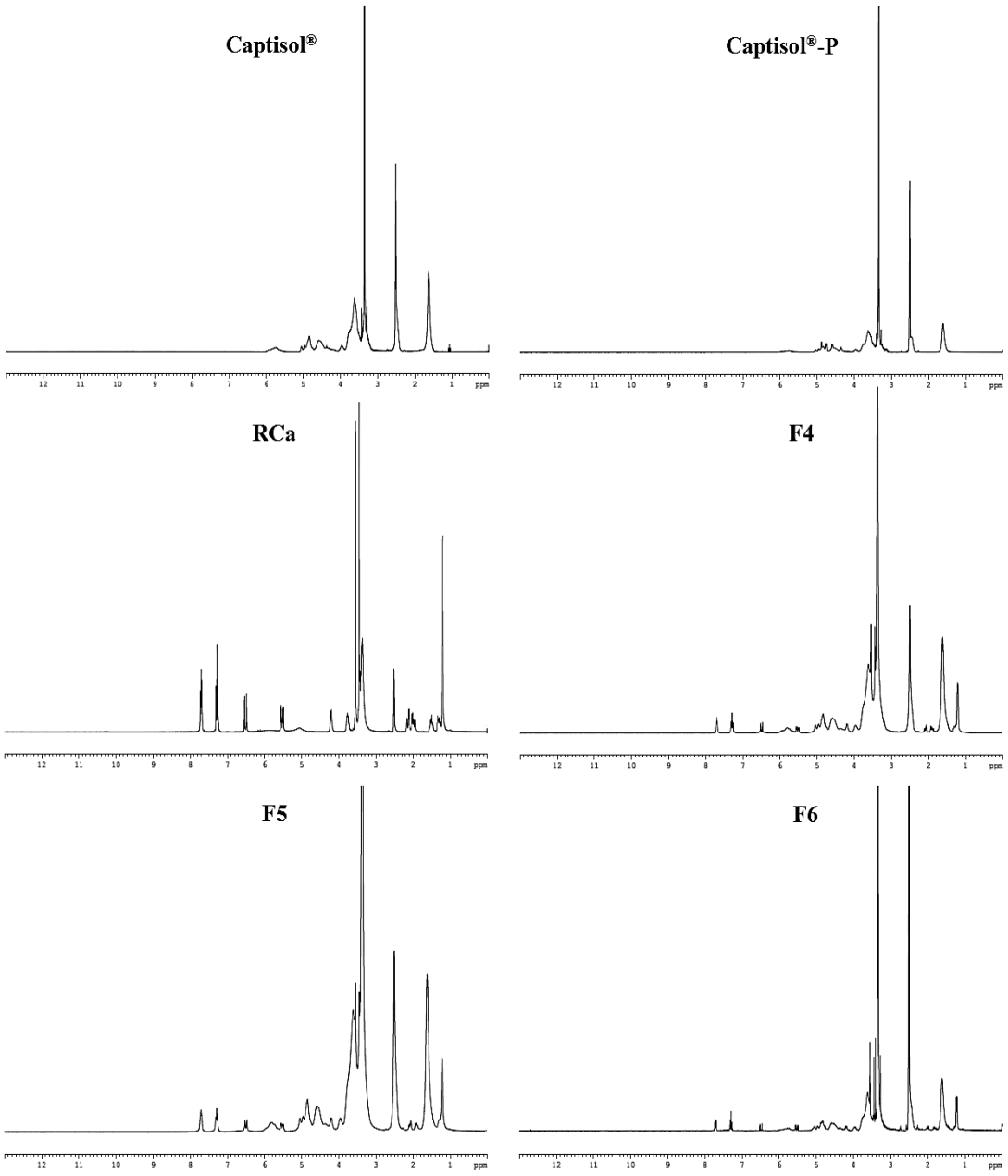


**Figure 4.38. (continued)** *$^{1}$H-NMR spectra of RCa, M-β-CD, Captisol®, Placebo and Inclusion Complexes*

### 4.5.4. *In vitro* release studies of CDs formulations

#### 4.5.4.1. *In vitro release studies of RCa/ M-β-CDs inclusion complexes*

The profiles and data of *in vitro* release of RCa from the M-β-CDs inclusion complexes are shown in Table 4.27 and Figure 4.39.

**Table 4.27.** *% Cumulative Release of RCa from the M-β-CDs Inclusion Complexes at pH 6.8 (n= 3)*

| (Time Hour) | % Cumulative Release (mean ± SE) | | | |
|---|---|---|---|---|
| | Pure RCa | F1 | F2 | F3 |
| 0.5 | 31.96 ± 2.31 | 34.33 ± 19.82 | 35.46 ± 20.47 | 25.59 ± 1.57 |
| 1 | 53.07 ± 3.75 | 55.98 ± 32.32 | 57.73 ± 33.33 | 41.91 ± 2.01 |
| 2 | 75.81 ± 4.69 | 81.55 ± 47.08 | 83.34 ± 48.12 | 67.56 ± 2.18 |
| 3 | 86.22 ± 5.0 | 92.21 ± 53.24 | 94.20 ± 54.39 | 80.04 ± 2.51 |
| 4 | 91.60 ± 4.97 | 96.52 ± 55.72 | 99.64 ± 57.53 | 86.71 ± 2.45 |
| 6 | 95.46 ± 4.73 | 98.71 ± 56.99 | 102.99 ± 59.46 | 92.71 ± 2.44 |

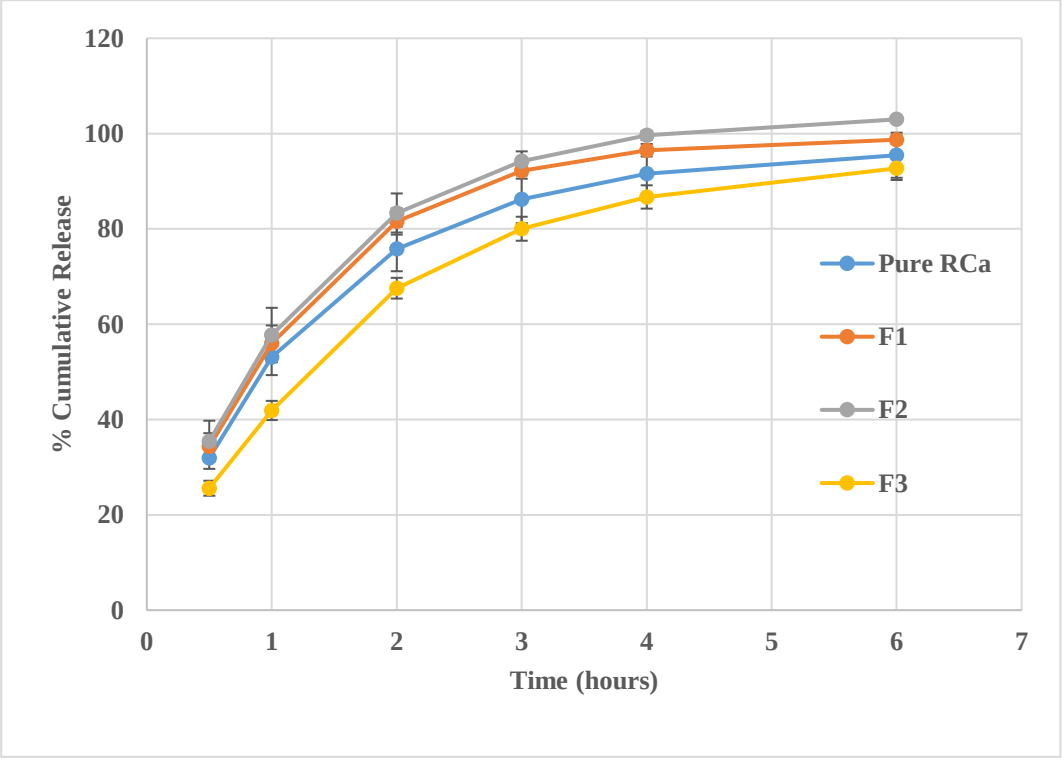


**Figure 4.39.** *% Cumulative Release of RCa from RCa/ M-β-CDs Inclusion Complexes at pH 6.8 (mean ± SE) (n= 3)*

### 4.5.4.2. *In vitro release studies of RCa/Captisol® inclusion complexes*

The profiles and data of *in vitro* release of RCa from the Captisol® inclusion complexes are demonstrated in Table 4.28 and Figure 4.40.

**Table 4.28.** *% Cumulative Release of RCa from The RCa/ Captisol® Inclusion Complexes at pH 6.8 (n=3)*

| (Time Hour) | % Cumulative Release (mean ± SE) | | | |
|---|---|---|---|---|
| | Pure RCa | F4 | F5 | F6 |
| **0.5** | 31.96 ± 2.31 | 35.82 ± 20.68 | 37.17 ± 21.46 | 33.57 ± 19.38 |
| **1** | 53.07 ± 3.75 | 60.44 ± 34.89 | 62.22 ± 35.92 | 56.36 ± 32.54 |
| **2** | 75.81 ± 4.69 | 82.55 ± 47.66 | 84.18 ± 48.60 | 78.31 ± 45.21 |
| **3** | 86.22 ± 5.0 | 92.71 ± 53.53 | 93.04 ± 53.72 | 87.53 ± 50.54 |
| **4** | 91.60 ± 4.97 | 96.44 ± 55.68 | 96.30 ± 55.60 | 91.30 ± 52.71 |
| **6** | 95.46 ± 4.73 | 97.67 ± 56.39 | 98.30 ± 56.75 | 93.17 ± 53.79 |

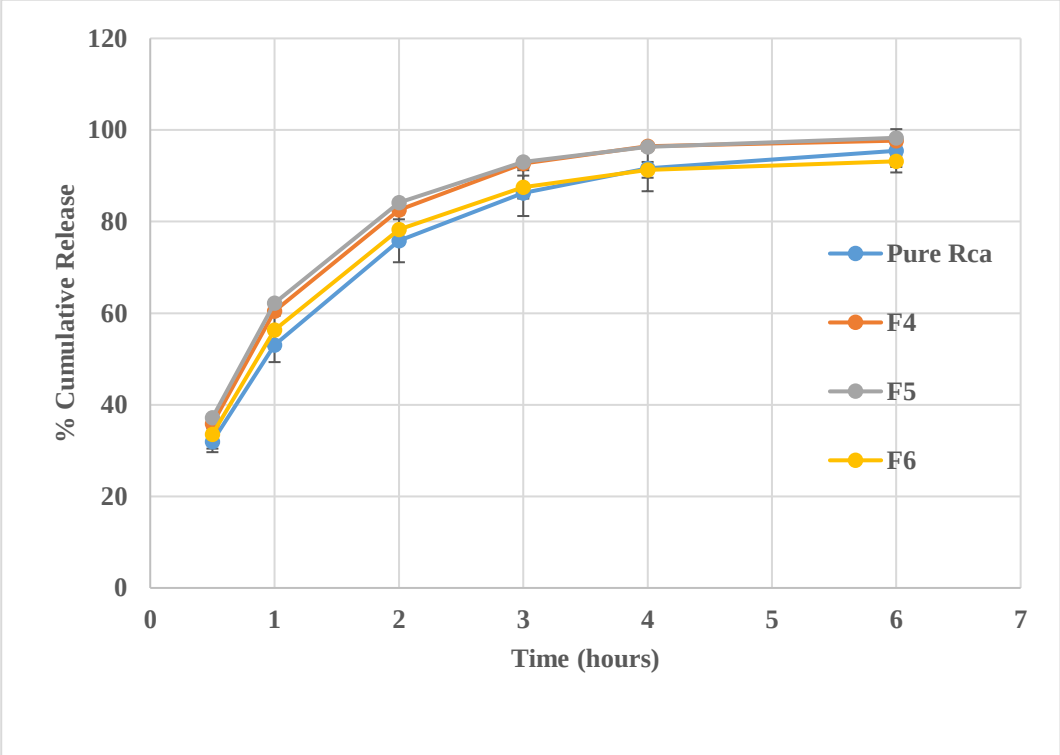


**Figure 4.40.** *% Cumulative Release of RCa from RCa/ Captisol® Inclusion Complexes at pH 6.8 (mean ± SE) (n= 3)*

### 4.5.5. Investigation of similarity of dissolution profiles for CDs inclusion complexes

The similarity factor values of the CDs inclusion complexes dissolution rate profiles were determined using DDSolver software program (Zhang *et al.*, 2010, p.263–271) according to the equation (3.7). The obtained $f_2$ values for the CDs inclusion complexes (F1, F2, F3, F4, F5 and F6) were (67, 58, 57, 62, 59, and 82), respectively.

### 4.5.6. Solubility study of RCa in CDs inclusion complexes formulations

Molar solubility of RCa in form of RCa/ CDs inclusion complex were studied according to the method and conditions which were explained in section (3.6.7). The solubility study results are shown in Table 4.29.

**Table 4.29.** *Molar Solubility ($m\mathcal{M}\,mL^{-1}$) of Pure RCa, RCa-CDs Physical Mixtures and RCa/ Inclusion Complexes in Distilled Water at 25 °C.*

| Code | Mean Solubility $m\mathcal{M}.\ mL^{-1}$ | ± SE |
|---|---|---|
| **Pure RCa** | 15.35 | 0.11 |
| **RCa/ M-β-CD Physical Mixture** | 39.56 | 2.15 |
| **RCa / Captisol® Physical Mixture** | 53.48 | 0.38 |
| **F1** | 42.61 | 2.28 |
| **F2** | 55.66 | 1.49 |
| **F3** | 57.18 | 0.91 |
| **F4** | 29.37 | 3.01 |
| **F5** | 45.88 | 0.91 |
| **F6** | 62.10 | 1.81 |

## 4.6. Formulation of Cyclodextrin-Poly(anhydride) Nanoparticles (CDs-PAD NPs)

The CDs F2 and CDs F6 formulations which represent M-β-CDs inclusion complex and the Captisol® inclusion complex respectively, were used to prepare CDs-PAD NPs formulations. The selection of CDs inclusion complexes was carried out according to the evaluation their physicochemical properties, *in vitro* RCa release profile, and the effect of CDs inclusion complex on molar solubility of RCa. The characterization of CDs-PAD NPs are given as follow.

### 4.6.1. Physicochemical characterization of CDs-PAD NPs

#### 4.6.1.1. *PS, PID, ZP, and DC % of CDs-PAD NPs*

The evaluated PS, PDI and ZP of the CDs-PAD NPs are illustrated in Table 4.30. The DC % was calculated using equation (3.4) Table 4.30.

**Table 4.30.** *PS, PDI, ZP and DC % of CDs-PAD NPs (mean ± SE) (n= 3)*

| Code | PS (nm) | PDI | ZP (mV) | DC (%) |
|---|---|---|---|---|
| **F1-CD-PAD** | 215.22 ± 1.25 | 0.203 ± 0.006 | -36.2 ± 0.06 | 63.371 ± 1.025 |
| **F2-CD-PAD** | 189.13 ± 1.03 | 0.182 ± 0.003 | -39.27 ± 0.30 | 67.921 ± 0.114 |

#### 4.6.1.2. *Morphology of CDs-PAD NPs*

For the evaluation of morphological structures of the CDs-PAD NPs and standard RCa, SEM microphotographs were shown in the Figure 4.41.

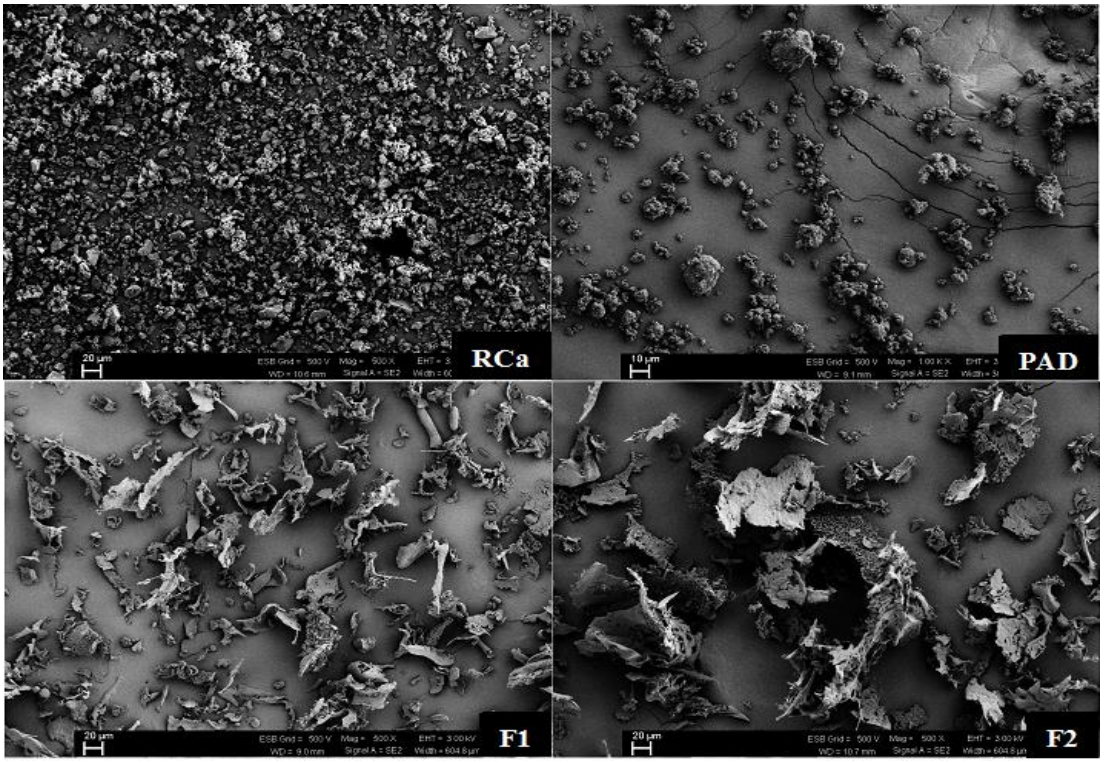


**Figure 4.41.** *SEM images of RCa, PAD and Formulations of CDs-PAD NPs*

#### 4.6.1.3. *Thermal analysis of CDs-PAD NPs*

The DSC thermogram of RCa, PAD, the CDs-PAD NPs formulations containing the active agent ingredient and the placebo are presented in Figure 4.42.

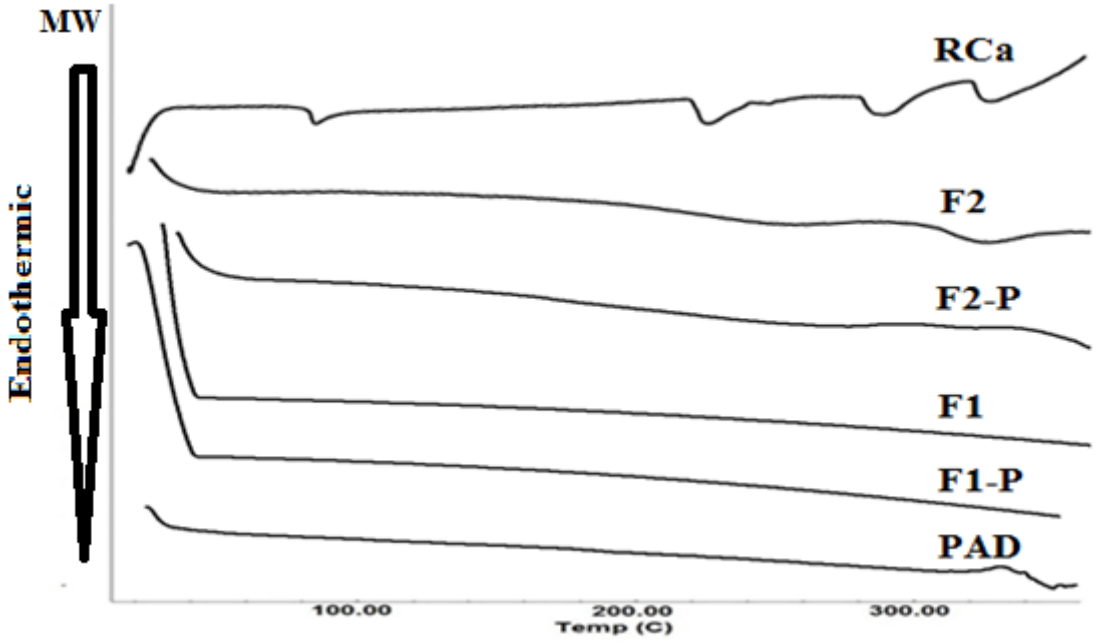


**Figure 4.42.** *DSC Thermograms of RCa, PAD, CDs-PAD NPs and Their Placebo*

#### 4.6.1.4. *FT-IR analysis of CDs-PAD NPs*

The FT-IR spectra analysis was carried out to investigate the characteristic peaks of the active molecule RCa, PAD, CDs-PAD NPs formulation and their placebo. Figures 4.43 is shown the FTIR spectra.

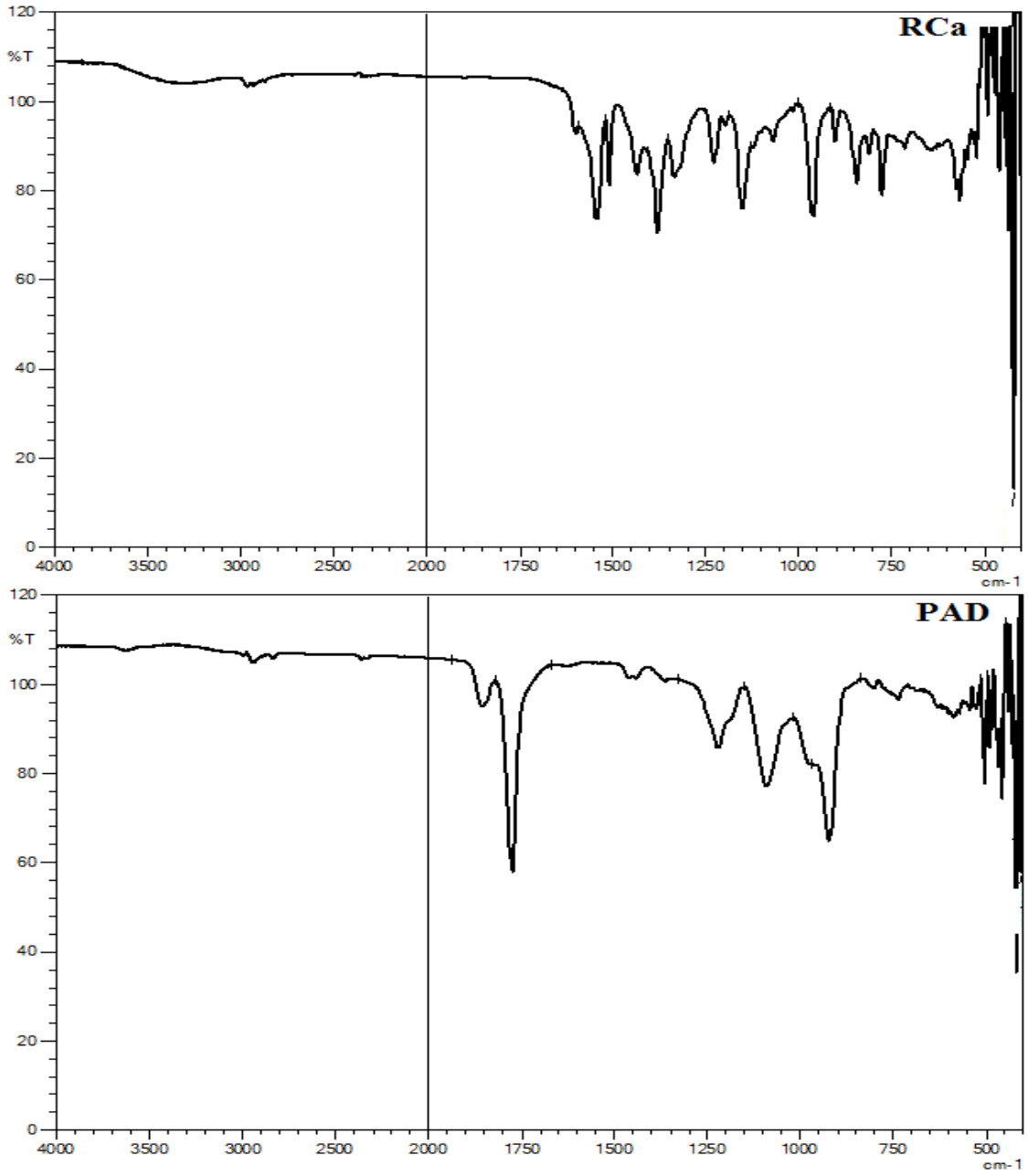


**Figure 4.43.** *FT-IR Spectra of RCa, PAD, CD-PAD NPs Formulations and Their Placebo*

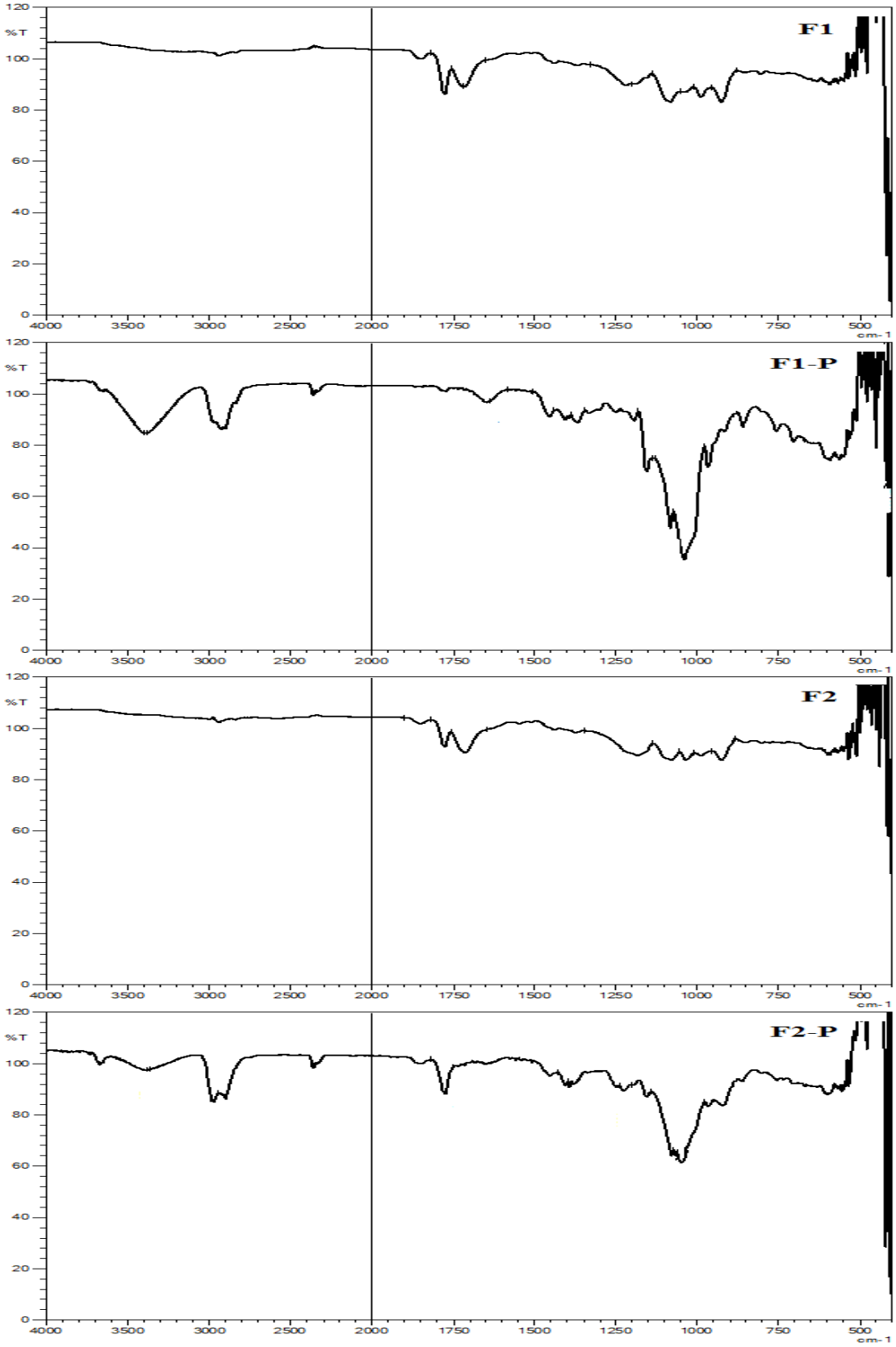


**Figure 4.43. (continued)** *FT-IR Spectra of CDs-PAD NPs Formulations and Their Placebo*

#### 4.6.1.5. *XRD analysis of CDs-PAD NPs*

The XRD patterns of RCa, PAD, the CDs-PAD NPs formulations containing the active agent ingredient and the placebo are shown in Figure 4.44.

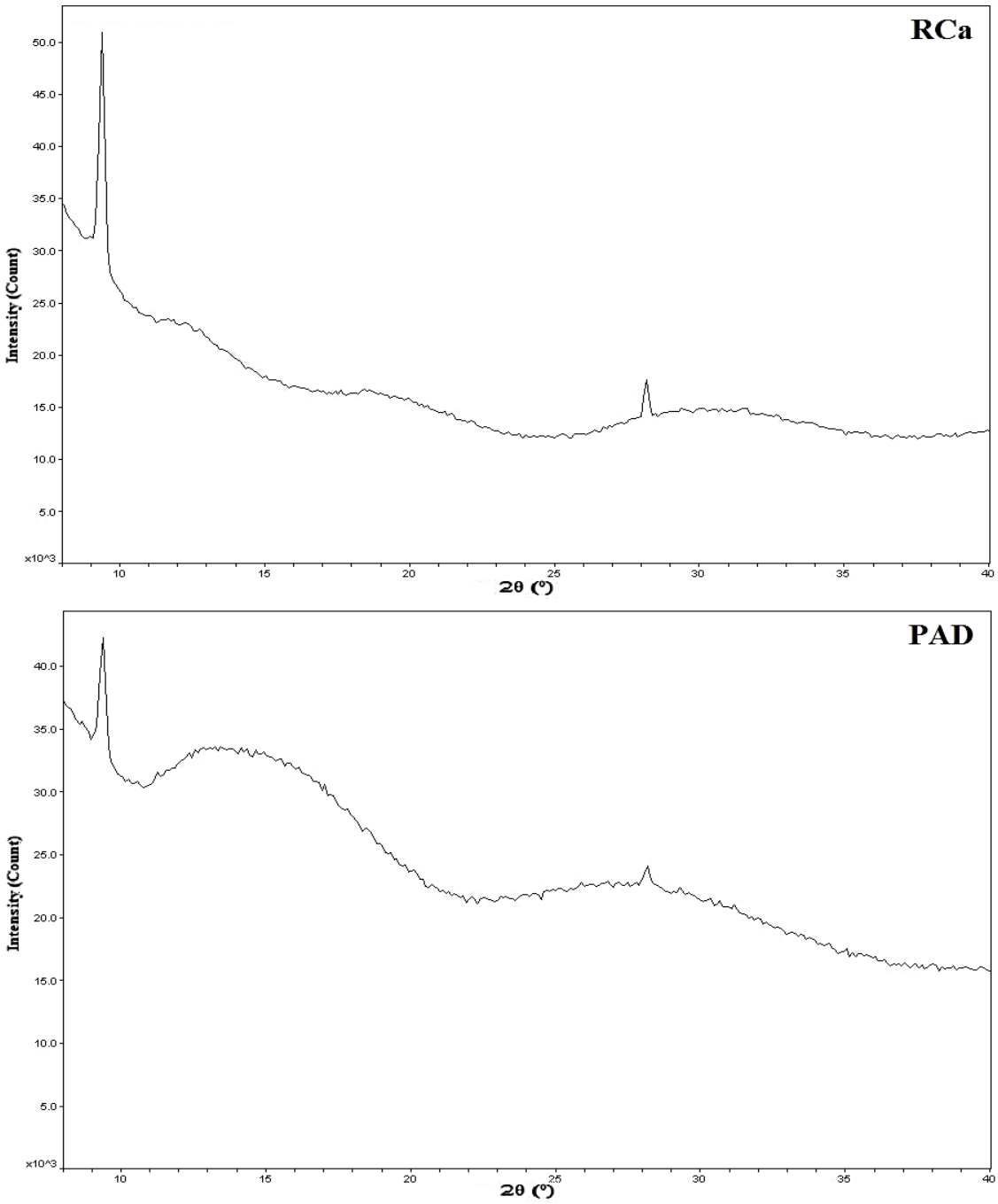


**Figure 4.44.** *XRD Spectra of RCa, PAD, CDs-PAD NPs Formulations and Their Placebo*

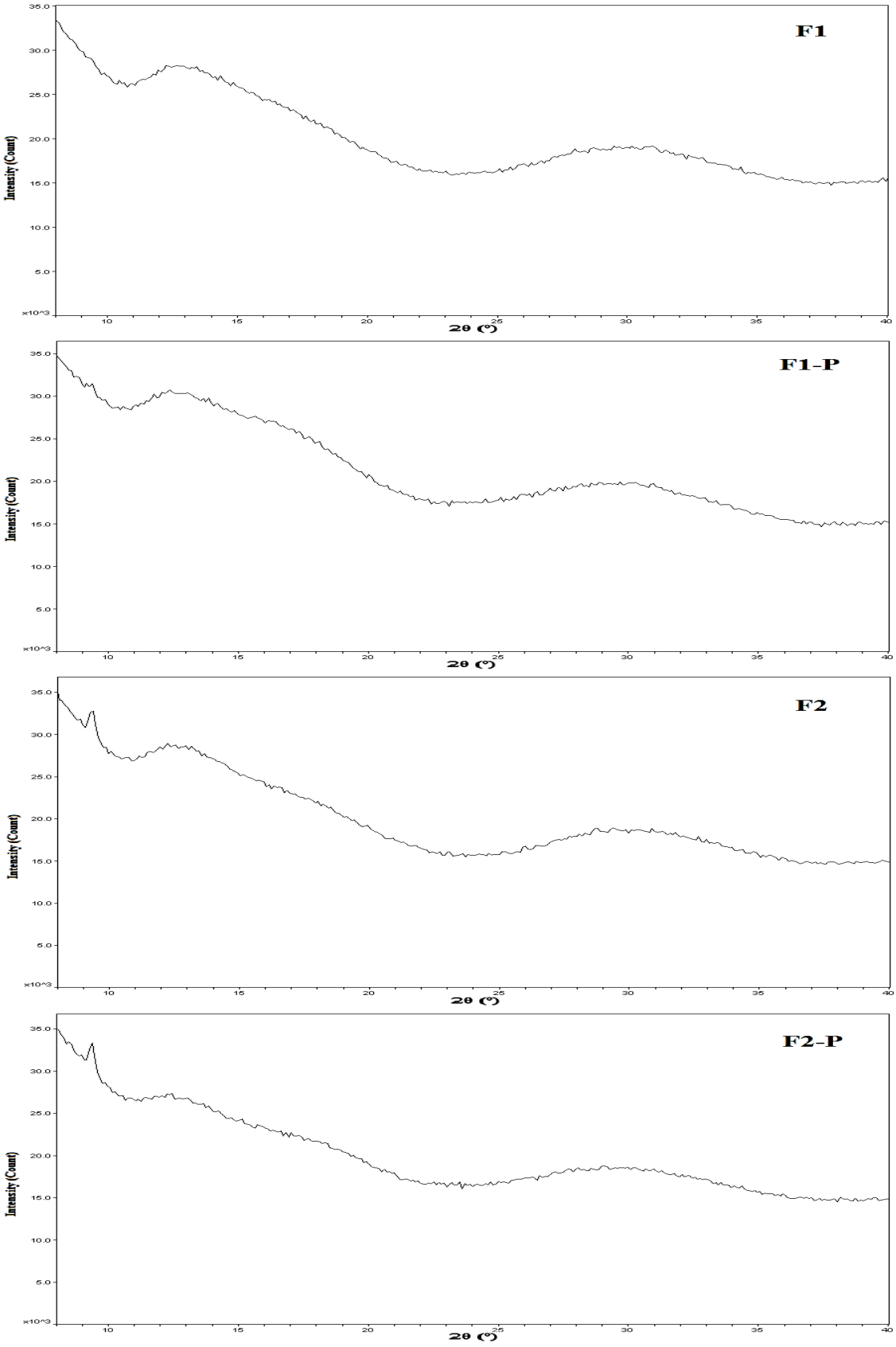


**Figure 4.44. (continued)** *XRD Spectra of RCa, PAD, CDs-PAD NPs Formulations and Their Placebo*

### *4.6.1.6.* $^{1}$H-NMR analysis of CDs-PAD NPs

The $^{1}$H-NMR spectra of RCa, PAD, the CDs-PAD NPs formulations containing RCa and their placebo are presented in Figure 4.45.

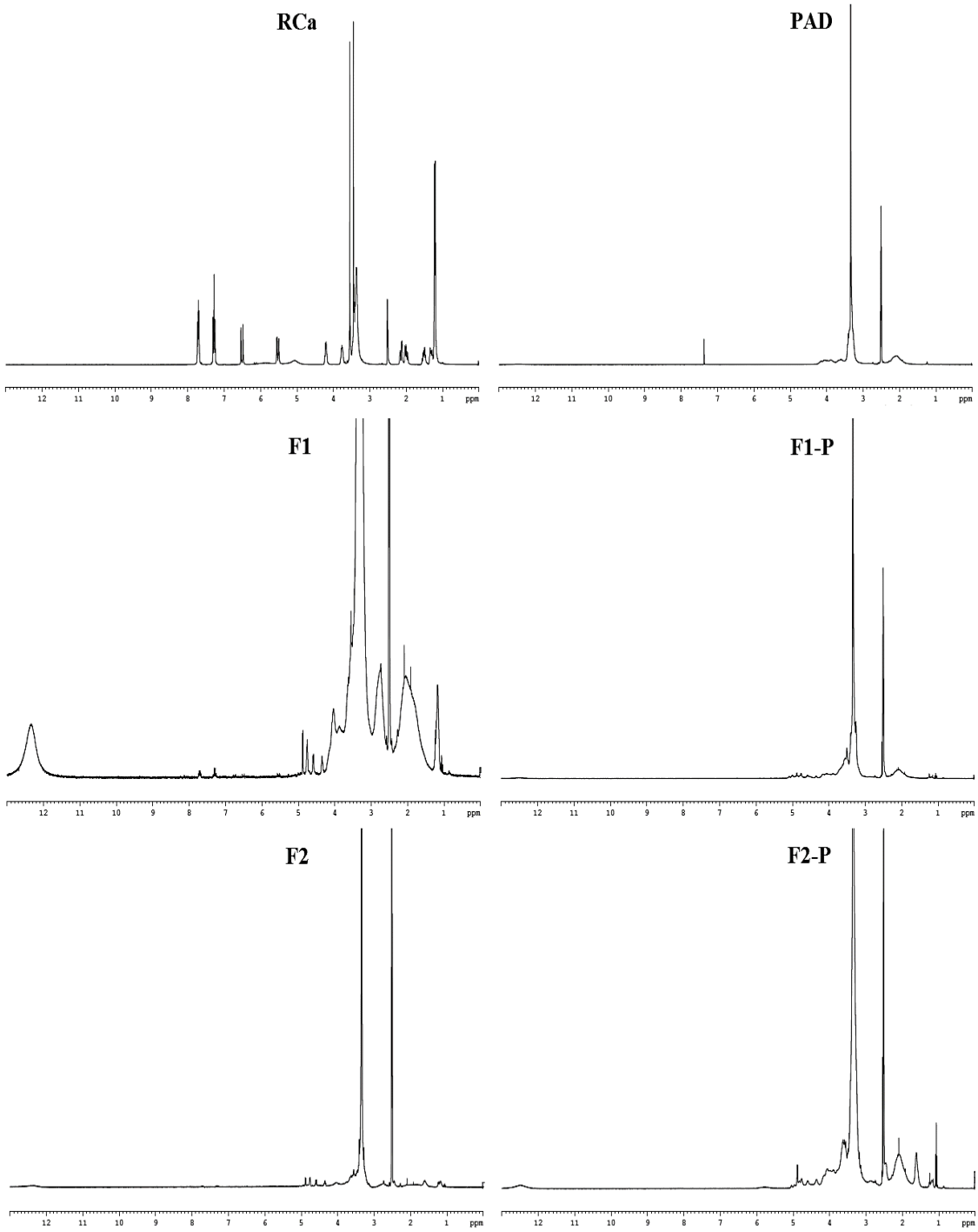


**Figure 4.45.** *$^{1}$H-NMR Spectra of RCa, PAD, CDs-PAD NPs and Their Placebo*

### 4.6.2. *In vitro* release studies of RCa from CDs-PAD NPs

The profiles and data of *in vitro* release of RCa from the CDs-PAD NPs formulations are shown in Table 4.31 and Figure 4.46.

**Table 4.31.** *% Cumulative Release of RCa from the CDs-PAD NPs at pH 6.8 (n= 3)*

| (Time Hour) | % Cumulative Release (mean ± SE) | | |
|---|---|---|---|
| | Pure RCa | F1 | F2 |
| **0,5** | 31.96 ± 2.31 | 26.36 ± 3.37 | 25.85 ± 2.26 |
| **1** | 53.07 ± 3.75 | 48.62 ± 5.61 | 43.63 ± 3.09 |
| **2** | 75.81 ± 4.69 | 72.04 ± 5.15 | 63.40 ± 3.97 |
| **3** | 86.22 ± 5.0 | 83.88 ± 2.75 | 71.88 ± 2.34 |
| **4** | 91.60 ± 4.97 | 89.92 ± 1.90 | 77.31 ± 3.15 |
| **6** | 95.46 ± 4.73 | 93.73 ± 3.97 | 81.52 ± 2.39 |
| **8** | - | 95.75 ± 4.14 | 82.64 ± 2.23 |
| **24** | - | 96.84 ± 4.17 | 83.77 ± 2.19 |

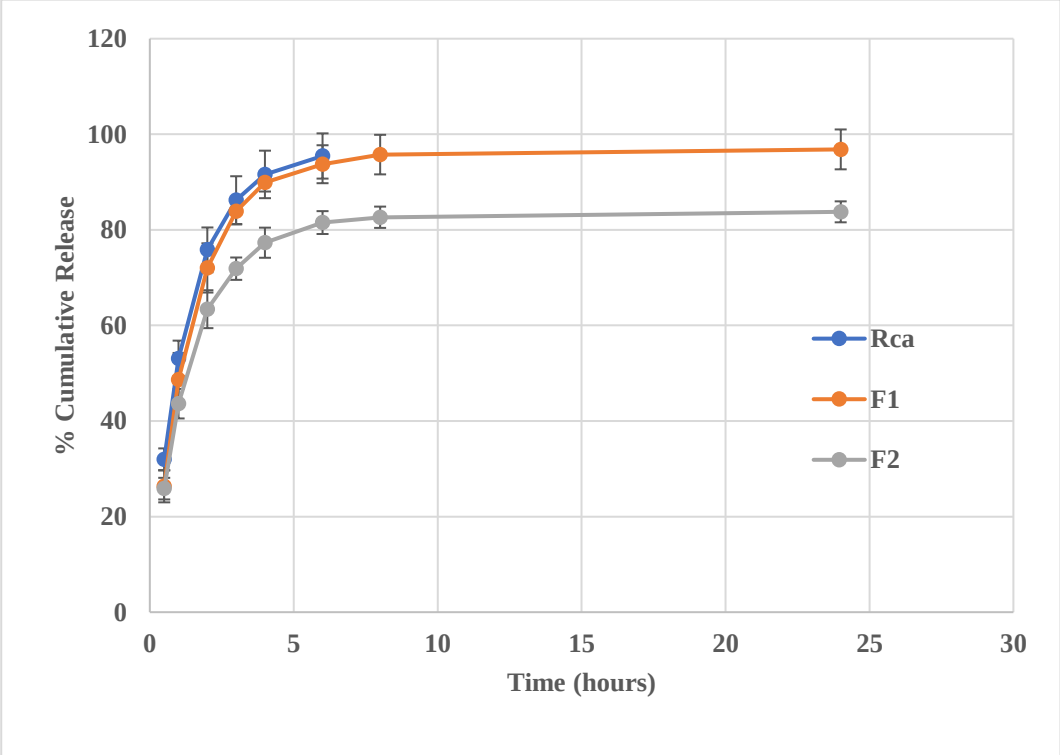


**Figure 4.46.** *% Cumulative Release of RCa from the CDs-PAD NPs at pH 6.8 (mean ± SE) (n= 3)*

### 4.6.3. Kinetics and mechanism of RCa release from CDs-PAD NPs

*In vitro* release profiles of RCa from CDs-PAD NPs in phosphate buffer (pH 6.8) were applied to different kinetic models (zero order kinetics, first order kinetics, Higuchi model, Korsmeyer-Peppas model and Hixson-Crowell model). The release data were investigated by k, $r^2$ and AIC for the selection of best suitable kinetic model Table 4.32. and Figure 4.47.

**Table 4.32.** *Kinetic Modeling of RCa Release from CDs-PAD NPs by DDsolver Software Program*

| Code | | Kinetic Model | | | | |
|---|---|---|---|---|---|---|
| | | **Zero order** | **First order** | **Higuchi** | **Korsmeyer-Peppas*** | **Hixson-Crowell** |
| **Pure RCa** | **k** | 0.021 | 0.001 | 0.045 | 0.048 | 0.000 |
| | **$r^2$** | 0.001 | 0.001 | 0.001 | 0.001 | 0.001 |
| | **AIC** | 0.078 | 0.048 | 0.059 | 0.065 | 0.051 |
| **F1** | **k** | 0.006 | 0.000 | 0.030 | 0.054 | 0.000 |
| | **$r^2$** | -0.004 | 0.000 | 0.000 | 0.001 | 0.000 |
| | **AIC** | 0.082 | 0.064 | 0.072 | 0.063 | 0.071 |
| **F2** | **k** | 0.005 | 0.000 | 0.026 | 0.049 | 0.000 |
| | **$r^2$** | -0.004 | 0.000 | -0.001 | 0.001 | -0.001 |
| | **AIC** | 0.080 | 0.070 | 0.070 | 0.059 | 0.072 |

**Reference:** *DDsolver Program, Zhang et al., 2010, p.263–271*

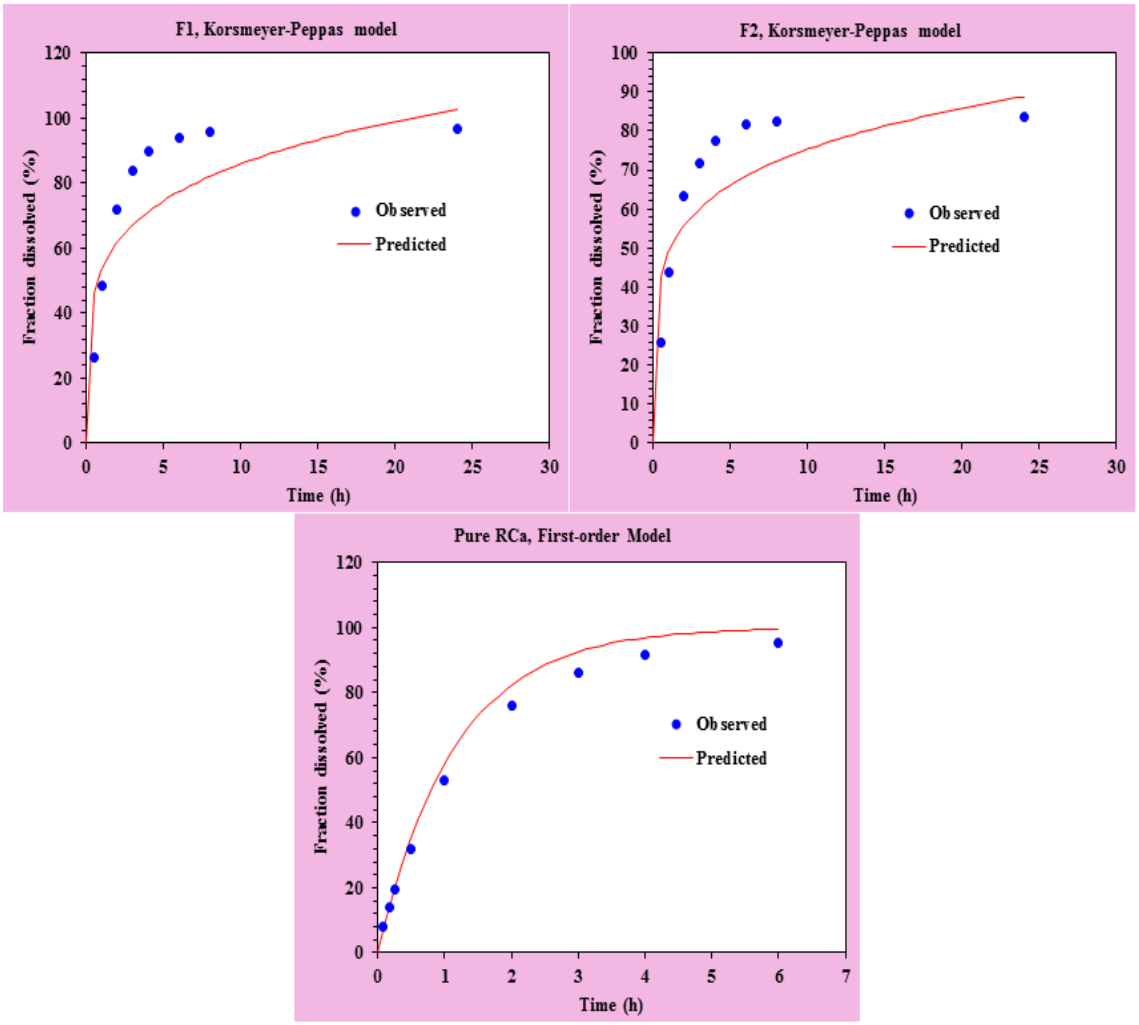


**Figure 4.47.** *Kinetic Modeling of RCa Release from CDs-PAD NPs by DDsolver Software Program*

**Reference:** *DDsolver Program, Zhang et al., 2010, p.263–271.*

### 4.7 Cytotoxicity Studies of Formulations

The best Cs NPs (F4, F6), SLNs (F2, F4), CDs inclusion complexes (F2, F6) and CDs-PAD NPs (F1, F2) formulations were selected according to physicochemical characterization tests results to be applied to cytotoxicity studies with their placebo forms.

The $IC_{50}$ value was calculated using (3.8) equation. The obtained results showed that the $IC_{50}$ values for the F4 (Cs NPs), F4-P (Cs NPs), F6 (Cs NPs), F6-P (Cs NPs) formulations were 36.298, 37.375, 35.241, 38.839 µM respectively after 24 hours of incubation. In accordance with these data, the formulations (F4 (Cs NPs), F4-P (Cs NPs), F6 (Cs NPs), F6-P (Cs NPs)) are within cytotoxic level. For this reason, these formulations have not been used in further studies. The results obtained from this study are shown in Figure 4.48.

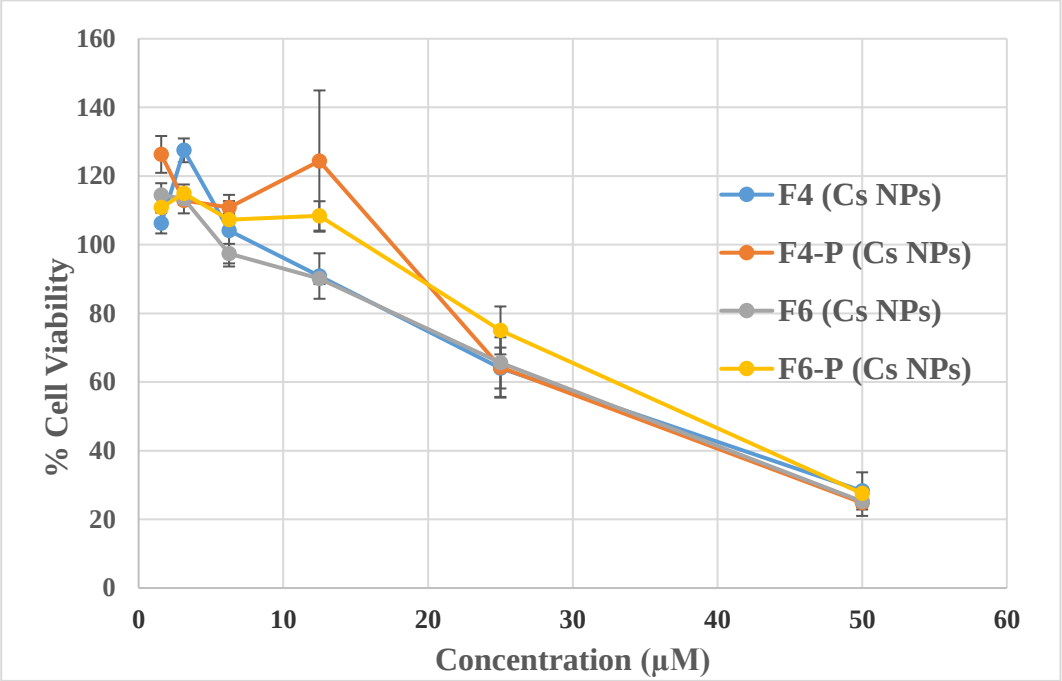


**Figure 4.48.** *% Cell Viability for F4 (Cs NPs), F4-P (Cs NPs), F6 (Cs NPs) and F6-P (Cs NPs) Formulations (mean ± SE) (n= 3)*

At the same time, The $IC_{50}$ cytotoxic values as a result of the MTT studies for the other formulations (CDs-F2, CDs-F2-P, CDs-F6, CDs-F6-P, F1 (CDs-PAD), F1-P (CDs-PAD), F2 (CDs-PAD), and F2-P (CDs-PAD) , SLNs-F2, SLN F2-P, SLNs-F4, SLNs-F4-P, RCa) were calculated to be (161.898, 87.563, 117.071, 139.492, 74.803, 94.741, 63.217, 163.354, 87.852, 335.238, 52.137, 52.138 and 149.470) µM, respectively, but none of these values were IC50 cytotoxic values. The % cell viability was plotted versus

the molar concentrations of pure RCa and the used formulations as demonstrated in the following Figures 4.49, 4.50, 4.51, and 4.52.

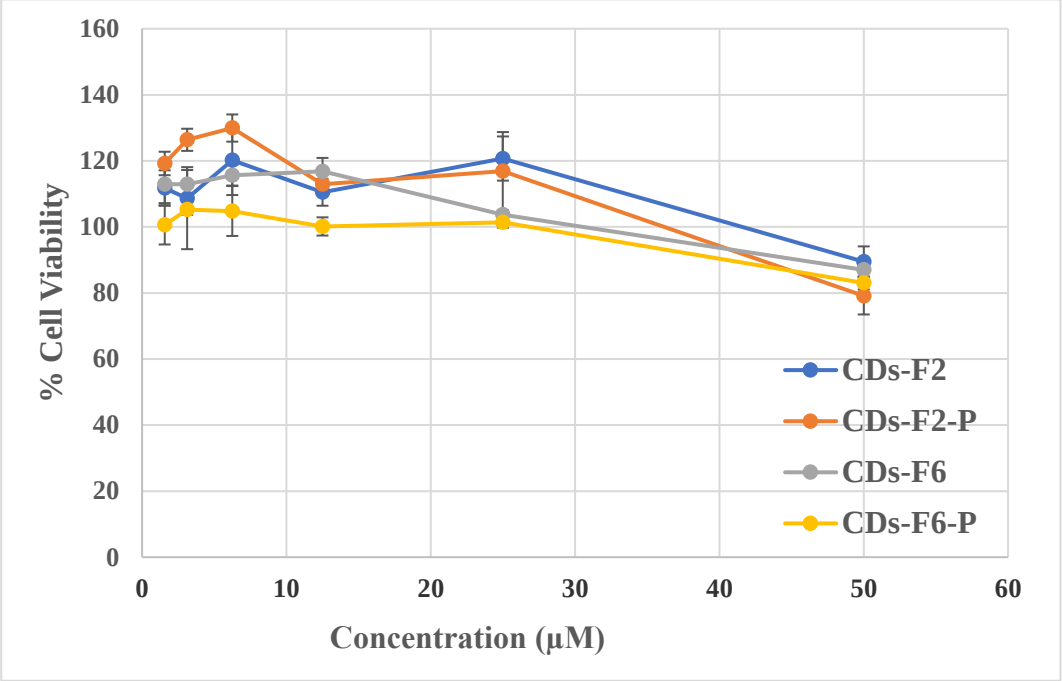


**Figure 4.49.** *% Cell Viability for CDs-F2, CDs-F3-P, CDs-F6, and CDs-F6-P Formulations (mean ± SE) (n= 3)*

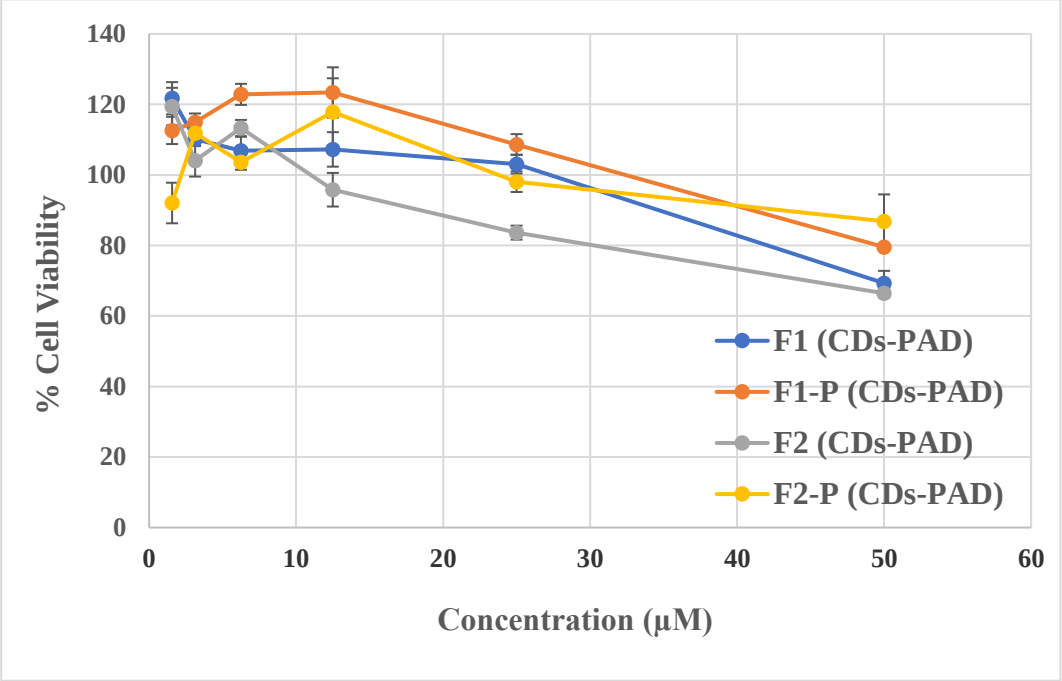


**Figure 4.50.** *% Cell Viability for F1 (CDs-PAD), F1-P (CDs-PAD), F2 (CDs-PAD), and F2-P (CDs-PAD) Formulations (mean ± SE) (n= 3)*

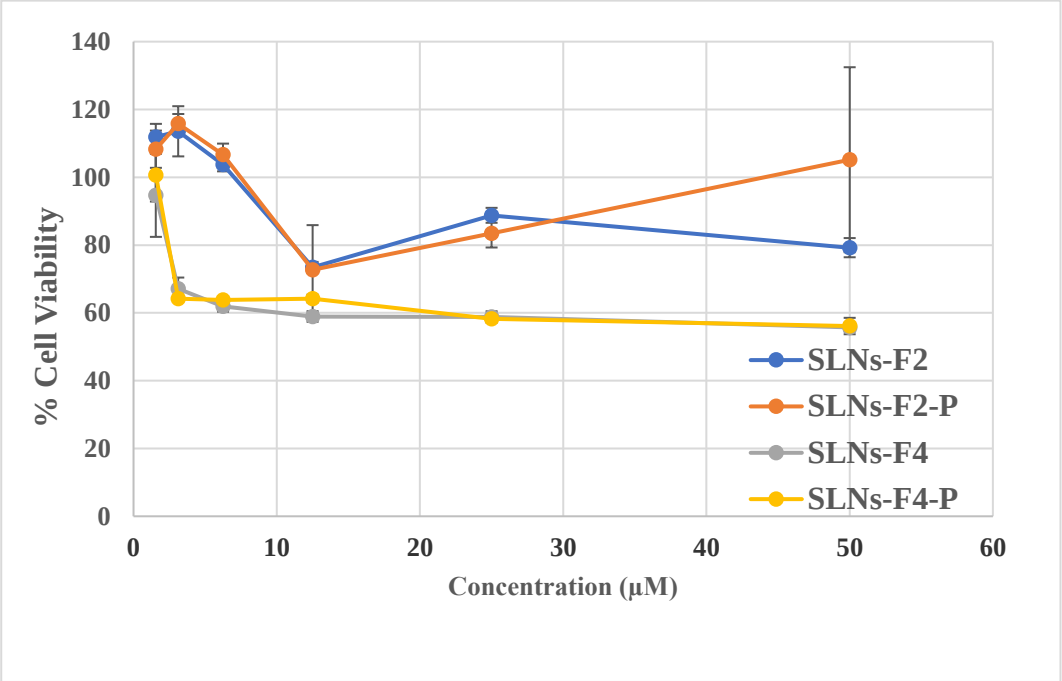


**Figure 4.51.** *% Cell Viability for SLNs-F2, SLN F2-P, SLNs-F4, and SLNs-F4-P Formulations (mean ± SE) (n= 3)*

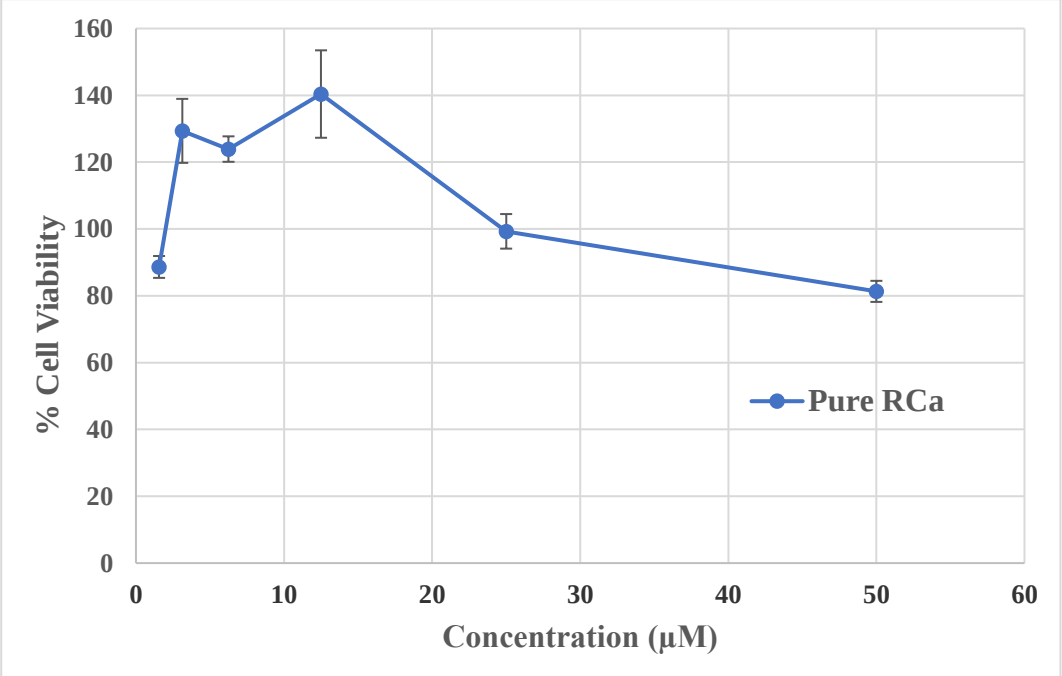


**Figure 4.52.** *% Cell Viability for Pure RCa (mean ± SE) (n= 3)*

### 4.7.1. Statistical analysis of MTT cytotoxicity studies

As a result of MTT study for cell viability, Two-way ANOVA statistical analysis was performed using GraphPad Prism 7 software for formulations of CDs-F2, CDs-F6, F1 (CDs-PAD), F2 (CDs-PAD) and SLNs-F2 in which they were found to be non-cytotoxic and fit for permeability study. As a result of the analysis, the significance relation between the formulations was examined in the constant concentration. The graph of the statistical study was derived from the data of MTT results, Figure 4.53.

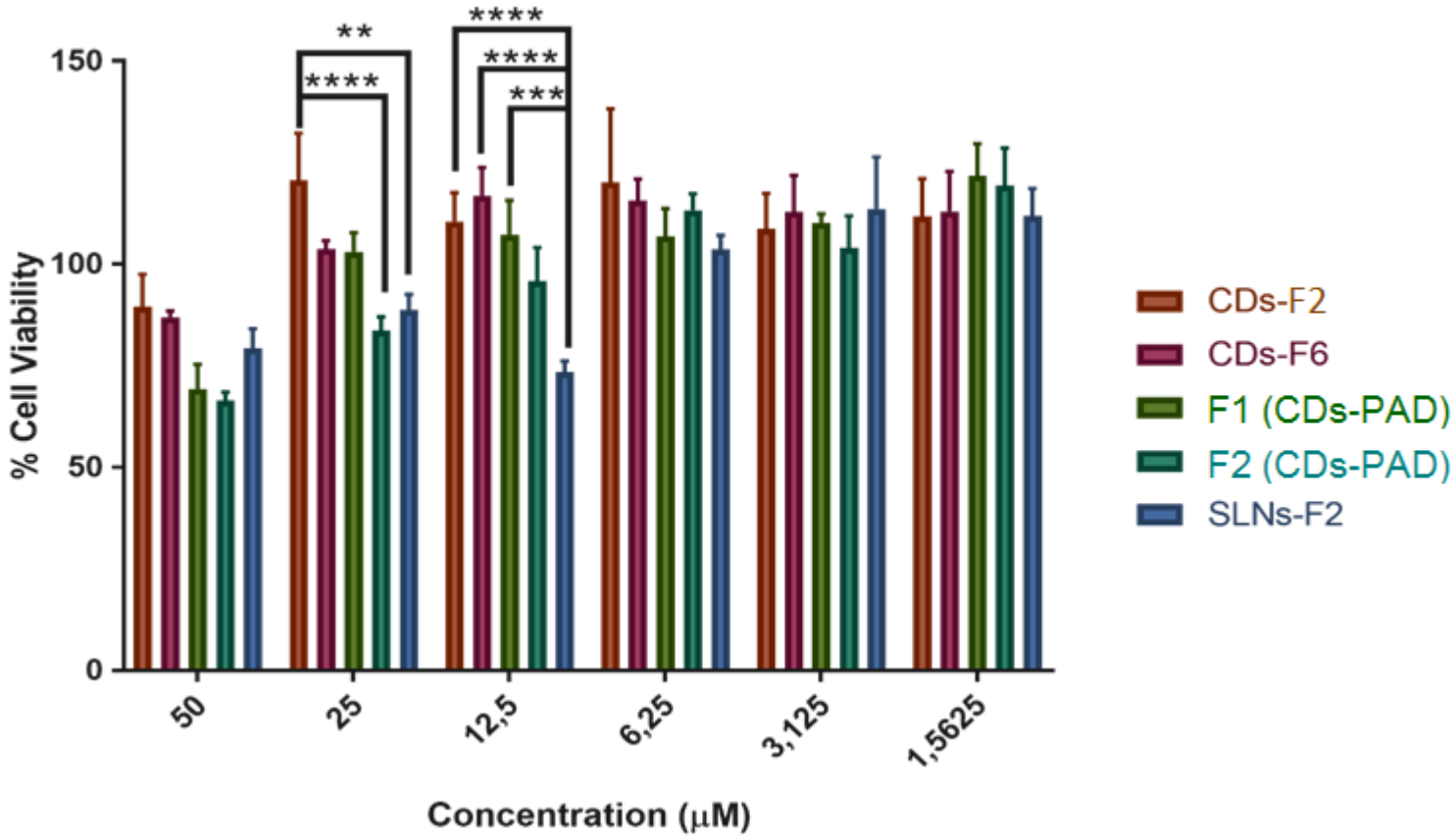


**Figure 4.53.** *Two-Way ANOVA Statistic Results for Formulations of CDs-F2, CDs-F6, F1 (CDs-PAD), F2 (CDs-PAD) and SLNs-F2*

As a result of MTT studies, the significant changes in cell viability according to concentrations of each formulation (CDs-F2, CDs-F6, F1 (CDs-PAD), F2 (CDs-PAD) and SLNs-F2) considered to be suitable for permeability study. Consequently, statistical analyzes were performed using the two-way ANOVA method. The % change in cell viability between concentrations is indicated by an asterisk (*) according to the level of significance (Figures 4.54-4.58).

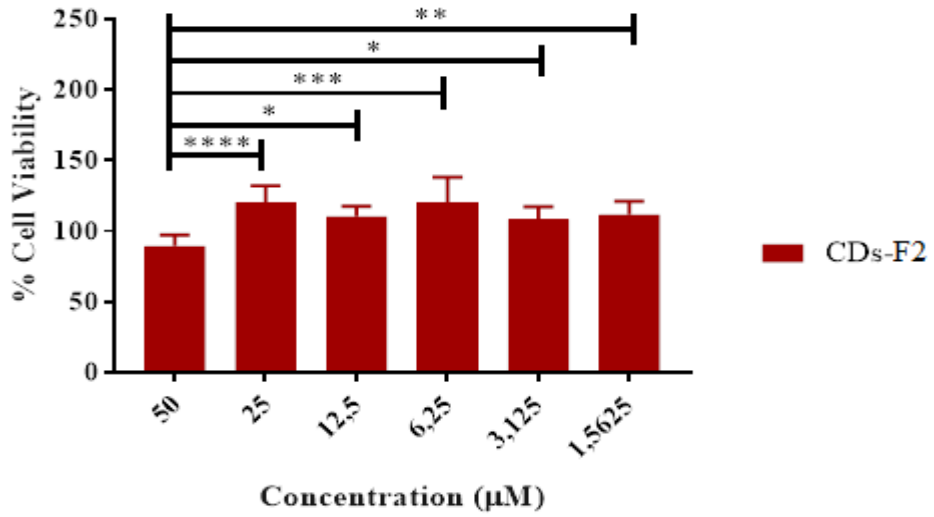


**Figure 4.54.** *Two-Way ANOVA Statistic Results for Different Concentration of CDs-F2 Formulation*

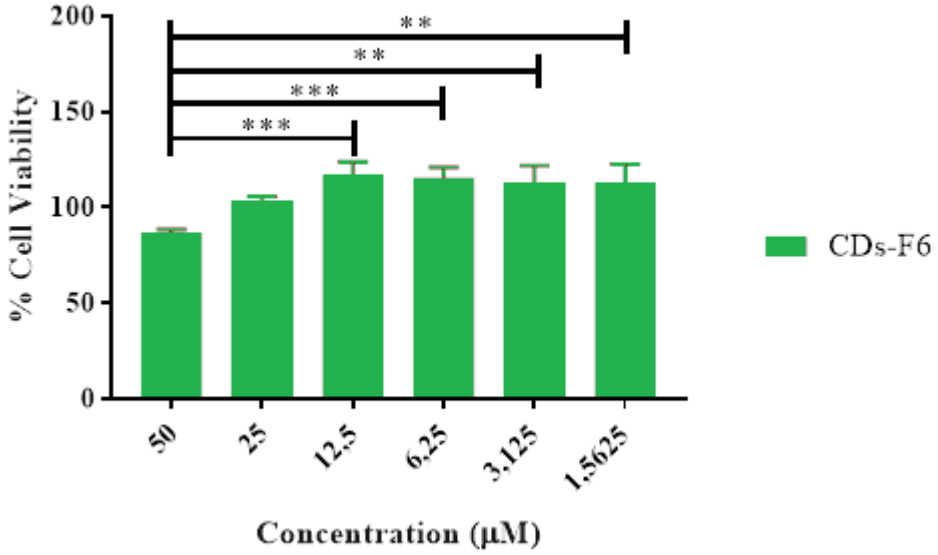


**Figure 4.55.** *Two-Way ANOVA Statistic Results for Different Concentration of CDs-F6 Formulation.*

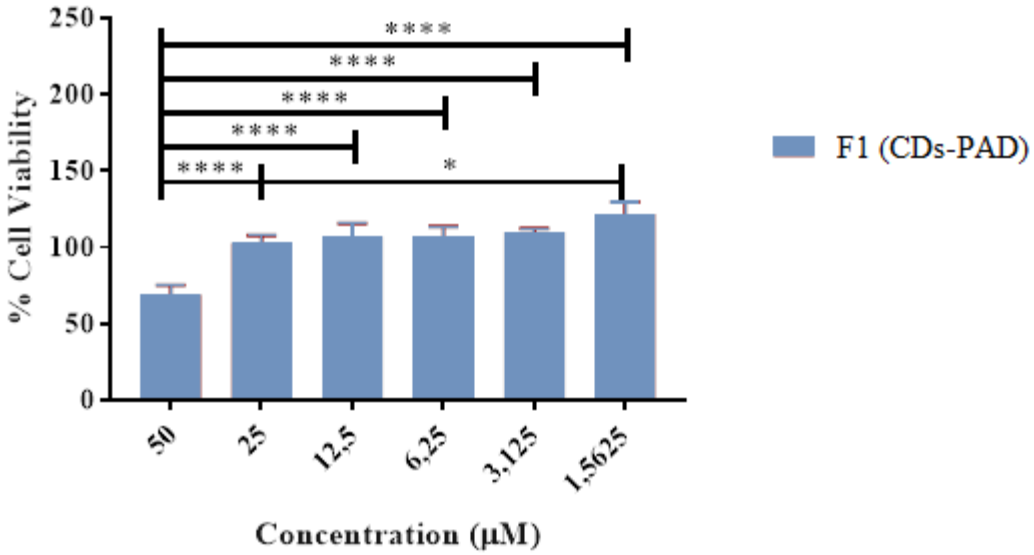


**Figure 4.56.** *Two-Way ANOVA Statistic Results for Different Concentration of F1 (CDs-PAD) Formulation.*

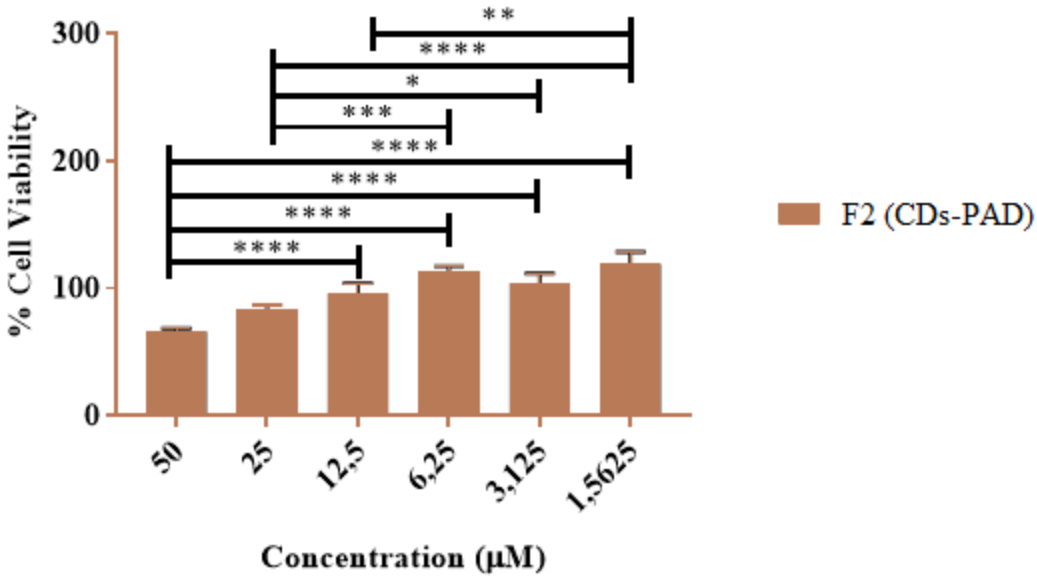


**Figure 4.57.** *Two-Way ANOVA Statistic Results for Different Concentration of F2 (CDs-PAD), Formulation.*

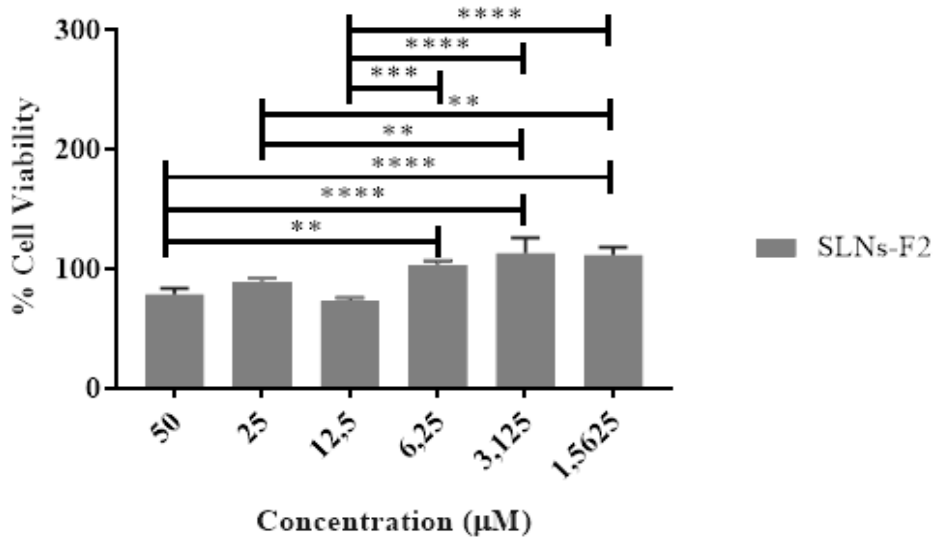


**Figure 4.58.** *Two-Way ANOVA Statistic Results for Different Concentration of SLNs-F2 Formulation.*

### 4.8. RCa permeation studies

The permeation studies carried out on standard RCa and five formulations (CDs-F3, CDs-F6, F1 (CDs-PAD), F2 (CDs-PAD), SLNs-F2) which have the best cytotoxicity test results. The results of permeation studies after two hours indicate that the permeation of RCa from (F1 (CDs-PAD), F2 (CDs-PAD), and SLNs-F2) formulations through tissue membrane better than standard RCa and other formulations. Table 4.33. demonstrate the permeated RCa (mean ± SE) in µg. $mL^{-1}$. The experiments were repeated four times for each formulation.

**Table 4.33.** *Detected Level of RCa in the Basolateral Media of Caco-2 Cell Monolayers Treated with 50 µM RCa as Pure RCa and Formulations Samples for 2 Hours (mean ± SE) (n= 4)*

| Code | RCa (µg. $mL^{-1}$) |
|---|---|
| **RCa Standard** | 0.12 ± 0.022 |
| **CDs-F2** | 0.06 ± 0.002 |
| **CDs-F6** | 0.13 ± 0.058 |
| **F1 (CDs-PAD)** | 4.90 ± 0.226 |
| **F2 (CDs-PAD)** | 4.00 ± 0.084 |
| **SLNs-F2** | 2.04 ± 0.044 |

The $P_{app}$ for RCa and studied formulations was calculated using equations (3.10), the results of $P_{app}$ calculations were shown in Table 4.34. and Figure 4.59.

**Table 4.34.** *$P_{app}$ Values of RCa for Caco-2 Permeability Assays (mean ± SE) (n= 4)*

| Code | $P_{app}$ (cm. $sec^{-1}$) |
|---|---|
| **RCa Standard** | $3.08 \times 10^{-7} \pm 5.15 \times 10^{-8}$ |
| **CDs-F2** | $1.37 \times 10^{-7} \pm 4.41 \times 10^{-9}$ |
| **CDs-F6** | $3.01 \times 10^{-7} \pm 1.35 \times 10^{-7}$ |
| **F1 (CDs-PAD)** | $1.36 \times 10^{-5} \pm 6.29 \times 10^{-7}$ |
| **F2 (CDs-PAD)** | $1.12 \times 10^{-5} \pm 2.39 \times 10^{-7}$ |
| **SLNs-F2** | $5.72 \times 10^{-6} \pm 1.39 \times 10^{-7}$ |

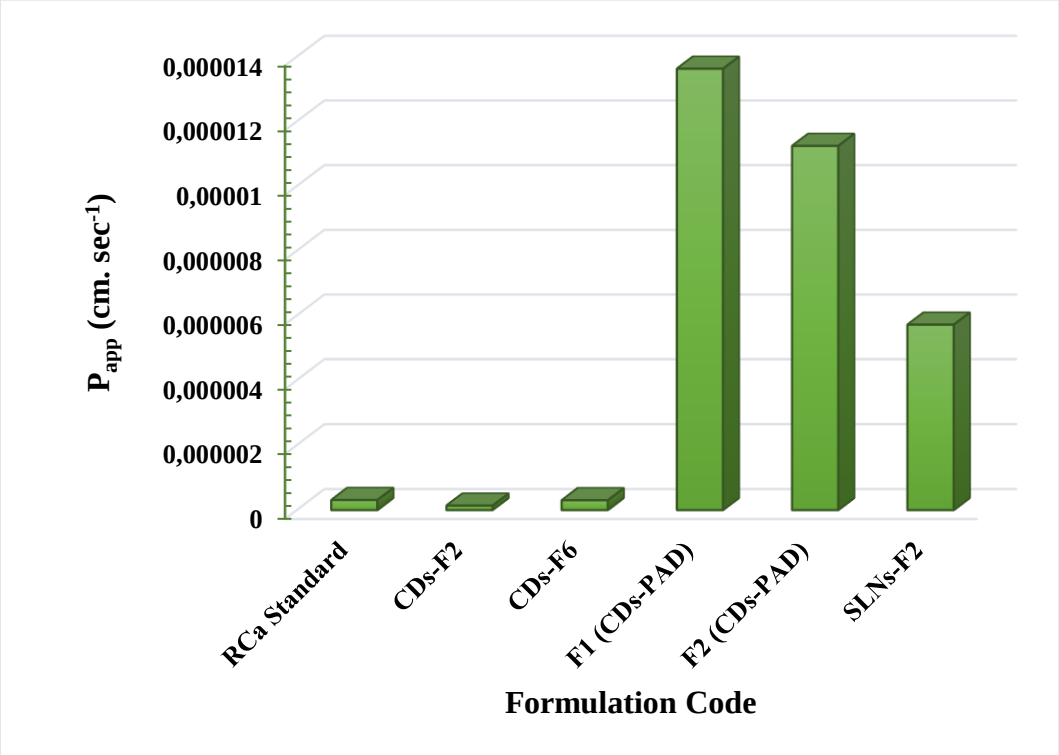


**Figure 4.59.** *$P_{app}$ Values of RCa for Caco-2 Permeability Assays (mean ± SE) (n= 4)*

### 4.9. Stability Studies

DC %, PS, PDI, and ZP were evaluated for the fresh formulations SLN F2, F1 (CD-PAD) and F2 (CD-PAD) and during three months.

#### 4.9.1. DC % studies result

The DC % analysis results of the fresh formulations SLN F2, F1 (CD-PAD) and F2 (CD-PAD) were (61.18 ± 0.51, 76,11 ± 0.43, and 66.18 ± 0.58), respectively. The Table 4.35 and Figure 4.57 are shown the results of DC % analysis after three months of stability studies.

**Table 4.35.** *The Drug Content % of the Studied Formulations after Three Months (mean ± SE) (n= 3)*

| Formulation | Storage Conditions | | |
|---|---|---|---|
| | 4 °C ± 1 °C | 25 °C ± 1°C | 40 °C ± 1 °C |
| SLNs-F2 | 60.02 ± 0.54 | 58.24 ± 1.57 | 39.98 ± 10.62 |
| F1-(CD-PAD) | 75.96 ± 0.40 | 75.78 ± 0.50 | 63.40 ± 6.73 |
| F2-(CD-PAD) | 65.68 ± 0.69 | 65.29 ± 0.55 | 56.92 ± 4.64 |

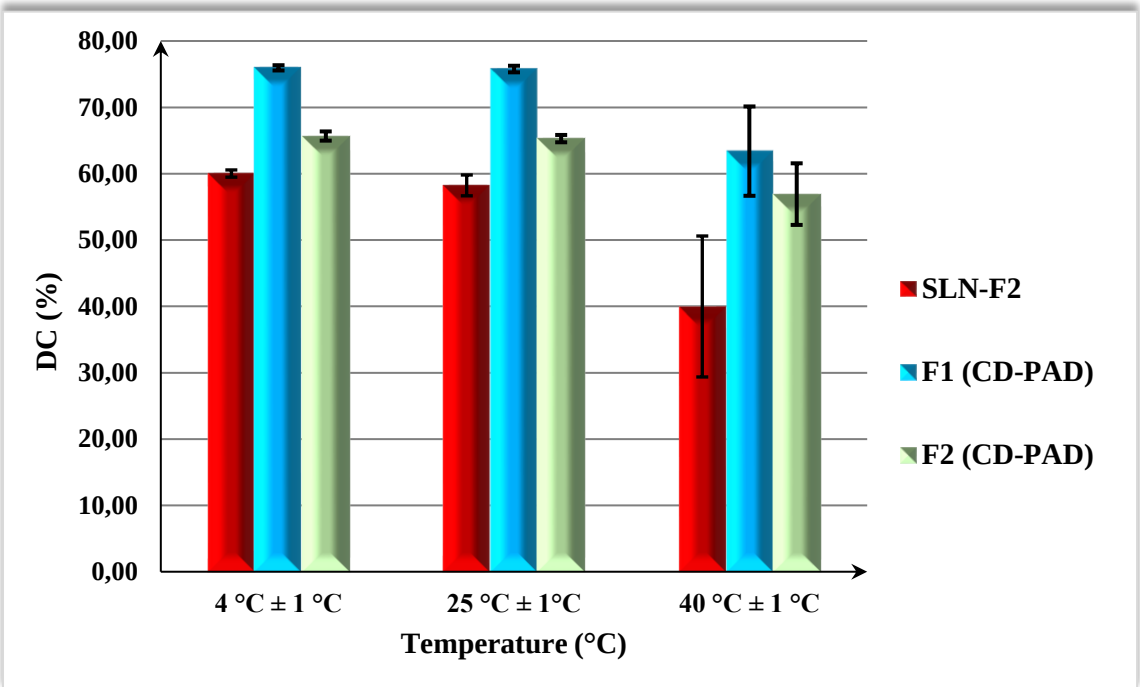


**Figure 4.60.** *The Drug Content % of the Studied Formulations after Three Months (mean ± SE) (n= 3)*

### 4.9.2. PS and PDI studies results

The PS and PDI analysis studies results for the formulation SLN-F2, F1-(CD-PAD), F2-(CD-PAD) are demonstrated in Table 4.36. respectively. The Figures 4.61., 4.62. are shown the comparison of the three formulations study's results for PS and PDI.

**Table 4.36.** *The PS and PDI of the Formulations after Three Months (mean ± SE) (n= 3)*

| Time | Storage Conditions | | | | | |
|---|---|---|---|---|---|---|
| | 4 °C ± 1 °C | | 25 °C ± 1°C | | 40 °C ± 1 °C | |
| | SLN-F2 | | | | | |
| | PS (nm) | PDI | PS (nm) | PDI | PS (nm) | PDI |
| 1st day | 134.4 ±0.91 | 0.13 ±0.01 | 134.4 ±0.91 | 0.13 ±0.01 | 134.4 ±0.91 | 0.13 ±0.01 |
| 30th day | 155.3 ±6.38 | 0.23 ±0.06 | 181.0 ±1.53 | 0.26 ±0.02 | 527.7 ±11.8 | 0.41 ±0.04 |
| 60th day | 255.0 ±6.10 | 0.37 ±0.02 | 264.7 ±8.65 | 0.44 ±0.01 | 561.0 ±23.5 | 0.60 ±0.05 |
| 90th day | 286.3 ±5.55 | 0.43 ±0.01 | 348.0 ±6.35 | 0.46 ±0.01 | 621.0 ±16.6 | 0.77 ±0.02 |
| | F1 (CD-PAD) | | | | | |
| | PS (nm) | PDI | PS (nm) | PDI | PS (nm) | PDI |
| 1st day | 215.2 ±1.25 | 0.20 ±0.01 | 215.2 ±1.25 | 0.20 ±0.001 | 215.2 ±1.25 | 0.20 ±0.01 |
| 30th day | 225.2 ±1.08 | 0.21 ±0.01 | 232.9 ±1.56 | 0.22 ±0.001 | 263.6 ±5.42 | 0.31 ±0.01 |
| 60th day | 230.2 ±6.03 | 0.24 ±0.01 | 253.6 ±6.55 | 0.27 ±0.01 | 367.2 ±4.82 | 0.40 ±0.03 |
| 90th day | 240.6 ±3.36 | 0.34 ±0.02 | 350.2 ±9.59 | 0.37 ±0.01 | 423.9 ±7.88 | 0.43 ±0.01 |
| | F2 (CD-PAD) | | | | | |
| | PS (nm) | PDI | PS (nm) | PDI | PS (nm) | PDI |
| 1st day | 189.1 ±1.03 | 0.18 ±0.01 | 189.1 ±1.03 | 0.18 ±0.01 | 189.1 ±1.03 | 0.18 ±0.01 |
| 30th day | 213.5 ±2.22 | 0.27 ±0.01 | 232.6 ±1.88 | 0.32 ±0.02 | 270.6 ±3.30 | 0.37 ±0.02 |
| 60th day | 266.2 ±8.05 | 0.34 ±0.01 | 283.6 ±5.41 | 0.37 ±0.01 | 437.9± 19.7 | 0.35 ±0.01 |
| 90th day | 336.3 ±8.94 | 0.36 ±0.01 | 354.2 ±4.93 | 0.37 ±0.01 | 444.2± 11.8 | 0.38 ±0.01 |

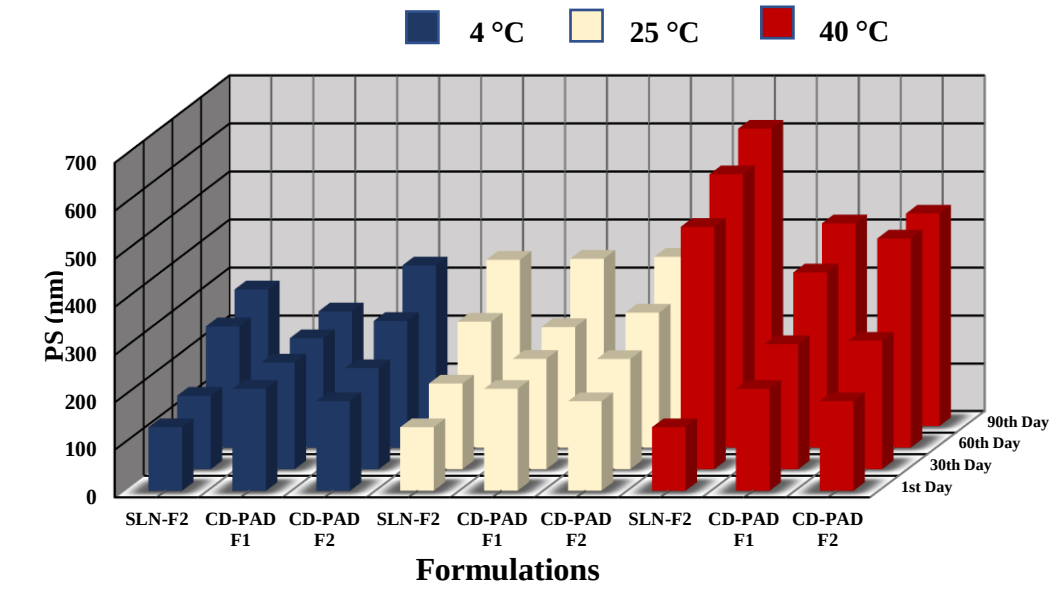


**Figure 4.61.** *The PS of the Studied Formulations after Three Months (mean ± SE) (n= 3)*

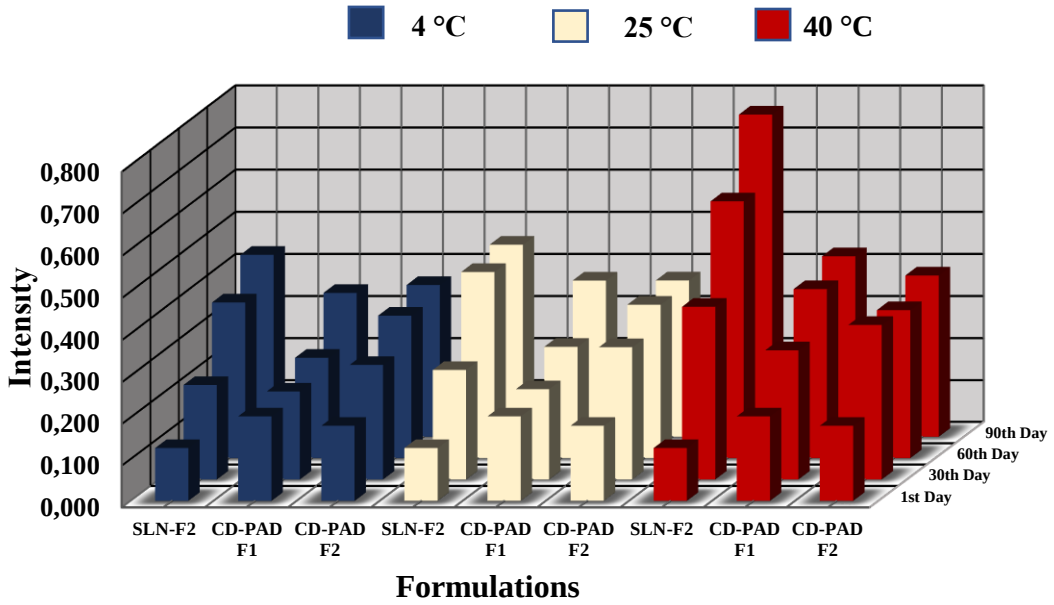


**Figure 4.62.** *The PDI of the Studied Formulations after Three Months (mean ± SE) (n= 3)*

The statistical analysis studies between values were carried out by two-way ANOVA where the *P*-value calculated to demonstrate the significant changes in PS, PDI, and ZP during three months. The *P*-values in figures were represented by stars in which $P > 0.05$ (null hypothesis) (no significant changes). The alternative hypothesis (significant changes) if, $P \leq 0.05$ (*), $P \leq 0.01$ (**), $P \leq 0.001$ (***), and $P \leq 0.0001$ (****).

The statistical analysis of the PS measurement results for three formulations SLN-F2, F1(CD-PAD), and F2 (CD-PAD) are illustrated in Figure 4.63, 4.64, 4.65. respectively.

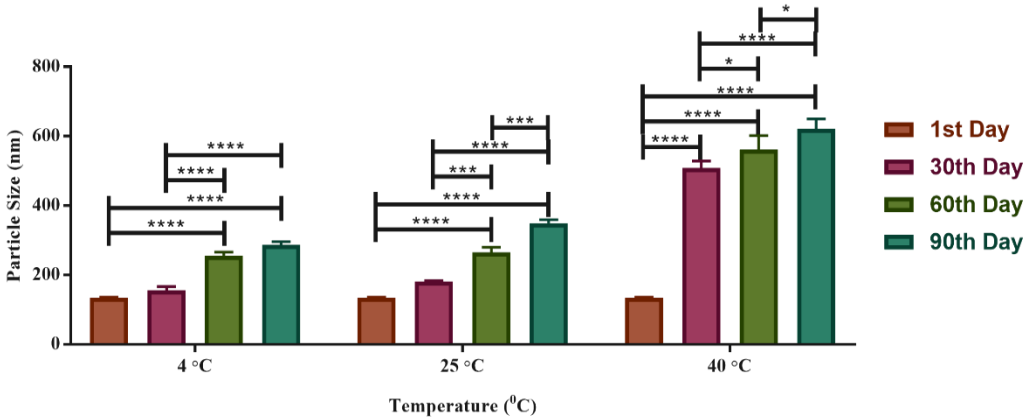


**Figure 4.63.** *Statistical Analysis of the PS Measurement Results for SLN-F2*

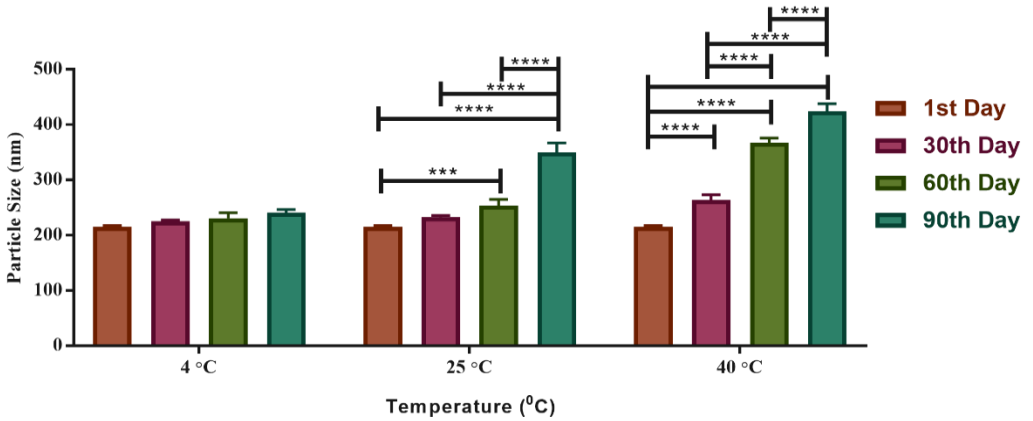


**Figure 4.64.** *Statistical Analysis of the PS Measurement Results for F1-(CD-PAD)*

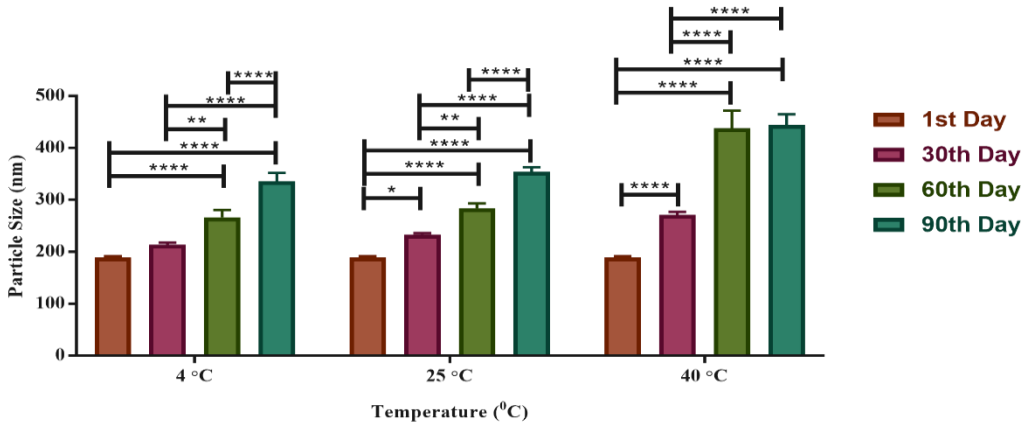


**Figure 4.65.** *Statistical Analysis of the PS Measurement Results for F2-(CD-PAD)*

The statistical analysis of the PDI measurement results for three formulations SLN-F2, F1(CD-PAD), and F2 (CD-PAD) are illustrated in Figure 4.66., 4.67., 4.68. respectively.

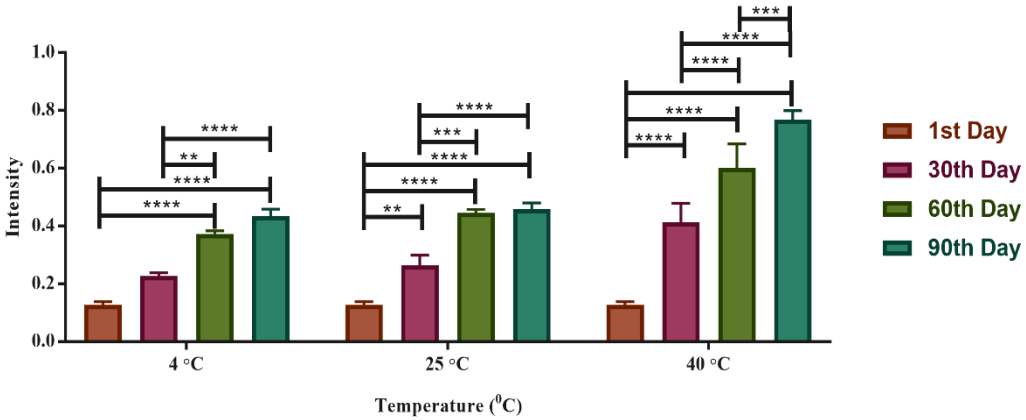


**Figure 4.66.** *Statistical Analysis of the PDI Measurement Results for SLN-F2*

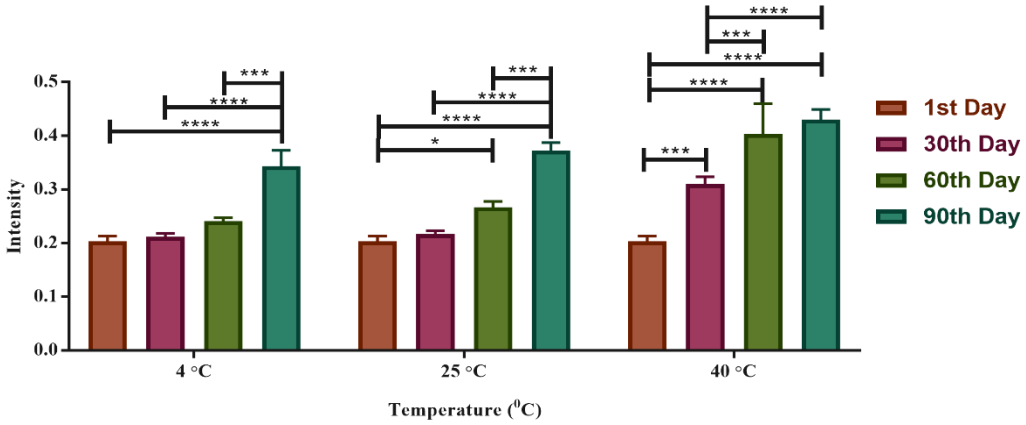


**Figure 4.67.** *Statistical Analysis of the PDI Measurement Results for F1-(CD-PAD)*

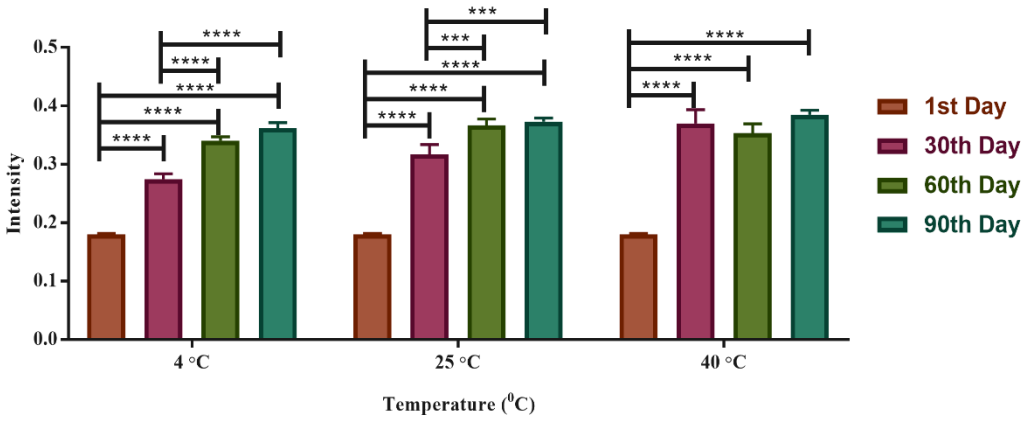


**Figure 4.68.** *Statistical Analysis of the PDI Measurement Results for F2-(CD-PAD)*

### 4.9.3. ZP studies results

The ZP analysis studies results for the formulation SLN-F2, F1-(CD-PAD), F2-(CD-PAD) are demonstrated in Tables 4.37. The Figures 4.69. is shown the comparison for the ZP analysis results for the three formulations.

**Table 4.37.** *The ZP of the Formulations after Three Months (mean ± SE) (n= 3)*

| Time | Storage Conditions | | |
|---|---|---|---|
| | **4 °C ± 1 °C** | **25 °C ± 1°C** | **40 °C ± 1 °C** |
| | | **SLN-F2** | |
| **1st day** | -18.77 ± 0.20 | -18.77 ± 0.20 | -18.77 ± 0.20 |
| **30th day** | -19.10 ± 0.51 | -23.43 ± 1.60 | -34.77 ± 1.96 |
| **60th day** | -28.10 ± 1.97 | -30.77 ± 1.00 | -37.43 ± 1.36 |
| **90th day** | -36.43 ± 0.69 | -36.10 ± 0.98 | -35.77 ± 0.78 |
| | | **F1 (CD-PAD)** | |
| **1st day** | -36.20 ± 0.06 | -36.20 ± 0.06 | -36.20 ± 0.06 |
| **30th day** | -33.20 ± 1.70 | -33.20 ± 1.54 | -36.53 ± 1.71 |
| **60th day** | -23.20 ± 1.68 | -23.53 ± 1.78 | -24.53 ± 0.85 |
| **90th day** | -31.20 ± 1.21 | -32.20 ± 0.64 | -32.53 ± 1.22 |
| | | **F2 (CD-PAD)** | |
| **1st day** | -39.20 ± 0.23 | -39.20 ± 0.23 | -39.20 ± 0.23 |
| **30th day** | -35.53 ± 0.92 | -34.53 ± 1.24 | -35.20 ± 0.64 |
| **60th day** | -34.60 ± 0.64 | -34.87 ± 0.86 | -34.53 ± 0.85 |
| **90th day** | -37.53 ± 1.24 | -36.35 ± 0.55 | -37.20 ± 1.16 |

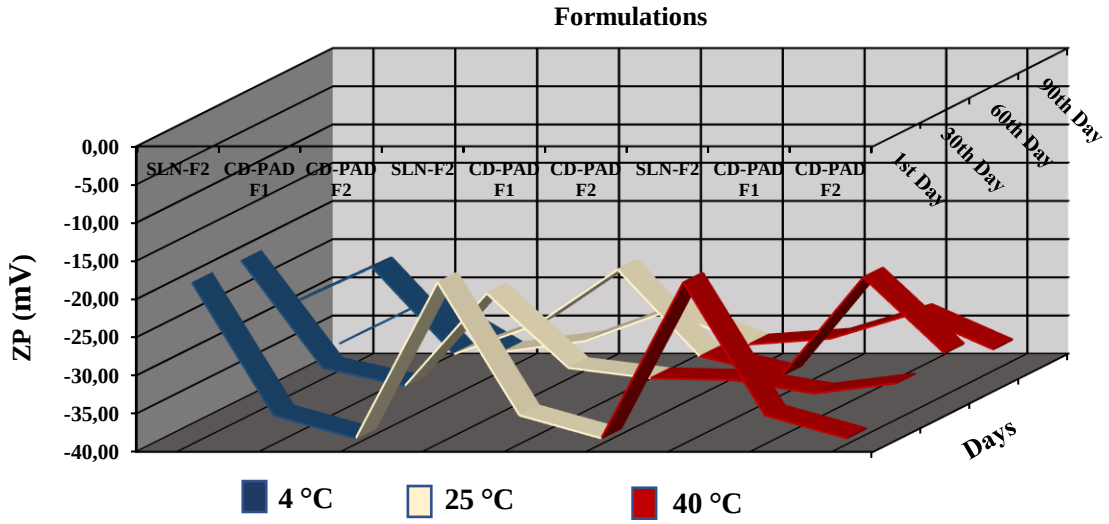


**Figure 4.69.** *The ZP of the Studied Formulations after Three Months (mean ± SE) (n= 3)*

The statistical analysis of the ZP measurement results for three formulations SLN-F2, F1-(CD-PAD), and F2-(CD-PAD) are illustrated in Figure 4.70., 4.71., and 4.72. respectively.

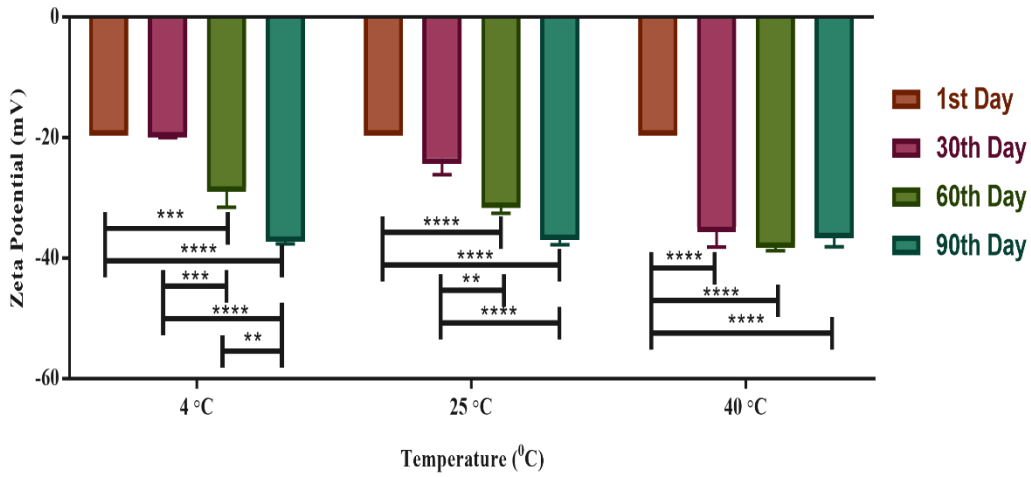


**Figure 4.70.** *Statistical Analysis of the ZP Measurement Results for SLN-F2*

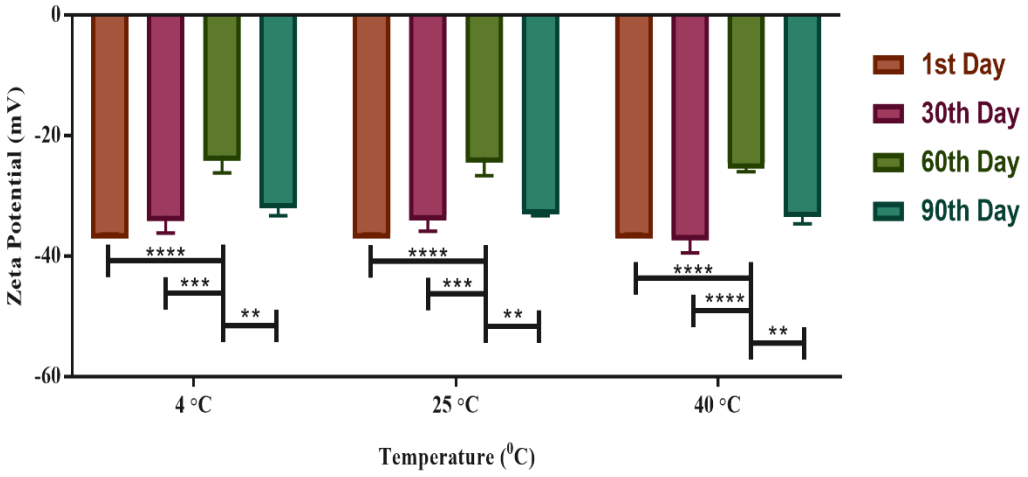


**Figure 4.71.** *Statistical Analysis of the ZP Measurement Results for F1-(CD-PAD)*

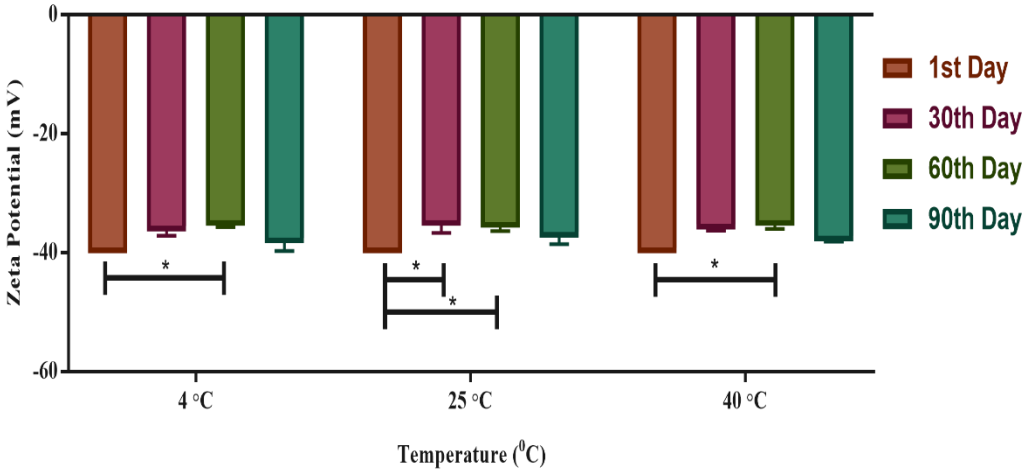


**Figure 4.72.** *Statistical Analysis of the ZP Measurement Results for F2-(CD-PAD)*

### 4.10. *In Vivo* Studies (Pharmacokinetic studies)

The detected RCa plasma concentrations in the three animal groups which were given the pure RCa suspension and the two formulations SLN-F2 and F2 (CD-PAD), are shown in Table 4.38., 4.39., and 4.40.

**Table 4.38.** *RCa Plasma Concentrations (μg. $mL^{-1}$) in A Group of Rat Which Was Fed with Pure RCa Suspension*

| Time | Plasma Con. in 1st Rat | Plasma Con. in 2nd Rat | Plasma Con. in 3rd Rat | Plasma Con. in 4th Rat | Plasma Con.in 5th Rat | Mean | SE |
|---|---|---|---|---|---|---|---|
| **0.5** | 0.1237 | 0.0670 | 0.0577 | 0.0554 | 0.0578 | 0.0723 | 0.0130 |
| **1** | 0.2415 | 0.0971 | 0.1148 | 0.2507 | 0.1160 | 0.1640 | 0.0337 |
| **2** | 0.2615 | 0.1443 | 0.1289 | 0.3217 | 0.1523 | 0.2017 | 0.0381 |
| **4** | 0.9008 | 0.2081 | 0.3836 | 0.4485 | 0.5013 | 0.4885 | 0.1143 |
| **6** | 1.1496 | 3.7214 | 2.0521 | 0.5152 | 2.3445 | 1.9566 | 0.5478 |
| **9** | 0.2432 | 0.0597 | 0.1312 | 0.0425 | 0.3519 | 0.1657 | 0.0584 |
| **24** | 0.2335 | 0.0564 | 0.1119 | 0.0365 | 0.1247 | 0.1126 | 0.0344 |
| **48** | 0.2203 | 0.0189 | 0.1086 | 0.0182 | 0.0118 | 0.0756 | 0.0404 |
| **72** | 0.0608 | 0.0000 | 0.0435 | 0.0118 | 0.0000 | 0.0219 | 0.0130 |

**Table 4.39.** *RCa Plasma Concentrations (μg. $mL^{-1}$) in A Group of Rat Which Was Fed with (SLN-F2)*

| Time | Plasma Con. in 1st Rat | Plasma Con. in 2nd Rat | Plasma Con. in 3rd Rat | Plasma Con. in 4th Rat | Plasma Con.in 5th Rat | Mean | SE |
|---|---|---|---|---|---|---|---|
| **0.5** | 0.6359 | 0.6486 | 0.6740 | 0.6049 | 0.6237 | 0.6374 | 0.0116 |
| **1** | 1.3200 | 1.5842 | 1.4479 | 1.6458 | 1.5600 | 1.5116 | 0.0576 |
| **2** | 1.5499 | 1.8879 | 1.9743 | 1.8554 | 1.6954 | 1.7926 | 0.0756 |
| **4** | 2.0970 | 2.2337 | 2.4969 | 2.3998 | 1.9033 | 2.2261 | 0.1059 |
| **6** | 2.4966 | 3.1804 | 3.0613 | 3.3078 | 2.2510 | 2.8594 | 0.2057 |
| **9** | 2.1381 | 2.7802 | 2.6822 | 2.7903 | 2.1476 | 2.5077 | 0.1501 |
| **24** | 1.7590 | 2.7035 | 1.9019 | 2.2019 | 1.8110 | 2.0755 | 0.1747 |
| **48** | 0.5586 | 0.6222 | 0.5291 | 0.6361 | 0.3090 | 0.5310 | 0.0589 |
| **72** | 0.4329 | 0.2921 | 0.2659 | 0.2698 | 0.2964 | 0.3114 | 0.0310 |

**Table 4.40.** *RCa Plasma Concentrations in (μg. mL$^{-1}$) A Group of Rat Which Was Fed with F2-(CD-PAD)*

| Time | Plasma Con. in 1st Rat | Plasma Con. in 2nd Rat | Plasma Con. in 3rd Rat | Plasma Con. in 4th Rat | Plasma Con.in 5th Rat | Mean | SE |
|---|---|---|---|---|---|---|---|
| **0.5** | 0.4105 | 0.3777 | 0.3516 | 0.3836 | 0.3696 | 0.3786 | 0.0096 |
| **1** | 1.2475 | 1.1583 | 1.1883 | 1.1623 | 1.1701 | 1.1853 | 0.0164 |
| **2** | 1.7131 | 1.5972 | 1.3059 | 1.3897 | 1.5415 | 1.5095 | 0.0728 |
| **4** | 2.4575 | 2.1857 | 1.9653 | 2.0036 | 2.1381 | 2.1500 | 0.0870 |
| **6** | 2.6718 | 2.5793 | 2.7227 | 2.6647 | 2.6705 | 2.6618 | 0.0231 |
| **9** | 2.2918 | 2.2892 | 2.3420 | 2.2444 | 1.9237 | 2.2182 | 0.0752 |
| **24** | 1.9637 | 1.9767 | 1.3349 | 1.5030 | 1.4594 | 1.6475 | 0.1346 |
| **48** | 0.7108 | 1.0188 | 0.7589 | 0.5964 | 1.0179 | 0.8206 | 0.0850 |
| **72** | 0.2993 | 0.5865 | 0.2512 | 0.3633 | 0.5391 | 0.4079 | 0.0661 |

The plasma concentration time curves of pure RCa suspension, SLN-F2 and F2-(CD-PAD) formulations which were orally fed to the rats are shown in Table 4.41 and Figure 4.73. The chromatogram representing bioanalysis of RCa in rat plasma for SLN-F2 is illustrated as an example of pharmacokinetic studies, Figure 4.74.

**Table 4.41.** *Average of RCa Plasma Concentration (μg. mL$^{-1}$) of All Time Points for Each Studied Rats Group (mean ± SE)*

| Time | Mean of Plasma Con. for Pure RCa Group | Mean of Plasma Con. for SLN-F2 Group | Mean of Plasma Con. for F2 (CD-PAD) Group |
|---|---|---|---|
| **0.5** | 0.0723 ± 0.0130 | 0.6374 ± 0.0116 | 0.3786 ± 0.0096 |
| **1** | 0.1640 ± 0.0337 | 1.5116 ± 0.0576 | 1.1853 ± 0.0164 |
| **2** | 0.2017 ± 0.0381 | 1.7926 ± 0.0756 | 1.5095 ± 0.0728 |
| **4** | 0.4885 ± 0.1143 | 2.2261 ± 0.1059 | 2.1500 ± 0.0870 |
| **6** | 1.9566 ± 0.5478 | 2.8594 ± 0.2057 | 2.6618 ± 0.0231 |
| **9** | 0.1657 ± 0.0584 | 2.5077 ± 0.1501 | 2.2182 ± 0.0752 |
| **24** | 0.1126 ± 0.0344 | 2.0755 ± 0.1747 | 1.6475 ± 0.1346 |
| **48** | 0.0756 ± 0.0404 | 0.5310 ± 0.0589 | 0.8206 ± 0.0850 |
| **72** | 0.0219 ± 0.0130 | 0.3114 ± 0.0310 | 0.4079 ± 0.0661 |

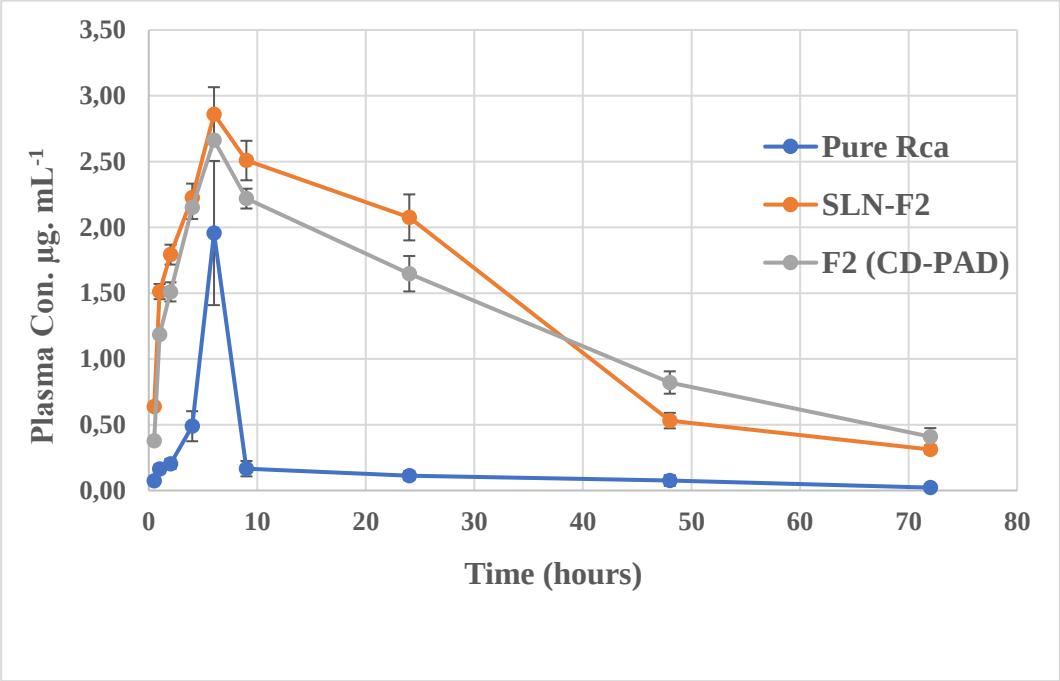


**Figure 4.73.** *The Plasma Concentration Time Curves of Pure RCa Suspension, SLN-F2 and F2-(CD-PAD) Formulations*

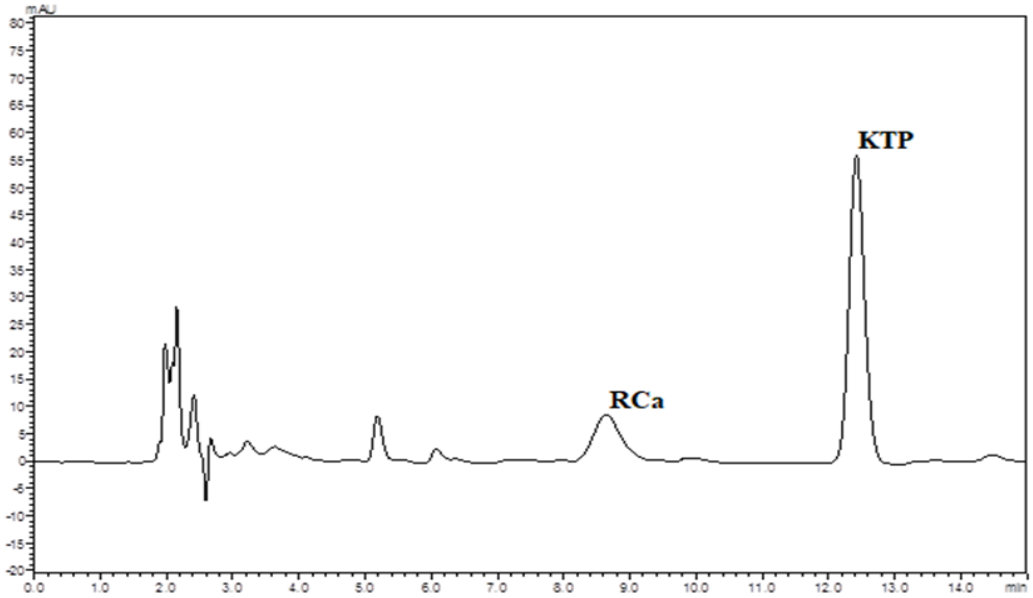


**Figure 4.74.** *Chromatogram Illustrating the Bioanalysis of RCa and KTP (IS) in Rat Plasma for Pharmacokinetic Studies.*

The RCa plasma concentrations in rats fed with SLN-F2 and F2-(CD-PAD) were significantly higher than those fed with pure RCa. The pharmacokinetic parameters ($C_{max}$. $T_{max}$ and $AUC_{last}$, $AUC_{total}$, $t_{1/2}$ and MRT) after oral administration of two formulations

and pure RCa suspension are calculated using Kinetica 50. software (Table 4.42).

**Table 4.42.** *The Pharmacokinetic Parameters after Oral Administration of Pure RCa, SLN-F2, and F2 (CD-PAD), (n= 5)*

| Parameters | Pure RCa $\bar{x}$ ± SD ± SE | SLN-F2 $\bar{x}$ ± SD ± SE | F2 (CD-PAD) $\bar{x}$ ± SD ± SE |
|---|---|---|---|
| **$C_{max}$ (µg. mL$^{-1}$)** | 2.03 ± 1.17 ± 0.53 | 2.86 ± 0.46 ± 0.21 | 2.58 ± 0.19 ± 0.08 |
| **$T_{max}$ (h)** | 6.00 | 6.00 | 6.00 |
| **$AUC_{last}$ (µg. h. mL$^{-1}$)** | 10.62 ± 4.74 ± 2.12 | 90.64 ± 12.85 ± 5.74 | 85.60 ± 11.71 ± 5.24 |
| **$AUC_{total}$ (µg. h. mL$^{-1}$)** | 12.00 ± 5.55 ± 2.48 | 98.87 ± 12.70 ± 5.68 | 96.71 ± 17.61 ± 7.87 |
| **$t_{1/2}$ (h)** | 25.58 ± 13.11 ± 5.86 | 19.68 ± 2.76 ± 1.24 | 21.47 ± 3.74 ± 1.67 |
| **MRT (h)** | 27.17 ± 14.74 ± 6.59 | 30.14 ± 3.68 ± 1.65 | 33.89 ± 5.74 ± 2.56 |

### 4.10.1 Statistical analysis of pharmacokinetic studies

The statistical analysis of plasma pharmacokinetic parameters is illustrated in Figure 4.75., 4.76. and 4.77.

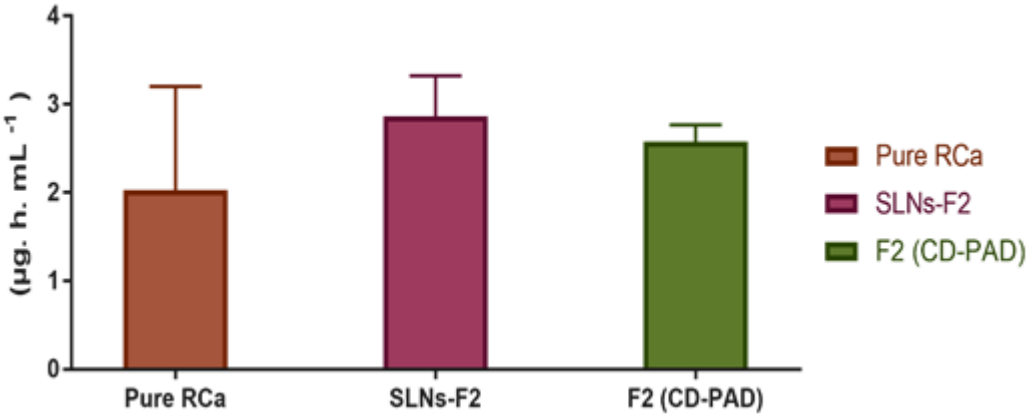


**Figure 4.75.** *$C_{max}$ of Pure RCa, SLN-F2 and F2 (CD-PAD)*

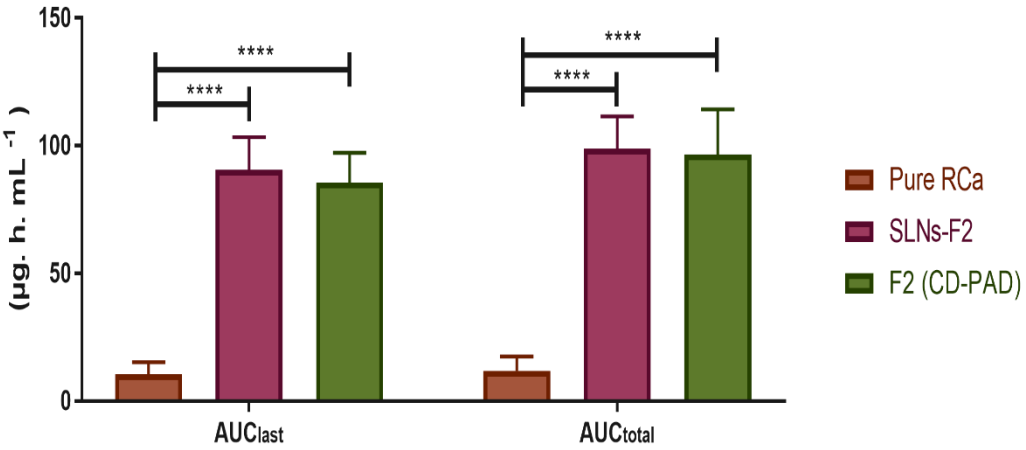


**Figure 4.76.** *$AUC_{last}$ and $AUC_{total}$ of Pure RCa, SLN-F2 and F2 (CD-PAD)*

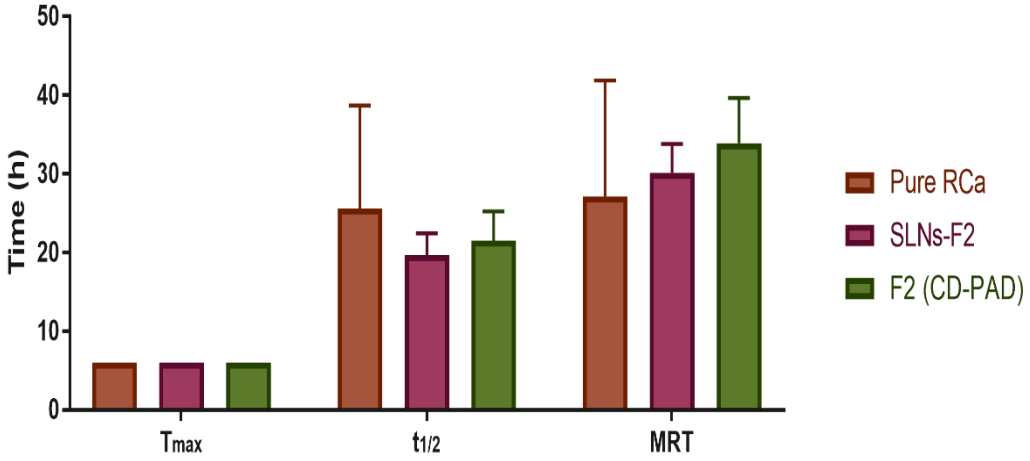


**Figure 4.77.** *$T_{max}$, $t_{1/2}$ and MRT of Pure RCa, SLN-F2 and F2-(CD-PAD)*

# 5. DISCUSSION

## 5.1. Analytical Method and Validation Studies

Isocratic reverse phase HPLC method (Kumar *et al.*, 2006, p.881–887) was used for the determination of RCa *in vitro* and *in vivo* studies. The method was validated and evaluation indicates that the used method confirms the ICH and USP system suitability test recommendations (ICH, 1996, p. 4–5), (U.S.P, 2016, p. 463–468). The method showed a good correlation coefficient which is (0.9998) (Figure 4.2.) for the calibration curve and the calculated LOQ and LOD were suitable for the intended studies. The percentages of recovery were between 99.0005 – 101.7392 % and RSD % for the precision of RCa standard solution was below 2 % which are within the permitted range (Table 4.2.- Table 4.5.) The specificity study was carried out by comparing the standard solution of RCa with the placebo solutions of the formulations and the chromatograms of the mobile phase and placebo solutions showed no interfering peak at the retention time of RCa (Figure 4.3.).

In case of permeability studies the same HPLC method was used except the solutions of RCa were prepared in the (HBSS + 2 % DMSO) solution. This method demonstrated a correlation coefficient which equal to a unity for the calibration curve and the determined LOD (0.23 µg. $mL^{-1}$) and LOQ (0.69 µg. $mL^{-1}$) were appropriate for the permeability studies. The percentage of recovery was within the required limit (100 % ± 2) and RSD % for the precision was less than 2 %. The specificity study was performed by comparing the standard RCa with the (HBSS + 2 % DMSO) solution. There was no interfering peak occurred. (Figure 4.6.).

In pharmacokinetic studies, the method was modified (Section 4.1.3.) in the step of plasma samples preparation in order to get better results (Kumar *et al.*, 2006, p. 881–887). ACN was used for the protein precipitation because it is more efficient for plasma protein precipitation (Polson *et al.*, 2003, p.263–275). Then HPLC method was used and validated (Section 4.1.2.) according to the official regulations (EMA, 2012, p.1–23). The validation of bioanalysis method was convenient for the determination of RCa in pharmacokinetic studies. The recovery % was within the required limit (100 % ± 15) and RSD % for the precision was less than 15 % (Table 4.14-4.17) (EMA, 2012, p.1–23) . The specificity study was carried out by comparing the standard RCa with pure plasma

sample and pure plasma spiked by IS (KTP) and no interference was detected neither from pure plasma nor IS (Figure 4.9.).

### 5.2. RCa Solubility in Water

RCa belongs to Class II drug in BCS classification i.e. low solubility and high permeability (Vidya *et al.*, 2016, p.4882–4892). It is sparingly soluble in water due to its crystalline nature. However, it has a partition coefficient (octanol/water) of 0.13 at pH of 7.0 (Vyas, 2013, p.37–46). The solubility of RCa in bidistilled water was found to be 7.32 ± 0.082 mg. $mL^{-1}$ (mean ± SE) correspond to the reference literature (http-1).

### 5.3. Cs NPs Formulation

Today, the most considerably used derivatives of Cs in drug delivery are water-soluble Cs salts. Cs forms water-soluble salts with both inorganic acids and organic acids such as hydrochloric acid, formic acid, GA, lactic acid, citric acid, AA and ascorbic acid. The reactive amino groups present in Cs chains can be the reason why the water-soluble polysaccharide is positively charged. Cs acid salts (mostly glutamate, aspartate, hydrochloride, and acetate) were used to improve the delivery of therapeutic agents across the intestinal epithelia (Cervera *et al.*, 2011, p.637–649).

Different techniques are used to prepare Cs-based NPs; including emulsification solvent diffusion method, spray drying, chemical cross-linking and ionotropic gelation (Viral *et al*., 2012, p.491–501). Among these techniques, spray drying is the most popular because of the facility of handling and the absence of toxic solvents. Spray drying is a well-establish technique for converting solutions, emulsions and suspensions into powders while controlling the size, density, morphology of the particles efficiently. Limited exposure to the heat makes the technique also advantageous for heat sensitive drugs. In addition, the technique is inexpensive, fast, and a one-step process, which is why it has been utilized in several applications in pharmaceutics, including preparation of Cs-based formulation (Alhalaweh *et al*., 2009, p.206–214; Cervera *et al*., 2011, p.637–649; Başaran *et al*., 2013, p.1–9). it should be taken into account that the drying procedure can result in amorphous structures compared to a semi-crystalline structure of pure substances, however, particle size reduction with the better dispersion formation can also be achieved (Maestrelli *et al*., 2004, p.257–267; Demirel *et al*., 2014, p.294–301).

Preparation yields of NPs were calculated with the amounts of pure materials used. In our study, the yields of the formulations were valued in a large scale between 10.43-

80.00% which correlates with the previous studies (Learoyd *et al.*, 2008, p.224–234). Loss during the preparation process may be due to the design of the spray-drying apparatus. Embryonic NPs which cannot be dried completely may lead to the formation of film on the surface of the drying component, resulting in reduced preparation yield (Hegazy *et al.*, 2002, p.171–174) .

Smaller particles possess an increased bioavailability with prolonged residence time showing more adhesive properties than larger particles (Başaran *et al.*, 2015, p.1180–1188). The most common and routine method for the determination of the mean hydrodynamic diameter of the particle is photon laser diffraction technique. For a monodisperse colloidal systems, the PDI should remain below 0.05, however values up to 0.5 can be regarded as homogenous and can be used for comparison purposes (Delair, 2011, p.10–18). As noted previously, the particle size increases with the molar mass of the Cs. Delair (Delair, 2011, p.10–18) obtained particles ranging in the 200-1000 nm, with a concomitant increase in PDI from 0.2 up to 0.6. According to the particle size analyses results F1 formulation which contain the highest amount Cs showed the highest particle size (446.9 ± 13.1 nm) while other particle sizes were ranged between the 388.1 ± 8.9 and 240.0 ± 10.7 nm (Table 4.19.). No concomitant increase in PDI data with particle size values were observed in our study however particle size distributions were relatively homogenous considering PDI values (Table 4.19).

ZP of NPs determine the performance of the NP system in the body considering interactions with cell membranes due to the electrostatic forces. ZP measurements also provide an information about the stability of dispersed NPs in aqueous media considering less aggregation, due to electric repulsion. ZP values higher than ± 30 mV indicate a stable colloidal dispersion (Genç and Demirel, 2013, p.701–709). In this study ZPs of prepared NPs were in the range of +21.9 ± 0.9 to +63.7±0.5 mV (except F6; -6.9 ± 0.1 mV) (Table 4.19.). Due to the presence of the quaternary ammonium groups of Cs, most of the Cs-based NPs have cationic characters which tend to adhere to the negatively charged surfaces, facilitating the penetration of NPs across the membranes (Bathool *et al.*, 2012:466–470; Bhattarai *et al.*, 2006, p.181–187).

HPLC method used for RCa was determined to be reliable, linear and precise, accurate, sensitive and selective through the validation studies (Section 4.1.). The comparison of DC % for all types of Cs salts were shown in (Table 4.19). For the batches which have same drug concentration (F1, F2, F4, and F6), the DC % ranged between

16.5-99.1 %. As reported before by Laungtana-anan et al. (Luangtana-anan *et al.*, 2005, p.189–196) acetate and lactate salts showed higher DC % than aspartate and glutamate salt forms also in our study.

SEM was used to visualize the particle diameter, structural and surface morphology of the spray-dried powders (Figure 4.10). SEM images showed that pure RCa has irregular shaped particles which were regarded as semi-crystalline structure (Figure 4.10). Flakes of pure Cs can also be seen in (Figure 4.10) showing the amorphous structure of the polymer. The images of spray-dried samples demonstrated spherical and regular in shapes with smooth surfaces (especially for F1 and F2) (Figure 4.10) which are general morphology of spray-dried amorphous materials (Learoyd *et al.*, 2008, p.224–234; Başaran *et al.*, 2014, p.49–57). Neither porous structures nor RCa residues were detected in the photomicrographs, showing that RCa was successfully incorporated into the particles as nanocapsule forms (Figure 4.10).

DSC thermograms of pure RCa showed glass transition onsets in the ranges of 78-85 °C, 188-198 °C and 237-252 °C showing the semi-crystalline structure of the active agent (Figure. 4.11) which also can be seen in SEM photomicrographs (Figure. 4.10). The DSC thermograms of NPs exhibited the amorphous character of the polymer which gives possibility to incorporate higher amounts of RCa within the spacings of the less ordered amorphous bonds compared to crystalline lattices (Portero and Remun, 1998, p.75–84) .

FT-IR spectra show absorption bands relating to bending or stretching of unique bond and the resulting spectrum is a fingerprint of the products. Cs can be identified by several absorption bands with specific wavenumbers. Cs base 3354 $cm^{-1}$ intermolecular hydrogen bonding, Amide II band 1649 cm-1 , CH2 bending 1379 cm-1 , C-O-C bridge 1058 cm-1 , C-O-C stretching 1028 $cm^{-1}$ (Buschmann *et al.*, 2013, p.1234–1270). Moreover, the spectrum of spray-dried CL, CA, CG shows a large peak (-NH2) at 1582 $cm^{-1}$, 1623 $cm^{-1}$, 1631 $cm^{-1}$ respectively (Figure 4.12). The large shift of these vibrations to higher wavenumbers compared with the usual wavenumbers of the amino group proves the formation of a carboxylate between the –COO- groups of the acids and the –NH3 + groups of Cs. Consequently, it seems reasonable to conclude the FT-IR analyses as -CH was ionically linked with the acids (Orienti *et al.*, 2002, p.51–59).

Powder XRD was used to determine the crystallinity of compounds. Polymorphic changes of the drugs are important factors which might affect the dissolution rate and the bioavailability. Besides DSC analyses, crystallinity of the drug and NPs were also

determined using XRD (Kamble *et al.*, 2014, p.197–204). RCa exhibited a characteristic semi-crystalline XRD pattern at 2θ that support the DSC analyses results (Figure 4.13) (Ponnuraj *et al.*, 2015 , p.2217–2231). Similarly no sharp peaks owing to the crystalline structure were recorded also for NPs showing no formation of crystals during the formulation stages (Portero and Remun, 1998, p.75–84).

$^{1}$H-NMR can also be used to identify Cs via particular chemical shifts of protons and carbons. Physicochemical properties of NPs can be identified by $^{1}$ H-NMR analyses in a variety of dosage forms to elucidate the status of active agent incorporated into a solid matrix, its molecular mobility and molecular interactions between the active material and the excipients (Başaran *et al.*, 2014, p.49–57) . $^{1}$H-NMR spectra of pure RCa and pure polymers were used as references and according to our analyses results the intensities of the peaks around 3 ppm, 5 ppm and 7 ppm ranges were changed upon the entrapment of RCa showing the molecular distribution of RCa in the polymeric matrix compared to pure substances (Figure. 4.14., marked with arrows).

Dissolution is frequently the rate-limiting step in gastro-intestinal absorption and the bioavailability of poor water-soluble drugs from solid dosage forms. The potent well-known dyslipidemic RCa is representative example of this type of drugs. RCa is sparingly soluble in water (7.32 ± 0.08 mg. $mL^{-1}$, experimental data) and as a consequence it exhibits low bioavailability values after oral administrations. Therefore, the improvement of RCa dissolution from its solid dosage forms is an important issue for enhancing bioavailability and therapeutic efficiency.

The release of drug from Cs based dosage forms depend upon morphology, size, density and extent of cross-linking of the particulate system, physicochemical properties of the drug as well as the polymer characteristics (such as its hydrophobic character, gel formation ability, swelling capacity, muco-adhesive or bioadhesive properties) and also on the presence of other excipients present in the dosage forms. The release of drug from Cs particulate systems involves three mechanisms: (a) erosion, (b) diffusion, and (c) release from the surface of particles. The release of drug follows more than one type of kinetic model. In case of release from the surface, adsorbed drug dissolves rapidly and leads to burst effect when it comes in contact with the release medium (Bansal *et al.*, 2011, p.28–37). According to dissolution studies, an initial burst release was achieved for F1 and F2 formulations, which was approximately 58 % within 5 min. On the other hand, F3-F6 formulations showed slower releases with biphasic profiles (Figure 4.15, 4.16).

Similar results were recorded at former studies (He *et al.*, 1999, p.53–65). He et al. observed that Cs based microspheres prepared by spray drying technique have shown burst release of cimetidine which correlates with our study. The lowest release rates were achieved for F4-F6 formulations which was attributed to a low DC % (Table 4.19.).

It is evident that all Cs salt types increased the dissolution rate of RCa with respect to the pure drug at the early stages of the release study (Table 4.20., Figure 4.15., Figure 4.16.). Although only 32% of the pure drug was dissolved in the release medium, approx. 85, 81, 58, and 63% release rates were recorded for the CA (F1), CL (F2), CAs (F4), and CG (F6) formulations, respectively just in 0.5 h (Figure 4.15, 4.16). In particular, the release of RCa from the NPs were ordered as: CA > CL > CG > CAs. There is a correlation between our results and former studies results showing that enhanced dissolution rate can be attributed to the decreased size and polymer wetting effect (Portero and Remun, 1998, p.75–84; Cerchiara *et al.*, 2003, p.1623–1627).

The mechanism of drug release from polymer based matrices is complex and not completely understood. Some systems may be classified as either purely diffusion or erosion controlled, while most systems exhibit a combination of these mechanisms. Korsmeyer-Peppas model characteristic of anomalous kinetics (non-Fickian, a combination of the diffusion and erosion mechanism) diffusion. Korsmeyer-Peppas model that fits the best the release data of Cs based NPs in our study (Table 4.21., Figure 4.17.) indicating that drug release is ruled by both diffusion of the drug and dissolution/erosion of the polymer matrix (Salih *et al.*, 2013, p.525–535; Arora *et al.*, 2011, p.163–169).

### 5.4. SLNs Formulation

Lipid nanoparticles with solid particle matrix have many advantages compared to other drug carries. They are mainly composed of bio-compatible lipids and provide a prolonged/controlled release, improve the bioavailability of the active substances and protect sensitive drugs from decomposition. They have been proposed for different administration routes, such as oral, topical application, ophthalmic, inhalation and nasal administration as well as parenteral injection (Sznitowska *et al.*, 2017, p.24–30; Olbrich *et al.*, 2002, p.119–128).

The most popular method of manufacturing solid lipid particles is to disperse the molten lipid phase in a warm aqueous phase containing surfactants. The lipid phase usually contains an active substance. Various methods can be used to produce fine

dispersion, resulting in lipid particles smaller than 1 μm in size (solid lipid nanoparticles-SLN): such methods can include a high pressure homogenization of a warm emulsion, high-shear homogenization, ultra-sonication, or a combination (Mäder and Mehnert, 2001, p.165–196). The SLN formulations were prepared with this commonly used method, whereby the molten lipid phase was emulsified in a heated aqueous phase and the emulsion was subjected to a cooling process in the study. High shear homogenization and ultrasonication techniques were employed to prepare SA and TP-SLNs.

General ingredients include solid lipid(s), surfactant(s) and water (Mäder and Mehnert, 2001, p.165–196). The term lipid is used here in a broader sense and includes triglycerides (e.g. tripalmitin), partial glycerides (e.g. Imwitor), fatty acids (e.g. stearic acid), steroids (e.g. cholesterol) and waxes (e.g. cetyl palimitate) (Mäder and Mehnert, 2001, p.165–96). Substances used to prepare these nanoparticles are physiologic and generally recognized as safe compounds (GRAS ingredients); this aspect makes SLNs preferable carriers for humans (Righeschi *et al.*, 2016, p.475–483).

In SLN composition, many different surfactants can be used (with respect to charge and molecular weight), such as non-ionic surfactants including poloxamer, polysorbate (Tween), sorbitan monopalmitate (Span), macrogolglycerol ricinoleate (Cremophor) and amphoteric surfactants such as soya lecithin, egg phosphatidyl choline, polymeric stabilizers (poly vinyl alcohol) and other have been used to stabilize the lipid dispersion (Sznitowska *et al.*, 2017, p.24–30; Mäder and Mehnert, 2001, p.165–196). The non-ionic surfactant (T80) was used in F1-F3 formulations. The F4 has T80 and amphoteric surfactant (PTC) together. It was reported that the use of surfactants as combinations might prevent particle agglomeration more efficiently compared to one surfactant alone (Mäder and Mehnert, 2001, p.165–96).

The effects of the type of components (lipid matrix and surfactant) and concentration of active agent on the properties of SLN were evaluated. Table 4.22 and 4.23 show the characteristics of prepared SLN formulations. The data in Table 4.22 show that all formulations possessed high EE ranged from 71.5±0.07% to 103.10±0.01%. SLN formulations prepared with TP as lipid matrices resulted in the higher drug entrapment than SA. The EE values of SA-SLNs (F1, F2) and TP-SLNs (F3, F4) were 71.5%, 80.2%, 103.10% and 100.14% respectively. The such values might be related to the structure of the lipid which had a great influence on the drug incorporation. TP has a long triglyceride chain and produced less ordered lipid crystals than SA which is composed solely of C18

carbon chains. During the SLN formation, the lipid that results in a highly crystalline structure with a perfect lattice would lead to drug expulsion (Westesen *et al.*, 1997, p.223–236; Hou *et al.*, 2003, p.1781–1785). As a result, the structure of the less ordered arrangement in the nanoparticles would be beneficial to the drug loading capacity like the samples in this study (Westesen *et al.*, 1997, p.223–236; Hou *et al.*, 2003, p.1781–1785). The EE values in SA-SLNs (F1, F2) were increased from 71.5 % to 80.2 % with decreased RCa amount in the formulation (Table 4.22). Also, the DL values in F1 and F2 increased from 0.71 % to 1.57 % with decreasing RCa content in the formulation. Although the EE of drug nearly not changed, the DL in TP-SLNs (F3, F4) decreased from 1.03 % to 0.25 % with decreasing RCa content in the formulation (Table 4.22).

Considering the analyses results, the formulations containing SA (F1 and F2) showed relatively higher particle sizes mean (±SE) 351.13±1.39 and 134.37±0.91 nm respectively while the formulations with TP (F3 and F4) resulted in particle size of 240.2±22.9 and 267.7±18.7 nm (Table 4.23.). A narrow particle size distribution was an indication of nanoparticle stability and homogeneous dispersion and PDI values ranging from 0 to 0.5 were considered to be monodisperse and homogenous, but those of more than 0.5 indicated non homogeneity and polydispersity (Senthil Kumar *et al.*, 2015, p.661–671). The size distribution of the SLNs was in the range of mean (±SE) 0.13±0.01 to 0.33±0.025, which indicates the existence of a monodisperse and homogenous populations (Table 4.23). Hence, the PDI of the particle size distributions of the present study are well correlated with the reported data in the literature (Oehlke *et al.*, 2017, p.1–19).

The surface charge is an important factor, influencing the stability of colloidal dispersion (Dudhipala and Veerabrahma, 2017, p.47–57). Nanoparticle with ZP values greater than +25 mV or less than -25 mV typically have high degrees of stability due to electric repulsion between particles (Senthil Kumar *et al.*, 2015, p.661–671). Dispersions with a low ZP values aggregate due to Van Der Waal inter-particle attraction (Senthil Kumar *et al.*, 2015, p.661–671). For SLN formulations all formulations were negatively charged and the ZP varied from -17.03±0.53 to -40.8±1.2 (mean ± SE) mV indicating a relatively good stability and dispersion of the system however the F4 formulation with TP showed higher ZP (Table 4.23). The negative value of the ZP of SLNs was attributed to the lipids used in the SLNs and in our study SA and TP provided the negative ZPs as expected considering the former information (Righeschi *et al.*, 2016, p.475–483).

RCa is available in crystalline, semi-crystalline and amorphous forms in the market. Morphology of RCa is semi-crystalline in sample investigated by SEM comprised of irregular rod-shaped particles of SA and TP (Figure 4.18). The shapes of SLNs were significantly differ from a spheres as they prefer to crystallize in the platelet form (Mäder and Mehnert, 2001, p.165–96). The non-spherical shapes of SLNs shown in Figure 4.19 were attributed to the crystalline structure of the matrix lipid.

Special attention must be paid to the characterization of the degree of lipid crystallinity and the modification of the lipid, considering the strongly correlation of the parameters with drug incorporation and release rates (Mäder and Mehnert, 2001, p.165–96). DSC is widely used to investigate the status of the lipid (Mäder and Mehnert, 2001, p.165–96). The thermograms of the pure substances, SLNs formulations and the placebos were presented in Figure 4.20. and 4.21. RCa sample with a heating rate 10°C.min$^{-1}$ showed a broad endothermic peak for water loss in the temperature range 75-80°C, followed by multiple glass transition onset in the temperature range of 180-290°C indicating its semi-crystalline nature Figure 4.20. and 4.21. The SA and TP showed the melting point of 72.20°C and 65.29°C respectively. However, for the formulations of SLNs (F1, F2, F3) a sharp peak of the lipid is present at its melting point, whereas the peaks of RCa have disappeared because the drug has been fully dissolved in the lipid and the F4 formulation demonstrated the melting peak of TP at 63°C and broad endothermic behavior between 190-320°C (Figure 4.20. and 4.21.).

Results of FT-IR study showed characteristic peaks of RCa at 2915, 1550, 1379, 1150 and 964 cm$^{-1}$ in Figure 4.22. as they reported also in the literature (Sathali and Nisha, 2013, p.536–548). All the characteristic peaks mentioned of RCa appeared in the spectra of the F1 and F2 formulations at the same wave number and no more additional of functional peaks were noticed (Figure 4.22.). It was demonstrated that there was no chemical reaction occurred between the RCa and SA, because the characteristic peaks of RCa did not show any shifts after encapsulation. The intensity of characteristic peaks of RCa was found to be reduced in the F1 and F2 formulations as seen Figure 4.22. which was mainly due to the molecular dispersion of semi-crystalline RCa in SA (Zhang *et al*., 1999, p.311–312; Agarwal *et al*., 2015, p.699–716). The characteristic peaks of RCa were also found in the spectrum of F3 formulation and there was no wave number change in the existing peaks (Figure 4.23.). It can be concluded as the RCa and TP were compatible with each other for F3 formulation however the major functional group peaks (964, 1150

and 1550 $cm^{-1}$) were not obtained in the F4 spectrum (Figure 4.23). However, other signature peaks of the drug remained unchanged (Figure 4.23).

The majority of active pharmaceutical ingredients (APIs) can exist in different solid-state forms like polymorphs, solvates, and the amorphous state. These solid forms can differ widely in their physicochemical properties, and thus can influence the quality, safety and efficacy of the drug product (Shete *et al.*, 2010, p.598–609). In addition, SEM and DSC analyses, semi-crystallinity of the drug was also determined using XRD. The XRD spectra of pure drug and pure lipids, SLNs and SLN-placebos are shown in the Figures 4.24 and 4.25. XRD pattern of RCa was indicating the semi-crystalline nature of the drug. The XRD pattern of SA was shown sharp crystalline peaks at 2Ɵ scattered angles at 6.8, 21.6, 24.2 and TP was shown at 19.2, 23.0 and 24.0 (Figures 4.24 and 4.25.). In F1-F3 and its placebos, decreased peak intensities of lipids were observed for RCa showing that the degree of crystallinity reduced in these formulations. On the other hand, in the F4, it was found that the lipid (TP) lost its crystalline nature (Figures 4.24 and 4.25.). The reducing crystallinity in F3 and F4 influenced the improvement of the encapsulation efficiency (Table 4.22) similar to reference (Li *et al.*, 2016, p.592–602).

The NMR is a powerful tool to investigate dynamic phenomena and the characteristics of nanocompartments in colloidal lipid dispersions (Müller *et al.*, 2000, p.161–177). NMR's active nuclei of interest is $^{1}H$. Due to the different chemical shifts it is possible to attribute the NMR signals to particular molecules or their segments. Simple $^{1}H$-spectroscopy permits an easy and rapid detection of supercooled melts (Müller *et al.*, 2000, p.161–177). Additional investigations on the SLNs performed in order to reveal the ionic interaction between RCa and solid lipids by $^{1}H$-NMR spectroscopy. The Figure 4.26 and 4.27 illustrated $^{1}H$-NMR spectroscopy RCa before and after preparation of the SLNs (as ppm). The characteristic peaks observed at 0.9 ppm (due to CH3 group) and 1.1 ppm (due to CH2 group) for SA and TP. The $^{1}H$-NMR spectrum of SLNs when compared with the spectra of pure RCa revealed mild alteration in the chemical shift for 3H (at 4.33 ppm) and 6H (at 4.41 ppm) (Figure 4.26 and 4.27). This indicated up-field nature of chemical shift and confirmed the formation hydrogen bonding reactions (Beg *et al.*, 2016, p.8173–8187).

*In vitro* release studies were performed using the dialysis bag technique in pH 6.8 phosphate buffer. The cumulative release of RCa from SLNs as a function of time were

shown in Table 4.24 and Figure 4.28. In order to evaluate the controlled release potential of the SLNs, the release of RCa from the nanoparticles was investigated over 48 h.

Comparing release profiles of lipids (SA and TP), different release rates were observed. SA-SLNs (F1 and F2) displayed a similar biphasic drug release pattern with a burst release within 6 hours, followed by relatively prolonged release (Sathali and Nisha, 2013, p.536–548; Kumar *et al.,* 2012:23–32). These formulations (F1 and F2) showed drug release of 78.88%, 74.36% at 6 h and 105.63%, 98.34% respectively at 48 h. For the pure RCa, the release rate was 31.96% within 0.5 h and reached to 95.46% by 6 h. The release profiles of SLNs resembled the drug-enriched core model were in agreement with the findings reported (Sathali and Nisha, 2013, p.536–548). Cumulative % of drug release profiles of TP-SLNs (F3 and F4) were not representing the prolonged release (Figure 4.28.). The cumulative releases of RCa pure form, F3 and F4 were 31.96%, 33.53% and 21.50% at 0.5 h and 95.46%, 92.16%, 92.40% at 6 h respectively. Obviously, the solid state of TP matrix could not prolong the release of drug from SLNs (Figure 4.28.).

Factors contributing to a release rate are the surface area of NPs, carbon chain length and melting point of lipid (Sathali and Nisha, 2013, p.536–548). In the present study, any relation between the given factors and the release behaviors could not be established. The release behavior of RCa from SLNs was attributed to the structure of SLNs, since the controlled adjustment of release can be achieved by modification of the chemical nature of the lipid matrix (Zur Muhlen *et al.,* 1998, p.149–155). When single solid lipid matrix was used as carrier material, the solution's ability of the drug was limited by the highly ordered lattice of solid lipid matrix (Li *et al.,* 2016, p.592–602).

SLNs, consist of a lipid core and outer shell of amphiphilic surfactant. If drug is loaded in the outer shell and on the particle surface, it is quickly released, displaying a burst effect. On the other hand, if it is incorporated into the particle core, it is released in a prolonged way. This makes the possibility of a controlled drug release from these carriers and represent an important tool to obtain a prolonged release of the drug (Righeschi *et al.,* 2016, p.475–483). TP is high melting point lipid has been used in modified/sustained release in oral solid dosage matrices.

The amount of the drug released was incorporated into the various release kinetic models (zero order, first order, Higuchi, Korsmeyer-Peppas and Hixson-Crowell) and among them the best fit model was determined on the basis of the k, $r^2$ and AIC (Zhang *et al.,* 2010, p.263–271). The pure RCa release was fitted to the first order kinetic model,

while all of the SLNs (F1, F2, F3 and F4) were fitted to Korsmeyer-Peppas model according to the highest k and r values with lowest AIC data (Table 4.25.). These k, r, AIC values for the models are presented in Table 4.25 and various kinetic models are illustrated in Figure 4.29. The first order release model showed that the release of the drug depends upon the concentration of the drug (Neupane *et al.*, 2013, p.1–11). Korsmeyer-Peppas was the best model that the SLNs fit since the release data indicates that the drug release is ruled by both diffusion of the drug and dissolution/erosion of the polymer/lipid matrix (Salih *et al.*, 2013, p.525–535; Arora *et al.*, 2011, p.163–169).

The formulation selected on the basis of the best properties in terms of PS, PDI, ZP and prolonged release profile was F2: it showed also an EE of 80.2±0.06 %, DL of 1.57±0.01 % therefore only F2 formulation was being evaluated in further investigations.

**5.5. CDs Inclusion Complexes**

Nanoparticulate systems have been developed using polymers like alginate, chitosan, gelatin or synthetic polymers such as poly (lactic acid), poly (lactide-co-glycolide) and poly-e-caprolactone. Now, the addition of modified CDs like sulfobutylether-β-CD (SBE-β-CD, Captisol®) and M-β-CD has added an exciting dimension to the nanoparticle approaches (Lakkakula and Macedo, 2014, p.877–894; Freitas *et al.*, 2012, p.1095–1100).

CDs are supramolecular oligosaccharide structures, containing six, seven or eight glucopyranose units (α, β or γ respectively) obtained by the enzymatic degradation of starch (Akbari *et al.*, 2011, p.1–8). CDs have been used for more than 30 years as pharmaceutical excipients (Lakkakula and Macedo, 2014, p.877–94). These are torus shaped molecules with a hydrophilic outer surface and lipophilic central cavity, which can accommodate a variety of lipophilic drugs (Akbari *et al.*, 2011, p.1–8). The nature of the CD (native chemically modified, crystalline or amorphous) may play a role in drug solubilization (Vyas, 2013, p.37–46). Natural CDs have limited water solubility. However, a significant increase in water solubility has been obtained by alkylation of the free hydroxyl groups of the CDs resulting in hydroxyl alkyl, methyl and sulfobutyl derivatives (Akbari *et al.*, 2011, p.1–8). Complexation of pharmaceutical compounds with CDs leads to alteration of physical, chemical and biological properties of guest molecules. The main advantages in the pharmaceutical use of CDs are the increase in solubility, improved stability, bioavailability and even palatability without affecting their intrinsic

lipophilicity or pharmacological properties (Vyas, 2013, p.37–46; Akbari *et al.,* 2011, p.1–8). Hence, chemical modifications often made to enhance and expand the functionalities of CDs. This includes of β-CD derivatives like 2-hydroxypropyl-β-CD (HP-β-CD), M-β-CD, Captisol® and maltosyl-β-CD. The complexation efficiency and solubilizing effect of CDs in an aqueous solution also increase by addition of water soluble polymers (Shiralashetti and Patil, 2014, p.88–96).

Present investigation was undertaken to enhance the solubility, dissolution rate and bioavailability of poorly soluble RCa through formation of an inclusion complex with M-β-CD, Captisol®. Higuchi and Connors have classified complexes based their effect on substrate solubiity as indicated by phase-solubility profiles (Higuchi and Connors, 1965, p.117–210). Phase-solubility analysis of the effect of complexing agents on the compound being solubilized is a traditional approach to determine not only the value of the stability constant but also to give insight into the stoichiometry of the equilibrium (Brewster and Loftsson, 2007, p.645–666). Figure 4.30 and 4.31 shows the phase-solubility diagrams of RCa for the different CDs (M-β-CD and Captisol®) tested. For the both oligosaccharides, the solubility of drug in the aqueous medium increased linearly as a function of CDs concentrations. The plots obtained for M-β-CD and Captisol® were typical of those ascribed to $A_L$ type diagrams (Higuchi and Connors, 1965, p.117–210). In fact, the linear host-guest correlations ($r^2 > 0.99$) suggested the formation of a 1:1 (RCa: CD) complex with respect to CDs concentrations.

The RCa/M-β-CD inclusion complexes were prepared by kneading method using (water: ethanol) (1:1) for formulation F1 and only distilled water used for F2 while the formulation F3 was prepared by the lyophilization method. The RCa/Captisol® formulations F4 and F5 were prepared by kneading method using (water: ethanol) (1:1, v/v) and distilled water, respectively whereas the formulation F6 was prepared by lyophilization method.

The morphological structure of the pure substances, RCa/M-β-CD and RCa/ Captisol® inclusion complexes obtained by SEM shown in Figure 4.32-4.33. The morphological structure of RCa has irregular shaped particles which were regarded as semi-crystals structure, while M-β-CD and Captisol® appears as amorphous particles. The complexes appear as irregular particles, in which the original morphology of all components disappeared and drastic changes in shapes were observed revealing an apparent interaction in the solid-state.

It was observed that all formulations had particle sizes in the range from 192.60±4.78 (PDI=0.364±0.02) to 532.80±15.35 (PDI=0.310±0.03), ZP in the range from -8.33±0.48 to -21.80±0.36 as shown in Table 4.26. These results had represented that all complexes had the desired particle size. For proper release of drug from particles, it is necessary that particles should have a size in a narrow range (Sarfraz *et al.*, 2015, p.1–9). The drug content percentage of different RCa complexes were shown in Table 4.26. The drug content percentage was found to be in the range of 93.50±1.70% to 105.40±0.93% (Table 4.26.). The low standard error values indicated the uniformity of drug content of the prepared complexes.

Figure 4.34. and 4.35. RCa showed a broad endotherm for water loss in temperature range 75-80ºC, followed by multiple glass transition onset in the temperature range of 180-290ºC indicating its semi-crystalline nature. The thermogram of Captisol® showed one endothermic peak is sharp at 259.7ºC indicating the beginning of decomposition events. Also, M-β-CD showed one endothermic peak, approximately at 165ºC related to broad endothermic peak. The glass transition enthalpies which are proportional to the degree of crystallinity of RCa was decreased when complexes were prepared by kneading (F1, F2, F4 and F5). On the other hand, transitions were almost disappeared in freeze dried samples of F3 and F6. Evidence of complexation was seen in the clear decrease of the RCa glass transitions due to its entrapment in the cavities of CDs and the decrease of CDs characteristic peaks in the complexes. There are similar observations in the previously researches (Darwish *et al.*, 2014, p.1756–1768; Pralhad and Rajendrakumar, 2004, p.333–339).

Results of FT-IR study showed characteristic peaks of RCa at 3300, 2915, 1543, 1379, 1151 and 961 $cm^{-1}$ in Figure 4.36. as reported in the literature (Sathali and Nisha, 2013, p.536–548). Spectra of M-β-CD and Captisol® complexes present the prominent peaks at the region of 3404, 1541, 1379, 1153 and 3381, 1544, 1379, 1151 $cm^{-1}$ respectively. RCa was observed at the region 3300 $cm^{-1}$ due to the (-OH stretching), a peak at 2915 $cm^{-1}$ due to the (N-H stretching) and a peak at 1543 $cm^{-1}$ observed due to carbonyl group Figure 4.36. At the lower frequencies 1379 $cm^{-1}$ (C-N stretching), 1151 $cm^{-1}$ (C-O stretching) observed. In case of complexes prepared using M-β-CD, Captisol® show considerable differences such as overlapping of O-H and N-H group peak resulting broadening of the peak was observed. This modification clearly indicates the presence of host-guest interaction suggesting the formation of stable hydrogen bonds between RCa

and CDs. However other peaks corresponding pure drug such as C-N, C-O can be clearly detected at the lower frequencies (Figure 4.36.). This indicates that overall symmetry of the molecule might not be significantly changed. These results were in compliance with the study conducted by Sarfraz *et al.* and Venkatesh *et al*. (Sarfraz *et al.,* 2015, p.1–9; Venkatesh *et al.,* 2014, p.685–690).

The XRD pattern of pure RCa presented two diffraction peaks at 9.39º(2θ), 28.19º(2θ) indicating the semi-crystalline nature of the drug (Figure 4.37.). The M-β-CD and Captisol® are a very amorphous material as there are no any sharp peak present as shown in Figure 4.37. In the XRD patterns of kneaded and lyophilizated samples, one crystalline peak was diminished or disappeared at 9.39º(2θ) while the peak 28.19º(2θ) corresponding to the native RCa crystal was absent (Figure 4.37.). This XRD experiment revealed that significant loss of crystalline RCa occurred from processing for all samples (Akbari *et al.,* 2011, p.1–8; Fukuda *et al.,* 2008, p.188–196). Disappearance or decrease in intensity of the drug peak might be related to possible drug-CD interaction or loss of drug crystallinity. The absence of the characteristic peak of drug is strong evidence of the inclusion of the drug into the CDs cavity in agreements with DSC and FT-IR analyses (Yurtdaş *et al.,* 2011, p.429–435; Demirel *et al.,* 2011, p.437–445).

NMR is the simplest experiment used to fast obtain direct evidence of the inclusion of a guest into the CD cavity by the observation of the difference in the proton ($^{1}$H NMR) or carbon ($^{13}$C NMR) chemical shifts (δ) between the free guest and host species and the presumed complex (Mura, 2014, p.238–250). As a consequence of a guest inclusion into their cavity, the $^{1}$H NMR spectra of CDs exhibit an upfield shift of their H-3 and H-5 protons, directed toward the interior of the cavity, indicative of the complex formation; moreover, the magnitude of the observed shift can be used as a measure of the complex stability (Figure 4.38.). In particular, it has been reported that Δδ H3 > Δδ H5 or Δδ H3 < Δδ H5 are indicative, respectively, of partial or total inclusion of the guest inside the CD cavity (Mura, 2014, p.238–250).

$^{1}$H-NMR spectra of M-β-CD complexes (F1, F2 and F3) exhibited the most significant downfield shift for the inner cavity proton H3 (0.0850, 0.0509 and 0.0527 ppm respectively), while relatively low down/upfield shift were observed for H5 proton (0.0092, 0.0329 and -0.0054 ppm respectively) suggesting that partial inclusion (Figure 4.38.). It is concluded that when Δδ H3 > Δδ H5, here occurs partial inclusion of the guest inside the cavity and when Δδ H3 < Δδ H5, a total inclusion takes place (Mura, 2014,

p.238–250). Therefore, it could say that partial inclusion occurs for F1, F2 and F3. $^{1}$H-NMR spectras of Captisol® complexes (F4, F5 and F6) exhibited the most significant upfield shift for the inner cavity proton H5 (-0.0233, -0.0235 and -0.0196 ppm respectively), while relatively low down/upfield shift were observed for H3' proton (0.0006, -0.0029 and -0.0065 ppm respectively) suggesting that inclusion complex (Figure 4.38.). These results were in compliance with the study prepared by Jain et al. (Jain *et al.*, 2011, p.1163–1175)

Comparing release profiles of complexes (M-β-CD and Captisol®), similar release rates were observed. M-β-CD complexes (F1, F2 and F3) showed drug release of 55.98±32.32%, 57.73±33.33%, 41.91±2.01% at 1 h and 98.71±56.99%, 102.99±59.46%, 92.71±2.44%, respectively at 6 h. In the native RCa, the release was 31.96% within 0.5 h and reached 95.46% by 6 h. Cumulative percent of drug release from Captisol® complexes (F4, F5 and F6) also were not show immediate release. The from F4, F5 and F6 showed drug release of 60.44±34.89%, 62.22±35.92%, 56.36±32.54% at 1 h and 97.67±56.39%, 98.30±56.75%, 93.17±53.79%, at 6 h respectively.

Various methods comparing drug dissolution profiles have been proposed. The one method is model-independent approaches based on a similarity factor. This approach proposed to measure the similarity between drug dissolution profiles of a test and reference formulation. Note that $f_2$=100 when the two dissolution curves are identical. When $f_2 \geq 50$, the two dissolution profiles are deemed to be similar according to the FDA guidance (Leblond *et al.*, 2016, p.14–23; Srinivas *et al.*, 2014, p.06–16). The obtained $f_2$ values for the CDs inclusion complexes (F1, F2, F3, F4, F5 and F6) were (67, 58, 57, 62, 59, and 82), respectively (Table 4.27., Table 4.28., Figure 4.39., Figure 4.40.). These values have indicated the equivalence of dissolution profile for RCa: M-β-CD (1:1 molar ratio) and RCa: Captisol® (1:1 molar ratio) to that of pure RCa. These results do not agreement with the results of solubility studies. From the solubility study of drug as well as CDs complex, it was observed that there had been a significant increase in the solubility of drug in water. However, dissolution profiles did not change. RCa is a weak acid in nature, so it shows ionization in basic medium and is therefore soluble in high pH solutions. The highest solubility was at pH 6.8 when compared with other buffers while the lowest data were at pH 1.2., however, highest solubility was observed in water in the ionic form (Sarfraz *et al.*, 2015, p.1–9). Thought that, since the rapid dissolution in the dialysis bag was seen, the reason of similar dissolution profiles of pure RCa and the

complexes could be related to the delayed transition of dissolved drug from dialysis bag to the dissolution medium which has shaded the rapid dissolution of the complexes.

The molar solubility data of RCa observed in various CD complexes are demonstrated in Table 4.29. Molar solubility of RCa was found to follow the order of F6 > F3 > F2 > F5 > F1 > F4. As highest solubility (62.10 $mM.mL^{-1}$) was observed in F6 which contain lyophilize RCa-Captisol® complex, it was selected as the complex for further CD-PAD formulation development studies.

## 5.6. CDs-PAD NP Formulations

NPs have been proposed as pharmaceutical dosage forms to improve the oral bioavailability of a number of drugs. The encapsulation of lipophilic drugs in polymeric NPs is usually hampered by its low aqueous solubility. One strategy to increase significantly the drug loading is encapsulation of the given drug as a complex with CDs. The incorporation of CDs in PAD (the copolymer of methyl ether and maleic anhydride) NPs permit the modification of the distribution and, to a certain degree, the intensity of the bioadhesive properties of these carriers (Agüeros *et al.*, 2011, p.721–734) In fact, when polyanhydrides hydrolytically degraded, the product of each cleaved anhydride bond contains two carboxylic acid groups. In accordance with the adsorption theory of adhesion, carboxylic groups would enhance the ability of polymers to form hydrogen bonds with components from the mucosa (Campanero *et al.*, 2003, p.19–30). This synthetic copolymer; PAD is widely used for pharmaceutical purposes as a thickening and suspending agent, denture adhesive and adjuvant for transdermal patches (Arbós *et al.*, 2002, p.321–330).

The one of the aim of this study was to combine the inclusion properties of CDs (M-β-CD and Captisol®) with the PAD NPs to modify drug release and to increase the oral bioavailability by enhanced bioadhesion in the GI tract. PAD characterized by its ability to easily get in touch with the molecules containing $–NH_2$ or –OH residues reach in aqueous environments. This fact permits the development of new NPs devices with different physico-chemical or biological properties. The association between CDs and PAD NPs provides a good strategy to both increase the loading capacity of lipophilic drugs by PAD NPs and modulate their release from these pharmaceutical forms (Agüeros *et al.*, 2005, p.495–502).

According to the analysis results, the best selected inclusion complexes of each CDs derivatives (M-β-CD and Captisol®) (F2 and F6) were used to being coated by PAD i.e. formulation of NPs (F1-CD-PAD contains M-β-CD complex and F2-CD-PAD–contains Captisol® complex respectively). The CD-PAD-NPs were prepared by a solvent displacement method and characterized by measuring PS, PDI, ZP, DC%, morphology, DSC, FT-IR, XRD, $^{1}$H-NMR analysis and *in vitro* release study.

The Figure 4.41. shows the morphological analysis by electron microscopy of RCa, PAD, and CD-PAD-NPs. RCa sample by SEM comprised of irregular rod-shaped particle. The irregular and platelet surface NPs were observed. The Table 4.30 summarizes the mean physico-chemical characteristics of the CD-PAD-NPs formulations. The size of PAD-NPs was about 200 nm with a very low PDI (~ 0.2) (Table 4.30.). Similarly, the PAD-NPs formulation displayed negative surface charges. The ZP values were ranged from -36 mV (F1-CD-PAD) to -39 mV (F2-CD-PAD) (Table 4.30.). Finally, the DC% of F1 and F2 were calculated to be 63.37%, 67.92% respectively (Table 4.30.). The encapsulation of RCa was found to be independent on the nature of the oligosaccharide used to form the complex with the drug. In general, the drug that was incorporated in PAD as free form, resulted in NPs of very low drug loading. On the contrary, when drug was incorporated as a complex with CDs, the drug loading increased and the results of study were confirmed with this literature (Agüeros *et al.*, 2010, p.2–8).

Temperature dependent structure and crystallinity changes in RCa and polymer were analyzed using DSC analyses (Başaran *et al.*, 2011, p.714–723).

The DSC thermograms of pure RCa showed glass transition onsets in the ranges of 78-85ºC, 188-19 ºC and 237-252 ºC showing the semi-crystalline structure of the active agent (Figure 4.42). The PAD did not show any thermal behavior. The formulations (F1 and F2) and placebo thermograms were identical with the thermogram of pure polymer. These results suggest that nanoencapsulation process produce a marked decrease in crystallinity of RCa and/or confers to this drug a nearly amorphous state or dilution effect of polymeric lattice leading to disappearance of drug peak (Başaran *et al.*, 2011, p.714–723).

The PAD present characteristic peak (aliphatic peak is shown at 1810 $cm^{-1}$) in the FT-IR spectra (Figure 4.43.). The presence of carboxylic acid groups in the polymer can be determined from the presence of a peak at 1700 $cm^{-1}$ (Domb et al., 1997, p.305)

Besides DSC analyses, amorphous structure of the PAD was also determined using XRD. RCa exhibited a characteristic semi-crystalline XRD pattern at 2θ that support the DSC analyses results (Fig. 4.44.) (Ponnuraj *et al.*, 2015 , p.2217–2231). Similarly no sharp peaks owing to the crystalline structure were recorded also for NPs showing no formation of crystals during the formulation stages (Portero and Remun, 1998, p.75–84).

$^{1}$H-NMR spectra of pure RCa and pure polymers were used as references and according to our analyses results the intensities of the peaks around 3, 5 and 7 ppm ranges were changed upon the entrapment of RCa showing the molecular distribution of RCa in the polymeric matrix compared to pure substances.

The Figure 4.46. shows the release profile of RCa from CD-PAD-NPs. Comparing release profiles of F1-CD-PAD and F2-CD-PAD, different release rates were observed. The F2-CD-PAD displayed a drug release pattern with a burst release within 2 hours followed by relatively prolonged release. It showed drug release of 63.40% at 2 h and 83.77% at 24 h. In the native RCa, the release was 31.96% within 0.5 h and reached 95.46% by 6 h. The F1-CD-PAD to F2-CD-PAD show drug release of 89.92% and 77.31% at 4 h and 96.84%, 83.77% at 24 h respectively. Since the PAD is a biocompatible and degradable material it has been widely applied in the drug controlled release system (Cai *et al.*, 2003, p.203–208). Generally, under acidic conditions no drug release was observed from PAD NPs (Agüeros *et al*., 2009, p.405–413). However, when PAD NPs were dispersed in neutral or basic conditions the release was completed Figure 4.46. This phenomenon has been described for PAD, showing that the release increases with increasing pH value, due to faster hydrolysis and erosion at these pHs (Agüeros *et al.*, 2009, p.405–413).

*In vitro* release profiles of RCa from CDs-PAD NPs in phosphate buffer (pH 6.8) were applied to different kinetic models (zero order kinetics, first order kinetics, Higuchi model, Korsmeyer-Peppas model and Hixson-Crowell model). The release data were investigated by k, $r^2$ and AIC for the selection of best suitable kinetic model. The pure RCa release was fitted to the first order kinetic model, while both of the CDs-PAD NPs (F1 and F2) were fitted to Korsmeyer-Peppas model according to the highest k and $r^2$ values with lowest AIC data. These k, $r^2$, AIC values for the models are presented in Table 4.32 and various kinetic models are illustrated in Figure 4.47. The first order release model showed that release of the drug depends upon the concentration of the drug (Neupane *et al.*, 2013, p.1–11). Korsmeyer-Peppas model was the best model that the

release data of NPs fit which indicates that the drug release is ruled by both diffusion of the drug and dissolution/erosion of the polymer matrix (Salih *et al.,* 2013, p.525–535; Arora *et al.,* 2011, p.163–169). Both of NPs formulations F1-CD-PAD and F2-CD-PAD were used for further investigations.

Therein, the bioadhesive properties of CD-PAD-NPs, and their performance for enhancing the oral bioavailability of lipophilic drugs such as paclitaxel, cyclosporin A and atovaquone were investigated (Agüeros *et al.,* 2011, p.721–734).

**5.7. Cytotoxicity Studies**

With a multitude of opportunities for nanomaterial use in pharmaceutical and medical applications, a thorough understanding of associated systemic toxicity is critical. Characterization of *in vivo* toxicity has been a daunting task as nanomaterials are quite complex and conflicting studies have led to different views of their use and safety. This makes it difficult to evaluate, generalize, and predict important aspects of toxicity (Aillon *et al.,* 2009, p.457–466). *In vitro* cytotoxicity studies of NPs using different cell lines, incubation times, and colorimetric assays are increasingly being published. However, these studies include a wide range of NPs concentrations and exposure times, making it difficult to determine whether the cytotoxicity observed is physiologically relevant (Lewinski *et al.,* 2008, p.26–49).

Consequently, the cytotoxicology of the pure RCa, selected Cs NPs (F4, F6), SLNs (F2, F4), CDs inclusion complexes (F2, F6) and CD-PAD NPs (F1, F2) formulations from preliminary studies and its placebos in the Caco-2 cell line was systematically investigated in the present study. The formulations selected on the basis of the best properties in terms of PS, PDI, ZP, prolonged release profile, EE %, and/or DC %.

The obtained results showed that the $IC_{50}$ values for the F4 (Cs NPs), F4-P (Cs NPs), F6 (Cs NPs), F6-P (Cs NPs) formulations were 36.298, 37.375, 35.241, 38.839 μM respectively after 24 hours of incubation. In accordance with these data, the formulations (F4 (Cs NPs), F4-P (Cs NPs), F6 (Cs NPs), F6-P (Cs NPs)) are within cytotoxic level (Figure 4.48). For this reason, these formulations have not been used in further studies. At the same time, The $IC_{50}$ cytotoxic values as a result of the MTT studies for the other formulations (CDs-F2, CDs-F2-P, CDs-F6, CDs-F6-P, F1 (CDs-PAD), F1-P (CDs-PAD), F2 (CDs-PAD), and F2-P (CDs-PAD), SLNs-F2, SLN F2-P, SLNs-F4, SLNs-F4-P, pure RCa were calculated to be (161.898, 87.563, 117.071, 139.492, 74.803, 94.741, 63.217, 163.354, 87.852, 335.238, 52.137, 52.138 and 149.470) μM, respectively. The percent

cell viability data was plotted versus the molar concentrations of pure RCa and the used formulations as demonstrated in the following Figures 4.49, 4.50., 4.51., and 4.52. These figures depict the percent cell viability data of Caco-2 cells treated with CDs-F2, CDs-F6, F1 (CDs-PAD), F2 (CDs-PAD), SLNs-F2, SLNs-F6 and pure drug. Figure 4.49. shows the cytotoxic effects of the CDs-F2 (M-β-CDs based) against Caco-2 cells in an MTT assay. The result demonstrated that the CDs-F2 had low cytotoxicity, and the all survival rate was approximately 100% when the concentration of the CDs-F2 was 50 μM, which was the concentration used for further permeability experiments. The cytotoxicity studies showed cell viability were ~100%, ~100%, 70%, 65%, 70%, 50% for CDs-F2, CDs-F6, F1 (CDs-PAD), F2 (CDs-PAD), SLNs-F2 and SLNs-F6 respectively for 50 μM concentration. The five formulations (CDs-F2, CDs-F6, F1 (CDs-PAD), F2 (CDs-PAD), SLNs-F2) which have the best cytotoxicity test results were selected for permeability studies.

Captisol® does not show any cytotoxic effects on intestinal epithelial Caco-2 cells, which corresponds to the reference literature (Beig *et al.*, 2015, p.73–78). Therefore Captisol® can be considered to be safe for oral administration. Indeed, seven FDA-approved Captisol®-enabled drug products can be found on the market: Noxafil IV, Kyprolis, Nexterone, Cerenia, VFend, Geodon, and Abilify (Beig *et al.*, 2015, p.73–78). The oral toxicity of PAD is quite low (i.e. $LD_{50}$ in guinea-pigs is ~ 8-9 g/kg *per os*). In addition, the copolymer is considered as GRAS and it can be used for the preparation of non-parenteral medicines licensed in the UK (Agüeros *et al.*, 2011, p.721–734).

### 5.8. Permeation Studies

CaCo-2 cell permeability test was considered as a reliable tool for screening the transport efficiency of new drugs and formulations through artificial biological membranes (Hubatsch *et al.*, 2007, p.2111–2119). To evaluate the effect of formulation on the oral bioavailability of the incorporated RCa, an *ex vivo* studies were performed using a CaCo-2 cell monolayer as intestinal absorption model. The permeation studies carried out on standard RCa and five formulations (CDs-F2, CDs-F6, F1 (CDs-PAD), F2 (CDs-PAD), SLNs-F2) which have the best cytotoxicity test results. Table 4.33 demonstrate the detected level (mean ± SE, μg. $mL^{-1}$) of RCa in the basolateral media of CaCo-2 cell monolayers treated apically with 50 μM RCa as pure RCa and formulations samples. The experiments were repeated four times for each formulation. The $P_{app}$ were calculated. The $P_{app}$ values of pure RCa and its formulations are shown in Table 4.34 and

Figure 4.59. The results of permeation studies after two hours indicate that the permeation of RCa from F1-(CDs-PAD), F2-(CDs-PAD), and SLNs-F2 formulations through tissue membrane better than standard RCa and other formulations.

According to obtained results, $P_{app}$ for pure RCa was found $3.08x10^{-7}$ $cm.sec^{-1}$. However, the permeability values for the CDs-F2 and CDs-F6 were $1.37x10^{-7}$ and $3.01x10^{-7}$ $cm.sec^{-1}$ respectively as much lower than the pure RCa. It can be concluded that RCa-M-β-CD (CDs-F2) and RCa-Captisol® (CDs-F6) did not promote permeability through the CaCo-2 cell monolayer. Conventional penetration enhancers, such as fatty acids and surfactants, enhance drug delivery by decreasing the barrier properties of the lipophilic membrane (i.e. by increasing $P_M$ -permeability coefficient within the membrane). In contrast, hydrophilic CDs, such as Captisol® (SBE-β-CD) increase drug delivery through biological membranes by enhancing drug permeation through the unstirred water layer (UWL) (i.e. by increasing $P_{Aq}$ – permeability coefficient in the aqueous exterior). The aqueous exterior layer consists of a stagnant water layer that is frequently referred to as the UWL. In general, hydrophilic CDs can only enhance drug delivery through biological membranes when $P_{Aq}$ is relatively small compared with $P_M$ (Loftsson and Brewster, 2010, p.1607–1621). Since aqueous solubility of CDs-F2 and CDs-F6 (55.66 and 62.10 mM. $mL^{-1}$ respectively) higher than pure RCa (15.35 $mM.mL^{-1}$) (Table 4.29) $P_{Aq}$ was resulted in relatively higher when compared with $P_M$. Therefore, the reason of low permeability of CDs-F2 and CDs-F6 was related to this phenomenon.

The permeation studies showed that the formulation composed of lipid and surfactant (SLNs-F2) showed better permeation than plain drug. The $P_{app}$ for the transport of plain drug was compared with that for SLNs-F2 in CaCo-2 cells shown in Table 4.34 and Figure 4.59. The $P_{app}$ for SLNs-F2 and plain drug are $5.72x10^{-6}$ and $3.08x10^{-7}$ $cm.sec^{-1}$ respectively. The result indicate that the $P_{app}$ were ordered as, SLN of RCa > plain RCa. Lipid nanoparticles have a major role in the increase of drug transport from intestine because they increase intestinal permeability and the surfactant which are present in the formulation mitigate the intestinal efflux by inhibition of the P-glycoprotein efflux pump which is present in the villus tip of enterocytes in the gastrointestinal tract. Digestive lipids comprised of dietary lipids such as fatty acids, glycosides, phospholipids, cholesterol esters as well as various synthetic derivatives increase in transport of the drug from the intestine (Neupane *et al.*, 2013, p.1–11).

The results showed that the permeability value for the F1 (CDs-PAD) and F2 (CDs-PAD) are $1.36x10^{-5}$ and $1.12x10^{-5}$ cm.sec$^{-1}$ respectively as the highest values in the study. Generally, substances with a $P_{app}$ of less than $1x10^{-6}$ cm.sec$^{-1}$ are classified as low permeability substances. Medium permeability substances have $P_{app}$ values between $1x10^{-6}$ and $1x10^{-5}$ cm.sec$^{-1}$ and high permeability substances exhibit $P_{app}$ of > $1x10^{-5}$ cm.sec$^{-1}$ (Yee, 1997, p.763–766). According to these information, pure RCa, CDs-F2 and CDs-F6 had low permeability data, while SLNs-F2 resulted in medium permeability, F1 (CDs-PAD) and F2 (CDs-PAD) gained high permeability data. These results indicate that the $P_{app}$ were ordered as, F1 (CDs-PAD) > F2 (CDs-PAD) > SLNs-F2 > CDs-F6 > CDs-F2 > pure RCa. In general, hydrophilic CDs do not enhance drug delivery through membranes if the lipophilic membrane barrier is the main permeation barrier (Loftsson and Brewster, 2010, p.1607–1621). In order to solve this problem, very recently, CD-PAD nanoparticles have been proposed. In the last years, these PAD nanoparticles have demonstrated a high ability to develop bioadhesive interactions within the GI tract (Agüeros *et al.*, 2009, p.405–413). In permeability studies, CDs formulations exhibited low permeability, however, when the RCa complexes (CDs-F2 and CDs-F6) were loaded in PAD nanoparticles F1-(CDs-PAD) and F2-(CDs-PAD), the permeability of RCa increased up high permeability. This improvement attributed to possible cytoadhesion to the cell surface of CDs-PAD-NPs (Ojer *et al.*, 2013, p.1891–1903).

### 5.9. Stability Studies

The stability studies were applied on three formulations which had the best permeability test results F1-(CD-PAD) and F2-(CD-PAD), and SLNs-F2. The prepared formulations were stored at temperature conditions of 4±1 °C, 25±1 °C, and 40±1 °C for stability studies at certain periods (first day, 30$^{th}$ day, 60$^{th}$, and 90$^{th}$ day). The stability studies for DC, PS, PDI, ZP were repeated in triplicate at every analyses term for every condition. All data are presented as a mean value with its standard error indicated (mean ±SE), *p*-values less than 0.05 were considered to be statistically significant.

PS of the formulations was determined and these results were evaluated together with PDI data, for the better characterization. Freshly prepared SLNs-F2 formulation had 61.18±0.51 nm mean PS (PDI=0.13±0.01) and at the end of 3 months mean PS of SLNs-F2 showed significant differences and the detected PS were 286.3±5.55 nm ($p \leq 0.0001$); (PDI=0.43±0.01; $p \leq 0.0001$), 348.0±6.35 nm ($p \leq 0.0001$); (PDI=0.46±0.01; $p \leq 0.0001$), 621.0±16.6 nm ($p \leq 0.0001$); (PDI=0.77±0.02; $p \leq 0.0001$) for the formulation kept at

4±1 °C, 25±1 °C, and 40±1 °C respectively. When F1-(CD-PAD) formulation had 215.2±1.25 nm mean PS (PDI= 0.2±0.01) at 1st day, mean PS were 240.6±3.36 nm ($p > 0.05$); (PDI=0.34±0.02; $p \leq 0.0001$), 350.2±9.59 nm ($p \leq 0.0001$); (PDI=0.37±0.01; $p \leq 0.0001$), 423.9±7.88 nm ($p \leq 0.0001$); (PDI=0.43±0.01; $p \leq 0.0001$) for the formulation kept at 4±1 °C, 25±1 °C, and 40±1 °C respectively after the 3 months storage period (Table 4.36. and Figure 4.61.-4.68). Despite of the variations in PS, particles remained in nanometer range (Başaran *et al.*, 2011, p.714–723). When F2-(CD-PAD) formulation had 189.1±1.03 nm mean PS (PDI= 0.18±0.01) at 1st day, mean PS were 336.3±8.94 nm ($p \leq 0.0001$); (PDI=0.36±0.01; $p \leq 0.0001$), 354.2±4.93 nm ($p \leq 0.0001$); (PDI=0.37±0.01; $p \leq 0.0001$), 444.2±11.8 nm ($p \leq 0.0001$); (PDI=0.38±0.01; $p \leq 0.0001$) for the formulation kept at 4±1 °C, 25±1 °C, and 40±1 °C respectively after the 3 months storage. These increases probably because of particle aggregation. This type of phenomenon has been reported earlier (Genç and Demirel, 2013, p.701–709). However, these batches showed mean sizes below 621 nm which is regarded as appropriate for oral application.

Surface charge of NPs determines the performance of the NP system in the body, e.g. electrostatic interaction with cell membranes and ZP measurements provide information about the particle surface charges. NPs dispersed in aqueous solutions can be stabilized either by electrostatic stabilization or by steric stabilization or by combination of both (Overbeek, 1977, p.408–422). ZP measurement is an adequate method in order to evaluate NPs surface properties and to detect any changes after the 3 months of storage.

Freshly prepared SLN-F2 formulation had -18.77±0.20 mV ZP value (Table 4.37.), while ZPs were -36.43±0.69 mV ($0.01 > p > 0.0001$), -36.10±0.98 mV ($0.01 > p > 0.0001$), -35.77±0.78 mV ($0.001 > p > 0.0001$) for formulation kept at 4±1°C, 25±1 °C, and 40±1°C respectively, at the end of 3 months (Table 4.37.). F1-(CD-PAD) formulation had -36.20±0.06 mV ZP value on the day of preparation and at the end of 3 months ZPs were -31.20±1.21 mV ($0.01 > p > 0.0001$), -32.20±0.64 mV ($0.01 > p > 0.0001$), -32.53±1.22 mV ($0.01 > p > 0.0001$) for formulation kept at 4±1 °C, 25±1°C, and 40±1°C respectively (Table 4.37.) and (Figure 4.69.-4.72.). F2-(CD-PAD) formulation had -39.20±0.23 mV ZP value at 1st day, while ZPs were -37.53±1.24 mV ($p \leq 0.05$), -36.35±0.55 mV ($p \leq 0.05$), -37.20±1.16 mV ($p \leq 0.05$) for formulation kept at 4±1 °C, 25±1 °C, and 40±1 °C respectively at the end of 3 months (Table 4.37. and Figure 4.69.-4.72.). There are big differences in ZP values between freshly- prepared formulations and 3 months of storage formulations SLN-F2 and F1-(CD-PAD) in different conditions.

However, ZP value of 3 months of storage F2-(CD-PAD) formulation is similar to ZP value of its 1st day. The ZP ought to be as a rule, stay higher than -60 mV for remaining physically stable (Lingayat *et al.*, 2012, p.80–102).

The DC% analysis results of the fresh formulations (SLNs-F2, F1-(CD-PAD) and F2-(CD-PAD) were 61.18±0.51, 76.11±0.43 and 66.18±0.58 respectively (Section 4.9.1.). The DC% values of SLNs-F2 were 60.02±0.54, 58.24±1.57 and 39.98±10.62% for the formulations kept at 4±1 °C, 25±1°C, and 40±1°C respectively after 3 months (Table 4.35.). The DC% values of F1-(CD-PAD) formulation were 75.96±0.40, 75.78±0.50 and 63.40±6.73; and of F2-(CD-PAD) formulation the results were 65.68±0.69, 65.29±0.55 and 56.92±4.64%, when the formulations kept at 4±1°C, 25±1°C, and 40±1°C respectively after 3 months of storage period (Table 4.35.).

There are significant differences in the DC% values between freshly-prepared formulations and 3 months of storage formulations at 40±1°C. The DC% of all formulations are not remained constant in this storage condition, indicating that possible chemical degradation. The DC% values are not extensively changed for other temperatures (4±1°C and 25±1°C). For example, SLN-F2 at 1st day had 61.18±0.51 DC%, while DC% were 60.02±0.54 and 58.24±1.57 for formulation kept at 4±1°C and 25±1°C respectively at the end of 3 months. These changes in the values is not exceed limit of ±10%. The similar results obtained with F1-(CD-PAD) and F2-(CD-PAD) for 4±1°C and 25±1°C (Table 4.35.).

When considering the physical and chemical changes, in a short term (3 months) stability studies, it can be concluded that the 4±1°C and 25±1°C seems to be better storage temperature for the all formulations (Section 4.9.). Also, the literature afformed these findings (Başaran *et al.*, 2013, p.1–9). Outer parameters, for example, temperature and light give off an impression of being of essential significance for long-term steadiness. The 4°C is the most positive stockpiling temperature. At 20°C, long term storage did not bring about medication stacked SLNs total or loss of medication. At 50°C, a fast development of particle size was watched (Lingayat *et al.*, 2012, p.80–102).

### 5.10. Pharmacokinetic Studies

Oral administration is the most preferred route for drug delivery because of its simplicity, convenience, and patient compliance, especially in the case of repeated dosing for chronic therapies (Xu *et al.*, 2013, p.1–15). However, many of the drugs remained poorly absorbed when administered by this route, owing to the physicochemical

properties of the drug (e.g., pKa, solubility, stability, lipophilicity, polar-nonpolar surface area, presence of hydrogen bonding functionalities and crystal form) and factors related to the dosage form (Agüeros *et al.*, 2011, p.721–734). The bioavailability of oral drugs is strongly influenced by two important parameters, solubility and permeability rates of the APIs (Xu *et al.*, 2013, p.1–15).

Frequent approaches to enhance oral bioavailability are the use of cyclodextrins, formulating oral microemulsions and formation of drug nanocrystals, (Müller *et al.*, 2006, p.82–89). In the past several years, SLNs have been extensively investigated and developed as a potential nanocarrier for oral drug delivery. Similar to liposomes, lipid nanoemulsions, and micelles, SLNs could improve oral absorption of many drugs because of their higher encapsulation efficiency (Chai *et al.*, 2016, p.5929–5940). Another alternative method to improve the oral bioavailability of drugs is the use of bioadhesive NPs, such as PAD NPs (Arbós *et al.*, 2002, p.321–330). The development of adhesive interactions between the drug and the absorption site can be of interest to increase the residence time of the drug delivery system in close contact with the absorptive membrane. This fact would facilitate the establishment of a concentration gradient between the pharmaceutical dosage form and the absorptive membrane increasing the possibilities for drug absorption. However, the capability of PAD NPs to load lipophilic drugs is limited. In order to minimize this drawback, one possible solution may be the incorporation of CDs as promoters of drug loading for the preparation of NPs. The resulting CDs-PAD-NPs have been proven effective to both develop intense bioadhesive interactions with the intestinal wall and to increase the drug loading of lipophilic drugs (Agüeros *et al.*, 2009, p.405–413; Agüeros *et al.*, 2009, p.231–240).

RCa is crystalline in nature so it reduces its aqueous solubility. RCa is ‘superstatin’ belonging to BCS class II having low bioavailability (20%) due to first-pass effect (Suares and Parbhakar, 2016, p.4856–4864). However, it has a partition coefficient (octanol/water) of 0.13 at pH of 7.0. Therefore, it is very important to introduce effective methods, to enhance the solubility and dissolution rate of drug, substantially leading to improve its bioavailability (Vyas, 2013, p.37–46). Some pharmaceutical technologies such as solid dispersions, inclusion complexes, nanocrystal technology, liquisolid technology, microemulsion technology, liquid self-nanoemulsifying drug delivery system (SNEDDS) and solid SNEDDS have been investigated in order to enhance solubility, dissolution rate and bioavailability of RCa (Alshora *et al.*, 2016, p.230–233; Beg *et al.*,

2017, p.333–356). Another possibility to overcome the problems and enhance the oral bioavailability of RCa prepared SLN and CD-PAD NP in this study.

Pharmacokinetic studies were performed on male (Spraque Dawley) rats to evaluate the efficiency of the selected SLN-F2 and F2 (CD-PAD) nanoparticle formulations in ameliorating oral bioavailability of RCa (Section 4.10.). The aqueous suspensions of pure drug and formulations were given orally to animals with gavage (2.2 $mg.kg^{-1}$) (n=5). The blood samples (0.5 mL) were withdrawn from the rat's tail at 0.5, 1, 2, 4, 6, 9, 24, 48, and 72 hours. The plasma concentration profiles of pure RCa and NPs after a single oral administration dose (2.2 $mg.kg^{-1}$) are shown in Figure 4.73. The peak plasma concentration ($C_{max}$) of pure RCa was 2.03±1.17 $\mu g.\ mL^{-1}$ (mean ± SD). The mean values obtained for $AUC_{total}$, half-life ($t_{1/2}$) and mean residence time (MRT) were 12.00±5.55 $\mu g.h.\ mL^{-1}$, 25.58±13.11 h and 27.17±14.74 h respectively. These pharmacokinetic parameters showed a slow removal of the RCa. Table 4.42. summarizes the main pharmacokinetic parameters derived from plasma concentrations curves.

SLN-F2 was developed using stearic acid as lipid carrier and T80 as surfactant, employing high-shear hot homogenization and ultrasonication combined method. The result of pharmacokinetic studies indicated remarkably superior drug absorption potential from SLN-F2 formulation over the pure RCa. SLN-F2 showed significant improvement ($p \leq 0.0001$) in the extent of drug absorption ($AUC_{last}$ and $AUC_{total}$) over the pure RCa. This might be due to lymphatic transport of drug from SLN-F2 formulation. Therefore, these systems enhance the lymphatic transport of the lipophilic drugs (Suresh *et al.*, 2007, p.2779–2785). The average $AUC_{last}$ and $AUC_{total}$ of pure RCa were 10.62±2.12 and 12.00±2.48 $\mu g.h.\ mL^{-1}$ respectively, whereas in the case of SLN-F2, $AUC_{last}$ and $AUC_{total}$ were 90.64±5.74 and 98.87±5.68 $\mu g.h.\ mL^{-1}$ respectively (Table 4.42.). Nearly, 1.41 and 1.11-fold improvement in $C_{max}$ and MRT were observed for the SLN-F2 over the pure RCa, while the value of $t_{1/2}$ was observed 1.30-fold reduction compared to the pure drug suspension and the $t_{max}$ value remained unchanged (Table 4.42.). It has been widely reported that drugs incorporated into lipid and stabilized by the use of various surfactants show high permeability of the intestine because lipids and these surfactants act as a good permeation enhancer of drugs from the gastrointestinal tract by solubilization of the drug in the intestinal milieu and reduce the first-pass metabolism of the drug by transport of the drug through a lymphatic route to the systemic circulation (Neupane *et al.*, 2013, p.1–11; Sznitowska *et al.*, 2017, p.24–30).

F2 (CD-PAD) were developed using Captisol® as CD and PAD as bioadhesive polymer. Evaluation of the pharmacokinetic parameters like $AUC_{last}$ and $AUC_{total}$ revealed significant improvement ($p \leq 0.0001$) corresponding to F2 CD-PAD over the pure drug suspension Figure (4.76.). The $AUC_{last}$ and $AUC_{total}$ average of the pure RCa, were 10.62±2.12 and 12.00±2.48 μg.h. $mL^{-1}$ respectively, whereas in the case of F2 (CD-PAD), $AUC_{last}$ and $AUC_{total}$ were 85.60±5.24 and 96.71±7.87 μg.h. $mL^{-1}$ respectively (Table 4.42.). These facts would be directly related with a synergistic effect obtained by the combination of the bioadhesive properties of PAD NPs and the inhibitory effect of CDs on the activity of P-glycoprotein and cytochrome P450 (Agüeros *et al.*, 2010, p.2–8). Nearly, 1.27 and 1.25-fold improvement in $C_{max}$ and MRT were observed for the F2 (CD-PAD) compared to the pure drug, while the value of $t_{1/2}$ was observed 1.19-fold reduction compared to the pure drug suspension and the $t_{max}$ value remained unchanged (Table 4.42.). From these findings, it may be hypothesized that the nanoparticles would transport the drug complexes to the surface of the mucosa where these carriers would remain immobilized witn intimate contact with the absorptive membrane. Then, nanoparticles would progressively release their contents, yielding, after dissociation, the free drug and the oligosaccharide molecules. The RCa would be rapidly absorbed, whereas the CDs would interact with lipophilic components of the membrane, disturbing the activity of the efflux pump and cytochrome P450 (Agüeros *et al.*, 2011, p.721–734). Captisol® inclusion complexes of some lipophilic drugs like BCS Class II (e.g. RCa) and Class IV API's have been investigated, and these inclusion complexes have been shown to increase total bioavailability of therapeutic efficacy of the drugs (Rajendrakumar *et al.*, 2005, p.39–46; Jain *et al.*, 2011, p.1163–1175; Kawabata *et al.*, 2011, p.1–10).

Enhanced bioavailability will also be achieved by PAD NPs which will improve the permeability through the intestinal mucosa and as a consequence, the oral bioavailability of the problematic drugs will be increased. Moreover, these NPs offer sustained RCa plasma levels for 72h. Interestingly, this sustained profile was found in parallel with high bioavailability values (Table 4.41., Figure 4.73.).

In addition to these, anionic NPs (SLN-F2 and F2 (CD-PAD) were -18.77±0.20 and -39.27±0.30 mV ZP respectively) encounter electrostatic repulsive forces from negatively charged matrix leading to faster lymphatic drainage and produce longer retention period of anionic particles in lymph nodes. This comportment will have an impact on sustained release of the drug from lipid nanocarriers (Suares and Parbhakar, 2016, p.4856–4864).

To sum up the study, both colloidal drug delivery systems (SLN-F2 and F2 (CD-PAD) showed approximately 8-9-fold relative oral bioavailability enhancements in term of rate ($AUC_{last}$ and $AUC_{total}$) compared to the pure active agent (Table 4.40.). No significant differences were found in $AUC_{last}$, $AUC_{total}$, as well as $C_{max}$ and $t_{max}$ between the two colloidal delivery systems (Table 4.42.).

In conclusion, these formulations may be a suitable delivery system to improve the bioavailability of RCa which has low water solubility. RCa SLNs and CD-PAD nanocarriers could be advantageous in reducing dose, by effectively providing sustained release, which will ultimately help in minimizing dose-dependent adverse effects.

## 6. CONCLUSION

RCa-loaded NPs could be prepared by Cs salts (acetate, lactate, aspartate and glutamate using spray drying method. The types of Cs salts play roles in the physicochemical properties of RCa-loaded NPs. CA and CL salts provided enhanced drug release while CAs and CG salts showed slower drug releases with respect to the pure drug in phosphate buffer (pH 6.8) medium. Therefore, the low aqueous solubility and bioavailability of RCa can be treated by using acetate and lactate salts of Cs as RCa delivery systems for oral route. The cytotoxicity test results of Cs RCa-loaded NPs were not satisfied so that, Cs NPs were not used in further studied (permeability, pharmacokinetic and stability studies).

In our study, RCa-loaded SLNs delivery system were successfully formulated by high shear homogenization followed by ultra-sonication technique. The studies of physicochemical properties of the RCa-Loaded SLNs showed that the SLNs have nano PS with narrow range, Furthermore, the RCa release from SLNs was sustained release profile with 98.34 % release up to 48 hours. The SA SLNs exhibited less cytotoxicity effect than TP SLNs, so that it was used in *Ex vivo* test and pharmacokinetic studies. The SA SLNs were able to enhance the RCa bioavailability compared with pure RCa and able to provide sustained release profile up to 72 hours. The SA formulation was found to be stable with no meaningful changes in drug content, PS, PDI and ZP at 4 ℃ over $90^{th}$ days.

The RCa-CD inclusion complexes were successfully prepared by kneading and lyophilization technique according to the determined phase solubility diagram. The physicochemical characterization test showed that the prepared inclusion complexes have nano size with a narrow range. *In vitro* release study carried out by using the dialysis bag in phosphate buffer medium at 6.8 pH. which was achieved within six hours. The RCa/CDs inclusion complexes showed low cytotoxicity effect on Caco-2 cell line which nominated them for *Ex vivo* test. The permeability studies demonstrated that the RCa/ M-β-CDs and RCa/ Captisol® inclusion complexes have very low permeation property due to their hydrophilicity properties and consequently, the pharmacokinetic studies were not carried out on RCa/CDs inclusion complexes.

The RCa/ CDs inclusion complexes were successfully coated with PAD by a solvent displacement method to form RCa /CD-PAD NPs. The physicochemical properties studies showed that the prepared RCa /CDs inclusion complexes were well incorporated into PAD NPs and resulted in NPs with nano size and typical PDI. The *In*

*vitro* studied of the RCa /CD-PAD NPs demonstrated the sustained release of RCa from CD-PAD NPs. The MTT test results exhibited that the RCa /CD-PAD NPs have very low cytotoxicity effect and so that, they were used in further studies. *Ex vivo* test of RCa /CD-PAD NPs demonstrated the highest permeation of RCa from CD-PAD NPs in comparison with pure RCa and other formulations. In our study, the synergistic effect gained from the combination of bioadhesive property of PAD NPs and CDs inclusion complexes in F2 (CD-PAD) enhanced the oral bioavailability of RCa. The F2 (CD-PAD) formulation was found to be stable with no significant changes in drug content, PS, PDI and ZP at 4 ℃ and 25 ℃ over $90^{th}$ days.

## REFERENCES


Agarwal, R., Malthar, H.P. and Chaitanya, B. (2015). Development and pharmacodynamic evaluation of rosuvastatin-loaded nanostructured lipid carriers, *J. Pharm. Pharm. Sci.,* 4 (7), 699–716.

Ageitos, J.M., Chuah, J.-A. and Numata, K. (2016). Design considerations for properties of nanocarriers on disposition and efficiency of drug and gene delivery, *Nanomedicines Des. Deliv. Detect.,* 1 (51), 1–22.

Agüeros, M., Areses, P., Campanero, M.A., Salman, H., Quincoces, G., Peñuelas, I. and Irache, J.M. (2009). Bioadhesive properties and biodistribution of cyclodextrin-poly(anhydride) nanoparticles, *Eur. J. Pharm. Sci.,* 37 (3–4), 231–240.

Agüeros, M., Ruiz-Gatón, L., Vauthier, C., Bouchemal, K., Espuelas, S., Ponchel, G. and Irache, J.M. (2009). Combined hydroxypropyl-β-cyclodextrin and poly(anhydride) nanoparticles improve the oral permeability of paclitaxel, *Eur. J. Pharm. Sci.,* 38 (4), 405–413.

Agüeros, M., Campanero, M.A. and Irache, J.M. (2005). Simultaneous quantification of different cyclodextrins and Gantrez by HPLC with evaporative light scattering detection, *J. Pharm. Biomed. Anal.,* 39 (3–4), 495–502.

Agüeros, M., Espuelas, S., Esparza, I., Calleja, P., Peñuelas, I., Ponchel, G. and Irache, J. (2011). Cyclodextrin-poly(anhydride) nanoparticles as new vehicles for oral drug delivery, *Expert Opin. Drug Deliv.,* 8 (6), 721–734.

Agüeros, M., Zabaleta, V., Espuelas, S., Campanero, M.A. and Irache, J.M. (2010). Increased oral bioavailability of paclitaxel by its encapsulation through complex formation with cyclodextrins in poly(anhydride) nanoparticles, *J. Control. Release*. 145 (1), 2–8.

Ai, F., Ma, Y., Wang, J. and Li, Y. (2014). Preparation, physicochemical characterization and In-vitro dissolution studies of diosmin-cyclodextrin inclusion complexes, *Iran J. Pharm. Res.*, 13 (4), 1115–1123.

Aillon, K.L., Xie, Y., El-Gendy, N., Berkland, C.J. and Forrest, M.L. (2009). Effects of nanomaterial physicochemical properties on in vivo toxicity, *Adv. Drug Deliv. Rev,* 61 (6), 457–466.

Ahmed, S. and Ikram, S. (2016). Chitosan based scaffolds and their applications in wound healing, *Achiev. Life Sci*., 10 (1), 27–37.

Akbari, B. V., Valaki, B.P., Maradiya, V.H., Akbari, A.K. and Vidyasagar, G. (2011). Effect of types of cyclodextrin on rosuvastatin calcium inclusion complex, *Indian J. Pharm.,* 2 (1), 1–8.

Alhalaweh, A., Andersson, S., & Velaga, S.P. (2009). Preparation of zolmitriptan-chitosan microparticles by spray drying for nasal delivery, *Eur. J. Pharm. Sci.,* 38 (3), 206–214.

Alshora, D.H., Haq, N., Alanazi, F.K., Ibrahim, M.A. and Shakeel, F. (2016). Solubility of rosuvastatin calcium in different neat solvents at different temperatures, *J. Chem. Thermodyn,* 94, 230–233.

Alves-Prado, H.F., Carneiro, A.A.J., Pavezzi, F.C., Gomes, E., Boscolo, M., Franco, C.M.L. and Da Silva, R. (2008). Production of cyclodextrins by CGTase from Bacillus clausii using different starches as substrates, *Appl. Biochem. Biotechnol,* 146 (1–3), 3–13.

Antonopoulos, A.S., Margaritis, M., Lee, R., Channon, K. and Antoniades, C. (2012). Statins as anti-inflammatory agents in atherogenesis, molecular mechanisms and lessons from the recent clinical trials, *Curr. Pharm. Des.,* 18, 1519–1530.

Arbós, P., Wirth, M., Arangoa, M.A., Gabor, F. and Irache, J.M. (2002). Gantrez® AN as a new polymer for the preparation of ligand-nanoparticle conjugates, *J. Control. Release,* 83 (3), 321–330.

Arora, G., Malik, K., Singh, I. and Arora, S. (2011). Formulation and evaluation of controlled release matrix mucoadhesive tablets of domperidone using Salvia plebeian gum, *J. Adv. Pharm. Tech. Res.,* 2 (3), 163–169.

Badimon, L., Padró, T. and Vilahur, G. (2012). Atherosclerosis, platelets and thrombosis in acute ischaemic heart disease, *Eur. Hear. Journal. Acute Cardiovasc. Care,* 1 (1), 60–74.

Badr-Eldin, S.M., Ahmed, T.A. and Ismail, H.R. (2013). Aripiprazole-cyclodextrin binary systems for dissolution enhancement, Effect of preparation technique, cyclodextrin type and molar ratio, *Iran J. Basic Med. Sci.,* 16 (12), 1223–1231.

Ballantyne, C.M. (2000). Primary prevention of coronary heart disease, *J. Clin. Endocrinol. Metab.,* 85 (6), 2089–2092.

Bansal, V., Sharma, P.K., Sharma, N., Pal, O.P. and Malviya, R. (2011). Applications of chitosan and chitosan derivatives in drug delivery, *Adv. Biol. Res. (Rennes),* 5 (1), 28–37.

Barrios, J.G. and Miranda, R.U. (2010). Biotechnological production and applications of statins, *Appl. Microbiol. Biotechnol.,* 85 (4), 869–883.

Başaran, E., Yenilmez, E., Berkman, M.S., Büyükköroğlu, G. and Yazan, Y. (2014). Chitosan nanoparticles for ocular delivery of cyclosporine A, *J. Microencapsul.,* 2048 (31), 49–57.

Başaran, E., Yenilmez, E., Berkman, M.S., Büyükköroğlu, G. and Yazan, Y. (2013). Chitosan nanoparticles for ocular delivery of cyclosporine A., *J. Microencapsul*., 2048, 1–9.

Başaran, E., Şenel, B.., Kırımlıoğlu, G.Y.., Güven, U.M. and Yazan, Y.. (2015). Ornidazole incorporated chitosan nanoparticles for ocular application, *Lat. Am. J. Pharm.,* 34 (6), 1180–1188.

Başaran, E., Demirel, M., Sirmagül, B. and Yazan, Y. (2011). Polymeric cyclosporine-A nanoparticles for ocular application, *J. Biomed. Nanotechnol.,* 7(5),714–723.

Basu, B., Garala, K., Bhalodia, R., Joshi, B. and Mehta, K. (2010). Solid lipid nanoparticles , A promising tool for drug delivery system, *J. Pharm. Res*., 3 (1), 84–92.

Bathool, A., Vishakante, G.D., Khan, M.S. and Shivakumar, H.G. (2012). Development and characterization of atorvastatin calcium loaded chitosan nanoparticles for sustain drug delivery, *Adv. Mater. Lett.,* 3 (6), 466–470.

Beg, S., Jain, S., Kushwah, V., Bhatti, G.K., Sandhu, P.S., Katare, O. and Singh, B. (2017). Novel surface-engineered solid lipid nanoparticles of rosuvastatin calcium for low-density lipoprotein-receptor targeting, a quality by design-driven perspective, *Nanomedicine,* 12 (4), 333–356.

Beg, S., Raza, K., Kumar, R., Chadha, R., Katare, O.P. and Singh, B. (2016). Improved intestinal lymphatic drug targeting via phospholipid complex-loaded nanolipospheres of rosuvastatin calcium, *RSC Adv. Royal Society of Chemistry,* 6 (10), 8173–8187.

Beig, A., Agbaria, R. and Dahan, A. (2015). The use of captisol (SBE7-ß-CD) in oral solubility-enabling formulations, Comparison to HP-ß-CD and the solubility-permeability interplay, *Eur. J. Pharm. Sci.*, (77), 73–78.

Bellosta, S., Paoletti, R. and Corsini, A. (2004). Safety of statins, focus on clinical pharmacokinetics and drug interactions, *Circulation,* 109 (23 Suppl 1), III-50-III-57.

Bhattarai, N., Ramay, H.R., Chou, S.H. and Zhang, M. (2006). Chitosan and lactic acid-grafted chitosan nanoparticles as carriers for prolonged drug delivery, *Int. J. Nanomedicine,* 1 (2), 181–187.

Blaser, D.W. (2007). Determination of drug absorption parameters in Caco-2 cell monolayers with a mathematical model encompassing passive diffusion , *J. Int. Adsorpt. Soc.,* 25–34.

Bonifácio, B.V., da Silva, P.B., Aparecido dos Santos Ramos, M., Maria Silveira Negri, K., Maria Bauab, T. and Chorilli, M. (2013). Nanotechnology-based drug delivery systems and herbal medicines, A review, *Int. J. Nanomedicine,* 9 (1), 1–15.

Brewster, M.E. and Loftsson, T. (2007). Cyclodextrins as pharmaceutical solubilizers, *Adv. Drug Deliv. Rev.,* 59 (7), 645–666.

Bunjes, H. and Unruh, T. (2007). Characterization of lipid nanoparticles by differential scanning calorimetry, X-ray and neutron scattering, *Adv. Drug Deliv. Rev*., 59 (6), 379–402.

Buschmann, M.D., Merzouki, A., Lavertu, M., Thibault, M., Jean, M. and Darras, V. (2013). Chitosans for delivery of nucleic acids, *Adv. Drug Deliv. Rev.*, 65 (9) ,1234–1270.

Cai, Q.X., Zhu, K.J., Chen, D. and Gao, L.P. (2003). Synthesis, characterization and in vitro release of 5-aminosalicylic acid and 5-acetyl aminosalicylic acid of polyanhydride - P(CBFAS), *Eur. J. Pharm. Biopharm.,* 55 (2), 203–208.

Campanero, M. a, Arangoa, M. a, Renedo, M.J. and Irache, J.M. (2003). I nfluence of the surface characteristics of PVM / MA nanoparticles on their bioadhesive properties, *J. Control. Release,* 89, 19–30.

Cerchiara, T., Luppi, B., Bigucci, F. and Zecchi, V. (2003). Chitosan salts as nasal sustained delivery systems for peptidic drugs, *J. Pharm. Pharmacol.,* 55, 1623–1627.

Cervera, M.F., Heinämäki, J., de la Paz, N., López, O., Maunu, S.L., Virtanen, T., Hatanpää, T., Antikainen, O., Nogueira, A., Fundora, J. and Yliruusi, J. (2011). Effects of spray drying on physicochemical properties of chitosan acid salts, *AAPS PharmSciTech*., 12 (2), 637–649.

Chai, G.-H., Xu, Y., Chen, S.-Q., Cheng, B., Hu, F.-Q., You, J., Du, Y.-Z., and Yuan, H. (2016). Transport mechanisms of solid lipid nanoparticles across Caco-2 cell monolayers and their related cytotoxicology, *ACS Appl. Mater. Interfaces*, 8 (9), 5929–5940.

Challa, R., Ahuja, A., Ali, J. and Khar, R.K. (2005). Cyclodextrins in drug delivery, an updated review, *AAPS PharmSciTech*., 6 (2), E329–E357.

Charcosset, C., El-Harati, A. and Fessi, H. (2005). Preparation of solid lipid nanoparticles using a membrane contactor, *J. Control. Release,* 108 (1), 112–120.

Chaudhary, V.B. and Patel, J.K. (2013). Cyclodextrin inclusion complex to enhance solubility of poorly water soluble drugs, a review, *Int J Pharm Sci Res*., 4 (1), 68–76.

Crouse III, J.R. (2008). An evaluation of rosuvastatin, pharmacokinetics, clinical efficacy and tolerability, *Expert Opin. Drug Metab. Toxicol*., 4 (3), 287–304.

Cui, B., Feng, L., Pan, Z., Yu, M., Zeng, Z., Sun, C., Zhao, X., Wang, Y. and Cui, H. (2015). Evaluation of stability and biological activity of solid nanodispersion of lambda-cyhalothrin, *PLoS One.,* 10 (8), 1–15.

Dahan, A., Miller, J.M. and Amidon, G.L. (2009). Prediction of solubility and permeability class membership, provisional BCS classification of the world's top oral drugs, *AAPS J.,* 11 (4), 740–746.

Darwish, M.K., Fouad, M.M., Zaazaa, H.E., Abdel-razeq, S.A. and Nasr, Z.A. (2014). Formulation , optimization and simultaneous determination of atorvastatin calcium and losartan potassium in pure and bilayer tablets, *J. Glob. Trends Pharm. Sci.,* 5 (3), 1756–1768.

Das, S.K., Rajabalaya, R., David, S., Gani, N., Khanam, J. and Nanda, A. (2013). Cyclodextrins-the molecular container, *Res. J. Pharm. Biol. Chem. Sci*., 4 (2), 1694–1720.

DeGorter, M.K., Urquhart, B.L., Gradhand, U., Tirona, R.G., and Kim, R.B. (2012). Disposition of atorvastatin, rosuvastatin, and simvastatin in oatp1b2-/- mice and intraindividual variability in human subjects, *J. Clin. Pharmacol.,* 52 (11), 1689–1697.

Del Valle, E.M.M. (2004). Cyclodextrins and their uses, A review, *Process Biochem*., 39 (9), 1033–1046.

Delair, T. (2011). Colloidal polyelectrolyte complexes of chitosan and dextran sulfate towards versatile nanocarriers of bioactive molecules, *Eur. J. Pharm. Biopharm.*, 78 (1), 10–18.

Demirel, M., Büyükköroğlu, G., Sırmagül, B., Kalava, B., Öztürk, N. and Yazan, Y. (2014). Enhanced bioavailability of cinnarizine using solid dispersion, in vitro and in vivo evaluation, *Curr. Drug ther.*, 9 (4), 294–301.

Demirel, M., Yurtdaş, G. and Genç, L. (2011). Inclusion complexes of ketoconazole with beta-cyclodextrin, physicochemical characterization and in vitro dissolution behaviour of its vaginal suppositories, *J. Incl. Phenom. Macrocycl. Chem.*, 70 (3–4), 437–445.

Dhiman, R., Kumar, D., Kumar, B. and Pandey, B.L. (2016). Quantitative determination of atorvastatin , atorvastatin in human plasma using rosuvastatin as internal standard by LC-MS / MS., *Int. J. Pharm. Chem. Sci.*, 4 (7), 487–500.

Divya, V.C. and Sathasivasubramanian, S. (2013). Submandibular sialolithiasis - A report of two cases, *Biomed.*, 33 (2), 279–283.

Domb, A.J., Kost, J., Sheva, B. and Wiseman, D.M. (1997). Edited by. *CRC Press Taylor and Francis Group*, Amsterdam.

Duchene, D. and Bochot, A. (2016). Thirty years with cyclodextrins, *Int. J. Pharm.*, 514 (1), 58–72.

Dudhipala, N. and Veerabrahma, K. (2017). Improved anti-hyperlipidemic activity of Rosuvastatin Calcium via lipid nanoparticles, pharmacokinetic and pharmacodynamic evaluation, *Eur. J. Pharm. Biopharm.*, 110, 47–57.

Eijsink, V., Hoell, I. and Vaaje-Kolstada, G. (2010). Structure and function of enzymes acting on chitin and chitosan, *Biotechnology and Genetic Engineering Reviews*, 27 (6), 331–366.

Ekambaram, P., Abdul Hasan Sathali, A. and Priyanka, K. (2012). Solid lipid nanoparticles , A review, *Sci. Rev. Chem. Commun.*, 2 (1), 80–102.

Ekambaram, P. and Abdul Hasan Sathali, A. (2011). Formulation and evaluation of solid lipid nanoparticles of ramipril, *J. Young Pharm.*, 3 (3), 216-220.

Elgadir, M.A., Uddin, M.S., Ferdosh, S., Adam, A., Chowdhury, A.J.K. and Sarker, M.Z.I. (2015). Impact of chitosan composites and chitosan nanoparticle composites on various drug delivery systems, A review. *J. Food Drug Anal.*, 23 (4), 619–629.

EMA. (2012). Guideline on bioanalytical method validation, *EMEA, Comm. Med. Prod., Hum. Use,* 44 (7), 1–23.

European Medicines Agency. (2014). Background review for cyclodextrins used as excipients, *Eur. Med. Agency,* 44 (11), 1–17.

Freitas, M.R. De, Rolim, L.A., Soares, M.F.D.L.R., Rolim-Neto, P.J., Albuquerque, M.M. De. and Soares-Sobrinho, J.L. (2012). Inclusion complex of methyl-ß-cyclodextrin and olanzapine as potential drug delivery system for schizophrenia, *Carbohydr. Polym.,* 89 (4), 1095–1100.

Fukuda, M., Miller, D.A., Peppas, N.A. and McGinity, J.W. (2008). Influence of sulfobutyl ether ß-cyclodextrin (Captisol®) on the dissolution properties of a poorly soluble drug from extrudates prepared by hot-melt extrusion, *Int. J. Pharm.,* 350 (1–2), 188–196.

Gaba, B., Fazil, M., Khan, S., Ali, A., Baboota, S. and Ali, J. (2015). Nanostructured lipid carrier system for topical delivery of terbinafine hydrochloride, *Bull. Fac. Pharmacy,* 53 (2), 147–159.

Gavandi, S., Jadhav, S. and Sapkale, G. (2015). Recent trends of nanotechnology in drug delivery and their application, *Asian J. Pharm. Technol. Innov*., 3 (10), 1–5.

Gavhane, Y.N. and Yadav, A.V. (2012). Loss of orally administered drugs in GI tract, *Saudi Pharm. J.,* 20 (4), 331–344.

Genç, L. and Demirel, M. (2013). Preparation and characterization of polymeric and lipid nanoparticles of pilocarpine HCl for ocular application, *Pharm. Dev. Technol.,* 18 (3), 701–709.

Girotra, P., Singh, S.K. and Nagpal, K. (2013). Supercritical fluid technology, a promising approach in pharmaceutical research, *Pharm. Dev. Technol*., 18 (1), 22–38.

Güleç, K. and Demirel, M. (2016). Characterization and antioxidant cyclodextrin complexes activity of quercetin / methyl- β -CD, *Curr. Drug Deliv.,* 13 (0), 444–452.

Gupta, D.R., Shah, Y.D., Vora, R.S. and Shah, D. (2016). Solubility enhancement by solid lipid nanoparticle, *IJPPR,* 7 (1), 351–367.

Gupta, H., Aqil, M., Khar, R.K., Ali, A., Bhatnagar, A. and Mittal, G. (2010). Sparfloxacin-loaded PLGA nanoparticles for sustained ocular drug delivery, *Nanomedicine Nanotechnology, Biol. Med.,* 6 (2), 324–333.

Gupta, K.C. and Kumar, M.N.V.R. (2000). An overview on chitin and chitosan applications with an emphasis on controlled, *J. Macromol. Sci.,* 40 (4), 273–308.

Hanumanaik, M., Patel, S.K. and Sree, K.R. (2013). Solid lipid nanoparticles; a review, *IJPSR,* 4 (3), 928–940.

He, P., Davis, S.S. and Illum, L. (1999). Chitosan microspheres prepared by spray drying, *Int. J. Pharm.,* 187, 53–65.

Hegazy, N., Demirel, M. and Yazan, Y. (2002). Preparation and *in vitro* evaluation of pyridostigmine bromide microparticles, *Int. J. Pharm.,* 242 (1–2), 171–174.

Higuchi, T. and Connors, K.A. (1965). Phase solubility techniques, *Adv. Anal. Chem. Instrum.,* 4, 117–210.

Hoell, I., Vaaje-Kolstad, G. and Eijsink, V.G.H. (2010). Structure and function of enzymes acting on chitin and chitosan, *Biotechnol. Genet. Eng. Rev*., 27 (7), 331–366.

Hou, D., Xie, C., Huang, K. and Zhu, C. (2003). The production and characteristics of solid lipid nanoparticles (SLNs), *Biomaterials,* 24 (10), 1781–1785.

Hubatsch, I., Ragnarsson, E.G.E. and Artursson, P. (2007). Determination of drug permeability and prediction of drug absorption in Caco-2 monolayers, *Nat. Protoc*., 2 (2119), 2111–2119.

ICH. (1996). Guidance for industry, Q2B validation of analytical procedures, methodology, *Int. Conf. Harmon. Tech. Requir. Regist. Tripart. Guidel.,* (11), 4–5.

Ingham, B. (2015). X-ray scattering characterisation of nanoparticles, *Crystallogr. Rev.,* 21 (4), 1–75.

Jadhav, S.B. and Jain, G.K. (2006). Statins and osteoporosis, new role for old drugs, *J. Pharm. Pharmacol.,* 58, 3–18.

Jain, A.S., Date, A.A., Pissurlenkar, R.R.S., Coutinho, E.C. and Nagarsenker, M.S. (2011). Sulfobutyl ether(7) β-cyclodextrin (SBE(7) β-CD) carbamazepine complex, preparation, characterization, molecular modeling, and evaluation of in vivo anti-epileptic activity, *AAPS Pharm Sci Tech*., 12 (4), 1163–1175.

Jambhekar, S.S. and Breen, P. (2016). Cyclodextrins in pharmaceutical formulations I, Structure and physicochemical properties, formation of complexes, and types of complex, *Drug Discov. Today*, 21 (2), 356–362.

Jin, Z.-Y. (2010). Cyclodextrin chemistry - preparation and application. first edit ed. , antimicrobial agents and chemotherapy, *World Scientific Publishing Co. Pte. Ltd,* Singapore, 5-8.

Kamaly, N., Yameen, B., Wu, J. and Farokhzad, O.C. (2016). Degradable controlled-release polymers and polymeric nanoparticles, mechanisms of controlling drug release, *Chem. Rev.*, 116 (4), 2602–2663.

Kamble, P.R., Shaikh, K.S. and Chaudhari, P.D. (2014). Application of liquisolid technology for enhancing solubility and dissolution of rosuvastatin, *Adv. Pharm. Bull.*, 4 (21), 197–204.

Kawabata, Y., Wada, K., Nakatani, M., Yamada, S. and Onoue, S. (2011). Formulation design for poorly water-soluble drugs based on biopharmaceutics classification system, basic approaches and practical applications, *Int. J. Pharm.*, 420 (1), 1–10.

Khan, N.A. and Durakshan, M. (2013). Cyclodextrin, An overview, *Int. J. Bioassays*, 2, 858–865.

Kheradmandnia, S., Vasheghani-Farahani, E., Nosrati, M. and Atyabi, F. (2010). Preparation and characterization of ketoprofen-loaded solid lipid nanoparticles made from beeswax and carnauba wax, *Nanomedicine Nanotechnology, Biol. Med.*, 6 (6), 753–759.

Klose, D., Delplace, C. and Siepmann, J. (2011). Unintended potential impact of perfect sink conditions on PLGA degradation in microparticles, *Int. J. Pharm.*, 404 (1–2), 75–82.

Kostapanos, M.S., Milionis, H.J. and Elisaf, M.S. (2010). Rosuvastatin-associated adverse effects and drug-drug interactions in the clinical setting of dyslipidemia, *Am. J. Cardiovasc. Drugs*, 10 (1), 11–28.

Kumar, B.P. and Karimulla, S. (2012). Solid lipid nanoparticles – a brief review, *Int. J. Adv. Pharm.*, 2 (1), 35–55.

Kumar, P.P., Gayatri, P., Sunil, R. and Rao, Y.M. (2012). Atorvastatin loaded solidlipid nanoparticles, formulation, optimization and *in - vitro* characterization, *IOSR J. Pharm.*, 2 (5), 23–32.

Kumar, T.R., Shitut, N.R., Kumar, P.K., Vinu, M.C.A., Pavan Kumar, V. V., Mullangi, R. and Srinivas, N.R. (2006). Determination of rosuvastatin in rat plasma by HPLC, validation and its application to pharmacokinetic studies, *Biomed. Chromatogr.*, 20 (9), 881–887.

Lakkakula, J.R. and Macedo, K.R.W. (2014). A vision for cyclodextrin nanoparticles in drug delivery systems and pharmaceutical applications, *Nanomedicine,* 9 (6), 877–894.

Learoyd, T.P., Burrows, J.L., French, E. and Seville, P.C. (2008). Chitosan-based spray-dried respirable powders for sustained delivery of terbutaline sulfate, *Eur. J. Pharm. Biopharm.,* 68 (2), 224–234.

Leblond, D., Altan, S., Novick, S., Peterson, J., Shen, Y. and Yang, H. (2016). In vitro dissolution curve comparisons, A critique of current practice, *Dissolution Technol.*, 23 (1), 14–23.

Lewinski, N., Colvin, V. and Drezek, R. (2008). Cytotoxicity of nanopartides, *Small*. 4 (1), 26–49.

Li, H.-Y. and Zhang, F. (2012). Preparation of nanoparticles by spray-drying and their use for efficient pulmonary drug delivery, *Methods Mol. Biol.,* 906, 295–301.

Li, M., Zahi, M.R., Yuan, Q., Tian, F. and Liang, H. (2016). Preparation and stability of astaxanthin solid lipid nanoparticles based on stearic acid, *Eur. J. Lipid Sci. Technol.,* 118 (4), 592–602.

Lingayat, V.J., Zarekar, N.S. and Shendge, R.S. (2012). Solid lipid nanoparticles , a review, *Nanosci. Nanotechnol. Res.,* 2 (1), 80–102.

Loftsson, T. and Brewster, M.E. (2010). Pharmaceutical applications of cyclodextrins, basic science and product development, *J. Pharm. Pharmacol.,* 62 (11), 1607–1621.

Luangtana-anan, M., Opanasopit, P., Ngawhirunpat, T., Nunthanid, J., Limmatvapirat, S., Lim, L.Y., Opanasopit, P., Ngawhirunpat, T. and Nunthanid, J. (2005). Effect of chitosan salts and molecular weight on a nanoparticulate carrier for therapeutic protein, *Pharm. Dev. Technol*., 10, 189–196.

Luo, Y.F., Chen, D.W., Ren, L.X., Zhao, X.L. and Qin, J. (2006). Solid lipid nanoparticles for enhancing vinpocetine's oral bioavailability, *J. Control. Release*, 114 (1), 53–59.

Luvai, A., Mbagaya, W., Hall, A.S. and Barth, J.H. (2012). Rosuvastatin, a review of the pharmacology and clinical effectiveness in cardiovascular disease, *Clin. Med. Insights Cardiol*., 6, 17–33.

Lyons, K.S. and Harbinson, M. (2009). Statins, In the beginning, *J. R. Coll. Physicians Edinb.,* 39 (4), 362–364.

Mabbott, N.A., Donaldson, D.S., Ohno, H., Williams, I.R. and Mahajan, A. (2013). Microfold (M) cells, important immunosurveillance posts in the intestinal epithelium, *Mucosal Immunol.,* 6 (4), 666–77.

Mäder, K. and Mehnert, W. (2001). Solid lipid nanoparticles, production, characterization and applications, *Adv. Drug Deliv. Rev.,* 47 (2–3), 165–96.

Maestrelli, F., Zerrouk, N., Chemtob, C. and Mura, P. (2004). Influence of chitosan and its glutamate and hydrochloride salts on naproxen dissolution rate and permeation across Caco-2 cells, *Int. J. Pharm.,* 271 (1–2), 257–267.

Mahajan, P.S., Mahajan, K.B. and Darekar, A.B. (2015). A review on solid lipid nanoparticle (SLN), An advanced treatment modality, *Int. J. Pharm. Sci. Res.,* 6 (9), 3698–3712.

Manmode, A.S., Sakarkar, D.M. and Mahajan, N.M. (2009). Nanoparticles-tremendous therapeutic potential, a review, *Int. J. PharmTech Res.,* 1 (4), 1020–1027.

Manzoni, M. and Rollini, M. (2002). Biosynthesis and biotechnological production of statins by filamentous fungi and application of these cholesterol-lowering drugs, *Appl. Microbiol. Biotechnol.,* 58 (5), 555–564.

Martin, P.D., Warwick, M.J., Dane, A.L., Hill, S.J., Giles, P.B., Phillips, P.J. and Lenz, E. (2003). Metabolism, Excretion, and pharmacokinetics of rosuvastatin in healthy adult male volunteers, *Clin. Ther.,* 25 (11), 2822–2835.

McTaggart, F. and Jones, P. (2008). Effects of statins on high-density lipoproteins, a potential contribution to cardiovascular benefit, *Cardiovasc. Drugs Ther.,* 22 (4), 321–338.

Mishra, B., Patel, B.B. and Tiwari, S. (2010). Colloidal nanocarriers, a review on formulation technology, types and applications toward targeted drug delivery, *Nanomedicine Nanotechnology, Biol. Med.,* 6 (1), 9–24.

Mohanraj, V., Chen, Y. and Chen, M. (2006). Nanoparticles – a review. *Trop J Pharm Res.,* 5 (6), 561–573.

M.S., Milionis, H.J. and Elisaf, M.S. (2010). Rosuvastatin-associated adverse effects and drug-drug interactions in the clinical setting of dyslipidemia, *Am. J. Cardiovasc. Drugs.,* 10 (1), 11–28.

Mudshinge, S.R., Deore, A.B., Patil, S. and Bhalgat, C.M. (2011). Nanoparticles, emerging carriers for drug delivery, *Saudi Pharm. J.,* 19 (3), 129–141.

Mukherjee, S., Ray, S. and Thakur, R.S. (2009). Solid lipid nanoparticles, a modern formulation approach in drug delivery system, *Indian J. Pharm. Sci.*, 4, 349–358.

Mura, P. (2014). Analytical techniques for characterization of cyclodextrin complexes in aqueous solution, a review, *J. Pharm. Biomed. Anal*., 101, 238–250.

Mura, P. (2015). Analytical techniques for characterization of cyclodextrin complexes in the solid state, a review. *J. Pharm. Biomed. Anal.*, 113, 226–238.

Mura, P., Adragna, E., Rabasco, A.M., Moyano, J.R., Pé Rez-Martnez, J.I., Arias, M.J. and Giné S, J.M. (1999). Effects of the host cavity size and the preparation method on the physicochemical properties of ibuproxam-cyclodextrin systems, *Drug Dev. Ind. Pharm.*, 25 (3), 279–287.

Müller, R.H., M, K. and Sven, G. (2000). Solid lipid nanoparticles ( SLN ) for controlled drug delivery - a review of the state of the art, *Eur. J. Pharm. Biopharm.*, 50, 161–177.

Müller, R.H., Runge, S., Ravelli, V., Mehnert, W., Thünemann, A.F. and Souto, E.B. (2006). Oral bioavailability of cyclosporine, solid lipid nanoparticles (SLNs) versus drug nanocrystals, *Int. J. Pharm.*, 317 (1), 82–89.

Nagavarma, B.V.N., Yadav, H.K.S., Ayaz, A., Vasudha, L.S. and Shivakumar, H.G. (2012). Different techniques for preparation of polymeric nanoparticles- a review, *Asian J. Pharm. Clin. Res.*, 5 (3), 16–23.

Nelson, R.H. (2014). Hyperlipidemia as a risk factor for cardiovascular disease robert, *Prim. Care*., 40 (1), 195–211.

Neupane, Y.R., Sabir, M.D., Ahmad, N., Ali, M. and Kohli, K. (2013). Lipid drug conjugate nanoparticle as a novel lipid nanocarrier for the oral delivery of decitabine, ex vivo gut permeation studies, *Nanotechnology*, 24 (41), 1–11.

Niwa, T., Takeuchi, H., Hino, T., Kunou, N. and Kawashima, Y. (1993). Preparations of biodegradable nanospheres of water-soluble and insoluble drugs with D,L-lactide/glycolide copolymer by a novel spontaneous emulsification solvent diffusion method, and the drug release behavior, *J. Control. Release*, 25 (1–2), 89–98.

Oehlke, K., Behsnilian, D., Mayer-miebach, E., Weidler, P.G. and Greiner, R. (2017). Edible solid lipid nanoparticles (SLN) as carrier system for antioxidants of different lipophilicity, *Pols one*, 12 (2), 1–19.

Ojer, P., Neutsch, L., Gabor, F., Irache, J.M. and López De Cerain, A. (2013). Cytotoxicity and cell interaction studies of bioadhesive poly(anhydride) nanoparticles for oral antigen/drug delivery, *J. Biomed. Nanotechnol.,* 9 (11), 1891–1903.

Olbrich, C., Kayser, O. and Müller, R.H. (2002). Lipase degradation of Dynasan 114 and 116 solid lipid nanoparticles (SLN) - effect of surfactants, storage time and crystallinity, *Int. J. Pharm.,* 237 (1–2), 119–128.

Orienti, I., Cerchiara, T., Luppi, B., Bigucci, F., Zuccari, G. and Zecchi, V. (2002). Influence of different chitosan salts on the release of sodium diclofenac in colon-specific delivery, *Int. J. Pharm.*, 238, 51–59.

Overbeek, J.T.G. (1977). Recent developments in the understanding of colloid stability, *J. Colloid Interface Sci.*, 58 (2), 408–422.

Özkan, Y., Atay, T., Dikmen, N., Işimer, A. and Aboul-Enein, H.Y. (2000). Improvement of water solubility and *in vitro* dissolution rate of gliclazide by complexation with β-cyclodextrin, *Pharm. Acta Helv.*, 74 (4), 365–370.

Pardeshi, C., Rajput, P., Belgamwar, V., Tekade, A., Patil, G., Chaudhary, K. and Sonje, A. (2012). Solid lipid based nanocarriers, an overview, *Acta Pharm.,* 62 (4), 433–72.

Patil, J.S., Kadam, D. V, Marapur, S.C. and Kamalapur, M. V. (2010). Inclusion complex system ; a novel technique to improve the solubility and bioavailability of poorly soluble drugs , a review, *Int. J. Res. Pharm. Si. Rev. Res.,* 2 (2), 29–34.

Peixoto, F.S., Dias, P.M., Ramaldes, G.A., Vilela, J.M.C., Andrade, M.S. and Cunha, A.S. (2005). Atomic force microscopy applied to the characterization of solid lipid nanoparticles, *Microsc. Microanal.*, 11 (3), 52–55.

Petros, R. a and DeSimone, J.M. (2010). Strategies in the design of nanoparticles for therapeutic applications, *Nat. Rev. Drug Discov.,* 9 (8), 615–627.

Pichandi, S., Pasupathi, P., Raoc, Y.Y., Farook, J., Ambika, A., Ponnusha, B.S., Subramaniyam, S. and Virumandye, R. (2011). The role of statin drugs in combating cardiovascular diseases, *Int. J. Cur. Sci. Res.*, 1 (2), 47–56.

Pinto Reis, C., Neufeld, R.J., Ribeiro, A.J. and Veiga, F. (2006). Nanoencapsulation I. Methods for preparation of drug-loaded polymeric nanoparticles, *Nanomedicine Nanotechnology, Biol. Med.*, 2 (1), 8–21.

Polson, C., Sarkar, P., Incledon, B., Raguvaran, V. and Grant, R. (2003). Optimization of protein precipitation based upon effectiveness of protein removal and ionization effect in liquid chromatography-tandem mass spectrometry, *J. Chromatogr. B Anal. Technol. Biomed. Life Sci*., 785 (2), 263–275.

Ponnuraj, R., K, J. and Gopalakrishnan, Sivaraman Arumugam, A. (2015). Formulation And Development of Capsules Containing Rosuvastatin, *Indo Am. J. Pharm. Res.*, 5 (6), 2217–2231.

Portero, A. and Remun, C. (1998). Effect of chitosan and chitosan glutamate enhancing the dissolution properties of the poorly water soluble drug nifedipine, *Int. J. Pharm.*, 175, 75–84.

Pralhad, T. and Rajendrakumar, K. (2004). Study of freeze-dried quercetin-cyclodextrin binary systems by DSC, FT-IR, X-ray diffraction and SEM analysis, *J. Pharm. Biomed. Anal.*, 34 (2), 333–339.

Pragati, S., Kuldeep, S., Ashok, S. and Satheesh, M. (2009). Solid lipid nanoparticles , a promising drug delivery technology, *Int. J. Pharm. Sci. Nanotechnol.*, 2 (2), 509–516.

Pragati1, S., Kuldeep, S., Ashok1, S. and Satheesh., M. (2014). Solid lipid nanoparticles – A promising drug delivery system. *Int. J. Pharm. Sci. Nanotechnol*., 2 (2), 187–237.

Puttananjaiah, M.K.H., Dhale, M.A., Gaonkar, V. and Keni, S. (2011). Statins, 3-Hydroxy-3-methylglutaryl-CoA (HMG-CoA) reductase inhibitors demonstrate anti-atherosclerotic character due to their antioxidant capacity, *Appl. Biochem. Biotechnol.*, 163 (2), 215–222.

Rajendrakumar, K., Madhusudan, S. and Pralhad, T. (2005). Cyclodextrin complexes of valdecoxib, properties and anti-inflammatory activity in rat, *Eur. J. Pharm. Biopharm.*, 60 (1), 39–46.

Ramteke, K.H., A., Joshi.S. A. and Dhole S N. (2012). Solid lipid nanoparticle, a review, *IOSR J. Pharm.*, 2 (6), 2250–3013.

Rao, J.P. and Geckeler, K.E. (2011). Polymer nanoparticles, preparation techniques and size-control parameters, *Prog. Polym. Sci.*, 36 (7), 887–913.

Rasheed, A., Kumar C.K., A. and Sravanthi, V.V.N.S.S. (2008). Cyclodextrins as drug carrier molecule, a review, *Sci. Pharm.*, 76 (4), 567–598.

Reddy, N.R. and Shariff, A. (2013). Solid lipid nanoparticles, an advanced drug delivery system, *Int. J. Pharm. Sci. Res*., 4 (1), 161-171.

Reiner, Ž. (2013). Statins in the primary prevention of cardiovascular disease, *Nat. Rev. Cardiol.,* 10 (8), 453–64.

Reis, C.P., Neufeld, R.J., Ribeiro, A.J. and Veiga, F. (2006). Nanoencapsulation I. Methods for preparation of drug-loaded polymeric nanoparticles, *Nanomedicine Nanotechnology, Biol. Med.,* 2 (1), 8–21.

Remington P, J. and Beringer, P. (2006). Remington the science and practice of pharmacy, Lippincott Williams and Wilkins, 1368–1369.

Righeschi, C., Bergonzi, M.C., Isacchi, B., Bazzicalupi, C., Gratteri, P. and Bilia, A.R. (2016). Enhanced curcumin permeability by SLN formulation, The PAMPA approach, *LWT - Food Sci. Technol.*, 66,475–483.

Rivedi, H.K.T. and Atel, M.C.P. (2012). Development and validation of a stability-indicating RP-UPLC method for determination of rosuvastatin and related substances in pharmaceutical dosage form, *Sci Pharm.,* 8, 393–406.

Sailaja, A.K., Amareshwar, P. and Chakravarty, P. (2012). Formulation of solid lipid nanoparticles and their applications, *Curr. Pharma Res.,* 2 (2), 508–510.

Saku, K., Zhang, B. and Noda, K., (2011). Randomized head-to-head comparison of pitavastatin, atorvastatin, and rosuvastatin for safety and efficacy (quantity and quality of LDL), *Circ. J*., 75 (6), 1493–1505.

Salih, O.S., Samein, L.H. and Ali, W.K. (2013). Formulation and *in vitro* evaluation of rosuvastatin calcium niosomes, *Int. J. Pharm. Pharm. Sci*., 5, 525–535.

Salústio, P.J., Pontes, P., Conduto, C., Sanches, I., Carvalho, C., Arrais, J. and Marques, H.M.C. (2011). Advanced technologies for oral controlled release, cyclodextrins for oral controlled release, *AAPS Pharm Sci Tech*., 12 (4), 1276–1292.

Sarfraz, R.M., Ahmad, M., Mahmood, A., Minhas, M.U. and Yaqoob, A. (2015). Development and evaluation of rosuvastatin calcium based microparticles for solubility enhancement, an in vitro study, *Adv. Polym. Technol.,* 0 (0), 1–9.

Sathali, A.A.H. and Nisha, N. (2013). Development of solid lipid nanoparticles of rosuvastatin calcium, *J. Pharm. Res*., 1 (5), 536–548.

Senthil Kumar, P., Arivuchelvan, A., Jagadeeswaran, A., Punniamurthy, N., Selvaraj, P., Richard Jagatheesan, P.N. and Mekala, P. (2015). Formulation of enrofloxacin SLNs and its pharmacokinetics in emu (Dromaius novaehollandiae) birds, *Appl. Nanosci.*, 5 (6), 661–671.

Severino, P., Andreani, T., Macedo, A.S., Fangueiro, J.F., Santana, M.H. a, Silva, A.M. and Souto, E.B. (2012). Current state-of-art and new trends on lipid nanoparticles (sln and nlc) for oral drug delivery, *J. Drug Deliv.*, 2012,1–10.

Schachter, M. (2005). Chemical, pharmacokinetic and pharmacodynamic properties of statins, an update, *Fundam. Clin. Pharmacol*., 19 (1), 117–125.

Schubert, M.A. and Müller-Goymann, C.C. (2003). Solvent injection as a new approach for manufacturing lipid nanoparticles - evaluation of the method and process parameters, *Eur. J. Pharm. Biopharm*., 55 (1), 125–131.

Shah, V.P., Tsong, Y., Sathe, P. and Liu, J.P. (1998). *In vitro* dissolution profile comparison- statistics and analysis of the similarity factor, f2. *Pharm. Res.*, 15 (6) 889-896.

Shete, G., Puri, V., Kumar, L. and Bansal, A.K. (2010). Solid state characterization of commercial crystalline and amorphous atorvastatin calcium samples, *AAPS PharmSciTech*., 11 (2), 598–609.

Shiralashetti S.S. and Patil J.S. (2014). Design , charecterization and evaluation of inclusion complexes of poorly soluble atorvastatin calcium, *UNIQUE J. Pharm. Biol. Sci. UJPBS*., 2 (4), 88–96

Singh, S. (2016). Green nanobiotechnology - an overview of synthesis , chracterisation and applications, *World Journal of Pharmacy And Pharmaceutical Sciences*, 5 (8), 501–531.

Soni, K., Kukereja, B.K., Kapur, M. and Kohli, K. (2015). Lipid nanoparticles, future of oral drug delivery and their current trends and regulatory issues, 7 (1), 1–18.

Soran, H. and Durrington, P. (2008). Rosuvastatin, efficacy, safety and clinical effectiveness, *Expert Opin. Pharmacother*., 9 (12), 2145–2160.

Srinivas, L., Hemalatha, B., VS Vinai Kumar, T., Naga Malleswara Rao, B. and B Teja, B. (2014). Studies on solubility and dissolution enhancement of itraconazole by complexation with sulfo-butyl7 ether β cyclodextrin, *Asian J. Biomed. Pharm. Sci.*, 4 (38), 06–16.

Surender, V., and Deepika, M. (2016). Solid lipid nanoparticles, a comprehensive review, *Journal of Chemical and Pharmaceutical Research*, 8 (8), 102–114.

Suares, D. and Parbhakar, B. (2016). Oral delivery of rosuvastatin lipid nanocarriers, investigation of *in vitro* and *in vivo* profile, *Int. J. Pharm. Sci. Res., IJPSR.* 7 (12), 4856–4864.

Suresh, G., Manjunath, K., Venkateswarlu, V. and Satyanarayana, V. (2007). Preparation, characterization, and in vitro and in vivo evaluation of lovastatin solid lipid nanoparticles, *AAPS Pharm. Sci. Tech*., 8 (1), 2779–2785.

Sznitowska, M., Wolska, E., Baranska, H., Cal, K. and Pietkiewicz, J. (2017). The effect of a lipid composition and a surfactant on the characteristics of the solid lipid microspheres and nanospheres (SLM and SLN), *Eur. J. Pharm. Biopharm.*, 110, 24–30.

Toth, P.P. and Dayspring, T.D. (2011). Drug safety evaluation of rosuvastatin, *Expert Opin. Drug Saf.*, 10 (6), 969–986.

Unlu, M., Aktas, Z., Gocun, P.U., Ilhan, S.O., Hasanreisoglu, M. and Hasanreisoglu, B. (2016). Neuroprotective effect of systemic and/or intravitreal rosuvastatin administration in rat glaucoma model, *Int. J. Ophthalmol.*, 9 (3), 340–347.

Urbán-Morlán, Z., Ganem-Rondero, A., Melgoza-Contreras, L. M., Escobar-Chávez, J. J., Nava-Arzaluz, M. G. and Quintanar-Guerrero, D. (2010). Preparation and characterization of solid lipid nanoparticles containing cyclosporine by the emulsification-diffusion method, *International Journal of Nanomedicine*, 5 (1), 611–620.

U.S.P, (2016). U.S. Pharmacopoeia-National Formulary [USP 39 NF 32], *USP, United States Pharmacop. (USP 37 NF 34), United States Pharmacopeial Convention, Inc;* 1, 463–468.

Üner, M. and Yener, G. (2007). Importance of solid lipid nanoparticles (SLN) in various administration routes and future perspective, *Int. J. Nanomedicine,* 2 (3), 289–300.

Venkatesh, N., Spandana, K., Sambamoorthy, U. and Suresh, K. (2014). Formulation development and evaluation of mouth dissolving film of zolmitriptan as an antimigraine medication, *Int. J. of Medicine Pharm. Res. IJMPR*, 2 (4), 685–690.

Vidya N., K., Chemate, S.Z. and Dharashive, V.M. (2016). Formulation development and solubility enhancement of rosuvastatin, *Int. J. Pharm. Sci. Res.,* 7 (12), 4882–4892.

Viral, H.S., Pragna, S. and Gaurang, B.S. (2012). Design and evaluation of thiolated chitosan based mucoadhesive and permeation enhancing bilayered buccal drug delivery system, *Afr. J. Pharm. Pharmacol*., 6 (7), 491–501.

Vyas, A. (2013). Preparation, characterization and pharmacodynamic activity of supramolecular and colloidal systems of rosuvastatin-cyclodextrin complexes, *J. Incl. Phenom. Macrocycl. Chem.,* 76 (1–2), 37–46.

Westesen, K., Bunjes, H. and Koch, M.H.J. (1997). Physicochemical characterization of lipid nanoparticles and evaluation of their drug loading capacity and sustained release potential, *J. Control. Release*, 48,223–236.

White, C.M. (2002). A review of the pharmacologic and pharmacokinetic aspects of rosuvastatin, *J. Clin. Pharmacol.,* 42 (9), 963–970.

Wilczewska, A.Z., Niemirowicz, K., Markiewicz, K.H. and Car, H. (2012). Nanoparticles as drug delivery systems, *Pharmacol Rep*., 7 (12), 1118–1122.

World Health Organization. (2002). Integrated management of cardiovascular risk, 1–35.

Xu, W., Ling, P. and Zhang, T. (2013). Polymeric micelles, a promising drug delivery system to enhance bioavailability of poorly water-soluble drugs, *J. Drug Deliv*., 2013 ,1–15.

Yadav, P., Soni, G., Mahor, A., Alok, S., Singh, P.P. and Verma, A. (2014). Solid lipid nanoparticles, an effective and promising drug delivery system- a review, *Int. J. Pharm. Sci. Res.,* 5 (4), 1152–1162.

Yee, S. (1997). *In vitro* prmeability across caco-2 cells (colonic) can redict *in vivo* (small intestinal) absorption in man - fact or myth., *Pharm. Res.,* 14 (6), 763-766.

Yong, Y., Saleem, A., Guerrero-Analco, J.A., Haddad, P.S., Cuerrier, A., Arnason, J.T., Harris, C.S. and Johns, T. (2016). Larix laricina bark, a traditional medicine used by the Cree of Eeyou Istchee, antioxidant constituents and *in vitro* permeability across Caco-2 cell monolayers, *J. Ethnopharmacol.,* 194 (3), 651–657.

Younes, I. and Rinaudo, M. (2015). Chitin and chitosan preparation from marine sources, structure, properties and applications, *Mar. Drugs*, 13 (3), 1133–1174.

Yu, W. and Xie, H. (2012). Parametric study of pool boiling heat transfer with nanofluids for the enhancement of critical heat flux, a review, *J. Nanomater.,* 87, 228–240.

Yuan, Y., Chesnutt, B.M., Haggard, W.O. and Bumgardner, J.D. (2011). Deacetylation of chitosan, Material characterization and *in vitro* evaluation via albumin adsorption and pre-osteoblastic cell cultures, *Materials,* 4 (8), 1399–1416.

Yurtdaş, G., Demirel, M. and Genç, L. (2011). Inclusion complexes of fluconazole with β-cyclodextrin, Physicochemical characterization and *in vitro* evaluation of its formulation, *J. Incl. Phenom. Macrocycl. Chem.,* 70 (3–4), 429–435.

Zhang, M., Yang, Z., Chow, L. and Wang, C. (2003). Simulation of drug release from biodegradable polymeric microspheres with bulk and surface erosions, *J. Pharm. Sci.,* 92 (10), 2040–2056.

Zhang, Q., Yie, G., Li, Y. and Yang, Q. (1999). Studies on the cyclosporin a loaded stearic acid nanoparticles, *Yaoxue Xuebao*., 34 (4), 311–312.

Zhang, Y., Huo, M., Zhou, J., Zou, A., Li, W., Yao, C. and Xie, S. (2010). DDSolver, an add-in program for modeling and comparison of drug dissolution profiles, *AAPS J,* 12 (3), 263–271.

Zur Muhlen, A., Schwarz, C. and Mehnert, W. (1998). Solid lipid nanoparticles (SLN) for controlled drug delivery drug release and release mechanism, *Eur J Pharm Biopharm*., 45, 149–155.

http-1: www.researchreview.com.au/Approved_Crestor_PI.pdf.

**Appendix 1**

T.C.
ESKİŞEHİR OSMANGAZİ ÜNİVERSİTESİ
REKTÖRLÜĞÜ
HAYVAN DENEYLERİ YEREL ETİK KURULU
( HADYEK)

# HAYVAN DENEYLERİ YEREL ETİK KURULU KARARI

| | |
|---|---|
| **TOPLANTI TARİHİ** | **: 21. 11. 2016** |
| **TOPLANTI SAYISI** | **: 103** |
| **DOSYA KAYIT NUMARASI** | **: 561** |
| **KARAR NUMARASI** | **: 561** |
| **ARAŞTIRMA YÜRÜTÜCÜSÜ** | **: Prof. Dr. Müzeyyen DEMİREL** |
| **YARDIMCI ARAŞTIRMACILAR** | **: Prof.Dr. Kevser EROL** |
| | **Doç.Dr. Rana ARSLAN** |
| | **Yrd.Doç.Dr. Ebru BAŞARAN** |
| | **Ecz. Fawaz AL HEIBSHY** |
| **HAYVAN TÜRÜ ve SAYISI** | **: Spraque Dawley (110 adet erkek)** |

Anadolu Üniversitesi Eczacılık Fakültesi Farmasötik Teknoloji Anabilim Dalı Öğretim üyesi **Prof. Dr. Müzeyyen DEMİREL**'in araştırma yürütücüsü olduğu 561/2016 kayıt numaralı ve **"Rosuvastatin Kalsiyum İçeren Siklodekstrin, Siklodekstrin+Polianhidrit ve Katı Lipit Bazlı Taşıyıcı Sistemler Üzerinde Farmakokinetik ve Farmakodinamik Çalışmalar"** konulu çalışma; Deney Hayvanları Etik Kurulu Yönergesi'ne göre değerlendirilmiş ve gerekçede belirtildiği şekilde yapılması uygun bulunmuştur.

Prof. Dr. Kevser EROL (Başkan)

Prof. Dr. Kubilay UZUNER (Üye)

Prof. Dr. Hasan V. GÜNEŞ (Üye)

Prof. Dr. Emel ULUPINAR. (Üye)

Doç. Dr. Engin YILDIRIM (Üye)

Yrd. Doç. Dr. Ünal ÖZELMAS (Üye)

Yrd.Doç.Dr.Nurdan KIRIMLIOĞLU (Üye)

Yrd. Doç. Dr. Vet. Hek. Oya ERALP İNAN (Üye)

Vet. Hek. Refik ARTAN (Üye)

Avukat Şükrü KIRDEMİR (Üye)

Adres: Meşelik Kampüsü 26480 Eskişehir
Telefon: 0 222 239 29 79 / (45 63)

MSN Laboratories Ltd
Factory : Sy. No. 317 & 323, Rudraram (vil), Patancheru (Mandal), Medak (Dist.)
A.P., India. Ph. : 08455 - 220372 & 220373 Fax : 08455 - 220415 PIN : 502329

# CERTIFICATE OF ANALYSIS

| | | | |
|---|---|---|---|
| Product | : Rosuvastatin Calcium | Customer Name | : ABDI IBRAHIM |
| Batch No. | : RNm0191112 | Date of Mfg. | : November 2012 |
| Batch Quantity | : 60.20 Kg | Date of Expiry | : October 2016 |
| A.R.No. | : IMD12100036 | Date of Analysis | : 29.11.2012 |
| Reference | : In house | Specification No. | : QC-FPRN-001/01 |

Storage: Preserve in well-closed containers, protected from light .Store at controlled room temperature.

| Sl. No. | TEST | RESULT | SPECIFICATION |
|---|---|---|---|
| 1.0 | Description | An off- white colored powder. | Off- white to light yellow colored powder. |
| 2.0 | Solubility | Complies | Soluble in N,N-Dimethyl formamide, Acetone and Acetonitrile. Insoluble in water |
| 3.0 | Identification by | | |
| 3.1 | IR-Spectrum | Complies | The sample infrared absorption spectrum should be concordant with that of the spectrum of standard. |
| 3.2 | Test for calcium | Positive | Positive |
| 3.3 | HPLC | Complies | The retention time of the major peak in the chromatogram of the assay preparation corresponds to that in the chromatogram of the standard preparation, as obtained in the Assay. |
| 4.0 | Water content by KFR | 4.9 % w/w | Not more than 6.0 % w/w |
| 5.0 | Calcium content (On anhydrous basis) | 4.0 % w/w | Should be between 3.5% to 4.5% w/w |
| 6.0 | Specific Optical rotation $[\alpha]_D^{25}$ C = 0.5, in Aqueous methanol | +17.9° | Between +14.0° and +19.0° |
| 7.0 | Heavy metals | Less than 10 ppm | Not more than 10 ppm |
| 8.0 | Related substances by HPLC | | |
| 8.1 | Anti Isomer | 0.06 % | Not more than 0.30 % |
| 8.2 | Lactone | Below detection limit (0.01%) | Not more than 0.30 % |
| 8.3 | Major Unknown Individual Impurity | 0.03 % | Not more than 0.10 % |
| 8.4 | Total impurities | 0.12 % | Not more than 1.0 % |

Q.A. Released
Sign.
Date 29/11/12

Compiled by ; Date : 29/11/2012

Checked by : Date : 29/11/2012

Head, Quality Control : Date : 29/11/2012

MSN Laboratories Ltd
Factory : Sy. No. 317 & 323, Rudraram (vil), Patancheru (Mandal), Medak (Dist.)
A.P., India. Ph. : 08455 - 220372 & 220373 Fax : 08455 - 220415 PIN : 502329

# CERTIFICATE OF ANALYSIS

| | | | |
|---|---|---|---|
| Product | : Rosuvastatin Calcium | Customer Name | : ABDI IBRAHIM |
| Batch No. | : RNm0191112 | Date of Mfg. | : November 2012 |
| Batch Quantity | : 60.20 Kg | Date of Expiry | : October 2016 |
| A.R.No. | : IMD12100036 | Date of Analysis | : 29.11.2012 |
| Reference | : In house | Specification No. | : QC-FPRN-001/01 |

Storage: Preserve in well-closed containers, protected from light .Store at controlled room temperature.

| Sl. No. | TEST | RESULT | SPECIFICATION |
|---|---|---|---|
| 9.0 | Assay by HPLC (On anhydrous basis) | 99.4 % w/w | Not less than 98.0% and Not more than 102.0 % w/w |
| 10.0 | Residual Solvents by GC | | |
| 10.1 | Isopropyl alcohol | Below Detection limit (20 ppm) | Not more than 5000 ppm |
| 10.2 | Acetonitrile | Less than LOQ (33 ppm) | Not more than 410 ppm |
| 10.3 | tert.Butanol | Below Detection limit (15 ppm) | Not more than 5000 ppm |
| 10.4 | tert.Butyl acetate | Below Detection limit (15 ppm) | Not more than 5000 ppm |
| 10.5 | Toluene | Below Detection limit (6 ppm) | Not more than 890 ppm |
| *11.0 | Particle size by Malvern | | |
| 11.1 | D(0.1) | 2.7 microns | Less than 5 microns |
| 11.2 | D(0.5) | 6.3 microns | Less than 10 microns |
| 11.3 | D(0.9) | 14.1 microns | Less than 20 microns |

The product CONFORMS to above specifications

* As per Customer requirement

Compiled by : Date : 29/11/2012

Checked by : Date : 29/11/2012

Head, Quality Control : Date : 29/11/2012

**Appendix 2**

*Latin American Journal of Pharmacy*
(formerly *Acta Farmacéutica Bonaerense)*
*Lat. Am. J. Pharm.* **35** (Suppl. 1): 1065-76 (2016)

Regular article
Received: December 7, 2015
Revised version: January 13, 2016
Accepted: January 15, 2016

# Studies on Rosuvastatin Calcium Incorporated Chitosan Salt Nanoparticles

Fawaz N.S. AL-HEİBSHY [1 2], Ebru BAŞARAN [2] & Müzeyyen DEMİREL [2] *

[1] *Doctorate Program in Pharmaceutical Technology, Graduate School of Health Sciences, Anadolu University, 26470, Eskişehir, Turkey.*
[2] *Anadolu University, Faculty of Pharmacy, Department of Pharmaceutical Technology, 26470, Eskişehir, Turkey.*

*SUMMARY.* **Cardiovascular diseases are the leading causes of death worldwide and rosuvastatin calcium (RCa) is one of the most effective drugs used for the prevention of coronary heart diseases. Considering low aqueous solubility oral bioavailability of RCa was hardly reached to almost 20%. Therefore there is still a demand for novel drug delivery systems with outstanding drug absorption, distribution, and elimination rates as well as less side effects. In this study RCa was incorporated into chitosan acetate (CA), chitosan lactate (CL), chitosan aspartate (CAs) and chitosan glutamate (CG) nanoparticles (NPs) for the enhancement of its preferential use. Spray drying method was used for the formation of the RCa incorporated NPs. Physicochemical characteristic properties were evaluated in detail and analyses results demonstrated that particle sizes were ranged between 240.0 ± 10.7-446.9 ± 13.1 nm with homogenous size distributions (with PDI data range of 0.490 ± 0.032 to 0.790 ± 0.090) while the zeta potentials mostly valued in the cationic scale. Entrapment efficiencies (EE) of RCa-CA-NPs and RCa-CL-NPs were the highest with 80.8 ± 3.1% and 99.1 ± 1.9%, respectively. *In vitro* release study results demonstrated initial burst releases for the RCa-CA-NPs and RCa-CL-NPs with almost 58% just within 5 min while the release rate of pure RCa was reached up to 53% in phosphate buffer solution (pH 6.8) only after 1 h. As a result of the study enhanced *in vitro* release rates were achieved from RCa incorpotared NPs showing that the chitosan (Cs) originated NPs have the potentials as novel drug delivery systems for RCa.**

*RESUMEN.* Las enfermedades cardiovasculares son las principales causas de muerte en todo el mundo y la rosuvastatina cálcica (RCa) es una de las drogas más eficaces utilizadas para la prevención de enfermedades coronarias. Teniendo en cuenta su baja solubilidad acuosa, la biodisponibilidad oral de la RCA apenas alcanza el 20%. Por lo tanto todavía hay una demanda de sistemas de administración de fármacos novedosos con buena absorción, distribución y tasas de eliminación, así como menos efectos secundarios. En este estudio RCa se incorporó en acetato de quitosano (CA), lactato de quitosano (CL), aspartato de quitosano (CAS) y glutamato de quitosano (CG) en nanopartículas (NPs) para mejorar su uso. El método de secado en aerosol se utilizó para la formación de los NPs con RCa incorporado. Las propiedades fisicoquímicas fueron evaluadas en detalle y el análisis de los resultados demostró que el tamaños de partícula osciló entre 240,0 ± 10,7 a 446,9 ± 13,1 nm con distribuciones de tamaño homogéneos (con rango de datos PDI de 0,490 ± 0,032 hasta 0,790 ± 0,090), mientras que los potenciales zeta se evaluaron sobre todo en la escala catiónica. Las eficiencias de atrapamiento (EE) de la RCa-CA-NP y RCa-CL-PN fueron las más altas con 80,8 ± 3,1% y 99,1 ± 1,9%, respectivamente. Los resultados del estudio de liberación *in vitro* demostraron comunicados de ráfagas iniciales para la RCa-CA-NP y RCa-CL-PN con casi el 58% sólo dentro de 5 min mientras se alcanzó una tasa de liberación pura de RCa hasta un 53% en solución tampón fosfato (pH 6,8) sólo después de 1 h. Como resultado del estudio fueron mejoradas las tasas de liberación *in vitro* de las RCa incorporadas en NPs que muestran que las NPs con quitosano (Cs) tienen potencial como sistemas de administración de la RCa.

## INTRODUCTION

Hyperlipidemia is a heterogeneous disorder commonly characterized by increased flux of free acids, triglyceride, low-density lipoprotein cholesterol (LDL-C) and apolipoprotein B levels, as well as decreased high-density lipoprotein cholesterol (HDL-C) plasma levels as a result of metabolic effects, dietary habits and life style [1]. Hyperlipidemia is the major cause of atherosclerosis

*KEY WORDS:* chitosan, chitosan salts, drug release, nanoparticles, rosuvastatin calcium.

* Author to whom correspondence should be addressed. *E-mail:* mdemirel@anadolu.edu.tr

ISSN 0326 2383 (printed ed.)
ISSN 2362-3853 (on line ed.)

and other conditions related to atherosclerosis like coronary heart diseases, peripheral vascular diseases, ischaemic cerebrovascular diseases and pancreatitis. It has been proved that elevated plasma levels of cholesterol and LDL are the main reasons of atherosclerosis whereas, plasma levels of HDL have a protective effect. Complications from high cholesterol and triglyceride levels affect the heart and lead to complications including heart diseases, heart attack, and stroke [2-4]. LDL-C is the primary target of cholesterol-lowering therapy with agents such as 3-hydroxy-3-methylglutaryl coenzyme A-reductase inhibitors (commonly referred to as statins) [5]. Such statins have become the keystone of therapies used for the treatment of dyslipidemia for both the primary and secondary prevention of cardiovascular disease [6].

Rosuvastatin calcium (RCa) is a member of the class of statins and highly efficacious in reducing plasma LDL-C levels and favorably modifying the other lipid and apolipoprotein variables in patiens with hypercholesterolemia in short-term (6-12 weeks) and long-term (52 weeks) trials [5,7]. The oral bioavailability of RCa is 20% because of its poor aqueous solubility and extensive metabolization by liver via oxidation, lactonisation, and direct secretion from the blood to the intestine. For these reasons, enhancing the solubility and by-passing the hepatic metabolism of RCa are desirable approaches to improve its therapeutic performance [8-12]. Studies have shown that novel drug delivery systems (solid dispersions, self nanoemulsifying drug delivery system (SNEDDS), nanoemulsions, solid lipid NPs etc.) improves the solubility, dissolution rates and bioavailability of the RCa [9,10,13,14]. However, chitosan (Cs) NPs of RCa have not fully investigated which makes the polymer more preferable.

Cs is a natural polymer obtained by deactylation of chitin. Chitin is known to be the most abundant biopolymer in nature that occurs as the major organic skeletal substance of invertebrates and as a cell wall constituent of fungi and green algae [15,16]. Cs is regarded as biologically safe, non-toxic, biocompatible and biodegradable polysaccharide [16] therefore Cs exhibits wide range of biological applications like hypobilirubinaemic and hyprocholesterolemic effects, antacid and antiulcer activities, wound and burn healing properties [17] and widely regarded as an efficient intestinal absorption enhancer of therapeutic macromolecules, owing to its inherent mucoadhesive feature and ability to modulate the integrity of epithelial tight junctions reversibly [18,19].

Cs has a weak base character with a pKa value of the D-glucosamine residue of about 6.2-7.0; therefore, it is insoluble at neutral and alkaline pH values. Cs salts can be formed easily with organic acids (such as hydrochloric acid, acetic acid, aspartic acid and glutamic acid) which allow it to be soluble in water [20]. By using Cs-based NPs, many studies have attempted to protect the loaded macromolecules against acidic denaturation and enzymatic degradation, prolong their intestinal residence time, and enhancement of the absorption by the intestinal epithelium [19]. In addition Cs NPs have many advantages like ability to control the release of active agents, avoidance of the hazardous organic solvent use while fabricating acid soluble particles. Its cationic nature also allows ionic crosslinking with multivalent anions, and shows mucoadhesive character which increases residence time at the site of absorbtion [21]. Furthermore, nano-sized drug delivery systems are very promising strategies for the improvement of the bioavailability of the incorporated drugs [22].

The improvement of dissolution from solid dosage forms is an important issue for enhancing bioavailability and therapeutic efficiency. The purpose of our investigation was the evaluation of the impact of Cs on the dissolution properties of RCa. Cs water-soluble acid salts (acetate, lactate, glutamate and aspartate) were selected as excipient to enhance the delivery of RCa for oral application.

## MATERIALS AND METHODS

### Materials

Rosuvastatin calcium was a generous gift from Abdi İbrahim İlaç (İstanbul, Turkey). Chitosan (medium molecular weight), chitosan oligosaccharide lactate, acetic acid, aspartic acid, glutamic acid and ethanol (99.8%) were purchased from Sigma-Aldrich (Steinheim, Germany). All the other chemicals and reagents used were of analytical grade.

### Preparation of Nanoparticles

The Cs NPs and Cs acid salts were prepared in a laboratory-scale spray dryer Buchi-190 mini spray dryer (Mini Spray Dryer, BUCHI Labortechnik AG, Switzerland), and organic acetic acid (AA), aspartic acid (AsA), and glutamic acid (GA) were used as solvent in the formulation process [23-25]. Briefly, the medium molecular weighted Cs powder was hydrated in 3% GA, 3% AsA and 2% AA solutions with a continuous stirring on a magnetic stirrer at 300 rpm at

room temperature for 16 h. Ethanol (99.8%) and RCa were added to the homogenous mixture of Cs solution with a continuous stirring about one hour. Spray drying process was accomplished for homogenous mixtures at flow rate 1 mL/min using a 0.5 mm nozzle. The inlet temperature was set to 160 °C and the outlet temperature was 95 °C. Finally dried NPs were put in well closed containers and stored in a desiccator at 25 ± 0.5 °C until being analyzed. Compositions of the RCa loaded NPs are shown in Table 1.

| Code | Rca (mg) | Cs (mg) | CL (mg) | AA 2% v/v (mL) | AsA 3% v/v (mL) | GA 3% v/v (mL) | Ethanol 99.8% (mL) | DW (mL) |
|---|---|---|---|---|---|---|---|---|
| F1 | 150 | 1000 | - | 150 | - | - | 150 | - |
| F2 | 75 | - | 500 | - | - | - | 250 | 250 |
| F3 | 50 | 500 | - | - | 500 | - | - | - |
| F4 | 75 | 500 | - | - | 500 | - | 500 | - |
| F5 | 50 | 500 | - | - | - | 500 | - | - |
| F6 | 75 | 500 | - | - | - | 250 | 250 | - |

**Table 1.** Compositions of rosuvastatin calcium incorporated chitosan nanoparticles. RCa: rosuvastatin calcium, Cs: chitosan medium molecular weight, CL: chitosan lactate, AA: acetic acid, AsA: aspartic acid, GA: glutamic acid, DW: distilled water.

The yield of NPs (%) was calculated using Eq. [1] [26].

$$Nanoparticle\ Yield = \frac{Mass\ of\ the\ nanoparticle\ recovered}{Mass\ of\ drug\ and\ polymer} \times 100 \quad [1]$$

**Physicochemical characterization of the nanoparticles**

***Particle size and zeta potential measurements***

The particle size and zeta potential measurements of NPs were carried out using Malvern Nano ZS (Zetasizer Nano Series, England). Prior to analyses, proper amounts of dry NPs were diluted with bidistilled water adjusted to a constant conductivity of 50 µS/cm with 0.9% NaCL and suspended completely for several minutes using vortex (Jeio Tech, VM-98B, Korea). All analyses were repeated in triplicate at 25 °C.

***Morphology of NPs***

Photomicrographs were taken at a voltage of 3 kV and 5.00 K X, 9.59 K X, 10.00 K X or 250 X magnification using a Field Emission Scanning Electron Microscope (SEM, Carl Zeiss, Ultra Plus, Germany).

***Entrapment efficiency***

The drug contents, which corresponds to the actual amount of drug incorporated into the NPs were determined by HPLC (Shimadzu 20-A, Japan) method [27]. Separation was achieved using $C_{18}$ column (250 × 4.6 mm, 5 µm) at a flow rate of 1.0 mL/min with an injection volume of 20 µL with detection wavelength at 240 nm. All the analyses were performed at 25 °C. The mobile phase was composed of formic acid (0.05 M) and acetonitrile 55:45 (v/v) [27]. For the reliability of the data, validation studies of the HPLC method were performed [28].

For the entrapment efficiency analyses briefly, 1 mg of formulations were dissolved in 1 mL mobile phase and 100 µL of solution was taken and adjusted to 1 mL with the mobile phase. The solution was analyzed by HPLC, and the entrapment efficiency was calculated by using Eq. [2] [29]. All analyses were repeated in triplicate.

$$Entrapment\ efficiency\ (\%) = \frac{Amount\ of\ drug\ actually\ present\ in\ the\ nanoparticles}{Amount\ of\ drug\ used} \times 100 \quad [2]$$

### Thermal, FT-IR, XRD and $^1$H NMR analyses

Melting transitions and changes in heat capacity of the drug and polymers were analyzed using differential scanning calorimetry (DSC, DSC-60, Shimadzu, Japan). The constant amount of sample was put in hermetically sealed aluminium crucibles and purged with inert nitrogen gas at the rate of 50 mL/min. Thermograms were obtained at 30-250 °C with an increase rate of 10° C/min. In order to evaluate the interaction possibilities between the drug and NPs Fourier Transform Infrared Spectroscopy (FT-IR) spectra were recorded on a Shimadzu 8400 FT-IR spectrophotometer (Japan) at the wavelenght range of 4000-400 $cm^{-1}$. The crystallinity of the spray dried powders was determined using powder X-ray diffractometer (XRD), Rikagu D/Max-3C (Japan) was used for diffraction studies. XRD studies were performed on the samples by exposing them to CuKα radiation (40 kV, 20 mA) and scanned from 2 to 40°, 2θ at a scanning rate 2°/min. Nuclear magnetic resonance ($^1$H-NMR) spectra were obtained in order to evaluate the modifications in the pure materials and polymeric matrixes during the formulation stages using a Bruker NMR equipment 500 MHz (USA). Deuterated chloroform was used as a cosolvent. DSC thermograms, FT-IR, XRD and $^1$H-NMR spectra of pure polymers and RCa were used as references for structural evaluations.

### *In vitro* release studies

RCa (26 mg) was dissolved in 10 mL at pH 6.8 [30]. To provide perfect sink conditions, 3 mg pure RCa or the NPs containing an equivalent amount of RCa were placed in 50 mL phosphate buffer (pH 6.8) [31,32]. Therefore sink conditions were achieved with the drug concentration in the release medium does not exceed 10% of the solubility of the drug in this medium at any time point. The study was performed at 37 ± 0.5°C with a stirring rate of 100 rpm (WiseStir, Korea). At predetermined time intervals (5, 10, 15 min, 0.5, 1, 2, 3, 4, 6, 8, 12, and 24 h) 1 mL samples were collected and fresh medium was added immediately to the release media with same amount to maintain sink conditions. The withdrawn samples were filtered through 0.2 µm polyamide filter and analyzed by HPLC. The experiments were repeated in triplicate. *In vitro* release studies were also performed in distilled water as described above.

### Kinetics and mechanism of release analyses

To evaluate the release kinetics, data obtained from *in vitro* drug release studies in phosphate buffer (pH 6.8) were analyzed by DDSolver software program [33].

## RESULTS

The production performance was calculated as the ratio of the dried product and the sum of the RCa and Cs masses. The yields were found, 10.43, 27.48, 41.82, 80.00, 41.82, and 27.83% for F1-F6 formulations, respectively. *In vitro* characteristics of the NPs are shown in Table 2. Particle size analyses results have demonstrated nanometer range with the particle sizes of 446.9 ± 13.1, 240.0 ± 10.7, 388.1 ± 8.9, 355.4 ± 14.5, 356.4 ± 6.5, and 247.2 ± 46.0 nm for F1-F6 formulations, respectively, with relatively homogenous size distribution (with PDI data range of 0.595±0.009-0.790 ± 0.090). An important parameter; zeta potentials were recorded as 37.3 ± 0.2, 21.9 ± 0.9, 63.7 ± 0.5, 24.9 ± 0.1, 49.4 ± 0.8, and -6.9 ± 0.1 mV for F1-F6 formulations, respectively. Zeta potential values of NP formulations were found indicating a good physical stability being in the range of 20-65 mV for most of the formulations (**Table 2**).

| Code | PS (nm) | PDI | ZP (mV) | EE (%) |
|---|---|---|---|---|
| F1 | 446.9 ± 13.1 | 0.595 ± 0.009 | 37.3 ± 0.2 | 80.8 ± 3.1 |
| F2 | 240.0 ± 10.7 | 0.693 ± 0.064 | 21.9 ± 0.9 | 99.1 ± 1.9 |
| F3 | 388.1 ± 8.9 | 0.620 ± 0.024 | 63.7 ± 0.5 | 4.9 ± 0.2 |
| F4 | 355.4 ± 14.7 | 0.671 ± 0.073 | 24.9 ± 0.1 | 16.5 ± 0.7 |
| F5 | 356.4 ± 6.5 | 0.490 ± 0.032 | 49.4 ± 0.8 | 4.3 ± 0.7 |
| F6 | 247.2 ± 46.0 | 0.790 ± 0.090 | -6.9 ± 0.1 | 21.2 ± 1.3 |

**Table 2.** Mean particle size, polydispersity index, zeta potential, and entrapment efficiency of nanoparticles prepared. PS: particle size, PDI: polydispersity Index, ZP: zeta potential, EE: entrapment efficiency, (mean ± SE, n = 3).

For the evaluation of morphological structures of the NPs SEM microphotographs are shown in **Fig. 1.**

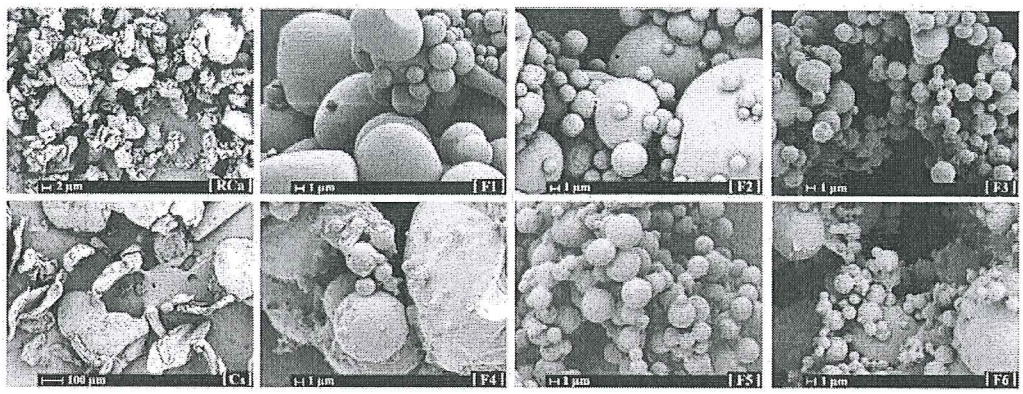


**Figure 1.** SEM images of rosuvastatin calcium, chitosan and nanoparticles prepared.

The drug concentrations of the samples were determined by a validated HPLC method. Regression equation and linearity ($r^2$) for concentration range of 1-100 µg/mL were $y = 50538.71x + 4444.51$ and *0.9999*, respectively (n = 3). Intra- and inter-day relative standard deviation (RSD) were less than 2.62 and 3.95%, respectively (n = 6). Recovery was 98-101%. Limit of detection (LOD) and quantification (LOQ) were 0.33 and 1.01 µg/mL, respectively. The drug-entrapment efficiency varied from 16.5 ± 0.7 to 99.1 ± 1.9% for the formulations prepared which have same drug concentrations (F1, F2, F4, and F6) (**Table 2**).

Thermodynamic variations related to morphological changes before and after formulation steps can be detected by DSC [34,35]. **Fig. 2** shows the DSC curves of the pure components as well as of the final NPs prepared. No sharp peaks were appeared in the thermograms showing the formation of amorphous structures [36]. The thermograms showed no evidence of the any chemical interaction between drug and polymer, however no structural changes were revealed related to the formulation steps.

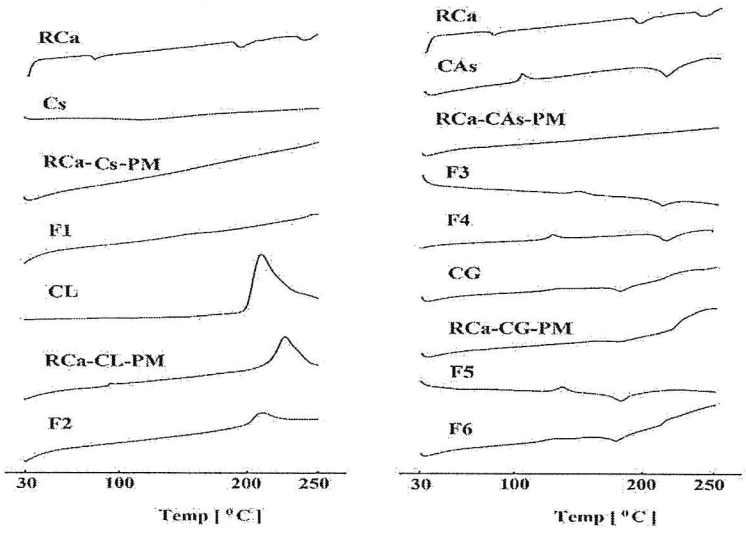


**Figure 2.** DSC thermograms of rosuvastatin calcium, chitosan and nanoparticles prepared. RCa: rosuvastatin calcium, Cs: chitosan medium molecular weight, RCa-Cs-PM: physical mixture of rosuvastatin calcium and chitosan medium molecular weight, CL: chitosan lactate, RCa-CL-PM: physical mixture of rosuvastatin calcium and chitosan lactate, CAs: chitosan aspartate, RCa-CAs-PM: physical mixture of rosuvastatin calcium and chitosan aspartate, CG: chitosan glutamate, RCa-CG-PM: physical mixture of rosuvastatin calcium and chitosan glutamate.

FT-IR analyses were proposed as the possible way to investigate the interactions between substances. In our study interaction possibilities between the salts and active agent were evaluated by FT-IR. The FT-IR spectra of pure materials and prepared NPs were given in **Fig. 3**. Cs spectrum has free amine, hydroxyl and ether functional groups. The peak at 3354 $cm^{-1}$; and also 2873 $cm^{-1}$ (C-H stretching vibrations) corresponds to stretching vibrations of hydroxyl group in Cs [37,38]. Cs exhibits main characteristic bands of carbonyl (C=O-NHR) and amine group (-$NH_2$) at 1649 cm-1 and 1379 $cm^{-1}$, respectively. The absorption bands at 1000-1200 $cm^{-1}$ are attributed to the saccharide structure of Cs [39-41]. RCa spectrum resembles characteristic peaks of aromatic N-H stretching and C=O stretching at 3302 $cm^{-1}$ and 1541 $cm^{-1}$, were revealed respectively (**Fig. 3**). Functional group of RCa was retained in NPs (F1, F2 and F4) spectra, suggesting the absence of chemical interaction with any of the Cs salts used in the preparation of spray dried products [36].

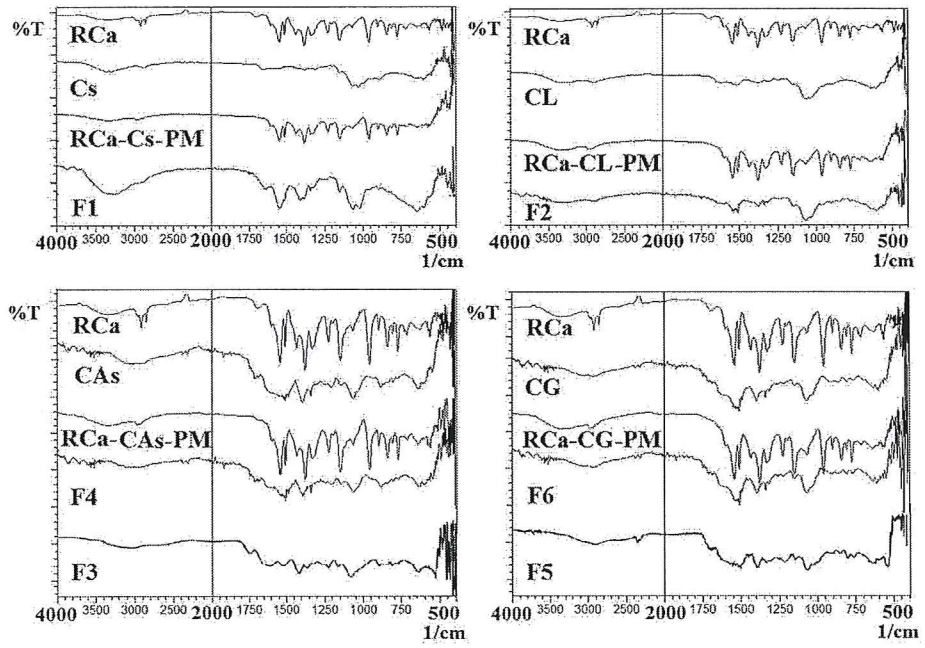


**Figure 3.** FT-IR spectra of rosuvastatin calcium, chitosan and nanoparticles prepared. RCa: rosuvastatin calcium, Cs: chitosan medium molecular weight, RCa-Cs-PM: physical mixture of rosuvastatin calcium and chitosan medium molecular weight, CL: chitosan lactate, RCa-CL-PM: physical mixture of rosuvastatin calcium and chitosan lactate, CAs: chitosan aspartate, RCa-CAs-PM: physical mixture of rosuvastatin calcium and chitosan aspartate, CG: chitosan glutamate, RCa-CG-PM: physical mixture of rosuvastatin calcium and chitosan glutamate.

Fig. 4 shows the XRD patterns of RCa, spray-dried Cs, Cs salts and NPs prepared. The XRD patterns of pure RCa, Cs, Cs salts and NPs prepared showed broad diffraction peaks at 2θ values indicating the amorphous status as expected [24,36].

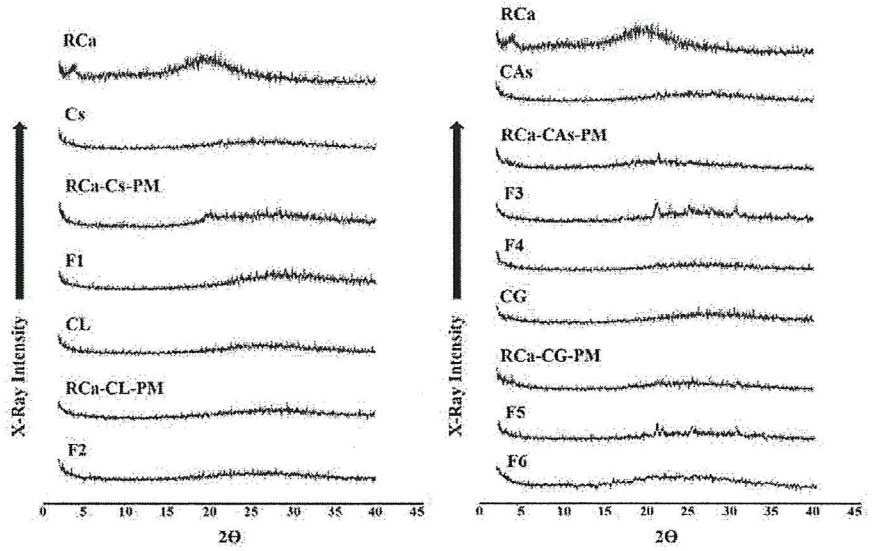


**Figure 4.** XRD spectra of rosuvastatin calcium, chitosan and nanoparticles prepared. RCa: rosuvastatin calcium, Cs: chitosan medium molecular weight, RCa-Cs-PM: physical mixture of rosuvastatin calcium and chitosan medium molecular weight, CL: chitosan lactate, RCa-CL-PM: physical mixture of rosuvastatin calcium and chitosan lactate, CAs: chitosan aspartate, RCa-CAs-PM: physical mixture of rosuvastatin calcium and chitosan aspartate, CG: chitosan glutamate, RCa-CG-PM: physical mixture of rosuvastatin calcium and chitosan glutamate.

$^{1}$H-NMR analyses of the NPs were performed in order to reveal the ionic interactions between RCa and Cs salts. Fig. 5 shows the characteristic peaks for Cs at 3 ppm (due to the acetyl group), and 7.5 ppm (considering H-3/6) for the ring structure of the sugar (marked with arrows) [42,43].

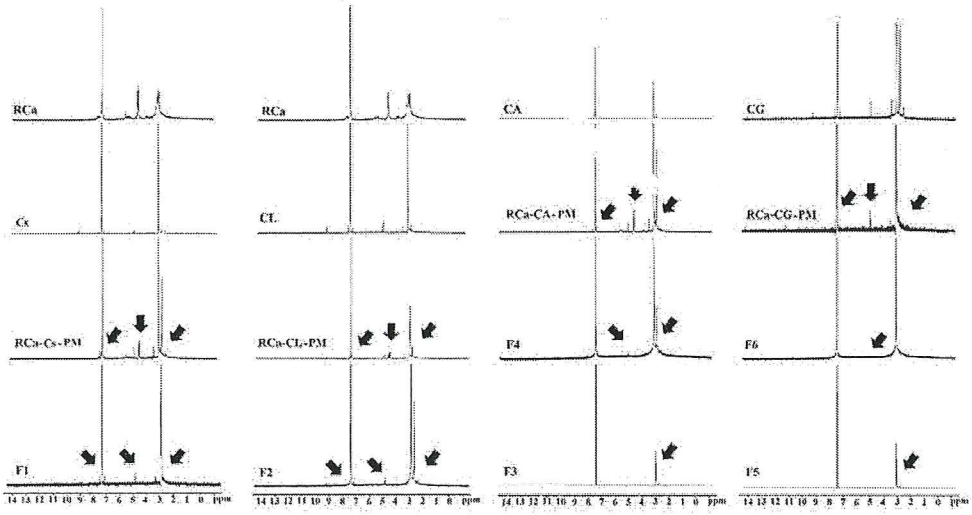


**Figure 5.** $^{1}$H-NMR spectra of rosuvastatin calcium, chitosan and nanoparticles prepared [RCa: rosuvastatin calcium, Cs: chitosan medium molecular weight, RCa-Cs-PM: physical mixture of rosuvastatin calcium and chitosan medium molecular weight, CL: chitosan lactate, RCa-CL-PM: physical mixture of rosuvastatin calcium and chitosan lactate, CAs: chitosan aspartate, RCa-CAs-PM: physical mixture of rosuvastatin calcium and chitosan aspartate, CG: chitosan glutamate, RCa-CG-PM: physical mixture of rosuvastatin calcium and chitosan glutamate.

The results of dissolution studies in phosphate buffer (pH 6.8) performed on NPs are shown in Fig. 6. The release data clearly indicated that RCa is released from the NPs under physiological conditions. An initial burst release achieved for the F1 and F2 formulations, which was approximately 58% just within 5 min. On the contrary, the release rate of pure RCa was relatively slower and sustained compared to F1 and F2 with 53% of drug release within 1 hour. The release rate of pure RCa was 32%, whereas 85, 81, 58, and 63% releases were observed from F1, F2, F4, and F6 in phosphate buffer (pH 6.8) within 0.5 h, respectively. Extented RCa releases (~91%) from pure substance and three formulations (F1, F2 and F6) were observed after 4 h (**Fig. 6**). On the other hand the release rate of pure RCa was 100%, whereas 71, 63, 35, and 100% releases were observed from F1, F2, F4, and F6 in distilled water within 10 min, respectively.

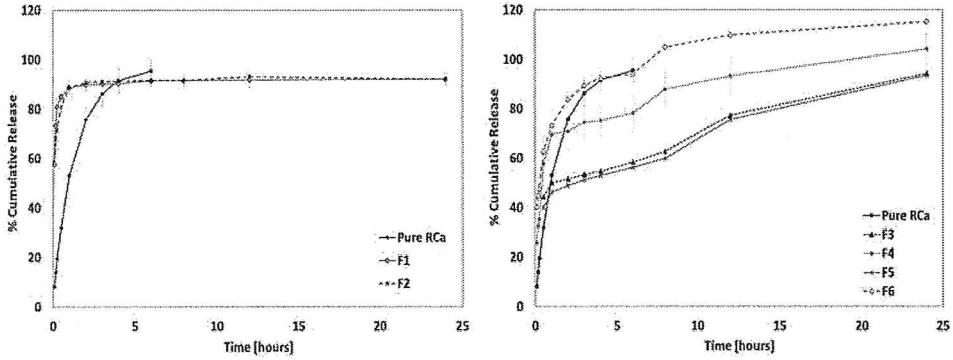


**Figure 6.** *In vitro* release of rosuvastatin calcium from chitosan nanoparticles in phosphate buffer (pH 6.8). RCa: Rosuvastatin Calcium.

*In vitro* release profiles in phosphate buffer (pH 6.8) for the selected NPs were applied on various kinetic model (zero order kinetics, first order kinetics, Higuchi model, Korsmeyer-Peppas model and Hixson-crowell model). The release data were evaluated by rate constant (k), r-values ($r^2$) and Akaike criteria (AIC) for the selection of best suited kinetic model. Pure RCa release was fitted to the first order kinetic model while, all of the NPs (F1, F2, F4, and F6) were fitted to Korsmeyer-Peppas model according to the highest k and r values with lowest AIC data (**Table 3**) [30].

| Code | | Kinetic Model | | | | |
|---|---|---|---|---|---|---|
| | | Zero order | First order | Higuchi | Korsmeyer-Peppas* | Hixson-Crowell |
| Pure RCa | k | 0.021 | 0.001 | 0.045 | 0.048 | 0.000 |
| | $r^2$ | 0.001 | 0.001 | 0.001 | 0.001 | 0.001 |
| | AIC | 0.078 | 0.048 | 0.059 | 0.065 | 0.051 |
| F1 | k | 0.007 | 0.000 | 0.032 | 0.082 | 0.000 |
| | $r^2$ | -0.043 | -0.022 | -0.021 | 0.001 | -0.026 |
| | AIC | 0.132 | 0.125 | 0.124 | 0.075 | 0.127 |
| F2 | k | 0.007 | 0.000 | 0.032 | 0.080 | 0.000 |
| | $r^2$ | -0.032 | -0.016 | -0.015 | 0.001 | -0.019 |
| | AIC | 0.132 | 0.123 | 0.123 | 0.074 | 0.126 |
| F4 | k | 0.007 | 0.000 | 0.030 | 0.062 | 0.000 |
| | $r^2$ | -0.003 | 0.000 | 0.000 | 0.001 | 0.000 |
| | AIC | 0.123 | 0.105 | 0.109 | 0.084 | 0.113 |
| F6 | k | 0.008 | 0.001 | 0.034 | 0.073 | 0.000 |
| | $r^2$ | -0.004 | 0.000 | -0.001 | 0.001 | -0.001 |
| | AIC | 0.128 | 0.102 | 0.114 | 0.079 | 0.118 |

**Table 3.** Kinetic modeling of the chitosan nanoparticles by DDSolver software program [33]. k: rate constant, $r^2$: correlation coefficient, AIC: Akaike criteria, *n (release exponent): 0.

## DISCUSSION

Water-soluble Cs salts are perhaps the most frequently used derivatives of Cs in drug delivery today. Cs forms water-soluble salts with both inorganic acids and organic acids such as hydrochloric acid, formic acid, GA, lactic acid, citric acid, AA and ascorbic acid. The reactive amino groups present in Cs chains can be the reason why the water-soluble polysaccharide is positively charged. Cs acid salts (mostly glutamate, aspartate, hydrochloride, and acetate) were used to enhance the delivery of therapeutic agents across the intestinal epithelia [24].

Several techniques are used to prepare Cs-based NPs; including chemical cross-linking, emulsification solvent diffusion method, ionotropic gelation and spray drying [41]. Among these techniques, spray drying became popular because of the ease of processing and the lack of involvement of toxic solvents. Spray drying is a well-establish method for processing solutions, emulsions and suspensions into powders while controlling the size, density, morphology of the particles efficiently. Limited exposure to the heat makes the method also useful for heat sensitive drugs. In addition, the method is cheap, fast, and a one-step process, which is why it has been employed in numerous applications in pharmaceutics, including preparation of Cs-based formulation [23,24,45]. It should be kept in mind that the drying process can result more amorphous structures compared to pure substances however particle size reduction with the better dispersion formation can also be achieved [46,47].

Preparation yields of NPs were calculated with the amounts of pure materials used. In our study the yield of the formulations were valued in a large scale between 10.43-80.00% which correlates with the previous studies [48]. Loss during the preparation process may be due to the design of the spray-drying apparatus. Embryonic NPs which can not be dried completely may lead to the formation of film on the surface of the drying component, resulting in reduced preparation yield [49].

Smaller particles possess an increased bioavailability with prolonged residence time showing more adhesive properties than larger particles [34]. The most common and routine method for the determination of the mean hydrodynamic diameter of the particle is photon laser diffraction technique. For a monodisperse colloidal systems, the PDI should remain below 0.05, however values up to 0.5 can be regarded as homogenous and can be used for comparison purposes [40]. As noted previously, the particle size increases with the molar mass of the Cs. Delair [40] obtained particles ranging in the 200-1000 nm, with a concomitant increase in PDI from 0.2 up to 0.6. According to the particle size analyses results F1 formulation which contain the highest amount Cs showed the highest particle size (446.9 ± 13.1 nm) while other particle sizes were ranged between the 388.1 ± 8.9 and 240.0 ± 10.7 nm (**Table 2**). No concomitant increase in PDI data with particle size values were observed in our study however particle size distributions were relatively homogenous considering PDI values (**Table 2**).

Zeta potentials of NPs determine the performance of the NP system in the body considering interactions with cell membranes due to the electrostatic forces. Zeta potential measurements also provide an information about the stability dispersed NPs in aqueous media considering less aggregation, due to electric repulsion. Zeta potential values higher than ± 30 mV indicate a stable colloidal dispersion [50]. In this study zeta potentials of prepared NPs were ranged between +21.9 ± 0.9 to +63.7 ± 0.5 mV (except F6;-6.9 ± 0.1 mV). Due to the presence of the quarternary ammonium groups of Cs, most of the Cs-based NPs have cationic characters which tend to adhere to the negatively charged surfaces, facilitating the penetration of NPs across the membranes [51,52].

SEM was used to visualize the particle diameter, structural and surface morphology of the spray-dried powders (**Fig. 1**). SEM images showed that pure RCa has irregular shaped particles which were regarded as amorphous structure (**Fig. 1**). Flakes of pure Cs can also be seen in **Fig. 1** showing the amorphous structure of the polymer. The images of spray-dried samples demonstrated spherical and regular in shapes with smooth surfaces (especially for F1 and F2) which are general morphology of spray-dried amorphous materials [48,53]. Neither porous structures nor RCa residues were detected in the photomicrographs, showing that RCa was successfully incorporated into the particles as nanocapsule forms (**Fig. 1**).

HPLC method used for RCa was determined to be reliable, linear and precise, accurate, sensitive and selective through the validation studies. The comparison of EE for all types of Cs salts was shown in **Table 2**. For the batches which have same drug concentra-

tion (F1, F2, F4, and F6), the EE ranged between 16.5-99.1%. As reported before by Laungtana-anan *et al.* [44] acetate and lactate salts showed higher EE than aspartate and glutamate salt forms also in our study.

DSC thermograms of pure RCa showed glass transition onsets in the ranges of 78-85 °C, 188-198 °C and 237-252 °C showing the amorphous structure of the active agent (**Fig. 2**) which also can be seen in SEM photomicrographs (**Fig. 1**). The DSC thermograms of NPs exhibited the amorphous character of the polymer which gives possibility to incorporate higher amounts of RCa within the spacings of the less ordered amorphous bonds compared to crystalline lattices [54].

FT-IR spectra show absorption bands relating to bending or stretching of unique bond and the resulting spectrum is a fingerprint of the products. Cs can be identified by several absorption bands with specific wavenumbers. Cs base 3354 $cm^{-1}$ intermolecular hydrogen bonding, Amide II band 1649 $cm^{-1}$, $CH_2$ bending 1379 $cm^{-1}$, C-O-C bridge 1058 $cm^{-1}$, C-O-C stretching 1028 $cm^{-1}$ [55]. Morever, the spectrum of spray-dried CL, CA, CG shows a large peak (-$NH_2$) at 1582, 1623, 1631 $cm^{-1}$ respectively (**Fig. 3**). The large shift of these vibrations to higher wavenumbers compared with the usual wavenumbers of the amino group proves the formation of a carboxylate between the –COO- groups of the acids and the $-NH_3^+$ groups of Cs. Consequently, it seems reasonable to conclude the FT-IR analyses as -CH was ionically linked with the acids [38].

Powder XRD was used to determine the crystallinity of compounds. Polymorphic changes of the drugs are important factors which might affect the dissolution rate and the bioavailability. Besides DSC analyses, crystallinity of the drug and NPs were also determined using XRD [36]. RCa exhibited a characteristic amorphous XRD pattern at 2θ that support the DSC analyses results (**Fig. 4**) [26]. Similarly no sharp peaks owing to the crystalline structure were recorded also for NPs showing no formation of crystals during the formulation stages [54].

$^1$H-NMR can also be used to identify Cs via particular chemical shifts of protons and carbons. Physicochemical properties of NPs can be identified by $^1$H-NMR analyses in a variety of dosage forms to elucidate the status of active agent incorporated into a solid matrix, its molecular mobility and molecular interactions between the active material and the excipients [53]. $^1$H-NMR spectra of pure RCa and pure polymers were used as references and according to our analyses results the intensities of the peaks around 3, 5 and 7 ppm ranges were changed upon the entrapment of RCa showing the molecular distribution of RCa in the polymeric matrix compared to pure substances (marked with arrows; **Fig. 5**).

Dissolution is frequently the rate-limiting step in gastro-intestinal absorption and the bioavailability of poor water-soluble drugs from solid dosage forms. The potent well-known dyslipidaemic RCa is representative example of this type of drugs. RCa is slightly soluble in water (7.2 ± 0.1 mg/mL, experimental data) and as a consequence it exhibits low bioavailability values after oral administrations. Therefore, the improvement of RCa dissolution from its solid dosage forms is an important issue for enhancing bioavailability and therapeutic efficiency.

The release of drug from Cs based dosage forms depend upon morphology, size, density and extent of cross-linking of the particulate system, physicochemical properties of the drug as well as the polymer characteristics (such as its hydrophobic character, gel formation ability, swelling capacity, muco-adhesive or bioadhesive properties) and also on the presence of other excipients present in the dosage forms. The release of drug from Cs particulate systems involves three mechanisms: (a) erosion, (b) diffusion, and (c) release from the surface of particles. The release of drug mostly follows more than one type of mechanism. In case of release from the surface, adsorbed drug dissolves rapidly and leads to burst effect when it comes in contact with the release medium [56]. According to dissolution studies, an initial burst release was achieved for F1 and F2 formulations, which was approximately 58% within 5 min. On the other hand, F3-F6 formulations showed slower releases with biphasic profiles (**Fig. 6**). Similar results were recorded at former studies [57]. He *et al.* [57] observed that Cs based microspheres prepared by spray drying technique have shown burst release of cimetidine which correlates with our study. The lowest release rates were achieved for F4-F6 formulations which was attributed to a low EE.

It is evident that all Cs salt types increased the dissolution rate of RCa with respect to the pure drug at

the early stages of the release study. Although only 32% of the pure drug was dissolved in the release medium, 85, 81, 58, and 63% release rates were recorded for the CA (F1), CL (F2), CAs (F4), and CG (F6) formulations, respectively just in 0.5 h (**Fig. 6**). In particular, the release of RCa from the NPs were ordered as: CA > CL > CG > CAs. There is a correlation between our results and former studies results showing that enhanced dissolution rate can be attributed to the decreased size and polymer wetting effect [54,58].

The mechanism of drug release from polymer-based matrices is complex and not completely understood. Some systems may be classified as either purely diffusion or erosion controlled, while most systems exhibit a combination of these mechanisms. Korsmeyer-Peppas model characteristic of anomalous kinetics (non-Fickian, a combination of the diffusion and erosion mechanism) diffusion. Korsmeyer-Peppas model that fits the best the release data of NPs indicates that drug release is ruled by both diffusion of the drug and dissolution/erosion of the polymer matrix [30,59].

## CONCLUSION

Cs salts (acetate, lactate, aspartate and glutamate) have potentials for the preparation of RCa-loaded NPs by spray drying method. The physicochemical properties of all NPs were dependent on types of Cs salts. CA and CL salts provided enhanced drug release while CAs and CG salts showed slower drug releases with respect to the pure drug in phosphate buffer (pH 6.8) medium. Considering poor aqueous solubility and bioavailability of RCa, acetate and lactate salts could serve as potential candidates for RCa delivery systems for oral applications.

**Acknowledgements.** The authors would like to thank Assist. Prof. Dr. Yasemin Süzen (Anadolu University, Faculty of Science) for SEM; Specialist Güner Saka (Anadolu University, Plant, Drug and Scientific Research Center, AUBIBAM) for $^{1}$H-NMR and Ceramic Technician Havva Duru (Anadolu University, Faculty of Engineering) for XRD analyses.

**Conflict of interest.** This study was supported by Anadolu University Scientific Research Project Foundation (No: 1404S289). The authors report no conflicts of interest. The authors alone are responsible for the content and writing of this article.

## REFERENCES

1. Panner Selvam, R., P.K. Kulkarni & V. Naga Sravan Kumar Varma (2015) *RSC Adv.* **5**: 69642-50.
2. Farooq, S.A., V. Saini, R. Singh & K. Kaur (2013) *J. Chem. Pharm. Sci.* **6**: 138-46.
3. Soran, H. & P. Durrington (2008) *Expert Opin. Pharmacother.* **9**: 2145-60.
4. Luvai, A., W. Mbagaya, A.S. Hall & J.H. Barth (2012) *Clin. Med. Insights Cardiol.* **6**: 17-33.
5. Jones, P.H., D.B. Hunninghake, K.C. Ferdinand, E.A. Stein, A. Gold, R.J. Caplan, *et al.* (2004) *Clin. Ther.* **26**: 1388-98.
6. Bhanu Prakash, K., K. Sridevi & P. Vijayasimha (2012) *Int. J. Biol. Pharm. Allied Sci.* **1**: 849-56.
7. Khedr, A., F. Belal, F. Ibrahim & T. Elawady (2013) *Anal. Methods* **5**: 6494-502.
8. Zhou, C., W. Gao, G. Lu, J. Ding, K. Wu, X. Huang, *et al.* (2013) *Carbohyd. Polym.* **96**: 156-62.
9. Swathi, T., M. Vamshi Krishna, D. Sudheer Kumar & J. Krishnaveni (2013) *J. Pharm. Sci. Innov.* **2**: 36-40.
10. Balakumar, K., C.V. Raghavan, N.T. Selvan, R.H. Prasad & S. Abdu (2013) Colloid *Surface B.* **112**: 337-43.
11. Vyas, A. (2013) *J. Incl. Phenom. Macrocycl. Chem.* **76**: 37-46.
12. Zalak, B.P., S.P. Kruti, S.S. Ankit & I.S. Naazneen (2012) *J. Pharm. Bioall. Sci.* **4**: 118-9.
13. Thimmaraju, M.K., V. Ramagiri, K. Bheemanapally, S. Bojja, V. Kola, R. Nerella, *et al.* (2013) *Lat. Am. J. Pharm.* **3**: 1-7.
14. Abdul Hasan Sathali, A. & N. Nisha (2013) *BioMedRx.* **1**: 536-48.
15. Kowalcsyk, D., M. Kordowska-Wiater, J. Nowak & B. Baraniak (2015) *Int. J. Biol. Macromol.* **77**: 350-9.
16. Shivashankar, M., B.K. Mandal, R. Yerappagari & V.P. Kumar (2011) *Int. Res. J. Pharm.* **2**: 1-6.
17. Sinha, V.R., A.K. Singla, S. Wadhawan, R. Kaushik, R. Kumria, K. Bansal, *et al.* (2004) *Int. J. Pharm.* **274**: 1-33.
18. Mainardes, R.M. & L.P. Silva (2004) *Curr. Drug Targets* **5**: 449-55.
19. Chen, M.C., F.L. Mi, Z.X. Liao, C.W. Hsiao, K. Sonaje, M.F. Chung, *et al.* (2013) *Adv. Drug Deliv. Rev.* **65**: 865-79.
20. Weecharangson, W., P. Opanasopit, T. Ngawhirunpat, A. Apirakaramwong, T. Rojanarata, U. Ruktanonchai, *et al.* (2008) *Int. J. Pharm.* **348**: 161-8.

21. Agnihotri, S.A., N.N. Mallikarjuna & T.M. Aminabhavi (2004) *J. Control. Release* **100**: 5-28.
22. Anwar, M., M.H. Warsi, N. Mallick, S. Akhter, S. Gahoi, G.K. Jain, *et al.* (2011) *Eur. J. Pharm. Sci.* **44**: 241-9.
23. Alhalaweh, A., S. Andersson & S.P. Velaga (2009) *Eur. J. Pharm. Sci.* **38**: 206-14.
24. Cervera, M.F., J. Heinämäki, N. de la Paz, O. López, S.L. Maunu, T. Virtanen, *et al.* (2011) *AAPS PharmSciTech.* **12**: 637-49.
25. Yenilmez, E., E. Başaran & Y. Yazan (2011) *Carbohyd. Polym.* **84**: 807-11.
26. Ponnuraj, P., K. Janakiraman, S. Gopalakrishnan, H.J. Jeyakumar, V. Venkateswartu & D.S. Narayanan (2015) *Indo. Am. J. Pharm. Res.* **5**: 767-79.
27. Kumar, T.R., N.R. Shitut, P.K. Kumar, M.C.A. Vinu, V.V.P. Kumar, R. Mullangi, *et al.* (2006) *Biomed. Chromatogr.* **20**: 881-7.
28. Shabir, G.A. (2003) *J. Chromatogr. A.* **987**: 57-66.
29. Gupta, H., M. Aqil, R.K. Khar, A. Ali, A. Bhatnagar & G. Mittal (2010) *Nanomed-Nanotechnol.* **6**: 324-33.
30. Salih, O.S., L.H. Samein & W.K. Ali (2013) *Int. J. Pharm. Pharm. Sci.* **5**: 525-35.
31. Akbari, B.V., B.P. Valaki, V.H. Maradiya, A.K. Akbari & G. Vidyasagar (2011) *Int. J. Pharm. Technol.* **3**: 1842-59.
32. Klose, D., C. Delplace & J. Siepmann (2011) *Int. J. Pharm.* **404**: 75-82.
33. Zhang, Y., M. Huo, J. Zhou, A. Zou, W. Li, C. Yao *et al.* (2010) *The AAPS J.* **12**: 263-71.
34. Başaran, E., B. Şenel, G. Kırımlıoğlu Yurtdaş, U.M. Güven & Y. Yazan (2015) *Lat. Am. J. Pharm.* **34**: 1180-8.
35. Demirel, M. & L. Genç (2015) *Lat. Am. J. Pharm.* **34**: 853-61.
36. Kamble, P.R., K.S. Shaikh & P.D. Chaudhari (2014) *Adv. Pharm. Bull.* **4**: 197-204.
37. Elmizadeh, H., M. Khanmohammadi, K. Ghasemi, G. Hassanzadeh, M. Nassiri-Asl & A.B. Garmarudi (2013) *J. Pharmaceut. Biomed.* **80**: 141-6.
38. Orienti, I., T. Cerchiara, B. Luppi, F. Bigucci, G. Zuccari & V. Zecchi (2002) *Int. J. Pharm.* **238**: 51-9.
39. Boonsongrit. Y., B.W. Mueller & A. Mitrevej (2008) *Eur. J. Pharm. Biopharm.* **69**: 388-95.
40. Delair, T. (2011) *Eur. J. Pharm. Biopharm.* **78**: 10-18.
41. Viral, H.S., S. Pragna & B.S. Gaurang (2012) *Afr. J. Pharm. Pharmacol.* **6**: 491-501.
42. Vllasaliu, D., L. Casettari, R. Fowler, R. Esposito-Harris, M. Garnett, L. Illum *et al.* (2012) *Int. J. Pharm.* **430**: 151-60.
43. Lavertu, M., Z. Xia, A.N. Serreqi, M. Berrada, A. Rodrigues, D. Wang *et al.* (2003) *J. Pharmaceut. Biomed.* **32**: 1149-58.
44. Laungtana-anan, M., P. Opanasopit, T. Ngawhirunpat, J. Nunthanid, P. Sriamornsak, S. Limmatvapirat *et al.* (2005) *Pharm. Dev. Technol.* **10**: 189-96.
45. Sormoli, M.E., M.I.U. Islam & T.A.G. Langrish (2012) *J. Food Eng.* **108**: 541-8.
46. Maestrelli, F., N. Zerrouk, C. Chemtob & P. Mura (2004) *Int. J. Pharm.* **271**: 257-67.
47. Demirel, M., G. Büyükköroğlu, B. Sırmagül, B.S. Kalava, N. Öztürk, Y. Yazan (2014) *Curr. Drug Ther.* **9**: 294-301.
48. Learoyd, T.P., J.L. Burrows, E. French & P.C. Seville (2008) *Eur. J. Pharm. Biopharm.* **68**: 224-34.
49. Hegazy, N., M. Demirel & Y. Yazan (2002) *Int. J. Pharm.* **242**: 171-4.
50. Genç, L. & M. Demirel (2013) *Pharm. Dev. Technol.* **18**: 701-9.
51. Bathool, A., G.D. Vishakante, M.S. Khan & H.G. Shivakumar (2012) *Adv. Matt. Lett.* **3**: 466-70.
52. Bhattarai, N., H.R. Ramay, S.H. Chou & M. Zhang (2006) *Int. J. Nanomed.* **1**: 181-7.
53. Başaran, E., E. Yenilmez, M.S. Berkman, G. Büyükköroğlu & Y. Yazan (2014) *J. Microencapsul.* **31**: 49-57.
54. Portero, A., C. Remuñán-López & J.L. Vila-Jato (1998) *Int. J. Pharm.* **175**: 75-84.
55. Buschmann, M.D., A. Merzouki, M. Lavertu, M. Thibault, M. Jean & V. Darras (2013) *Adv. Drug Deliver. Rev.* **65**: 1234-70.
56. Bansal, V., P.K. Sharma, N. Sharma, O.P. Pal & R. Malviya (2011) *Adv. Biol. Res.* **5**: 28-37.
57. He, P., S.S. Davis & L. Illum (1999) *Int. J. Pharm.* **187**: 53-65.
58. Cerchiara, T., B. Luppi, F. Bigucci & V. Zecchi (2003) *J. Pharm. Pharmacol.* **55**: 1623-7.
59. Arora, G., K. Malik, I. Singh, S. Arora & V. Rana (2011) *J. Adv. Pharm. Technol. Res.* **2**: 163-9.

SCHOOL OF PHARMACY

# NANOBIOTECHNOLOGY DAYS 2015

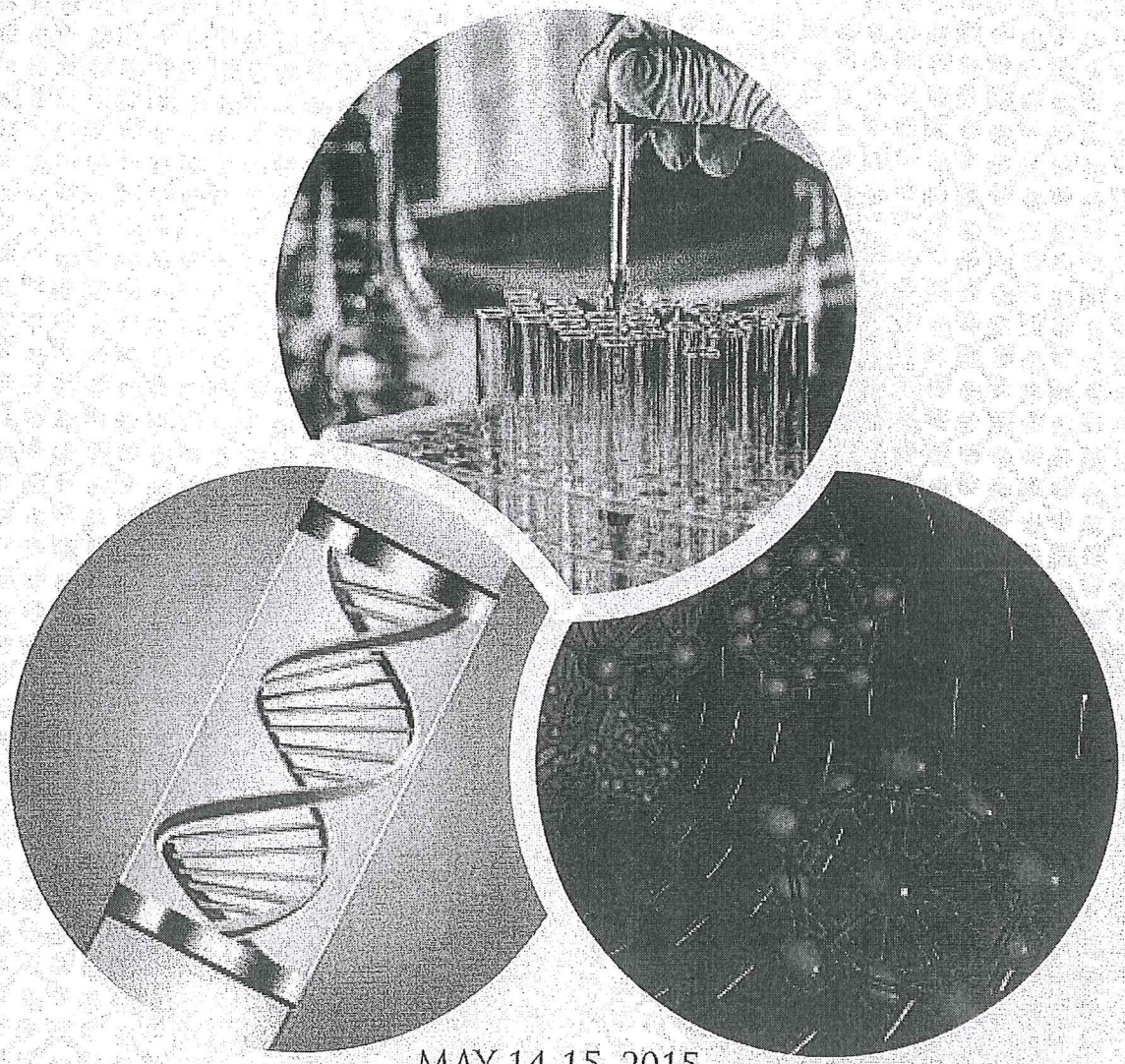

MAY 14-15, 2015
ISTANBUL, TURKEY

# ABSTRACT BOOK

ISTANBUL KEMERBURGAZ UNIVERSITY
GLOBAL · MODERN · REALIST · DYNAMIC

Poster presentation, P13

# FORMULATION AND CHARACTERIZATION STUDIES OF ROSUVASTATIN CALCIUM INCORPORATED STEARIC ACID BASED NANOPARTICLES

Fawaz Nasser Shekh Al-Heibshy*, Ebru Başaran, Müzeyyen Demirel
Anadolu University Faculty of Pharmacy, Department of Pharmaceutical Technology 26470 Eskişehir-Turkey
*Presenting author: Fawaz Nasser Shekh Al-Heibshy, e-mail: fnsaa.aden@gmail.com

**Purpose:** Stearic acid based solid lipid nanoparticles (SLNs) were formulated in order to refine the solubility /dissolution rate as well as the enhancement of bioavailability of the Rosuvastatin Calcium (RCa) which is one of the most effective drug among the cholesterol-lowering Statin Group agents that used for the treatment of high cholesterol, blood-lipid metabolic disorders. RCa has very low solubility and dissolution rate in water with oral bioavailability of approx. 20% therefore there is a need for formulation of novel drug delivery systems for the enhancement of efficacy with lowered side effects of the RCa while enhancing the bioavailability.

**Methods:** SLN formulations were prepared according to hot homogenization method. Briefly lipid was heated up to 90°C±1°C and RCa was added to the molted lipid under mild agitation. Aqueous phase with 2%Tween®80 was heated up to same temperature and was added to the lipid phase under stirring at 13500 rpm using Ultraturrax (T25 Janke & Kunkel IKA® Labortechnik, Staufen, Germany). Resulting emulsion was cooled down to room temperature. For the determination of characteristic properties of the formulations prepared particle size, polydispersity index, zeta potential analyses were performed. In order to evaluate the changes in lipid structure thermal analyses by differential scanning calorimetry (DSC) and X-ray diffractometry (XRD) analyses were performed. Fourier transform infrared spectrophotometry (FT-IR) and nuclear magnetic resonance (NMR) analyses results were used for the evaluation of bond formation during the formulation steps. A validated HPLC method was used for the determination of incorporated RCa into the particles. Release characteristics of the particles prepared were evaluated at 37°C±1°C in buffer solution (pH 1.2 ) during 120 minutes.

**Results:** Considering particle size and zeta potential data F9 and F32 coded formulations were selected for further studies. Particle sizes of the formulations selected were remained in the nanometer range with 228.57±6.51nm and 351.13±13.91nm and PDI data were valued 0.368±0.032 0.327±0.025 respectively for F9 and F32 formulations showing the homogenous size distribution of the suspensions. Zeta potentials were recorded as -16.07±0.22 and -17.03±0.53 for F9 and F32 respectively. According to the HPLC analyses results RCa was successfully incorporated into the SLNs with 280.07±2.23 µg.mL-1 519.05±5.32 $\mu g.mL^{-1}$ concentrations for F9 and F32 respectively. Approx. 90% and %92 of the incorporated RCa was released within 120 minutes from F9 and F32 respectively in buffer solution during in vitro release studies.

**Conclusion:** RCa incorporated stearic acid based SLNs were successfully prepared by hot homogenization method and characteristic properties of the formulation were revealed in detail by *in vitro* characterization studies.

**Keywords:** Rosuvastatin calcium, solid lipid nanoparticles, bioavailability

ANKARA UNIVERSITY
FACULTY OF PHARMACY

# ISOPS 11th International SYMPOSIUM ON PHARMACEUTICAL SCIENCES

## BOOK OF ABSTRACT

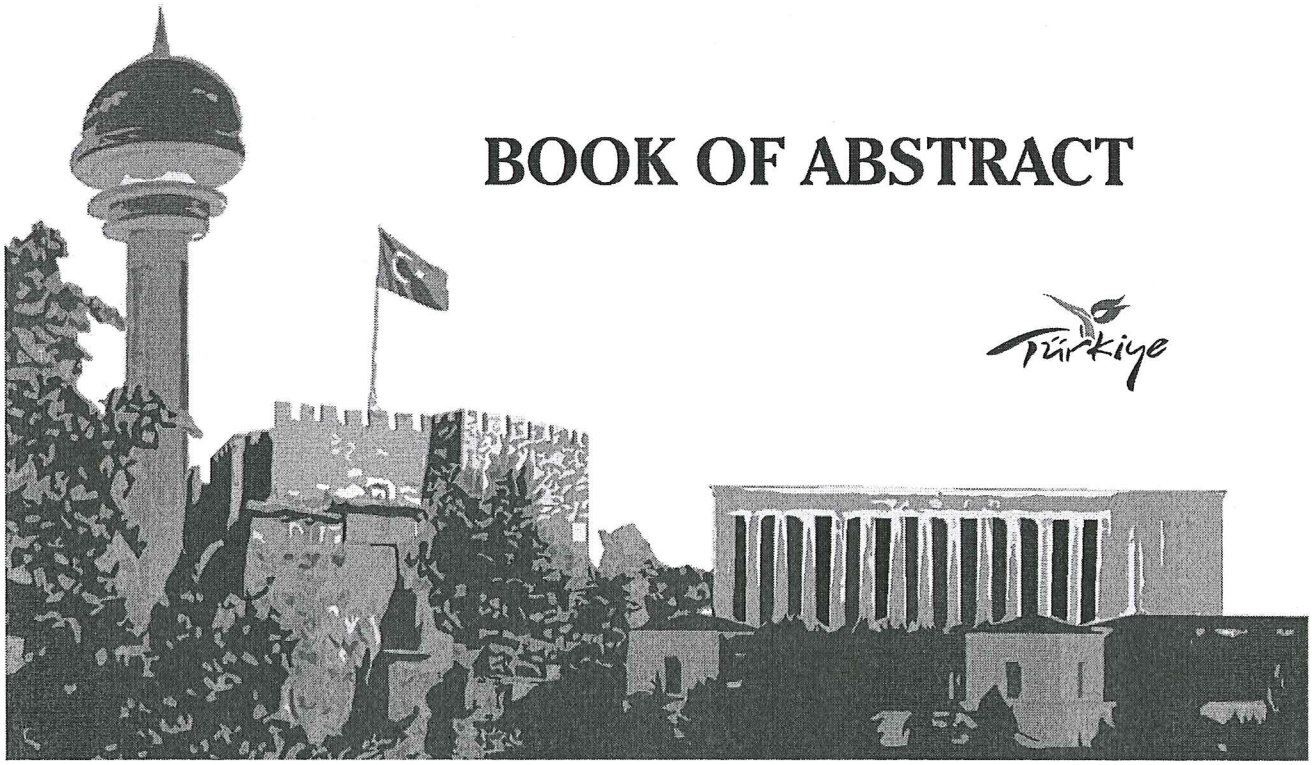

T.C. KÜLTÜR VE TURİZM BAKANLIĞI

TUBİTAK

JUNE 09-12, 2015
ANKARA, TURKEY

## P-81: *IN VITRO* CHARACTERIZATION STUDIES OF ROSUVASTATIN CALCIUM INCORPORATED TRIPALMITIN BASED SLNS

F.N.S. Al Heibshy, E. Başaran, M. Demirel

Anadolu University, Faculty of Pharmacy, Department of Pharmaceutical Technology,
26470 Eskişehir, TURKEY

Rosuvastatin calcium (RCa) was successfully incorporated into Tripalmitin based solid lipid nanoparticles (SLNs) in order to enhance oral bioavailability of RCa.

### INTRODUCTION

Rosuvastatin calcium (RCa) which is the member of the most effective cholesterol lowering drugs; Statins, is relatively high potent statin with good clinical efficacy with a long elimination half-life (approx. 20 hrs) [1, 2] however it has a low bioavailability due to low aqueous solubility because of its crystalline structure [3], therefore, RCa was incorporated into Tripalmitin (TP) based solid lipid nanoparticles (SLNs) in order to enhance its bioavailability in the treatment of dyslipidemia.

### MATERIALS AND METHODS

*Formulation*: SLNs were prepared according to the hot homogenization method using high shear stirrers at 9500 rpm (Table 1) [4].

Table 1. Compositions of the Formulations Prepared

| Code | TP (%) | RCa (%) | Tween (%) | PC (%) | Water (q.s. mL) |
|---|---|---|---|---|---|
| LTF3-PL | 4 | - | 2 | - | 50 |
| LTF3 | 4 | 0.3 | 2 | - | 50 |
| LTF4-PL | 4 | - | 1 | 1 | 50 |
| LTF4 | 4 | 0.2 | 1 | 1 | 50 |

*PL:Placebo TP: Tripalmitin, RCa: Rosuvastatin calcium, Tween: Tween® 80, PC: Phosphatidylcholine, Water: Distilled Water*

*Characterization*: Particle size, polydispersity index, zeta potential analyses were performed. In order to evaluate structural changes of the lipid DSC, XRD, FT-IR and NMR analyses results were used. A validated HPLC method was used for the determination of incorporated RCa. Release characteristics of the particles prepared were evaluated at 37°C±1°C in phosphate buffer solution (pH 6.8) during 24 hrs.

### RESULTS AND DISCUSSION

Primary characterization analyses (particle size, polydispersity index, zeta potential analyses) with RCa amount of the formulations were given in Table 2.

Analyses results revealed that the particle sizes were in the nanometer range with homogenous size distribution. RCa was successfully incorporated into SLNs and encapsulation of RCa did not effect the the anionic character of the particles (Table 2). RCa was detected in the release medium up to 24 hrs showing incorporation of RCa into SLN has extended the RCa release as expected (Figure 1).

Table 2. Primary Characterization Analyses Results with RCa Amount of the Formulations Prepared (n=3, mean ±SE)

| Code | PS (nm) | PDI | Zeta (mV) | RCa ($\mu g.mL^{-1}$) |
|---|---|---|---|---|
| LTF3-PL | 107.5±3.8 | 0.7±0.0 | -25.1±1.3 | - |
| LTF3 | 240.2±22.9 | 0.2±0.0 | -23.9±1.5 | 436.5±7.9 |
| LTF4-PL | 216.8±15.9 | 0.3±0.0 | -48.5±1.0 | - |
| LTF4 | 267.7±18.7 | 0.3±0.0 | -40.8±1.2 | 321.9±2.7 |

*PS:Particle Size, PDI:Polydispersity Index*

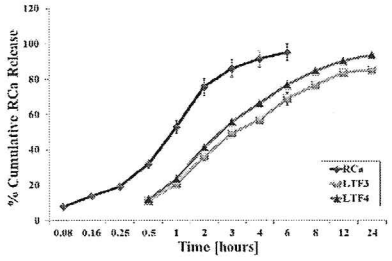


Fig. 1. Release profiles of RCa from SLNs Prepared versus Pure RCa (n=4, mean ±SE)

### CONCLUSIONS

As a conclusion RCa incorporated SLNs were successfully formulated for the treatment of dyslipidemia.

### ACKNOWLEDGMENTS

This study was financed by Anadolu University Scientific Research Project Foundation (No: 1404S289).

### REFERENCES

1. Litvić, M.; Šmic, K.; Vinković, V.; Filipan-Litvić, M., A study of photodegradation of drug rosuvastatin calcium in solid state and solution under UV and visible light irradiation: The influence of certain dyes as efficient stabilizers. *J Photoch Photobio A* **2013**, *252*, 84-92.

2. Lai, S-W.; Lin, C-L.; Liao, K-F., Rosuvastatin and risk of acute pancreatitis in a population-based case–control study. *Int J Cardiol* **2015**, *187*, 417-420.

3. Balakumara, K.; Raghavan, C.V.; Tamil selvana, N.; Hari prasad, R.; Abdu, S., Self nanoemulsifying drug delivery system (SNEDDS) of Rosuvastatin calcium: Design, formulation, bioavailability and pharmacokinetic evaluation. *Colloid Surface B* **2013**, *112*, 337-343.

4. Basaran, E.; Demirel, M.; Sırmagül, B.; Yazan, Y., Cyclosporine-A incorporated cationic solid lipid nanoparticles for ocular delivery. *J Microencapsul* **2010,** *27*(1), 37-47.

## P-82: MODIFIED CHITOSAN NANOPARTICLES FOR ENHANCED VACCINE DELIVERY BY NASAL ROUTE

G. Sinani[1,2] M.K. Gök[3], S. Özgümüş[3], H.O. Alpar[2,4] and E. Cevher[1]

[1]Faculty of Pharmacy, Istanbul University, Istanbul, 34116, Turkey; [2]Faculty of Pharmacy, Istanbul Kemerburgaz University, Istanbul, 34217, Turkey; [3]Faculty of Engineering, Istanbul University, Istanbul, 34320, Turkey; [4]School of Pharmacy, University of London, London, WC1N 1AX, UK

### INTRODUCTION

Nanotechnology offers the opportunity to design particulate delivery systems varying in composition, size, shape and surface properties for vaccine development [1]. In particular, biodegradable and biocompatible chitosan nanoparticles (NPs) have shown mucosal adjuvant activity [2]. In this study, new chitosan derivative NPs have been prepared and evaluated as nanocarrier system for nasal immunisation.

### MATERIALS AND METHODS

*Preparation of nanoparticles*

Aminated derivative of chitosan (CSA) as a polymer was synthesised in house and NPs were prepared by ionotropic gelation of CSA with tripolyphosphate (TPP).

*Characterisation of nanoparticles*

The particle size and size distribution was determined by photon correlation spectroscopy and zeta potential was measured by Zetasizer Nano-ZS (Malvern Instruments, UK). The percentage yields of chitosan NPs were calculated after centrifugation at 15,000 rpm and following freeze-drying at -50°C. The morphology was examined by scanning electron microscopy. The entrapment efficiency of BSA in NPs was determined by Bradford assay (Sigma-Aldrich, Germany) and SDS-PAGE integrity of BSA released from the NPs was demonstrated (Bio-Rad, USA).

*Cytotoxicity studies*

The safety of NPs was tested *in vitro* on Calu-3 cell lines by MTT assay and cell viability was evaluated at a concentration range of 0-2 mg.mL$^{-1}$.

*In vivo studies and systemic antibody response*

For in vivo studies, dispersion of NP formulation in distilled water with optimum physicochemical characteristics and free BSA were administered intranasally (i.n.) (20µl) and subcutaneously (s.c.) (100µl) to Balb/c mice (n=5) equivalent to 40µg BSA/mice. Blood samples were collected at different time points and BSA specific antibodies (IgG) titres were analysed by ELISA.

### RESULTS AND DISCUSSION

NPs with appropriate particle size, polydispersity and zeta potential for nasal delivery of vaccines were obtained. The CSA NPs showed good reproducibility and good stability at +4±1°C for 12 months (Table 1).

Table1. Z-Average diameter and zeta potential of BSAloaded NPs (n=3)

| For m. | CSA/ TPP (m/m) | After preparation | | After 12 months | |
|---|---|---|---|---|---|
| | | Z-Average diameter nm±SD | Zeta potential mV±SD | Z-Average diameter nm±SD | Zeta potential mV±SD |
| F1 | 1/1 | aggregation | | aggregation | |
| F2 | 2/1 | aggregation | | aggregation | |
| F3 | 3/1 | 125.2±5.5 PDI: 0.40 | 31.4±4.5 | 144.8±0.7 PDI:0.36 | 33.7±4.6 |
| F4 | 4/1 | 139.5±0.1 PDI: 0.36 | 41.2±5.4 | 140.5±0.3 PDI:0.35 | 39.6±4.1 |
| F5 | 5/1 | 146.7±4.0 PDI: 0.38 | 42.4±5.4 | 127.1±6.6 PDI:0.34 | 40.4±5.4 |
| F6 | 6/1 | 161.3±6.2 PDI: 0.34 | 44.2±5.7 | 147.3±9.9 PDI:0.39 | 42.9±5.6 |
| F7 | 7/1 | 177.3±10.2 PDI: 0.35 | 47.8±7.2 | 168.3±4.2 PDI:0.36 | 46.5±4.9 |
| F8 | 8/1 | 184.6±11.7 PDI: 0.40 | 46.9±4.6 | 154.9±3.7 PDI:0.40 | 43.4±4.9 |

Formulation 3 was selected for the *in vivo* delivery of vaccines on the basis of high encapsulation efficiency (78.38%±5.73), small particle size, positive zeta potential and high yield (60.54%±9.82). These particles were spherical in shape, showed good cell viability up to concentrations as high as 2mg.ml$^{-1}$ in Calu-3 cell line and preparation process did not affect the SDS-PAGE integrity of the encapsulated BSA. CSA particles containing BSA were compared with free BSA dispersions with the same dose of BSA administered as CSA particles. Serum BSA spesific IgG titres for CSA particles at 13., 21. and 60. day were significantly different ($p<0.05$) than the equivalent dose of BSA solution.

### CONCLUSIONS

Modified chitosan NPs with suitable size, surface charge and stability for enhanced nasal vaccine delivery were successfully prepared and can be promising carrier systems for i.n. administration of vaccines.

### REFERENCES

1.Smith, JD., et al., *Curr Opin Biotech* **2015**, *34*, 217–224.
2.Bal, SM., et al., *Eur J Pharm Sci* **2012,** *45* (4), 475–81.


12th International Conference of the European Chitin Society
13th International Conference on Chitin and Chitosan

MÜNSTER
Germany

**August 30th to September 2nd**
2015

B1

## *In vitro* evaluation of Rosuvastatin calcium incorporated chitosan and chitosan lactate nanoparticles

F. N. S. Alheibshy, M. Demirel, E. Başaran

Anadolu University, Turkey

Rosuvastatine calcium (RCa) is one of the most effective statin group member has major drawback as low bioavailability due to limited solubility in water and severe side effects. Therefore need for novel drug delivery systems are required in order to enhance the bioavailability while minimizing the side effects by reducing the applied dose. In this study RCa was incorporated into Chitosan and Chitosan lactate nanoparticles by spray drying method.

SEM analyses results demonstrated that particles are round in shape and particle size analyses results also showed that, particle sizes were 313.3±22.3, 446.9±13.1, 624.4±33.4 and 240.0±10.7 nm with homogenous size distribution (0.888±0.051, 0.595±0.009, 0.492±0.123 and 0.693±0.064 of PDI data) while the zeta potentials valued in the cationic scale as 24.1±0.2, 27.3±0.2, 21.7±0.9 and 21.9±0.9 mV for the formulations CF1-P, CF1, CLF2-P and CLF2 respectively.

DSC, XRD, FT-IR and $^{1}$H-NMR analyses showed that both RCa and polymer remained unchanged during formulation steps. Incorporated RCa was found 0.106±0.004 and 0.149±0.011 ($mg.mg^{-1}$) while the release rate of the RCa was 92.04±2.34 % and 92.12±0.76 % CF1 and CLF2 respectively wich was extended up to 24 hrs compared to pure RCa wich was released almost 95 % just within 6 hrs.

As a conclusion incorporation and extended release of RCa was achieved with chitosan based nanoparticles.

Acknowledgement

This study was financed by Anadolu University Scientific Research Project Foundation (No: 1404S289). AUBIBAM management, Faculty of Science (Assoc. Prof. Dr. Murat Erdem) and Faculty of Engineering were acknowledged for $^{1}$H-NMR, SEM and XRD analyses respectively.

D11

## Formulation and characterization studies of Rosuvastatin calcium incorporated chitosan aspartate and chitosan glutamate nanoparticles

**F. N. S. Alheibshy, M. Demirel, E. Başaran**

Anadolu University, Turkey

Despite being the most effective statin group member, severe side effects and limited bioavailability limits the use of Rosuvastatine calcium (RCa) in clinical trials. Therefore in this study RCa was incorporated into two extraordinary chitosan salts; chitosan aspartate and chitosan glutamate for the enhancement of its preferential use.

Spray drying method was used for the formation of the nanoparticles. A validated HPLC method was used for the determination of RCa. SEM analyses results demonstrated that particles are spherical with small particle sizes and particle size analyses results showed that particles were 503.0±33.6, 355.4±14.7, 712.7±56.4 and 247.2±46.0 nm with relatively homogenous size distribution (0.565±0.043, 0.671±0.073, 0.566±0.081 and 0.790±0.090 of PDI data) while the zeta potentials valued as 5.6±0.6, 24.9±0.1, -5.5±0.4 and -6.9±0.1 mV for the formulations CAF4-P, CAF4, CGF6-P and CGF6 respectively.

DSC, XRD, FT-IR and $^{1}$H-NMR analyses showed that both incorporated RCa and polymers remained unchanged during formulation stages. Incorporated RCa was found 0.022±0.001 and 0.039±0.002 (mg.mg$^{-1}$). The 100 % of the incorporated RCa was released (104.00±6.35 % and 115.28±2.65 % CAF4 and CGF6 respectively) within 24 hrs while almost 95 % of pure RCa was released immediately just within 6 hrs.

As a conclusion RCa was successfully incorporated into chitosan salts while maintaining sustained release during 24 hrs as expected.

### Acknowledgement

This study was financed by Anadolu University Scientific Research Project Foundation (No: 1404S289). AUBIBAM management, Faculty of Science (Assoc. Prof. Dr. Murat Erdem) and Faculty of Engineering were acknowledged for 1H-NMR, SEM and XRD analyses respectively.

**CURRICULUM VITAE**